

From THE DEPARTMENT OF NEUROSCIENCE  
Karolinska Institutet, Stockholm, Sweden

**CELLULAR AND SYNAPTIC PROPERTIES IN THE  
LAMPREY STRIATUM**

Jesper Ericsson



**Karolinska  
Institutet**

Stockholm 2012

All previously published papers were reproduced with permission from the publisher.

Published by Karolinska Institutet. Printed by Larserics digital print.

© Jesper Ericsson, 2012  
ISBN 978-91-7457-862-1

## ABSTRACT

The striatum is the main input structure of the basal ganglia, a group of subcortical nuclei that are central to the control of different patterns of motor behaviours and for the selection of actions, a fundamental problem facing all animals. The main focus of this thesis has been to characterize the cellular and synaptic mechanisms of the striatum and its relation to other basal ganglia nuclei in the lamprey.

To understand how the basal ganglia input structure, the striatum, processes motor related information we first needed to understand the basic architecture of the striatal microcircuitry. Individual neurons were characterized based on their electrophysiological properties and we showed that there are two main types of striatal neurons: inwardly rectifying neurons (IRNs) that are distinguished by a prominent rectification due to a  $K_{ir}$  type  $K^+$  conductance, and non-IRNs. IRNs are in this and other respects very similar to the mammalian medium spiny projection neurons (MSNs). IRNs are projection neurons of two types, those that express substance P, dopamine receptors of D1 type and GABA, or enkephaline and D2 receptors and GABA. Non-IRNs are a mixed group of neurons and contain neurons similar to the fast-spiking type found in mammals.

We then investigated how the striatum is activated by the main excitatory inputs from the lateral pallium (the homolog of the cortex) and from thalamus. As recently demonstrated in mammals, the pallium and thalamus in lamprey provide synaptic inputs with very different dynamic properties to the striatum, as evoked by extracellular stimulation of the respective pathway. Repetitive activation of the synapses from the lateral pallium result in a progressive facilitation over several hundred milliseconds due to a low presynaptic release probability. In contrast, activation of thalamic afferents instead evokes strongly depressing synapses throughout a stimulus train due to a high presynaptic release probability. The conserved difference between the thalamic and pallial inputs most likely has functional implications for processing within striatum.

The lamprey striatum receives prominent dopaminergic innervation that, when depleted, leads to hypokinetic symptoms. As dopamine is thought to bias the striatal networks towards selecting actions by differentially modulating the excitability of D1 and D2 receptor expressing striatal projection neurons, we investigated this in lamprey. We cloned the lamprey D2 receptor and demonstrated that it was expressed in striatum. We showed that the neurons that project directly to the basal ganglia output nuclei (the substantia nigra pars reticulata (SNr) and the globus pallidus interna (GPi)) express dopamine D1 receptors, while separate populations that project to the mixed GPi/GPe nucleus express either dopamine D1 or D2 receptors. As in mammals, activation of D1 receptors furthermore leads to an increase in the excitability, whereas D2 activation decreases the excitability of IRNs.

Lastly, we identified the SNr and pedunculopontine nucleus (PPN) in lamprey and showed that the SNr provides tonic inhibition to downstream motor centers while the cholinergic neurons of the PPN modulates basal ganglia nuclei.

In summary, the organization of striatum and the properties of the synaptic input, cellular properties and molecular markers are conserved throughout vertebrate evolution.

## LIST OF PUBLICATIONS

- I. **Ericsson J**, Robertson B, Wikström MA (2007) A lamprey striatal brain slice preparation for patch-clamp recordings. *J Neurosci Methods* 165:251-256.
- II. **Ericsson J**, Silberberg G, Robertson B, Wikström MA, Grillner S (2011) Striatal cellular properties conserved from lampreys to mammals. *J Physiol* 589:2979-2992.
- III. **Ericsson J**, Stephenson-Jones M, Kardamakis A, Robertson B, Silberberg G, Grillner S (2012) Evolutionarily conserved differences in pallial and thalamic short-term synaptic plasticity in striatum. (*Under revision*)
- IV. Robertson B, Huerta-Ocampo I, **Ericsson J**, Stephenson-Jones M, Perez-Fernandez J, Bolam JP, Diaz-Heijtz R, Grillner S (2012) The dopamine D2 receptor gene in lamprey, its expression in the striatum and cellular effects of D2 receptor activation. *PloS one* 7:e35642.
- V. **Ericsson J\***, Stephenson-Jones M\*, Pérez-Fernández J, Robertson B, Silberberg G, Grillner S (2012) Dopamine differentially modulates the excitability of striatal neurons in the direct and indirect pathways in lamprey. *Manuscript*  
(\* Equal contribution)
- VI. Stephenson-Jones M, **Ericsson J**, Robertson B, Grillner S (2012) Evolution of the basal ganglia; Dual output pathways conserved throughout vertebrate phylogeny. *J Comp Neurol.* 520(13):2957-73.



## TABLE OF CONTENTS

<b>1</b>	<b>INTRODUCTION .....</b>	<b>1</b>
1.1	ACTION SELECTION .....	1
1.2	THE LAMPREY MODEL .....	1
1.3	THE BASAL GANGLIA – OVERALL STRUCTURE AND FUNCTION .....	1
1.3.1	<i>The mammalian striatum.....</i>	<i>4</i>
1.3.2	<i>Dopaminergic modulation of striatal neurons.....</i>	<i>7</i>
1.4	CELLULAR BASIS OF MOTOR BEHAVIOUR IN LAMPREY AND OTHER NON-MAMMALIAN VERTEBRATES .....	8
1.4.1	<i>The basal ganglia in lamprey .....</i>	<i>9</i>
1.4.2	<i>The striatum in lamprey.....</i>	<i>10</i>
1.4.3	<i>Striatal afferents.....</i>	<i>11</i>
1.4.4	<i>Striatal efferents.....</i>	<i>12</i>
<b>2</b>	<b>AIMS .....</b>	<b>14</b>
<b>3</b>	<b>METHODS.....</b>	<b>15</b>
3.1	THE <i>IN VITRO</i> SLICE PREPARATION .....	15
3.2	ELECTROPHYSIOLOGY.....	15
3.3	NEUROANATOMY AND IMAGING .....	16
<b>4</b>	<b>RESULTS AND DISCUSSION.....</b>	<b>17</b>
4.1	THE LAMPREY STRIATAL BRAIN SLICE PREPARATION (PAPER I) .....	17
4.2	STRIATAL CELLULAR PROPERTIES CONSERVED FROM LAMPREYS TO MAMMALS (PAPER II)...	18
4.3	EVOLUTIONARILY CONSERVED DIFFERENCES IN PALLIAL AND THALAMIC SHORT-TERM SYNAPTIC PLASTICITY IN STRIATUM (PAPER III) .....	20
4.4	THE DOPAMINE D2 RECEPTOR GENE IN LAMPREY, ITS EXPRESSION IN THE STRIATUM AND CELLULAR EFFECTS OF D2 RECEPTOR ACTIVATION (PAPER IV).....	23
4.5	DOPAMINE DIFFERENTIALLY MODULATES THE EXCITABILITY OF STRIATAL NEURONS OF THE DIRECT AND INDIRECT PATHWAYS IN LAMPREY (PAPER V) .....	24
4.6	EVOLUTION OF THE BASAL GANGLIA; DUAL OUTPUT PATHWAYS CONSERVED THROUGHOUT VERTEBRATE PHYLOGENY (PAPER VI) .....	26
<b>5</b>	<b>CONCLUDING REMARKS .....</b>	<b>28</b>
<b>6</b>	<b>ACKNOWLEDGEMENTS.....</b>	<b>30</b>
<b>7</b>	<b>REFERENCES .....</b>	<b>32</b>

## LIST OF ABBREVIATIONS

AChE	acetylcholinesterase
aCSF	artificial cerebrospinal fluid
AHP	afterhyperpolarization
AMPA	$\alpha$ -amino-3-hydroxy-5-methyl-4-isoxazolepropionic acid
AP-5	D-(-)-2-Amino-5-phosphonopentanoic acid
BAC	bacterial artificial chromosome
ChAT	choline acetyltransferase
CNS	central nervous system
CNQX	6-cyano-7-nitroquinoxaline-2,3-dione
CPG	central pattern generator
D1	dopamine 1 receptor
D2	dopamine 2 receptor
D5	dopamine 5 receptor
DARPP-32	dopamine- and cAMP-regulated neuronal phosphoprotein
DPh	habenula projecting dorsal pallidum
EPSP	excitatory postsynaptic potential
FS	fast-spiking
FSI	fast-spiking interneuron
GABA	$\gamma$ -Aminobutyric acid
GPe	globus pallidus externa
GPI	globus pallidus interna
HCN	hyperpolarization-activated cyclic nucleotide-gated
I <sub>A</sub>	A-type potassium current
I <sub>h</sub>	hyperpolarization-activated monovalent cation current
IRN	inwardly rectifying neuron
K <sub>ir</sub>	inwardly rectifying potassium channels
LPal	lateral pallium
LTS	low-threshold Ca <sup>2+</sup> spiking
LVA	low-voltage activated
MPTP	1-methyl-4-phenyl-1,2,3,6-tetrahydropyridine
MSN	medium spiny neuron
NBQX	2,3-Dioxo-6-nitro-1,2,3,4-tetrahydrobenzo[f]quinoxaline-7-

	sulfonamide
NMDA	N-Methyl-D-aspartic acid
non-IRN	non-inwardly rectifying neuron
NOS	nitric oxide synthase
NPY	neuropeptide y
OT	optic tectum
PIR	post-inhibitory rebound
PLTS	persistent and low-threshold $\text{Ca}^{2+}$ spiking
PPN	pedunculopontine nucleus
SKF 81297	( $\pm$ )-6-Chloro-2,3,4,5-tetrahydro-1-phenyl-1H-3-benzazepine hydrobromide
SNC	substantia nigra pars compacta
SNr	substantia nigra pars reticulata
SOM	somatostatin
STN	subthalamic nucleus
SP	substance P
TNPA	R(-)-2,10,11-Trihydroxy-N-propyl-noraporphine 123 hydrobromide hydrate
TH	tyrosine hydroxylase
TSC	torus semicircularis
vLPal	ventral lateral pallium
VTA	ventral tegmental area
ZD 7288	4-Ethylphenylamino-1,2-dimethyl-6-m ethylaminopyrimidinium chloride



# 1 INTRODUCTION

## 1.1 ACTION SELECTION

Writing this thesis is one example of a goal-directed behaviour that requires me to select between different competing actions. This action selection is a basic problem facing not just us humans but all animals, including the earliest vertebrates such as lampreys that, however, have a more limited repertoire of choices to act upon. Because action selection is such a fundamental challenge for all vertebrates, it likely involves similar brain structures that were developed already at the dawn of vertebrate evolution. The basal ganglia, a group of subcortical nuclei, are central to these processes (DeLong, 1990; Mink, 1996; Redgrave et al., 1999). The basal ganglia receives input from competing motor systems where one behaviour is promoted while others are inhibited through segregated pathways to motor centers of the brainstem and thalamus (Grillner et al., 2005). Although the need to select actions to achieve their goals is common to all animals, it was at the onset of this study unknown if they share common mechanisms for these functions. This thesis analyzes the cellular and synaptic mechanisms of the input structure of the basal ganglia, the striatum, and its relation to other basal ganglia nuclei in the lamprey that diverged from the main vertebrate line 560 million years ago (Kumar and Hedges, 1998).

## 1.2 THE LAMPREY MODEL

Lampreys are jawless vertebrates known as cyclostomes that occupy a key position in phylogeny, with their ancestors having diverged from the main vertebrate lineage at the beginning of vertebrate evolution. The nervous system of lamprey shares many of the physiological and anatomical characteristics of other vertebrates (Rovainen, 1979; Nieuwenhuys R, 1998), including mammals, and has been used extensively over the past few decades to study the detailed neural architecture of goal-directed locomotion and posture (Deliagina and Orlovsky, 2002; Grillner, 2003; Grillner et al., 2008). The relative simplicity and limited number of neurons of the lamprey CNS compared to mammals, together with the similarity in anatomical properties, makes it an attractive model to study neural networks controlling motor functions. Another advantage of the lamprey model is the ease of using different *in vitro* and *in vivo* preparations such as intact, semi-intact, isolated and slice CNS preparations. The intrinsic function and network activity of the central pattern generators (CPGs) (Grillner, 1985; Grillner and Wallen, 1985) in the spinal cord that can generate locomotion has been studied in great detail and provided a deep understanding of the general principles governing initiation of movement (Grillner, 2006).

## 1.3 THE BASAL GANGLIA – OVERALL STRUCTURE AND FUNCTION

The basal ganglia are involved in a wide range of motor-related tasks, such as planning, memory, and selection of motor-sequences, but are also important for cognitive and attention-related functions (DeLong, 2000; Middleton and Strick, 2000). Malfunctions of the basal ganglia are related to a multitude of disorders such as Parkinson's disease, Tourette's syndrome, Huntington's disease and certain types of attention disorders

(Albin et al., 1989; DeLong, 2000; Middleton and Strick, 2000; Mink, 2001). The striatum is the main input structure of the basal ganglia and receives glutamatergic afferents from practically all areas of the cerebral cortex, including the primary motor and sensory cortex, and the intralaminar nuclei of the thalamus (e.g. centromedian and parafascicular nucleus) (Bolam et al., 2000; Van der Werf et al., 2002; Smith et al., 2004; Lacey et al., 2007; Reiner et al., 2010). Different striatal subregions receive inputs from distinct cortical areas and participate in different behaviours through cortico-basal ganglia-motor system loops. On a simplified level, the sensorimotor circuits are processed in the putamen nucleus of the striatum in primates (dorsal/lateral/posterior striatum in rodents), associative circuits in the caudate nucleus (dorsal/medial striatum in rodents) and the limbic circuitry in the accumbens nucleus (Kreitzer and Berke, 2011). The striatal architecture does however appear relatively homogeneous, suggesting that there is a core striatal computation that can operate on various forms of information in different parts of the striatum. The striatum as a whole can be thought of as serving as a filter for cortical and thalamic signals, which takes part in determining which actions should be performed at a given moment. The striatum projects either directly (the “direct pathway”) to the output nuclei of the basal ganglia, the globus pallidus interna (GPi) and the substantia nigra pars reticulata (SNr), or polysynaptically via the globus pallidus externa (GPe) and the subthalamic nucleus (STN) to the output nuclei (the “indirect pathway”) (DeLong, 1990). The substantia nigra also includes the dopaminergic substantia nigra pars compacta (SNc) that sends projections to the basal ganglia. Although the striatum is the main functional target of dopamine, there is also dopaminergic innervation of the pallidum and STN to different extents (Rommelfanger and Wichmann, 2010; Rice et al., 2011). The majority of neurons in the basal ganglia are GABAergic projection neurons, whereas the STN contains glutamatergic neurons and the SNc neurons are almost exclusively dopaminergic (Utter and Basso, 2008).

The basal ganglia has traditionally been considered to be dominated by two principal pathways by which cortical and thalamic information is transmitted to the output structures GPi/SNr (Alexander and Crutcher, 1990), although this is presumably a simplification of the situation in mammals (Bertran-Gonzalez et al., 2010). The direct pathway comprises striatal GABAergic medium spiny projection neurons (MSNs) that project directly to the SNr/GPi where they make direct synaptic contact with the GABAergic output neurons. These MSNs also send collaterals to the GPe (Kawaguchi et al., 1990; Bertran-Gonzalez et al., 2010). The directly projecting MSNs also contain substance P and dynorphin and primarily express D1 receptors. This direct pathway through the basal ganglia mediates facilitation of motor actions through disinhibition. The indirect pathway comprises MSNs that project almost exclusively to the GABAergic neurons of the GPe and contain enkephaline in addition to GABA and primarily express D2 receptors and A2a adenosine receptors (Schiffmann et al., 1991). The GPe neurons, in turn, innervate the GABAergic output neurons in the SNr/GPi and the glutamatergic neurons of the STN that then innervate the GABAergic output neurons in the SNr/GPi. The indirect pathway has the opposite effect to that of the direct pathway and mediates motor suppression (Surmeier and Kitai, 1994; Nicola et al., 2000). Kreitzer and colleagues recently demonstrated results in favour of the direct/indirect pathways antagonistically controlling motor activity by using an *in vivo* transgenic mouse model where channelrhodopsin-2 was expressed in either the direct or indirect pathway MSNs (Kravitz et al., 2010). By stimulating indirect-pathway

MSNs they elicited a parkinsonian state with increased freezing and decreased locomotion. In contrast, activation of direct MSNs reduced freezing and increased locomotion.

The GABAergic neurons of the GPe send extensive axon collaterals that innervate the STN nucleus, the basal ganglia output nuclei and the striatum, making it possible to influence neurons throughout the basal ganglia (Kita, 2007). In addition to the striatum, there are also significant excitatory inputs from the cortex and thalamus to the STN that represent the other input layer of the basal ganglia (Tepper et al., 2007). This is referred to as the hyperdirect pathway because of the fast access from the cortex to the GPi/SNr (Nambu et al., 2002), see a schematic overview of the basal ganglia in Figure 1. The GABAergic GPi/SNr neurons have high tonic discharge rates and project to the thalamus and motor centers in the brainstem, including the optic tectum/superior colliculus and mesencephalic locomotor region (Garcia-Rill et al., 1981; Garcia-Rill et al., 1983b; Garcia-Rill et al., 1983a).

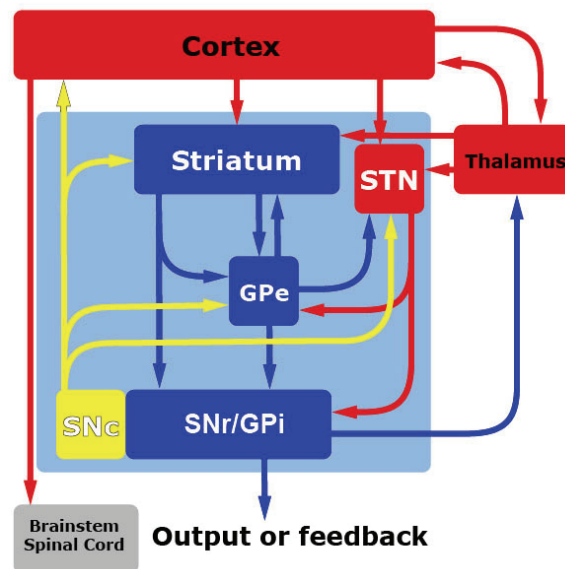


Figure 1. Simplified diagram of the basal ganglia in mammals. Blue indicates structures that are principally GABAergic; red indicates structures that are principally glutamatergic and yellow indicates structures that are dopaminergic. Figure reprinted from Tepper et al., 2007.

The way these GABAergic circuits can activate or pause movements is by disinhibition/inhibition of the output structures of the basal ganglia. Activation of the direct pathway MSNs will inhibit the tonic firing of GPi/SNr neurons which in turn will remove inhibition and thereby facilitate thalamocortical and brainstem motor center activity through the process of disinhibition and thereby promote movement. In contrast, activation of the indirect pathway MSNs will inhibit the tonic firing of GPe neurons and, via the multiple indirect pathways, increase GPi/SNr firing rates and suppress downstream motor cortices and movement (Nambu et al., 2002). Experiments of the superior colliculus support the role of the basal ganglia in selecting specific actions. Studies of saccadic eye movements, one type of goal-directed behaviour, have

shown that the SNr tonically inhibits the saccade-related activity in the superior colliculus, and that the SNr neurons decrease or cease their firing when a saccade is initiated, leading to disinhibition of specific parts of the superior colliculus (Hikosaka and Wurtz, 1983, 1985). The saccade-related decrease of firing in the SNr is directly caused by saccade-related increases in firing of the striatum (Yoshida and Precht, 1971). Similarly, stimulation of D1 MSNs optogenetically *in vivo* has been demonstrated to be directly related to reduced SNr firing and, conversely, stimulation of D2 MSNs led to increased SNr activity (Kravitz et al., 2010).

### 1.3.1 The mammalian striatum

In the mammalian striatum, 95% of all neurons are GABAergic medium spiny neurons (MSNs) (Tepper et al., 2004), also called spiny projection neurons, and they can be identified by their projection targets and the selective expression of different neuropeptides and receptors as previously discussed (D1R and substance P or D2R and enkephaline). MSNs are characterized electrophysiologically by a negative resting potential due to the presence of potassium channels of the inward rectifier type ( $K_{ir}$ ) that are open at negative potentials, but closed when the membrane potential is brought to more depolarized levels by synaptic excitatory drive. This property of MSNs makes them difficult to activate by the glutamatergic input from cortex and thalamus (Wilson & Kawaguchi, 1996; Tepper et al. 2004; Grillner et al. 2005). The responsiveness of MSNs is, however, regulated by the degree of dopaminergic modulatory drive (Surmeier et al. 2007; Redgrave et al. 2008). Without the presence of a dopamine input, mammals become hypokinetic and acquire parkinsonian symptoms. Conversely, an enhanced level of dopamine leads to hyperkinesias with an unintended initiation of motor programs. The corticostriatal terminals form synapses almost exclusively onto dendritic spines as do the majority of thalamic terminals although a proportion also contact dendritic shafts. There is no clear difference in the cortical and thalamic innervation of D1R and D2R MSNs specifically (Doig et al., 2010). The dopaminergic input to the dorsal striatum mainly originates in the SNc while the ventral striatum (the nucleus accumbens and olfactory tubercle) is innervated by both the SNc and the ventral tegmental area (Smith and Villalba, 2008). The dopaminergic terminals mainly make synaptic contacts with spine necks and may therefore influence cortical and thalamic signals reaching the spine head (Smith and Bolam, 1990). Other modulatory input includes serotonin from the raphe nucleus, noradrenaline from the locus coeruleus and histamine from the tuberomammillary nucleus of the hypothalamus (Aston-Jones and Bloom, 1981; Ellender et al., 2011; Parent et al., 2011). Intrastrially, MSNs are sparsely connected to other D1R or D2R expressing MSNs via variable, depressing and facilitating synapses while fast-spiking (FS) neurons provide strong depressing inhibition (Planert et al., 2010). They also receive input from other GABAergic and cholinergic interneurons (Tepper and Bolam, 2004; Ding et al., 2010).

Corticostriatal and thalamostriatal synaptic transmission have recently been shown to regulate striatal activity in opposing ways (Ding et al., 2008; Ellender et al., 2011). Corticostriatal short-term synaptic plasticity onto identified D1R or D2R MSNs was shown to be facilitatory for several different interstimulus intervals and for several consecutive responses in a stimulus train (Ding et al., 2008). In contrast, thalamostriatal synaptic responses in both MSN types were strongly depressing. This was shown to be mainly due to presynaptic differences in release probabilities. The



facilitatory cortical synaptic dynamics is in accordance with the view of the cortical signaling to the striatum, where coherent cortical input is thought to mediate membrane potential transitions (Wilson and Kawaguchi, 1996). The facilitatory nature of the synapses ensures that persistent afferent input is effectively integrated and drives the membrane potential towards discharge threshold. Conversely, thalamic input is thought to be activated upon salient sensory events and shifts in attention (Ewert et al., 1999; Matsumoto et al., 2001). Thalamostriatal synapses with depressing synaptic responses would in contrast to corticostriatal responses evoke action potential discharge upon precisely timed, coincident thalamic inputs (Ding et al., 2008). In lamprey, we have shown (**Paper III**) that the pallial (cortical) and thalamic synaptic transmission show similar dynamics to that of mammals and activates the striatum via facilitating (pallial) and depressing synapses (thalamus), indicating that these are fundamental components of the vertebrate mechanisms for action/selection.

MSNs are medium-sized neurons with dense and extensive local axon collaterals and spiny dendrites. They have distinct electrophysiological properties, including inward rectification due to  $K_{ir}$ , hyperpolarized resting membrane potentials and a ramping response with a long delay to the first action potential due to low-voltage-activated A-type  $K^+$  channels (Kawaguchi et al. 1989; Uchimura et al. 1989; Nisenbaum & Wilson, 1995). MSNs are silent at rest with little spontaneous activity as a consequence of their strong expression of  $K_{ir}$  channels that keep them very hyperpolarized at rest (Nisenbaum and Wilson, 1995). The resting hyperpolarized state in MSNs is also referred to as the “down-state” as these neurons are capable of producing a two-state behaviour with an up-state just below action potential threshold (Wilson and Kawaguchi, 1996). The up-states are driven by phasic changes in cortical and thalamic inputs where strong coherent inputs promote the up-state, which is further facilitated by dopamine acting via pre- and/or postsynaptic D1 receptors or inhibited via pre- and/or postsynaptic D2 receptors (Wilson and Kawaguchi, 1996; Grillner et al., 2005; Surmeier et al., 2007).  $K_{ir}$  is also a characteristic feature of MSNs in birds (Farries and Perkel, 2000; Farries et al., 2005) and reptiles as recently shown by Barral and colleagues in turtles (Barral et al., 2010). As reptiles are the evolutionary origin of both mammals and birds, this suggest that  $K_{ir}$  provides an important property of striatal function in amniotes. Using lamprey striatal brain slices (**Paper I**), we demonstrated for the first time in an anamniote species that the main type of striatal neurons are inwardly rectifying neurons with  $K_{ir}$ -channels and a characteristic long delay to first spike due to activation of A-type potassium channels (**Paper II**).

The remaining population of striatal neurons consist of at least three electrophysiologically distinct types of GABAergic interneurons (Kawaguchi, 1993; Kawaguchi et al., 1995; Tepper and Bolam, 2004), four newly discovered tyrosine hydroxylase-expressing/GABAergic interneurons (Ibanez-Sandoval et al., 2010) and large aspiny cholinergic interneurons (Bolam et al., 1984). Although striatal interneurons are very few in relation to MSNs, they have a strong influence on striatal functioning. *Fast-spiking interneurons (FSIs)* are the best understood of the GABAergic striatal interneurons. They express the calcium-binding protein parvalbumin and are similar to the basket cells of the cortex. Although these cells make up less than 1% of striatal neurons, they exert very powerful inhibition on spiny projection neurons and primarily innervate the soma and proximal dendrites of MSN cell bodies (Tepper et al., 2004). They are characterized by medium-sized cell bodies and aspiny dendrites, narrow action potentials, short duration afterhyperpolarizations

(AHPs), high maximum firing frequencies up to several hundred Hz with little spike frequency adaptation, low input resistance with little or no inward rectification and hyperpolarized membrane potentials (Kawaguchi, 1993; Kawaguchi et al., 1995; Koos and Tepper, 1999). Many FS neurons also exhibit random stuttering discharge in response to steady depolarization during in vitro recordings (Kawaguchi, 1993; Klaus et al., 2011). They provide feed-forward inhibition of the striatum (Tepper et al., 2008; Planert et al., 2010) and receive powerful excitatory input from the neocortex as well as some thalamic innervation (Kita, 1993) although in non-human primates the thalamic input is more abundant (Sidibe and Smith, 1999). They also receive additional extrinsic inhibitory input from a subpopulation of GABAergic globus pallidus externa projection neurons (Kubota et al., 1987; Bevan et al., 1998) and dopaminergic inputs that appear to depolarize neurons through a D1/D5 receptor-mediated effect (Bracci et al., 2002). They also receive cholinergic input from cholinergic interneurons (Koos and Tepper, 2002) although the functional connectivity between cholinergic and FS interneurons is still largely unclear (English et al., 2012). Striatal FSIs make synapses onto both direct and indirect pathway MSNs (Planert et al., 2010) and are also often interconnected with other FSIs via electrical and chemical synapses (Gittis et al., 2010) but do not innervate cholinergic interneurons (Tepper et al., 2010). Fast-spiking like neurons have now also been identified in the lamprey striatum, where they may provide important inhibitory signals to the local striatal circuit (**Paper II**).

*Low-threshold  $Ca^{2+}$  spiking (LTS) GABAergic interneurons* that express somatostatin (SOM), neuropeptide y (NPY) and nitric oxide synthase (NOS) are medium sized neurons with round or fusiform somas with simple dendritic arborization (Kawaguchi, 1993). They are characterized by the presence of a low threshold  $Ca^{2+}$  spike, a high input resistance, a depolarized resting membrane potential and long-lasting plateau potentials following depolarization from rest as well as in rebound from strong hyperpolarization when they often also fire post-inhibitory rebound (PIR) spikes (Tepper and Bolam, 2004). These interneurons may contain even more specialized subclasses but the overall group are called LTS, persistent and low-threshold  $Ca^{2+}$  spiking (PLTS) or SOM/NOS/NPY interneurons (Kawaguchi, 1993; Kawaguchi et al., 1995; Ibanez-Sandoval et al., 2010). These interneurons receive cortical, cholinergic, dopaminergic and GABAergic input (Kubota et al., 1988; Bevan et al., 1998; Gittis et al., 2010) and mainly target MSNs, although they may be sparsely innervated (Gittis et al., 2010). A third type of GABAergic neuron that expresses calretinin has also been identified but not studied in detail electrophysiologically (Kawaguchi, 1993; Kawaguchi et al., 1995).

*Cholinergic interneurons* are immunolabeled by choline acetyltransferase and can be clearly visualized in rodent brain slices by their large cell bodies even though they comprise less than 0.5% of the neuronal population (Rymar et al., 2004) and they contain aspiny dendrites. Electrophysiological hallmarks are large and long-lasting AHPs, regular tonic firing, prominent sag to hyperpolarizing pulses and more depolarized resting membrane potentials than other striatal neurons (Wilson et al., 1990). They receive GABAergic input from MSNs, glutamatergic input from the thalamus and dopaminergic input from the SNc that bind to D2 and D5 receptors and mainly target MSNs as well as GABA interneurons (Tepper and Bolam, 2004; Smith and Villalba, 2008; Ding et al., 2010).

### 1.3.2 Dopaminergic modulation of striatal neurons

In mammals, dopamine serves a critical role in the action selection process, both as a short-term modulator of cellular excitability and for long-term changes in synaptic strength that shape network activity. The striatum receives a very dense dopamine innervation from the SNc that also project to the GPe and STN (Rommelfanger and Wichmann, 2010). Dopamine binds to G-protein-coupled receptors (GPCRs) that are classified into 5 different receptors, D1-D5. These receptors are grouped into two different families, where the D1 receptor family comprises D1 and D5 and that stimulate  $G_s$  and  $G_{olf}$  proteins. The D2 receptor family comprises D2, D3 and D4 receptors that stimulate  $G_o$  and  $G_i$  proteins (Neve et al., 2004). Binding of dopamine either stimulates (D1) or inhibits (D2) adenylyl cyclase that initiates different signaling cascades, such as protein kinase A (PKA) and DARPP-32 mediated effects on voltage sensitive ion channels and glutamate receptors (Cepeda et al., 1993; Greengard, 2001; Svenningsson et al., 2004). Dopamine receptor activation also raises intracellular calcium levels by modulating  $Ca^{2+}$  release from intracellular stores and targets enzymes like phospholipase C (PLC) (Surmeier and Kitai, 1994; Surmeier et al., 2007).

Dopamine differentially modulates the excitability of the striatal projection neurons by increasing the excitability of MSNs that project directly to the output layer of the basal ganglia (GPi/SNr) and decreasing the excitability of MSNs that project indirectly to these nuclei via GPe. This dichotomous effect is due to the differential expression of D1 and D2 receptors on direct and indirect MSNs respectively. Dopamine is therefore thought to bias the basal ganglia network towards selecting actions, by increasing the excitability of the direct pathway and decreasing the excitability of the indirect pathway. In addition, co-existence of multiple dopamine receptor subtypes has been identified in some MSNs suggesting that the dopamine modulation may sometimes be more complex than previously thought (Nicola et al., 2000; Bertran-Gonzalez et al., 2010). However, with the development of bacterial artificial chromosome (BAC) transgenic mice in which enhanced green fluorescent protein (eGFP) or Cre-recombinase are expressed under control of the D1 or D2 promoter, the segregation of D1 and D2 receptor expression in direct and indirect MSNs is further supported (Gertler et al., 2008; Valjent et al., 2009). This segregation of dopamine receptors is also present in the lamprey where we show that D1 receptors are expressed in direct pathway striatal projection neurons while D2 receptors are expressed in indirect pathway projection neurons (**Paper V**). In addition, subsequent application of dopamine receptor specific agonists preferentially activates one or the other receptor in the same neuron.

In mammals, birds and reptiles, D1 receptor activation preferentially enhances excitability at membrane potentials close to spike threshold and decrease it at hyperpolarized levels close to rest, whereas D2 receptor activation acts in the opposite direction by decreasing excitability (Hernandez-Lopez et al., 1997; Hernandez-Lopez et al., 2000; Ding and Perkel, 2002; Barral et al., 2010). These contrasting effects on excitability are due to a different modulation of voltage-gated channels. The low voltage activated (LVA) L-type  $Ca_v$  1.3  $Ca^{2+}$  channel has been suggested as the main mechanism underlying these excitability changes in mammals and reptiles (Levine et al., 1996; Hernandez-Lopez et al., 1997; Barral et al., 2010). These channels have similar voltage activation ranges as LVA T-type  $Ca_v$  3.1  $Ca^{2+}$  channels and activates around -60 mV with a maximum conductance around -30 mV (Lipscombe, 2002).

These activation ranges are in accordance with the level of voltage-dependence seen by dopamine modulation of excitability (Hernandez-Lopez et al., 1997; Surmeier et al., 2007). In lamprey striatal projection neurons, D1R activation excites neurons while D2R activation reduces neuronal spiking (**Paper IV and V**), presumably via LVA  $\text{Ca}^{2+}$  channels as in mammalian striatum and lamprey spinal neurons (Wang et al., 2011). Stimulation of both D1 and D2 receptors increases the inactivation of voltage gated  $\text{Na}^+$ -channels (Cepeda et al., 1995; Carr et al., 2003; Maurice et al., 2004) and affects potassium channels such as  $\text{K}_\text{ir}$  and A-type  $\text{K}^+$ -channels (Hernandez-Lopez et al., 1997; Ding and Perkel, 2002; Surmeier et al., 2007). It has recently been shown that D2 MSNs are more excitable than D1 MSNs in their naïve resting state, assessed by somatic current injections (Gertler et al., 2008). The dopaminergic modulation thus counterbalances these differences. This may be of importance for the dopaminergic modulation of up- and downstates in MSNs (Wilson and Kawaguchi, 1996) where D2 receptor signaling impedes the up-state transition, in indirect-pathway MSNs, whereas D1 receptor signaling promotes the transition from the downstate in direct-pathway MSNs (Grillner et al., 2005; Surmeier et al., 2007).

#### **1.4 CELLULAR BASIS OF MOTOR BEHAVIOUR IN LAMPREY AND OTHER NON-MAMMALIAN VERTEBRATES**

The detailed knowledge of spinal microcircuits in the lamprey has been paralleled with an increased understanding of the supraspinal control of CPGs (Dubuc et al., 2008; Grillner et al., 2008). Supraspinal activity initiates locomotion in response to internal cues and sensory inputs, such as light, pheromones or mechanical stimuli (Ullen et al., 1993; Derjean et al., 2010), that is relayed to reticulospinal (RS) neurons in the brainstem that constitute the main descending system (Dubuc et al., 1993; Di Prisco et al., 2000). Goal-directed locomotion is initiated by brain centers in the mesencephalon, diencephalon and forebrain that in turn activate the RS system. In the brainstem, several areas were identified early on by electrically stimulating specific regions and measuring the evoked movements (McClellan and Grillner, 1984). Within these brainstem regions, one important motor center is the mesencephalic locomotor region (MLR) that was characterized in detail by Dubuc and colleagues (Sirota et al., 2000). By electrical microstimulation of a small region in the caudal mesencephalon they elicited well-coordinated swimming with an intensity that was proportional to the stimulation strength. This is similar to the graded locomotor responses evoked in other vertebrates by stimulation of the MLR, such as in the cat where the MLR was first described by Orlovsky and colleagues (Shik and Orlovsky, 1976) where an increase in stimulation led to trotting and galloping from initial walking. Swimming in lamprey can also be elicited by a region in the ventral thalamus of the diencephalon called the diencephalic locomotor region (DLR) (El Manira et al., 1997; Menard and Grillner, 2008). The optic tectum/superior colliculus is another important motor center for visuomotor control and goal-directed behaviour. It has been studied for several decades in non-human primates, cats, rodents and many lower vertebrates (Jones et al., 2009; Isoda and Hikosaka, 2011). It receives retinotopic input from the retina and powerful GABAergic inhibition from the basal ganglia (Grillner et al., 2005; Stephenson-Jones et al., 2011). Stimulation of the optic tectum in lamprey elicits eye movements, orienting movements as well as swimming (Saitoh et al., 2007).

#### 1.4.1 The basal ganglia in lamprey

The MLR is known to be under tonic inhibition from the basal ganglia in vertebrates, shown by local injections of GABA antagonists that induce locomotion by disinhibition of the MLR and vice versa GABA agonists inhibit/pause movements (Garcia-Rill et al., 1985; Garcia-Rill et al., 1990). This was recently also shown in lamprey, where movements were inhibited/initiated by GABA agonists/antagonists locally administered into the MLR (Menard et al., 2007) and the DLR (Menard and Grillner, 2008). The lamprey tectum was also recently shown to receive GABAergic input from the forebrain (Robertson et al., 2006; de Arriba Mdel and Pombal, 2007). One of these nuclei is located in the diencephalon, ventrocaudal to the eminentia thalami just caudal to the medial pallidum, and the neurons in this area also send GABAergic projections to the MLR and DLR (Menard et al., 2007; Menard and Grillner, 2008). This nucleus has now been characterized as the dorsal pallidum in lamprey (Stephenson-Jones et al., 2011). GABAergic striatal neurons expressing substance P project directly to the pallidal output layer (GPi), whereas neurons expressing enkephaline project via nuclei homologous to the GPe and STN. The pallidal projection neurons (homologous to GPi neurons) are GABAergic and tonically active, inhibiting the tectum, MLR and DLR. Separate, but intermingled, pallidal neurons project to either the STN or tectum/MLR/DLR. The pallido-STN subpopulation receives input primarily from enkephaline-expressing striatal neurons whereas the pallido-motor center subpopulation is contacted by substance P-expressing striatal neurons. This shows that the dorsal pallidum is an intermingled GPi/GPe nucleus, which is also the case in the avian dorsal pallidum (Reiner et al., 1998). The dorsal pallidum study by Stephenson-Jones and colleagues is one of the first investigations in a series of studies that details the basal ganglia in the lamprey in recent years: striatal cellular properties (**Paper I-III**); the GPi, GPe and the STN (Stephenson-Jones et al., 2011); the direct and indirect pathway of the basal ganglia, including dopaminergic modulation of striatal projection neurons (**Paper IV and V**); the SNr and PPN (**Paper VI**); and the habenula-projecting dorsal pallidal (DPH) nucleus (Stephenson-Jones et al., 2012), showing that the detailed basal ganglia circuitry is present in the earliest vertebrates.

An SNr homolog was just identified in lamprey (**Paper VI**) while the homolog of the SNc has been known much longer and is located in the posterior tubercle (Pombal et al., 1997a; Thompson et al., 2008). The SNr is located in the mesencephalon and although this nucleus was not characterized in detail until recently, this area was known to contact the optic tectum (Robertson et al., 2006; de Arriba Mdel and Pombal, 2007) but was thought to be part of the lateral isthmus nuclei as they were presumed to be cholinergic cells (Pombal et al., 2001; de Arriba Mdel and Pombal, 2007). These neurons are now known to be GABAergic and are located just lateral to the previously described cholinergic neurons of isthmus region and MLR (Pombal et al., 2001; Le Ray et al., 2003). These GABAergic nigral neurons receive GABAergic striatal input from substance P expressing rectifying neurons, as expected from direct pathway neurons. They also receive afferents from the pallidum, STN and SNc and in turn project to tectum, thalamus, torus semicircularis, and pretectum but not to the MLR. In addition, they are reciprocally connected to the pedunculopontine nucleus (PPN) as described in detail for the first time in lamprey (**Paper VI**). The PPN is composed of two main groups of neurons, cholinergic and non-cholinergic (GABAergic, glutamatergic, dopaminergic) neurons that are intermingled with both ascending and descending projections (Lee et al., 2000; Mena-Segovia et al., 2009). It

has therefore been proposed that the descending neurons are part of the MLR (Skinner and Garcia-Rill, 1984; Le Ray et al., 2003; Menard et al., 2007; Le Ray et al., 2011). The region now characterized as a putative PPN in the lamprey has been recognized previously as a group of distributed cholinergic neurons in the lateral mesopontine tegmentum with characteristics of the PPN (Pombal et al., 2001; Le Ray et al., 2003). It is now shown to receive input from the dorsal pallidum and the habenula-projecting part of the dorsal pallidum (DPh), the STN and reciprocally with the SNR, while providing efferents to the striatum, DPh and SNc (**Paper VI**).

#### 1.4.2 The striatum in lamprey

The existence of a striatal region in the lamprey has been known for over a century (Johnston, 1902; Johnston, 1912). It was however not until recently that it was characterized anatomically and immunohistochemically in greater detail as a prominent band of several layers of packed cells close to the medial ventricle in the telencephalon (Pombal et al., 1997a, b). The lamprey striatum shows striking similarities to that of mammals with regard to organization of input structures and histochemical markers and the striatum is present in practically all vertebrates studied (lamprey, fish, amphibians, reptiles, birds and mammals) suggesting it is a highly conserved brain region (Reiner et al., 1998). Distinguishing characteristics of the striatum are a rich dopaminergic innervation from the SNc, the presence of acetylcholinesterase and cholinergic neurons, substance P and enkephaline neurons, a high percentage of GABAergic neurons and in addition glutamatergic afferents from the cortex/pallidum and thalamus as well as modulatory inputs of histamine, serotonin and noradrenaline (Reiner et al., 1998; Doya, 2002). Nozaki and Gorbman demonstrated that substance P (SP) was strongly expressed in and around the lamprey striatal cell band (Nozaki and Gorbman, 1986). This was confirmed by two other studies that showed scattered SP-positive neurons throughout the striatum and with a high density of cells in the dorsolateral part (Pombal et al., 1997b), and in a study by Dubuc and colleagues both substance P and additional tachykinin expressing cells were described (Auclair et al., 2004). Pombal et al also showed fibers immunoreactive to enkephaline (Enk) surrounding the striatal cell band. They did not discover any Enk-positive cells, which are difficult to immunostain also in rodents. It thus remained to be shown that both types of striatal neurons exist in the lamprey striatum and that they also project to possible pallidal and nigral structures. This has now been shown in (Stephenson-Jones et al., 2011) and **Paper VI**. Cells in the striatum have been shown in several studies to be GABAergic with a few weakly or unlabeled cells intermingled among the GABA-positive neurons (Pombal et al., 1997b; Robertson et al., 2007; Menard and Grillner, 2008). At least some of the unlabeled cells are most probably cholinergic interneurons, as a small number of neurons expressing choline acetyltransferase (ChAT) have been described (Pombal et al., 2001) and the rich innervation of acetylcholinesterase (AChE) in and around the striatal cell band (Pombal et al., 1997b), which is the region with the strongest AChE activity in the lamprey telencephalon (Wachtler, 1974) (**Paper II**). Pombal also showed that there are spiny neurons in the striatum but it was unknown if these neurons also corresponded to MSNs as no detailed physiological studies had yet been performed in the lamprey striatum (Pombal et al., 1997b). We show that the majority of lamprey striatal neurons are inwardly rectifying neurons (IRNs) characterized by two potassium conductances,  $K_{ir}$  and LVA A-type currents, that shape their current voltage responses and that at least



some of these neurons are spiny and thus share the hallmarks of MSNs (**Paper II**). There are also neurons lacking rectification that have fast-spiking interneuron properties and some also resemble cholinergic interneurons. The lamprey striatal microcircuit properties thus indicate that similar mechanisms as those of mammals may underlie gating and facilitation of specific actions.

#### 1.4.3 Striatal afferents

The striatum receives dopaminergic innervation from neurons located in the ventral diencephalon in the nucleus tuberculi posterior, homologous to the SNc/ventral tegmental area (VTA) in mammals (Pombal et al., 1997a). Dopamine and tyrosine hydroxylase (TH) immunoreactive fibers surround the striatal cell band (Pierre, 1994; Pombal et al., 1997a). We have now also showed with electron microscopy that TH-positive fibers form asymmetric synapses onto spine-like or stubby striatal dendritic processes, and that these are mainly located in the area lateral to the cell band (**Paper IV**). In addition to the demonstration of dopaminergic input, a partial D1-like receptor gene had also been cloned previously and shown to be expressed in a subpopulation of striatal neurons as well as in the olfactory bulbs, pretectal region and the periventricular hypothalamic organ (Vernier, 1997; Pombal MA, 2007). It was however not until recently that the detailed expression of D1 (**Paper V**) and D2 receptors (**Paper IV and V**) was shown, as described in chapter 1.3.2. Striatal cells have also been shown to express dopamine- and cAMP-regulated neuronal phosphoprotein (DARPP-32) and dopamine depletion with 1-methyl-4-phenyl-1,2,3,6-tetrahydropyridine (MPTP) renders the lamprey hypokinetic, as in Parkinson's, an effect that can be counteracted by dopamine agonists (Grillner et al., 2008; Thompson et al., 2008). Thus, the direct and indirect pathways exist also in lamprey, and loss of the striatal dopaminergic modulation leads to the same motor disturbances as those of mammals. It thus appears that with regard to nigrostriatal function, the role of the striatum and parts of the basal ganglia is conserved. Recent evidence has shown that a minor subpopulation of lamprey striatal cells co-express both dopamine and GABA (Barreiro-Iglesias et al., 2009) that may be similar to the recently identified mammalian dopaminergic/GABAergic striatal interneurons (Ibanez-Sandoval et al., 2010). Electrophysiologically, three of these four newly characterized neurons have very pronounced  $I_h$  currents, a characteristic property also of a subclass of lamprey striatal neurons (**Paper II**). In addition to dopamine, the striatum also receives a modulatory 5-HT input from the raphe nucleus in the caudal mesencephalon/rostral rhombencephalon (Brodin et al., 1990a; Pierre et al., 1992; Antri et al., 2006), a histaminergic input from the ventral hypothalamus (Brodin et al., 1990a) as well as galanin (Jimenez et al., 1996) and neurotensin input (Brodin et al., 1990b).

The largest striatal input arises from the lateral pallium (the homologue of the cortex) and the thalamus (Polenova and Vesselkin, 1993; Northcutt and Wicht, 1997; Pombal et al., 1997a). Large numbers of cells were also identified in the olfactory bulb (Pombal et al., 1997a) but recent findings have shown that the majority of these neurons were probably labeled from fibers of passage projecting to the posterior tubercle (Derjean et al., 2010) and **Paper III**. The LPal projects heavily to the striatum and is the largest recipient of olfactory projections (Northcutt and Wicht, 1997; Derjean et al., 2010). Recent findings have also shown that electrical stimulation of a restricted area in LPal is capable of evoking mouth- and eye movements, neck-

trunk bending or swimming movements (Ocaña FM, 2011). Tract tracing by injection of neurobiotin in the effective stimulation points showed that efferent projections were distributed in the striatum and to the optic tectum, STN and the DLR and MLR. This part of the LPal is the same area that contacts the striatum with facilitating synapses and with a low presynaptic release probability (**Paper III**). The lamprey thalamus receives a different input from that of the LPal, including direct retinal and tectal input (Vesselkin et al., 1980).

#### 1.4.4 Striatal efferents

As described previously, direct pathway rectifying striatal neurons express D1R, substance P and GABA and contact the SNr and the dorsal pallidum (GPi-homolog). Conversely, indirect pathway striatal neurons express D2R, enkephaline and GABA and contact the dorsal pallidum (GPe-homolog), in (**Paper II, IV-VI**) and Stephenson-Jones et al., 2011, see Fig. 2.

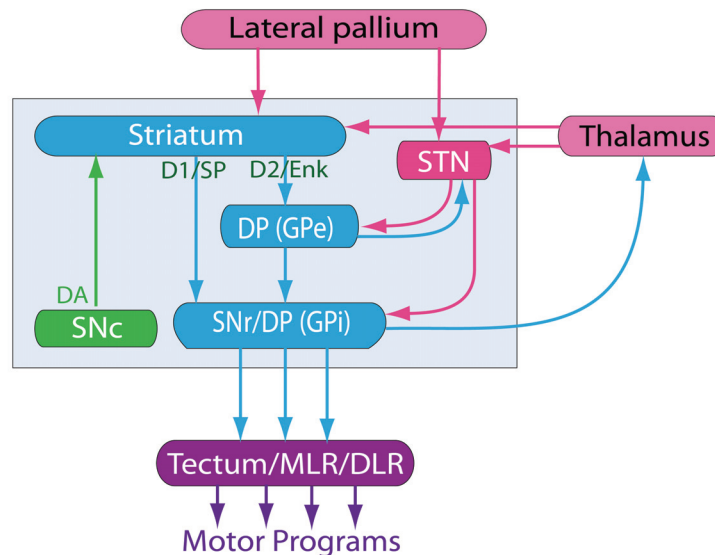


Figure 2. Schematic overview of the lamprey basal ganglia. Blue arrows represent GABAergic projections, red glutamatergic projections and in green the dopaminergic projection from the SNc homolog.

Leading up to these papers, it had been shown that the optic tectum, MLR and DLR receive input from GABAergic sources suspected to correspond to these basal ganglia output nuclei (Robertson et al., 2006; Menard et al., 2007; Menard and Grillner, 2008), especially the dorsal pallidum (Medina and Reiner, 1995; Grillner et al., 2008; Menard and Grillner, 2008). An important part was the demonstration that local injections of gabazine in the DLR and MLR facilitates or evokes locomotion (Menard et al., 2007; Menard and Grillner, 2008) and these motor command centers may thus be inhibited/disinhibited by striatal activity via the pallidum/SNr. It was also shown



directly that the striatum may facilitate movements, by electrically stimulating the striatum that evoked polysynaptic EPSPs in reticulospinal cells and induced locomotion, and that the DLR contributed to these responses (Menard and Grillner, 2008). These studies also showed that striatal GABAergic projection neurons project, in addition to pallidal projections, directly to the DLR and MLR. In addition, stimulation of specific parts of the tectum evokes eye, head and locomotor movements (Saitoh et al., 2007).

In the first detailed investigations of the striatum, striatal fibers were detected in the ventral LPal (vLPal) and this area was also shown to contain GABAergic neurons (Pombal et al., 1997b). Striatal neurons were also retrogradely labeled from the same area. Anterograde labeling of fibers from the vLPal demonstrated axonal projections to the DLR (Pombal et al., 1997b), and reciprocally the DLR received input from this area (El Manira et al., 1997) and it was therefore thought to possibly represent a basal ganglia output nucleus (Pombal et al., 1997b). Later studies also confirmed that there are GABAergic projection neurons in the vLPal that send axons to the DLR and MLR (Menard et al., 2007; Menard and Grillner, 2008). The vLPal does, however, not project to the tectum (Robertson et al., 2006), although a few vLPal neurons were retrogradely labeled from large tectal injections in a separate study (de Arriba Mdel and Pombal, 2007). It is still unclear if this represents a pallidal structure. Cells in this area actually provide input to the striatum (Pombal et al., 1997a), which is however also known to be the case for a subpopulation of GPe neurons but not GPi cells (Mallet et al., 2012). However, although the vLPal cells seem to be rather few the responses elicited by stimulation are glutamatergic, not GABAergic (**Paper III**). This rather indicates that this may be a pallial structure.

## 2 AIMS

The overall aim of this thesis has been to characterize the striatal microcircuit of the lamprey, to enhance our understanding of the basic cellular processes that underlie selection of actions.

The specific objectives are:

- To develop a method to study the detailed cellular and synaptic processes of lamprey striatal neurons.
- To characterize the different types of neurons in the striatum electrophysiologically, including projection neurons and putative interneurons.
- To study the synaptic transmission to the striatum from the pallium (cortex) and thalamus.
- To investigate if dopamine receptors are expressed in the striatum and how dopamine modulates neuronal activity.

### 3 METHODS

Detailed descriptions of the methods employed in this thesis are given in the individual papers. Some general aspects of the methodology are discussed below.

#### 3.1 THE *IN VITRO* SLICE PREPARATION

Acute lamprey *in vitro* brain slices were the main preparations used in this study, prepared from adult lampreys (*Lampetra Fluviatilis*). There are several advantages of this *in vitro* method compared to *in vivo* experiments, including direct access to neurons and even dendrites visible with differential interference contrast (DIC) microscopy, enhanced mechanical stability and the possibility of directly manipulating the aCSF and ease of applying different pharmacological agents. The slice maintains the local microcircuit and enables the possibility of multi-patch clamp recordings to study the neuronal communication between neighbouring cells and high quality recordings of cellular and synaptic function. The afferent and efferent connections are often cut off from their source of origin during slicing, but depending on the cutting angle the fibers can be preserved within the slice and hence be activated by for instance electrical stimulation. This was used in paper III of this thesis to study thalamic and pallial afferents that are conserved in a coronal slice of the lamprey brain at the level of the striatum. Although patch clamp recordings have been performed from lamprey CNS preparations before (Alford et al., 1995; Wikstrom et al., 1999; Brocard et al., 2005; Gariépy et al., 2012), the development of the lamprey slice preparation has enabled an additional method for detailed studies of cellular properties because of the advantages described.

#### 3.2 ELECTROPHYSIOLOGY

The development of the patch clamp technique has had a tremendous impact on the understanding of cellular and synaptic processes of neurons as it enables the detailed study of membrane properties, including the possibility of recording activity through single ion channels (Neher and Sakmann, 1976). The technique allows for several different recording configurations, such as whole-cell and cell-attached recordings, that all have their respective uses, advantages and disadvantages. We have mainly performed whole-cell patch clamp recordings in current clamp mode. This allows the experimenter the possibility of controlling the current going into and out of the cell while recording the voltage responses. It thus makes it possible to study specific properties of single neurons, such as discharge behaviour, the function of specific membrane channels and how they are activated/inactivated at certain voltages or by intracellular signals etc.

Whole-cell current clamp recording were used in all studies included in this thesis to study spontaneous and evoked synaptic input, to characterize different neurons based on their electrophysiological “fingerprint”, to study cellular effects of receptor activation (e.g. dopamine D1 receptors) and investigate the expression and function of specific channels by voltage activation/inactivation combined with application of pharmacological agents (e.g. LVA A-type K<sup>+</sup> channels). The striatum of rodents have been studied in detail with these methods and hence different neurons

have been classified according to their electrophysiological properties. MSNs, fast-spiking interneurons and other striatal neurons are easily identified by their differences in cellular properties by analyzing the current-voltage responses (see for instance Ibañez-Sandoval et al., 2010). We have adopted these established principles and classified lamprey striatal neurons based on several patch clamp protocols, including the voltage responses to 1 s long consecutive negative and positive current steps. These were adjusted for the input resistance of individual neurons and set so that recordings captured the cellular behaviour from around -100 mV to suprathreshold potentials. All recorded neurons were visualized under the microscope and patch electrodes were advanced onto cells by electrical micromanipulators before Giga-seal formation with the soma of identified neurons.

### **3.3 NEUROANATOMY AND IMAGING**

To visualize neurons after patch clamp experiments, neurons were filled with neurobiotin (0.2-0.5% w/v) intracellularly during recordings. Neurobiotin labels all processes of a neuron, such as the soma and dendrites and even spines and thin axons depending on how well the tracer has diffused into all these compartments. The tissue was fixed after recordings and processed for visualization either by brightfield microscopy or fluorescence and confocal microscopy. Confocal microscopy offered the advantage of higher resolution of the morphological properties and also to construct 3D-stacks of stained neurons. For these experiments we used avidin-conjugated fluorophores such as Cy-2 for binding with the biotin-stained tissue. One disadvantage of this method is the sometimes fairly rapid fading of fluorescence. We therefore sometimes instead visualized the neurobiotin stained neurons with a complex of avidin, biotin and horseradish peroxidase (ABC-kit) which was then incubated with 3,3'-Diaminobenzidine (DAB) for a permanent staining. For retro- and anterograde tracing experiments, injections were performed with neurobiotin (20% in distilled water) and/or Alexa fluor 488-dextran 10-kD (12%).

## 4 RESULTS AND DISCUSSION

The questions that have been addressed in this thesis are as follows:

### **Paper I**

In order to study the detailed cellular properties of striatal neurons, can an acute brain slice preparation of the lamprey telencephalon be developed that enables whole-cell patch clamp recordings?

### **Paper II**

Is the striatal microcircuit organized into different types of neurons with specific cellular properties such as inwardly rectifying potassium ( $K_{ir}$ ) channels?

### **Paper III**

How is the striatum activated from the thalamus and pallidum, the two principal glutamatergic inputs, and what are the characteristics of its synaptic dynamics?

### **Paper IV**

Where is the dopamine D2 receptor expressed in the telencephalon and how does its activation modulate striatal excitability?

### **Paper V**

Does dopamine differentially modulate the excitability of direct and indirect striatal projection neurons by activating segregated dopamine D1 and D2 receptors?

### **Paper VI**

Are dual output pathways of the basal ganglia conserved throughout evolution with the homolog of the substantia nigra pars reticulata present in the lamprey?

### **4.1 THE LAMPREY STRIATAL BRAIN SLICE PREPARATION (PAPER I)**

In order to study the detailed cellular and synaptic properties of the striatum, we first had to develop a preparation and method that enabled single-cell physiological recordings. A powerful approach to study the behaviour of single ion-channels and synaptic transmission of individual neurons is the patch-clamp technique in acute *in vitro* slice preparations. This technique is well established in rodent studies and a preferred *in vitro* method as it preserves much of microcircuitry while still providing direct control over the extracellular and intracellular environments and easy access to neurons. Patch recordings in slice preparations had however never been performed in lamprey. After adapting this method to lamprey tissue, we were able to produce viable slice preparations at the level of the striatum with healthy neurons. The small size of the lamprey brain, less compact brain tissue and the age of animals were all challenging to obtaining optimal cell recordings and this technique has been perfected over the course of this thesis.

Once the technique was established, we assessed the health of neurons by voltage- and current-clamp recordings to investigate basic cellular properties such as current responses to stepwise depolarizations, action potential properties and

spontaneous synaptic activity. The aim of this paper was thus to establish the slice preparation (Fig. 3) for single- and multielectrode patch clamp recordings to be used alone or with extracellular stimulation of afferents, retrograde tracing to target projection neurons, intracellular staining with neurobiotin followed by confocal, fluorescent and light microscopy.

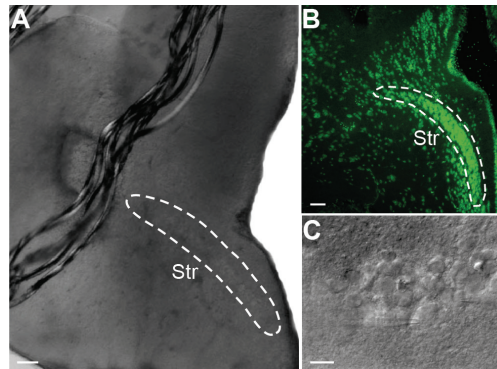


Figure 3. A, coronal brain slice showing the striatal cell band inside the white lines. B, fluorescent Nissl staining of a coronal section displaying the band of striatal cell bodies. C, photograph of individual striatal neurons in the recording chamber. Scale bars = 100 μm in A and B, 15 μm in C.

Although the cellular properties reported were mainly intended as an assessment of the health of neurons, one discovered property of some cells was occasional membrane potential oscillations. This finding was a first indication of the potential presence of  $K_{ir}$  in lamprey striatal neurons that have been well described in MSNs (Kawaguchi et al., 1989; Nisenbaum and Wilson, 1995; Wilson and Kawaguchi, 1996).  $K_{ir}$  channels are important properties as these channels are thought to underlie part of the cellular mechanisms that enable the striatum to function as a gating or selection structure for actions (Wilson and Kawaguchi, 1996; Grillner et al., 2005).

## 4.2 STRIATAL CELLULAR PROPERTIES CONSERVED FROM LAMPREYS TO MAMMALS (PAPER II)

As described in the introduction, the macroscopic structure of the lamprey striatum with its main input and output was known from immunohistochemical and tract tracing studies. However, nothing was known about the physiology of the lamprey striatum and its individual neurons, a prerequisite for understanding the basic operations of the striatal microcircuit and the mechanisms involved in selection of movements and control of locomotion. The aim of this study was to characterize the detailed cellular properties of individual lamprey striatal neurons, using the established patch clamp method in acute slices. Whole-cell current clamp recordings were used to study the voltage responses of neurons in response to current steps to record their electrophysiological "fingerprint" and activation/inactivation of specific voltage-gated conductances that shape supra- and subthreshold properties.

We showed that there are two main types of neurons; inwardly rectifying neurons (IRNs) characterized by a prominent rectification due to a  $K_{ir}$  type  $K^+$  conductance, and non-IRNs that represent a smaller and more heterogeneous group of neurons (Fig. 4). Pronounced inward rectification is a hallmark of MSNs in mammals

and differentiates these neurons from other striatal interneurons and is therefore of special interest (Kawaguchi et al., 1989; Grillner et al., 2005).

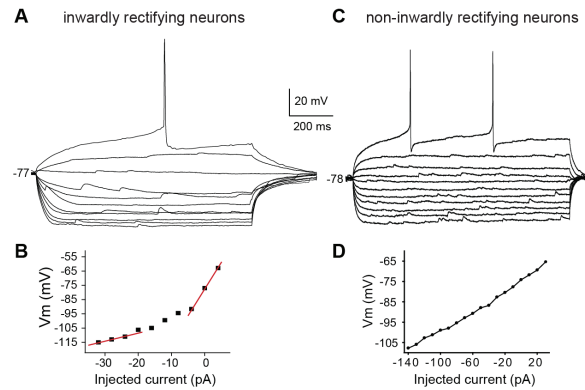


Figure 4. Inwardly rectifying neurons and non-inwardly rectifying neurons. A, Voltage responses of an inwardly rectifying neuron (IRN) with smaller responses at hyperpolarized potentials when  $K_{ir}$  channels are open and progressively larger responses at more depolarized potentials due to closing of these potassium channels. B, I-V plot of the steady-state voltage deflections in response to current steps of the IRN in A. C, similar voltage responses of a non-IRN without rectification, seen also in the close to linear relationship of the IV-plot in D.

Rectification was identified by lower input resistance/increased conductance at hyperpolarized potentials as  $K_{ir}$  channels are, in contrast to the majority of voltage-gated potassium channels, opened by hyperpolarization (Uchimura et al., 1989).  $K_{ir}$  channels were blocked by extracellular barium chloride (Fig. 5A) that significantly reduced the inward rectification and increased the responsiveness of neurons to stimulation due to a more electrotonically compact neuron with increased input resistance. Neuronal discharge was shaped by a low-voltage-activated  $K^+$  current,  $I_A$ , which resulted in a slower depolarization and thereby delayed the action potential onset. Some of the identified IRNs had spines that were detected on their distal dendrites. In addition to inward rectification, a third of the IRNs responded to hyperpolarization with a time- and voltage dependent depolarizing sag (Fig. 5B). This was characterized pharmacologically as the monovalent cation current  $I_h$ , also termed hyperpolarization-activated cyclic nucleotide-gated (HCN) channels (Harris and Constanti, 1995). A distinct voltage sag due to  $I_h$  is one of the distinguishing properties of large striatal cholinergic interneurons in mammals (Bennett et al., 2000; Wilson, 2005) that are required for spontaneous firing. Many of these cells had broad action potentials with large and slow AHPs and responded to hyperpolarization by post-inhibitory rebound spiking. The behaviour of these cells was clearly different from another identified subpopulations of cells characterized by narrow action potentials and fast AHPs with high spiking frequencies and low spike frequency adaptation, similar to the mammalian parvalbumin-expressing fast spiking interneurons.

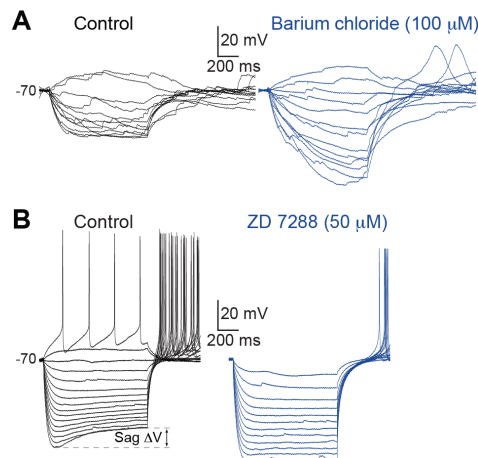


Figure 5. Pharmacological analyses of  $K_{ir}$  and  $I_h$  in IRNs. A, Voltage responses of an IRN before (left) and during bath application of barium chloride (right, blue) that blocks  $K_{ir}$  channels. B, The left voltage traces shows an IRN that also displays an  $I_h$ -induced sag (see Sag  $\Delta V$ ), followed by a post-inhibitory rebound with action potentials at the end of the hyperpolarising current steps. Under control conditions (black traces) the  $I_h$  sag is seen clearly at hyperpolarised levels while bath application of the  $I_h$  antagonist ZD 7288 almost completely removes the sag (blue traces).

The results thus showed that the striatal microcircuit is composed of different cell types. The majority of cells had hyperpolarized resting membrane potentials and also actively resisted depolarization by two types of potassium channels active at subthreshold potentials. These properties are in support of the mechanisms thought to underlie the striatal involvement in action selection. These neurons are silent at rest and partly clamped at negative potentials and thus need synchronized excitatory input to depolarize them closer to threshold, and in addition, the delayed action potential discharge may also be a mechanism to integrate input from several sources over a persistent time period.

#### 4.3 EVOLUTIONARILY CONSERVED DIFFERENCES IN PALLIAL AND THALAMIC SHORT-TERM SYNAPTIC PLASTICITY IN STRIATUM (PAPER III)

Recent studies have shown that the striatum and the basal ganglia are to a remarkable degree conserved throughout the vertebrate phylum, but the characteristics of the synaptic input to the striatum was unknown. As the basic organization of the neural machinery for action selection is present in the lamprey, it is essential to understand how the striatum is activated. We therefore went on to characterize the pharmacology and synaptic dynamics from the lateral pallium and thalamus, representing the main excitatory input to the striatum.

We first mapped out the exact location of thalamo- and palliostriatal afferents in the established coronal slice preparation. These fibers were shown to contact the striatum through topographically separate fiber bundles, indicating that their synaptic contacts onto striatal cells may be investigated separately. Extracellular stimulation of lateral pallial fibers evoked glutamatergic synaptic responses that activated both NMDA and AMPA receptors (Fig. 6A-C). The glutamatergic drive also recruited activity-dependent disynaptic GABAergic input, shown by evoking a train of



depolarizing synaptic potentials that resulted in a delayed GABAergic response (Fig. 6D). The GABAergic inhibition most likely originates from within the intrastriatal network that is densely populated with GABAergic neurons (Robertson et al., 2007).

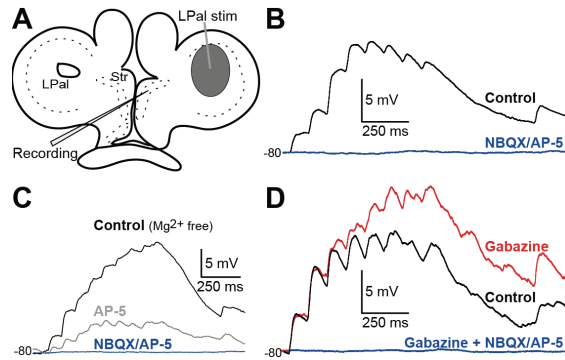


Figure 6. Lateral palliostriatal stimulation evokes glutamatergic synaptic responses.

A, Schematic drawing indicating the stimulation area in LPal. B, Current clamp recordings of striatal PSPs in regular aCSF evoked by LPal stimulation (artefacts removed), before (black trace) and after application of NBQX (40  $\mu$ M) and AP-5 (50  $\mu$ M, blue trace). C, NMDA and AMPA receptors were investigated in  $Mg^{2+}$ -free aCSF by current clamp recordings of striatal PSPs evoked by LPal stimulation before (black trace) and after sequential application AP-5 (grey trace) and both AP-5 and NBQX (blue trace) around -80 mV. D, Application of gabazine (20  $\mu$ M, red trace) increased responses in recorded neurons (rest Vm -80 mV) indicative of disynaptic inhibition. Responses were completely removed by further application of NBQX and AP-5 (blue trace).

Similarly, stimulation of thalamic afferents showed that also this direct synaptic transmission is glutamatergic that acts via both NMDA and AMPA receptors and upon repeated activation a disynaptic GABAergic signal was recruited (Fig 7).

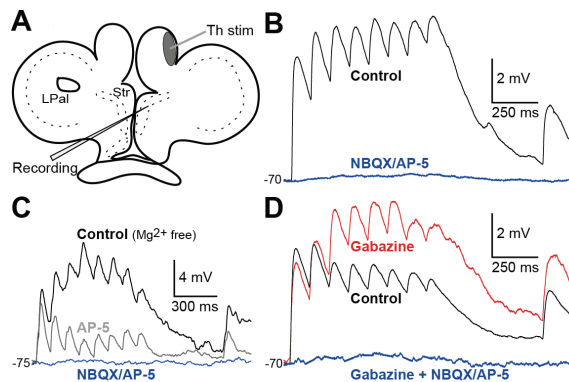


Figure 7. Thalamostriatal synaptic responses are glutamatergic.

A, Schematic drawing indicating stimulation area of thalamic fibers in the most lateral region of the medial pallium. B, Striatal PSPs in regular aCSF in response to stimulation of thalamic fibers (black trace) and application of NBQX (40  $\mu$ M) and AP-5 (50  $\mu$ M), that completely removed all responses (blue trace). C, NMDA and AMPA receptors were investigated in  $Mg^{2+}$ -free aCSF by current clamp recordings of striatal PSPs in response to stimulation of thalamic fibers (black trace) and after sequential application

of AP-5 (grey trace) and both AP-5 and NBQX (blue trace) around -75 mV. D, Application of gabazine (20  $\mu$ M, red trace) increased responses in recorded neurons (rest  $V_m$  -70 mV), indicative of disinaptic inhibition. Responses were completely removed by further application of NBQX and AP-5 (blue trace).

We next investigated the short-term activity-dependent synaptic plasticity from the lateral pallium and thalamus. Patch-clamp recordings were combined with presynaptic stimulus trains at 10 Hz. Synaptic responses from the LPal were facilitatory for the first several hundred milliseconds with clear paired-pulse facilitation, effectively summing sustained input and driving the cell towards threshold (Fig. 8, red traces). Thalamic input had directly opposite effects with an often large first response and smaller second response and with continued strong synaptic depression over the entire pulse train (Fig. 8, black traces). Responses thus quickly reached a plateau, while pallial input fully recovered after few hundred milliseconds the thalamic synaptic responses were still depressed. The paired-pulse and recovery test responses both indicated a difference in presynaptic release properties, which was confirmed by performing the same experiment in altered extracellular calcium concentrations. By lowering the  $Ca^{2+}$  concentration pallial synaptic facilitation was increased and thalamic depression reduced, in agreement with different presynaptic release probabilities underlying the difference in short-term synaptic plasticity.

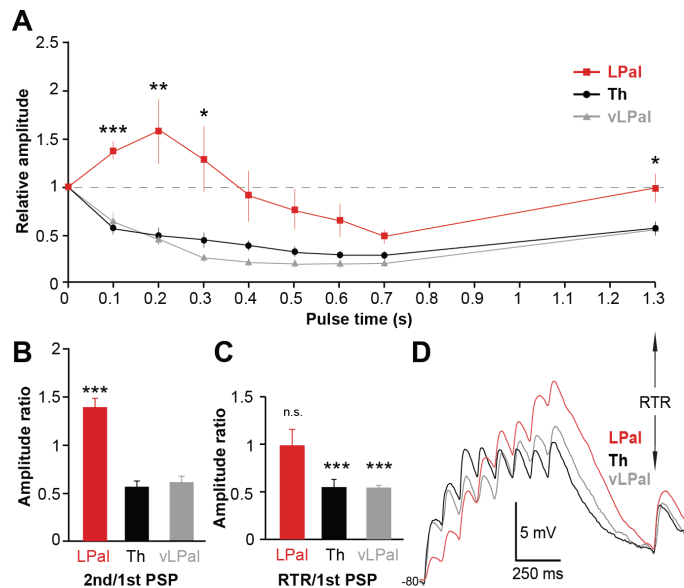


Figure 8. Lateral palliostriatal and thalamostriatal synapses have different dynamics.

A, Normalised postsynaptic responses to stimulations in LPal (red squares), vLPal (grey triangles) and thalamus (th, black circles) including the normalised recovery test response (RTR) 600 ms after the 8th pulse in the stimulus train. B, Comparison of the paired-pulse ratio of the second PSP to the first PSP in response to stimulations of fibers from the thalamus, LPal and vLPal. C, Comparisons of the recovery test response of LPal, vLPal and thalamic stimulation. D, Postsynaptic response patterns in the same neuron to LPal (red), vLPal (grey) and thalamic (black) stimulations.

The results thus show dramatic differences in the way that the striatum is activated from either the LPal or the thalamus. The facilitatory synaptic dynamics from LPal ensure that persistent afferent input is effectively summated, presumably together with the previously described intrinsic properties supporting this integrative behaviour, and drives the cell towards discharge only after receiving long enough input. Conversely, the activation of the thalamostriatal pathway indicate that precisely timed, coincident thalamic inputs will evoke immediate discharge but then rapidly become depressed and thus only activate an initial burst of striatal activity rather than prolonged firing. As these synaptic differences have recently also been characterized in the mammalian striatum (Ding et al., 2008), it strongly suggests that these are fundamental components of the vertebrate mechanisms for action/selection.

#### **4.4 THE DOPAMINE D2 RECEPTOR GENE IN LAMPREY, ITS EXPRESSION IN THE STRIATUM AND CELLULAR EFFECTS OF D2 RECEPTOR ACTIVATION (PAPER IV)**

At this stage, we thus had a fairly good understanding of the macroscopic connections and flow of information through the striatum and downstream pallidal structures. However, with regard to the main modulatory striatal input, dopamine, little was known about the expression of specific dopamine receptors and its cellular effects upon activation. We therefore investigated if dopamine D2 receptors (D2R), one of the functionally different classes of dopamine receptors, are expressed in striatal neurons and their potential role by using sequence analysis, *in situ* hybridization, electron microscopy and patch clamp recordings. A cDNA encoding the dopamine D2 receptor in the lamprey brain was identified, and it was shown that its amino acid sequence showed close relationship with other vertebrate D2 receptors.

Distinct D2 receptor mRNA expression was detected in a subpopulation of striatal neurons where also tyrosine hydroxylase-immunoreactive synaptic terminals were identified. The D2R expressing neurons were located throughout the striatal cell band and intermingled among non-expressing cells. As described in the introduction, D2Rs are expressed by MSNs of the indirect pathway in mammals. However, as the lamprey pallidum is a mixed GPe/GPi nuclei it is not possible to retrogradely label striatal neurons from this area to stain solely indirectly projecting striatal neurons. Instead, we retrogradely labeled neurons from the SNr and showed that these neurons never co-localized with the D2R expression, thus demonstrating they are not expressed on direct pathway striatal neurons. These results thus support the hypothesis that D2 receptors are expressed by indirect pathway neurons.

To investigate the effects of D2 receptor activation on lamprey striatal neurons and show that these receptors are functional, we applied the selective D2 agonist TNPA during whole cell current-clamp recordings. D2R reduced discharge, diminished post-inhibitory rebound spikes and also affected the size and shape of action potentials. Our findings indicate that a negative modulation of the L-type  $\text{Ca}_v 1.3 \text{ Ca}^{2+}$  channel by D2R activation may be a key mechanism underlying the change in excitability, which is consistent with results from both lamprey spinal neurons (Wang et al., 2011) mammalian striatal projection neurons (Hernandez-Lopez et al., 2000; Olson et al., 2005).

We conclude that functional dopamine D2 receptors are present in the lamprey striatum and that the resemblances in gene structure between different vertebrate D2 receptors show that its function is a conserved feature.

#### **4.5 DOPAMINE DIFFERENTIALLY MODULATES THE EXCITABILITY OF STRIATAL NEURONS OF THE DIRECT AND INDIRECT PATHWAYS IN LAMPREY (PAPER V)**

We thus knew from the previous study that D2 receptors were expressed in a subpopulation of striatal neurons, intermingled among non-D2R-expressing neurons, that could thus potentially be D1R expressing neurons, as a dopamine D1 gene had previously been identified in lamprey (Vernier, 1997; Pombal MA, 2007). We did however not know if the direct and indirect pathway with D1 and D2 receptor expression, respectively, existed also in lamprey. These pathways are key to the current understanding and working hypotheses of the function of the basal ganglia and its involvement in action selection (DeLong, 1990). The aim of this study was therefore to further investigate the mechanisms by which dopamine affects movements, by determining how dopamine modulates the striatal projection neurons of the direct and indirect pathways.

To investigate if neurons of the direct pathway preferentially express dopamine D1 receptors (D1Rs), we retrogradely labeled striatal neurons from the SNr and showed that the majority co-localized with the *in situ* hybridization signal for the D1 receptor (Fig. 9A-D). In contrast very few of the retrogradely labeled neurons co-localize with the *in situ* hybridization signal for the D2 receptor (Fig. 9E-G). To investigate how dopamine modulates striatonigral excitability, we subsequently applied D1- and D2 receptor agonists in patch-clamp experiments. Application of the D1 agonist SKF 81297 excited neurons with increased neuronal firing while the D2 agonist TNPA had no effect (Fig. 9I-K). The results thus show that striatal neurons that project directly to the output nuclei of the basal ganglia selectively express dopamine D1 receptors. When these receptors are activated they increase the excitability of these neurons. This may thus facilitate the promotion of actions by disinhibition of the tectum, MLR and DLR, by inhibiting the SNr/GPi that reduce/pause their tonic inhibition of these motor centers.

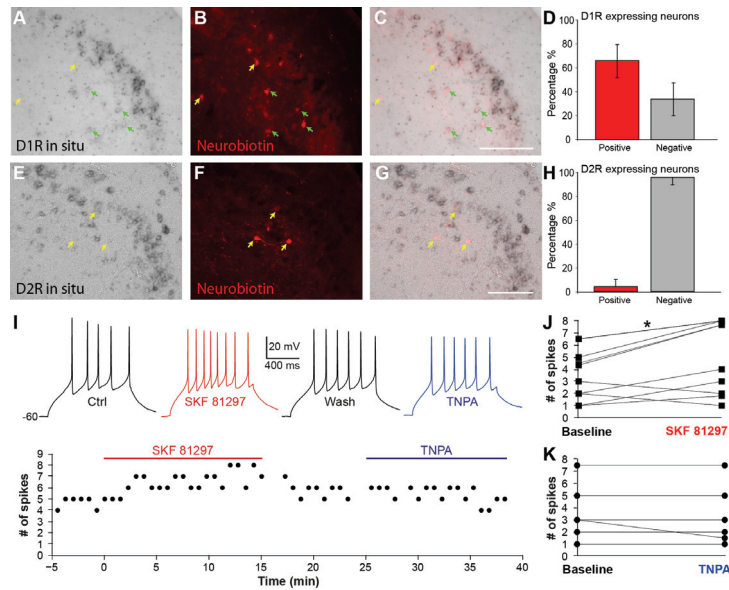


Figure 9. Striatonigral neurons express functional D1 receptors that excite neurons

A, D1 receptor riboprobe expressed in a subpopulation of striatal neurons. Yellow arrows indicate neurons that are retrograde labeled from the SNr but do not express D1 receptor mRNA. Green arrows indicate neurons that are retrograde labeled and express D1 receptor mRNA. B, Striatal neurons retrogradely labeled after injections of neurobiotin into the SNr. C, Merged image showing the overlap between retrograde labeled cells and D1 receptor mRNA. D, Quantification showing the percentage of retrogradely labeled neurons that express D1 receptor mRNA. E, D2 receptor riboprobe expressed in a subpopulation of striatal neurons. Yellow arrows, retrogradely labeled neurons that do not express D2 receptor mRNA. Green arrows, retrogradely labeled neurons that express D2 receptor mRNA. F, Striatal neurons retrogradely labeled from the SNr. G, Merged image showing the lack of overlap between retrogradely labeled cells and D2 receptor mRNA. H, Quantification showing the percentage of retrograde labeled neurons that express D2 receptor mRNA. I, Evoked action potentials in a striatonigral neuron during subsequent application of 10  $\mu$ M of SKF 81297 (red, second trace and bar below) and 100  $\mu$ M of TNPA (blue, last trace and bar below) shown in a corresponding plot of time and the number of spikes evoked by the same near rheobase current step. This neuron only responded to application of SKF 81297, which increased spiking seen in the plot, whereas TNPA had no effect on the number of evoked spikes. J, Application of SKF 81297 enhanced evoked spiking in striatonigral neurons, and all, but one, tested neurons were unresponsive to subsequent application of TNPA (I). Scale bars = 200  $\mu$ M.

To investigate if dopamine D1 and D2 receptors are segregated and expressed in the two different pathways of the intermingled dorsal pallidum, striatal neurons were retrogradely labeled together with *in situ* hybridization for either the D1 or D2 receptor. In line with a segregation of these receptors, just less than half of the retrogradely labeled neurons co-localized with the signal for the D2 receptor. Similarly, when the same experiment was performed to investigate the D1 receptor expression, around 50% of neurons were labeled by the D1R riboprobe. The results thus suggested that neurons of both the direct and indirect pathway project to the dorsal pallidum. From the distribution of receptor expression we hypothesized that neurons either expressed one or the other receptor and to test this functionally, we patched

retrogradely labeled neurons and applied D1 and D2 agonists in subsequent order to the same neurons. The results showed that neurons responded to either the D1 or D2 agonist by changes in excitability, but not to both agonists. The data thus suggest that the dopamine receptors are not co-localized in the same neuron. One subpopulation of striatopallidal neurons preferentially expresses D2 receptors that suppress discharge upon activation. These neurons are thus presumably part of the indirect pathway that preferentially targets the GPe-like neurons in the dorsal pallidum. Conversely, another subpopulation preferentially expresses D1 receptors that excite neurons and is presumed to project to GPi-like neurons of the dorsal pallidum.

The detailed analysis of the dopaminergic effects on cellular properties showed that D1R modulation of excitability is voltage-dependent but not the D2R modulation. The results also show a distinct separation of enhancing (D1-activation) or reducing (D2-activation) post inhibitory rebound-spiking in the subset of striatal neurons capable of producing such action potentials, further indicating LVA  $Ca^{2+}$ -channels as part of the downstream mechanisms modulated by dopamine signaling in striatal neurons.

Our results suggest that the dichotomous effect of dopamine on direct and indirect pathways has been conserved throughout the vertebrate phylum, likely as a mechanism to bias the network towards action selection. Taken together, our results support the classical action selection hypothesis where dopamine plays a fundamental role in facilitating or inhibiting the promotion of actions by modulating the excitability of striatal projection neurons. It still remains to be shown how dopamine modulates the synaptic input to the striatum, but considering the effects on cellular properties it seems likely that dopamine may also enhance or reduce synaptic release and synaptic dynamics via pre- and or postsynaptic receptors.

#### **4.6 EVOLUTION OF THE BASAL GANGLIA; DUAL OUTPUT PATHWAYS CONSERVED THROUGHOUT VERTEBRATE PHYLOGENY (PAPER VI)**

In this last study we examined the output structures of the basal ganglia in further detail. At this stage we had shown, prior to this investigation, that the basal ganglia, including the striatum, GPi/GPe, STN and SNc, are conserved throughout evolution. Here we aimed to determine if also the substantia nigra pars reticulata (SNr) and the pedunculopontine nucleus (PPN) are present in lamprey.

With tract tracing and immunohistochemistry, we show that an area homologous to the SNr is located in the caudal mesencephalon, receiving direct projections from inwardly rectifying GABAergic striatal neurons expressing substance P as expected by direct pathway neurons. The GABAergic SNr projection neurons in turn project to the thalamus and optic tectum. The SNr neurons are tonically active and can be silenced by GABA receptor activation, as expected by a basal ganglia output nucleus. The SNr is also contacted by the previously described STN and the intermingled dorsal pallidum, as well as from the homologue of the SNc (the posterior tubercle) and the putative PPN. The PPN contains cholinergic neurons and is located just ventromedial to the SNr in the mesencephalon. This entire region was previously considered part of the MLR (Skinner and Garcia-Rill, 1984; Menard et al., 2007) although a putative PPN has been reported (Pombal et al., 2001; Le Ray et al., 2003). Retrograde labeling showed that it receives input from the habenula-projecting dorsal pallidum (DPh), the dorsal pallidum, the STN and potentially also from the SNr and

optic tectum. It also sends fibers to most areas of the basal ganglia, including the striatum, STN, SNc and optic tectum.

These results suggest that dual output nuclei (SNr/GPi) are part of the ancestral basal ganglia and that the PPN appears to have co-evolved as part of a mechanism for action selection common to all vertebrates. Separate groups of cholinergic neurons provide ascending projections to the basal ganglia and descending neurons that correspond to the MLR.

## 5 CONCLUDING REMARKS

The main findings of this thesis are that similar cellular properties characterize striatal circuits in vertebrates, from lampreys to mammals. This suggests that the mechanisms that govern the selection of specific movements are shared by all vertebrates.

The inwardly rectifying GABAergic projection neurons are silent at rest and kept at hyperpolarized potentials due to their  $K_{ir}$  conductances. This is a key property of the striatum and its potential filter function in action selection, as it has a high threshold for activation and needs strong excitatory input to discharge (Surmeier et al., 2007). This excitation is provided by the pallium and thalamus in functionally distinct inputs to the striatum via both NMDA and AMPA receptors. The fact that corticostriatal synapses are facilitating, but that thalamostriatal synapses are depressing in both lamprey and mammals strongly suggest that this difference is a fundamental component of the vertebrate mechanisms for action/selection (Ding et al., 2008). These results strengthen the view of the corticostriatal signaling, where persistent and coherent cortical input mediates the transition from the stable and silent, hyperpolarized resting potential to an upstate where  $K_{ir}$  channels are inactivated and neuronal discharge is easily evoked (Grillner et al., 2005). The facilitating nature of the synapses ensures that persistent temporal input is effectively integrated and drives the neuron towards discharge. The distinct difference of the thalamostriatal synapses instead indicate that precisely timed bursts of input will be effectively translated into striatal discharge whereas tonic input would be quickly depressed and have little influence over striatal output.

The dopaminergic modulation is tightly coupled to the cortico- and thalamostriatal signaling in mammals where dopamine may facilitate or inhibit the transition from rest to discharge depending on the specific receptor activation (Surmeier et al., 2011). We demonstrate that the mechanism by which dopamine modulates the activity of striatal projection neurons is conserved across the vertebrate phylum. The striatal neurons that project directly to the basal ganglia output nuclei express dopamine D1 receptors, while separate populations that project to the dorsal pallidum, the homolog of the GPi/GPe, express either dopamine D1 or D2 receptors. Furthermore, activation of these dopamine receptors leads to an increase in the excitability of D1 expressing neurons and a decrease in the excitability of D2 expressing neurons. Together these results suggest that the dichotomous effect of dopamine on the direct and indirect pathways was present already in lamprey, likely as a mechanism to bias the network towards action selection. In addition, D1 receptors co-localize with substance P expressed by the directly projecting striatal neurons. Conversely, D2 receptors are expressed by the indirectly projecting neurons and are therefore likely to also express enkephaline.

Our results thus provide evidence in favour of the basal ganglia model by which actions are promoted via the direct pathway and inhibited via the indirect pathway. Together with colleagues in the field, we have shown not just that all nuclei of the basal ganglia were present already at the dawn of vertebrate evolution, but that the signaling through the pallium/thalamus-basal ganglia-motor center-spinal cord activation shares the same basic principles of promotion/inhibition of different motion processes.



For future perspectives, there are several interesting questions that need to be addressed to fully understand the mechanisms governing the signaling through the striatum. First, we have indicated that LVA  $\text{Ca}^{2+}$  channels may be one of the key cellular mechanisms that are modulated downstream of dopamine receptor activation. This should be characterized in detail by pharmacological agents. The lamprey striatum offers a unique opportunity in that a subpopulation of IRNs are capable of producing post-inhibitory rebound (PIR) spikes that are positively (D1R) and negatively (D2R) modulated by dopamine. The PIR spikes are thus an easy “readout” of downstream effects of dopamine that, together with specific calcium channel blockers, can provide a better understanding of the neural mechanisms modulated by dopamine.

It is also important to understand the complete microcircuitry and its morphological properties. What interneurons exist? Our electrophysiological data clearly suggest the presence of fast-spiking interneurons, but also cholinergic cells and possibly even LTS/PLTS neurons. The role of the strong  $I_h$  current, often coupled to substantial PIR discharge, seen in some neurons should also be addressed. Many of these cells show resemblance to the newly identified mammalian tyrosine hydroxylase-expressing GABAergic neurons (Ibanez-Sandoval et al., 2010). However, regardless if they are analogous to these neurons or not, the fact that more and more neuronal subtypes of striatal cells are being identified in mammals shows how complex this microcircuitry is. The lamprey striatum can thus serve as an important model to understand the basic striatal circuitry needed for action selection, in the same way as this odd creature has provided ground breaking insights of the central pattern generators of the spinal cord.

## 6 ACKNOWLEDGEMENTS

This thesis is the result of a passion for curiosity and a roller coaster ride of new findings, challenging experiments and a collaborative effort together with great colleagues and friends.

First and foremost, I want to thank my team of supervisors without whom this work would have never been done.

- **Sten Grillner**, I see you. And you amaze me. With your passion for science. Your generosity. A never-ending drive and extreme knowledge of details on all levels. You embody the quest “from gene to behaviour”. I humbly thank you for your encouragement and guidance. And, importantly, for allowing me to follow my personalized entrepreneurial scientific journey. The quest has just begun!

- **Gilad Silberberg**, you came in at a critical period and are truly part of the fact that this thesis exists. Brilliant experimentalist. And microcircuit expert superior. I am utterly grateful for your help, tips and patience. And for being young at heart. And empathic. Someday I will also comeback and master you in ping-pong.

- **Martin Wikström**, for believing in me early on and pushing a possibility into reality. And, very important, for following your own passion. Different paths, similar dreams.

- **Jeanette Hellgren Koteleski**, for your support and guidance early on.

- **Brita Robertson**, for all your guidance and help. For always having time. For also being young at heart. Vibratome. Yes!

My research education has been paralleled by entrepreneurial courses, initiatives and ventures of strong interest and importance to me. In this, several people should be acknowledged but none more than super facilitator and positive hurricane Carl Johan:

- **Carl-Johan Sundberg**! You embody energy and generosity. Apart from family, no single person has boosted my opportunities like you. Just by being you. I thank you by translating learnings into action for the better of mankind. You saw me like few others and empowered me from day one. THANK YOU.

- **Otto Skolling and Jörgen Thorball**, for your passion in building a better future for life. For building me. For making BiotechBuilders my platform. For being genuine. Together with CJS, your importance for global biotech cannot be overstated.

- **Micke Nygård**, for everything. The early phase, the decider. The discussions.

Friendship de lux. Science of course, but most importantly, for true honesty and goodness that is touchable. It has just begun, yes yes yes.

- **Marcus and Andreas**, two great scientists in their early blossoming. You made it real. And together we created new knowledge. Pretty cool. Never stop your quests by following your own paths. Beer is science and science without beer is unthinkable.

- **Ebba**. I believe I saw you. Truly. In the end. Too late for me. Much too early for you. This thesis is partly for you Ebba.

- **Henrike, Susanne, Ramon, Elham, Isaac, Carolina, Kostas and Stylianos** for so many fun times and sharing this journey.

- **Paul Bolam, Icnelia Huerta-Ocampo, Juan Pérez-Fernández and Rochellys Diaz-Heijtj** for valuable collaborations and scientific discussions.

- **Mikael Berglund, Therese Högfeldt and Jessica Norrbom** and the **Biotech Builders committee**, for a life of opportunities. We worked too hard, but had fun fun fun and it was extremely rewarding. Less suits and ever more creative entrepreneurial spirit rules.
- **Sanna, Hanna, Lena, Charlotta, Danielle, Paulina and Bosse** – for showing all is possible and that internal structure is not the decider for true value. We live, we build.
  
- to what must now be described as the early phase heroes. To **Jenny and Mimi**. For all, especially those late nighters.
- **Seth, Zoltan, Olle, Fredrik, Evanthea, Arianne, Di, Anders, Stefan, Isaac** and late phase **Andreas Fahlström!**
- **Ida**. You are superduper. Just so. For making science known in the real world.
- **Dave**. You are meant to create new knowledge. Let the system work with you, the world deserves your findings. You are utterly unique. Smartness and punk in a new life form. Don't you dare not pushing the borders of wisdom for life. To **Sabs** – you too, unique!
  
- **Peter W and Russ**, for all your help with techniques and good discussions.
- **Iris, Tommy and Lasse**. For endless help. And. Much laughter. Again, young at heart.
  
- **Mia Lindskog**, for being a true inspiration. Honest, good superstars always prevail long-term. Go Tiger, Go!
  
- **Tom Davidson**, for bringing new dimensions during this journey. You build futures!
  
- **P2M** for being you. The same goes for **Abdel El-Manira, Ole Kiehn and Ola Hermansson**. For scientific, political and art discussions. And to **Tomas Hökfelt**, for an inspiring passion for science.
  
- to the inner circle – **Erik O, Adam, Calle, Lars, DV, Daniel D, Cribba, Mange, Mangemange, Danne S, Reite, Jocke, Fredde J, Jess, Sara, Kajsa, Carro, Perra, Erik L, Inca, Tom, Kakan**
  
- to my **SUPER FAMILY** and **extended family**. For being real and for always being there. For being perfectly imperfect. Titles could not mean less to us. True value, not facades. THANK U.
  
- to **Hanna Yeah Yeah Yeah**. For life. You are my rock n roll. Every day. Always and forever. For endless support, ultra positive energy and patience with the all-in man of your life. I literally wake up with a smile every day. Every day. No science. Just pure, honest, happiness. Jehafools!

## 7 REFERENCES

- Albin RL, Young AB, Penney JB (1989) The functional anatomy of basal ganglia disorders. *Trends Neurosci* 12:366-375.
- Alexander GE, Crutcher MD (1990) Functional architecture of basal ganglia circuits: neural substrates of parallel processing. *Trends Neurosci* 13:266-271.
- Alford S, Zompa I, Dubuc R (1995) Long-term potentiation of glutamatergic pathways in the lamprey brainstem. *J Neurosci* 15:7528-7538.
- Antri M, Cyr A, Auclair F, Dubuc R (2006) Ontogeny of 5-HT neurons in the brainstem of the lamprey, *Petromyzon marinus*. *J Comp Neurol* 495:788-800.
- Aston-Jones G, Bloom FE (1981) Activity of norepinephrine-containing locus coeruleus neurons in behaving rats anticipates fluctuations in the sleep-waking cycle. *J Neurosci* 1:876-886.
- Auclair F, Lund JP, Dubuc R (2004) Immunohistochemical distribution of tachykinins in the CNS of the lamprey *Petromyzon marinus*. *J Comp Neurol* 479:328-346.
- Barral J, Galarraga E, Tapia D, Flores-Barrera E, Reyes A, Bargas J (2010) Dopaminergic Modulation of Spiny Neurons in the Turtle Striatum. *Cell Mol Neurobiol*.
- Barreiro-Iglesias A, Villar-Cervino V, Anadon R, Rodicio MC (2009) Dopamine and gamma-aminobutyric acid are colocalized in restricted groups of neurons in the sea lamprey brain: insights into the early evolution of neurotransmitter colocalization in vertebrates. *J Anat* 215:601-610.
- Bennett BD, Callaway JC, Wilson CJ (2000) Intrinsic membrane properties underlying spontaneous tonic firing in neostriatal cholinergic interneurons. *J Neurosci* 20:8493-8503.
- Bertran-Gonzalez J, Herve D, Girault JA, Valjent E (2010) What is the Degree of Segregation between Striatonigral and Striatopallidal Projections? *Front Neuroanat* 4.
- Bevan MD, Booth PA, Eaton SA, Bolam JP (1998) Selective innervation of neostriatal interneurons by a subclass of neuron in the globus pallidus of the rat. *J Neurosci* 18:9438-9452.
- Bolam JP, Wainer BH, Smith AD (1984) Characterization of cholinergic neurons in the rat neostriatum. A combination of choline acetyltransferase immunocytochemistry, Golgi-impregnation and electron microscopy. *Neuroscience* 12:711-718.
- Bolam JP, Hanley JJ, Booth PA, Bevan MD (2000) Synaptic organisation of the basal ganglia. *J Anat* 196 ( Pt 4):527-542.
- Bracci E, Centonze D, Bernardi G, Calabresi P (2002) Dopamine excites fast-spiking interneurons in the striatum. *J Neurophysiol* 87:2190-2194.
- Brocard F, Bardy C, Dubuc R (2005) Modulatory effect of substance P to the brain stem locomotor command in lampreys. *J Neurophysiol* 93:2127-2141.
- Brodin L, Hokfelt T, Grillner S, Panula P (1990a) Distribution of histaminergic neurons in the brain of the lamprey *Lampetra fluviatilis* as revealed by histamine-immunohistochemistry. *J Comp Neurol* 292:435-442.
- Brodin L, Theodorsson E, Christenson J, Cullheim S, Hökfelt T, Brown J, Buchan A, Panula P, Verhofstad A, Goldstein M (1990b) Neurotensin-like Peptides in the CNS of Lampreys: Chromatographic Characterization and Immunohistochemical Localization with Reference to Aminergic Markers. *Eur J Neurosci* 2:1095-1109.
- Carr DB, Day M, Cantrell AR, Held J, Scheuer T, Catterall WA, Surmeier DJ (2003) Transmitter modulation of slow, activity-dependent alterations in sodium

- channel availability endows neurons with a novel form of cellular plasticity. *Neuron* 39:793-806.
- Cepeda C, Buchwald NA, Levine MS (1993) Neuromodulatory actions of dopamine in the neostriatum are dependent upon the excitatory amino acid receptor subtypes activated. *Proc Natl Acad Sci U S A* 90:9576-9580.
- Cepeda C, Chandler SH, Shumate LW, Levine MS (1995) Persistent Na<sup>+</sup> conductance in medium-sized neostriatal neurons: characterization using infrared videomicroscopy and whole cell patch-clamp recordings. *J Neurophysiol* 74:1343-1348.
- de Arriba Mdel C, Pombal MA (2007) Afferent connections of the optic tectum in lampreys: an experimental study. *Brain, behavior and evolution* 69:37-68.
- Deliaquina TG, Orlovsky GN (2002) Comparative neurobiology of postural control. *Curr Opin Neurobiol* 12:652-657.
- DeLong MR (1990) Primate models of movement disorders of basal ganglia origin. *Trends Neurosci* 13:281-285.
- DeLong MR (2000) The basal ganglia. In: *Principles of Neural Sciences*, fourth Edition (Kandel ER, Schwartz JH, Jessel TM, eds), pp 853-867: McGraw-Hill.
- Derjean D, Moussaddy A, Atallah E, St-Pierre M, Auclair F, Chang S, Ren X, Zielinski B, Dubuc R (2010) A novel neural substrate for the transformation of olfactory inputs into motor output. *PLoS biology* 8:e1000567.
- Di Prisco GV, Pearlstein E, Le Ray D, Robitaille R, Dubuc R (2000) A cellular mechanism for the transformation of a sensory input into a motor command. *J Neurosci* 20:8169-8176.
- Ding J, Peterson JD, Surmeier DJ (2008) Corticostriatal and thalamostriatal synapses have distinctive properties. *J Neurosci* 28:6483-6492.
- Ding JB, Guzman JN, Peterson JD, Goldberg JA, Surmeier DJ (2010) Thalamic gating of corticostriatal signaling by cholinergic interneurons. *Neuron* 67:294-307.
- Ding L, Perkel DJ (2002) Dopamine modulates excitability of spiny neurons in the avian basal ganglia. *J Neurosci* 22:5210-5218.
- Doig NM, Moss J, Bolam JP (2010) Cortical and thalamic innervation of direct and indirect pathway medium-sized spiny neurons in mouse striatum. *J Neurosci* 30:14610-14618.
- Doya K (2002) Metalearning and neuromodulation. *Neural networks : the official journal of the International Neural Network Society* 15:495-506.
- Dubuc R, Bongianni F, Ohta Y, Grillner S (1993) Dorsal root and dorsal column mediated synaptic inputs to reticulospinal neurons in lampreys: involvement of glutamatergic, glycinergic, and GABAergic transmission. *J Comp Neurol* 327:251-259.
- Dubuc R, Brocard F, Antri M, Fenelon K, Garipey JF, Smetana R, Menard A, Le Ray D, Viana Di Prisco G, Pearlstein E, Sirota MG, Derjean D, St-Pierre M, Zielinski B, Auclair F, Veilleux D (2008) Initiation of locomotion in lampreys. *Brain Res Rev* 57:172-182.
- El Manira A, Pombal MA, Grillner S (1997) Diencephalic projection to reticulospinal neurons involved in the initiation of locomotion in adult lampreys *Lampetra fluviatilis*. *J Comp Neurol* 389:603-616.
- Ellender TJ, Huerta-Ocampo I, Deisseroth K, Capogna M, Bolam JP (2011) Differential modulation of excitatory and inhibitory striatal synaptic transmission by histamine. *J Neurosci* 31:15340-15351.
- English DF, Ibanez-Sandoval O, Stark E, Tecuapetla F, Buzsaki G, Deisseroth K, Tepper JM, Koos T (2012) GABAergic circuits mediate the reinforcement-related signals of striatal cholinergic interneurons. *Nat Neurosci* 15:123-130.

- Ewert JP, Buxbaum-Conradi H, Glasgow M, Röttgen A, Schürg-Pfeiffer E, Schwippert WW (1999) Forebrain and midbrain structures involved in prey-catching behaviour of toads: stimulus-response mediating circuits and their modulating loops. *Eur J Morphol* 37:172-176.
- Farries MA, Perkel DJ (2000) Electrophysiological properties of avian basal ganglia neurons recorded in vitro. *J Neurophysiol* 84:2502-2513.
- Farries MA, Meitzen J, Perkel DJ (2005) Electrophysiological properties of neurons in the basal ganglia of the domestic chick: conservation and divergence in the evolution of the avian basal ganglia. *J Neurophysiol* 94:454-467.
- Garcia-Rill E, Skinner RD, Gilmore SA (1981) Pallidal projections to the mesencephalic locomotor region (MLR) in the cat. *The American journal of anatomy* 161:311-321.
- Garcia-Rill E, Skinner RD, Fitzgerald JA (1985) Chemical activation of the mesencephalic locomotor region. *Brain Res* 330:43-54.
- Garcia-Rill E, Skinner RD, Jackson MB, Smith MM (1983a) Connections of the mesencephalic locomotor region (MLR) I. Substantia nigra afferents. *Brain research bulletin* 10:57-62.
- Garcia-Rill E, Skinner RD, Gilmore SA, Owings R (1983b) Connections of the mesencephalic locomotor region (MLR) II. Afferents and efferents. *Brain research bulletin* 10:63-71.
- Garcia-Rill E, Kinjo N, Atsuta Y, Ishikawa Y, Webber M, Skinner RD (1990) Posterior midbrain-induced locomotion. *Brain research bulletin* 24:499-508.
- Gariépy JF, Missaghi K, Chevallier S, Chartre S, Robert M, Auclair F, Lund JP, Dubuc R (2012) Specific neural substrate linking respiration to locomotion. *Proc Natl Acad Sci U S A* 109:E84-92.
- Gertler TS, Chan CS, Surmeier DJ (2008) Dichotomous anatomical properties of adult striatal medium spiny neurons. *J Neurosci* 28:10814-10824.
- Gittis AH, Nelson AB, Thwin MT, Palop JJ, Kreitzer AC (2010) Distinct roles of GABAergic interneurons in the regulation of striatal output pathways. *J Neurosci* 30:2223-2234.
- Greengard P (2001) The neurobiology of slow synaptic transmission. *Science* 294:1024-1030.
- Grillner S (1985) Neurobiological bases of rhythmic motor acts in vertebrates. *Science* 228:143-149.
- Grillner S (2003) The motor infrastructure: from ion channels to neuronal networks. *Nat Rev Neurosci* 4:573-586.
- Grillner S (2006) Biological pattern generation: the cellular and computational logic of networks in motion. *Neuron* 52:751-766.
- Grillner S, Wallen P (1985) Central pattern generators for locomotion, with special reference to vertebrates. *Annual review of neuroscience* 8:233-261.
- Grillner S, Hellgren J, Menard A, Saitoh K, Wikstrom MA (2005) Mechanisms for selection of basic motor programs--roles for the striatum and pallidum. *Trends Neurosci* 28:364-370.
- Grillner S, Wallen P, Saitoh K, Kozlov A, Robertson B (2008) Neural bases of goal-directed locomotion in vertebrates--an overview. *Brain Res Rev* 57:2-12.
- Harris NC, Constanti A (1995) Mechanism of block by ZD 7288 of the hyperpolarization-activated inward rectifying current in guinea pig substantia nigra neurons in vitro. *J Neurophysiol* 74:2366-2378.
- Hernandez-Lopez S, Bargas J, Surmeier DJ, Reyes A, Galarraga E (1997) D1 receptor activation enhances evoked discharge in neostriatal medium spiny neurons by modulating an L-type  $Ca^{2+}$  conductance. *J Neurosci* 17:3334-3342.

- Hernandez-Lopez S, Tkatch T, Perez-Garci E, Galarraga E,argas J, Hamm H, Surmeier DJ (2000) D2 dopamine receptors in striatal medium spiny neurons reduce L-type Ca<sup>2+</sup> currents and excitability via a novel PLC[ $\beta$ ]-IP3-calcineurin-signaling cascade. *J Neurosci* 20:8987-8995.
- Hikosaka O, Wurtz RH (1983) Visual and oculomotor functions of monkey substantia nigra pars reticulata. IV. Relation of substantia nigra to superior colliculus. *J Neurophysiol* 49:1285-1301.
- Hikosaka O, Wurtz RH (1985) Modification of saccadic eye movements by GABA-related substances. I. Effect of muscimol and bicuculline in monkey superior colliculus. *J Neurophysiol* 53:266-291.
- Ibanez-Sandoval O, Tecuapetla F, Unal B, Shah F, Koos T, Tepper JM (2010) Electrophysiological and morphological characteristics and synaptic connectivity of tyrosine hydroxylase-expressing neurons in adult mouse striatum. *J Neurosci* 30:6999-7016.
- Isoda M, Hikosaka O (2011) Cortico-basal ganglia mechanisms for overcoming innate, habitual and motivational behaviors. *Eur J Neurosci* 33:2058-2069.
- Jimenez AJ, Mancera JM, Pombal MA, Perez-Figares JM, Fernandez-Llebrez P (1996) Distribution of galanin-like immunoreactive elements in the brain of the adult lamprey *Lampetra fluviatilis*. *J Comp Neurol* 368:185-197.
- Johnston JB (1902) The brain of *Petromyzon*. *J Comp Neurol* 12:11-86.
- Johnston JB (1912) The telencephalon in cyclostomes. *J Comp Neurol* 22:341-404.
- Jones MR, Grillner S, Robertson B (2009) Selective projection patterns from subtypes of retinal ganglion cells to tectum and pretectum: distribution and relation to behavior. *J Comp Neurol* 517:257-275.
- Kawaguchi Y (1993) Physiological, morphological, and histochemical characterization of three classes of interneurons in rat neostriatum. *J Neurosci* 13:4908-4923.
- Kawaguchi Y, Wilson CJ, Emson PC (1989) Intracellular recording of identified neostriatal patch and matrix spiny cells in a slice preparation preserving cortical inputs. *J Neurophysiol* 62:1052-1068.
- Kawaguchi Y, Wilson CJ, Emson PC (1990) Projection subtypes of rat neostriatal matrix cells revealed by intracellular injection of biocytin. *J Neurosci* 10:3421-3438.
- Kawaguchi Y, Wilson CJ, Augood SJ, Emson PC (1995) Striatal interneurons: chemical, physiological and morphological characterization. *Trends Neurosci* 18:527-535.
- Kita H (1993) GABAergic circuits of the striatum. *Prog Brain Res* 99:51-72.
- Kita H (2007) Globus pallidus external segment. *Prog Brain Res* 160:111-133.
- Klaus A, Planert H, Hjorth JJ, Berke JD, Silberberg G, Kotaleski JH (2011) Striatal fast-spiking interneurons: from firing patterns to postsynaptic impact. *Frontiers in systems neuroscience* 5:57.
- Koos T, Tepper JM (1999) Inhibitory control of neostriatal projection neurons by GABAergic interneurons. *Nat Neurosci* 2:467-472.
- Koos T, Tepper JM (2002) Dual cholinergic control of fast-spiking interneurons in the neostriatum. *J Neurosci* 22:529-535.
- Kravitz AV, Freeze BS, Parker PR, Kay K, Thwin MT, Deisseroth K, Kreitzer AC (2010) Regulation of parkinsonian motor behaviours by optogenetic control of basal ganglia circuitry. *Nature* 466:622-626.
- Kreitzer AC, Berke JD (2011) Investigating striatal function through cell-type-specific manipulations. *Neuroscience* 198:19-26.
- Kubota Y, Inagaki S, Kito S, Wu JY (1987) Dopaminergic axons directly make synapses with GABAergic neurons in the rat neostriatum. *Brain Res* 406:147-156.



- Kubota Y, Inagaki S, Kito S, Shimada S, Okayama T, Hatanaka H, Pelletier G, Takagi H, Tohyama M (1988) Neuropeptide Y-immunoreactive neurons receive synaptic inputs from dopaminergic axon terminals in the rat neostriatum. *Brain Res* 458:389-393.
- Kumar S, Hedges SB (1998) A molecular timescale for vertebrate evolution. *Nature* 392:917-920.
- Lacey CJ, Bolam JP, Magill PJ (2007) Novel and distinct operational principles of intralaminar thalamic neurons and their striatal projections. *J Neurosci* 27:4374-4384.
- Le Ray D, Juvin L, Ryczko D, Dubuc R (2011) Chapter 4--supraspinal control of locomotion: the mesencephalic locomotor region. *Prog Brain Res* 188:51-70.
- Le Ray D, Brocard F, Bourcier-Lucas C, Auclair F, Lafaille P, Dubuc R (2003) Nicotinic activation of reticulospinal cells involved in the control of swimming in lampreys. *Eur J Neurosci* 17:137-148.
- Lee MS, Rinne JO, Marsden CD (2000) The pedunculopontine nucleus: its role in the genesis of movement disorders. *Yonsei medical journal* 41:167-184.
- Levine MS, Li Z, Cepeda C, Cromwell HC, Altemus KL (1996) Neuromodulatory actions of dopamine on synaptically-evoked neostriatal responses in slices. *Synapse* 24:65-78.
- Lipscombe D (2002) L-type calcium channels: highs and new lows. *Circulation research* 90:933-935.
- Mallet N, Micklem BR, Henny P, Brown MT, Williams C, Bolam JP, Nakamura KC, Magill PJ (2012) Dichotomous organization of the external globus pallidus. *Neuron* 74:1075-1086.
- Matsumoto N, Minamimoto T, Graybiel AM, Kimura M (2001) Neurons in the thalamic CM-Pf complex supply striatal neurons with information about behaviorally significant sensory events. *J Neurophysiol* 85:960-976.
- Maurice N, Mercer J, Chan CS, Hernandez-Lopez S, Held J, Tkatch T, Surmeier DJ (2004) D2 dopamine receptor-mediated modulation of voltage-dependent Na<sup>+</sup> channels reduces autonomous activity in striatal cholinergic interneurons. *J Neurosci* 24:10289-10301.
- McClellan AD, Grillner S (1984) Activation of 'fictive swimming' by electrical microstimulation of brainstem locomotor regions in an in vitro preparation of the lamprey central nervous system. *Brain Res* 300:357-361.
- Medina L, Reiner A (1995) Neurotransmitter organization and connectivity of the basal ganglia in vertebrates: implications for the evolution of basal ganglia. *Brain, behavior and evolution* 46:235-258.
- Mena-Segovia J, Micklem BR, Nair-Roberts RG, Ungless MA, Bolam JP (2009) GABAergic neuron distribution in the pedunculopontine nucleus defines functional subterritories. *J Comp Neurol* 515:397-408.
- Menard A, Grillner S (2008) Diencephalic locomotor region in the lamprey--afferents and efferent control. *J Neurophysiol* 100:1343-1353.
- Menard A, Auclair F, Bourcier-Lucas C, Grillner S, Dubuc R (2007) Descending GABAergic projections to the mesencephalic locomotor region in the lamprey *Petromyzon marinus*. *J Comp Neurol* 501:260-273.
- Middleton FA, Strick PL (2000) Basal ganglia and cerebellar loops: motor and cognitive circuits. *Brain Res Brain Res Rev* 31:236-250.
- Mink JW (1996) The basal ganglia: focused selection and inhibition of competing motor programs. *Progress in neurobiology* 50:381-425.
- Mink JW (2001) Basal ganglia dysfunction in Tourette's syndrome: a new hypothesis. *Pediatr Neurol* 25:190-198.



- Nambu A, Tokuno H, Takada M (2002) Functional significance of the cortico-subthalamo-pallidal 'hyperdirect' pathway. *Neuroscience research* 43:111-117.
- Neher E, Sakmann B (1976) Single-channel currents recorded from membrane of denervated frog muscle fibres. *Nature* 260:799-802.
- Neve KA, Seamans JK, Trantham-Davidson H (2004) Dopamine receptor signaling. *Journal of receptor and signal transduction research* 24:165-205.
- Nicola SM, Surmeier J, Malenka RC (2000) Dopaminergic modulation of neuronal excitability in the striatum and nucleus accumbens. *Annual review of neuroscience* 23:185-215.
- Nieuwenhuys R NC (1998) Lampreys, Petromyzontoidea. In: *The central nervous system of vertebrates* (Nieuwenhuys R tDH, Nicholson C, ed), pp p 397–486. Berlin: Springer Verlag.
- Nisenbaum ES, Wilson CJ (1995) Potassium currents responsible for inward and outward rectification in rat neostriatal spiny projection neurons. *J Neurosci* 15:4449-4463.
- Northcutt RG, Wicht H (1997) Afferent and efferent connections of the lateral and medial pallia of the silver lamprey. *Brain, behavior and evolution* 49:1-19.
- Nozaki M, Gorbman A (1986) Occurrence and distribution of substance P-related immunoreactivity in the brain of adult lampreys, *Petromyzon marinus* and *Entosphenus tridentatus*. *Gen Comp Endocrinol* 62:217-229.
- Ocaña FM SK, Rodriguez F, Robertson B and Grillner S. (2011) Is there a motor pallium in the lamprey. *International Brain Research Organization*.
- Olson PA, Tkatch T, Hernandez-Lopez S, Ulrich S, Ilijic E, Mugnaini E, Zhang H, Bezprozvanny I, Surmeier DJ (2005) G-protein-coupled receptor modulation of striatal CaV1.3 L-type Ca<sup>2+</sup> channels is dependent on a Shank-binding domain. *J Neurosci* 25:1050-1062.
- Parent M, Wallman MJ, Gagnon D, Parent A (2011) Serotonin innervation of basal ganglia in monkeys and humans. *Journal of chemical neuroanatomy* 41:256-265.
- Pierre J, Reperant J, Ward R, Vesselkin NP, Rio JP, Miceli D, Kratskin I (1992) The serotonergic system of the brain of the lamprey, *Lampetra fluviatilis*: an evolutionary perspective. *Journal of chemical neuroanatomy* 5:195-219.
- Pierre J, J.P. Rio, M. Mahouche, and J. Repérant. (1994) Catecholamine systems in the brain of cyclostomes, the lamprey, *Lampetra fluviatilis*. In: *Phylogeny and Development of Catecholamine Systems in the CNS of Vertebrates*. (Reiner WJASaA, ed), pp pp. 7–19. Cambridge: Cambridge University Press.
- Planert H, Szydlowski SN, Hjorth JJ, Grillner S, Silberberg G (2010) Dynamics of synaptic transmission between fast-spiking interneurons and striatal projection neurons of the direct and indirect pathways. *J Neurosci* 30:3499-3507.
- Polenova OA, Vesselkin NP (1993) Olfactory and nonolfactory projections in the river lamprey (*Lampetra fluviatilis*) telencephalon. *Journal fur Hirnforschung* 34:261-279.
- Pombal MA, El Manira A, Grillner S (1997a) Afferents of the lamprey striatum with special reference to the dopaminergic system: a combined tracing and immunohistochemical study. *J Comp Neurol* 386:71-91.
- Pombal MA, El Manira A, Grillner S (1997b) Organization of the lamprey striatum - transmitters and projections. *Brain Res* 766:249-254.
- Pombal MA, Marin O, Gonzalez A (2001) Distribution of choline acetyltransferase-immunoreactive structures in the lamprey brain. *J Comp Neurol* 431:105-126.
- Pombal MA MM, Moussa CE-H, Sidhu A, Vernier P. (2007) Distribution of the dopamine D1 receptor in the lamprey brain: evolutionary implications. *Society for Neuroscience* 35129.

- Redgrave P, Prescott TJ, Gurney K (1999) The basal ganglia: a vertebrate solution to the selection problem? *Neuroscience* 89:1009-1023.
- Reiner A, Medina L, Veenman CL (1998) Structural and functional evolution of the basal ganglia in vertebrates. *Brain Res Brain Res Rev* 28:235-285.
- Reiner A, Hart NM, Lei W, Deng Y (2010) Corticostriatal projection neurons - dichotomous types and dichotomous functions. *Front Neuroanat* 4:142.
- Rice ME, Patel JC, Cragg SJ (2011) Dopamine release in the basal ganglia. *Neuroscience* 198:112-137.
- Robertson B, Saitoh K, Menard A, Grillner S (2006) Afferents of the lamprey optic tectum with special reference to the GABA input: combined tracing and immunohistochemical study. *J Comp Neurol* 499:106-119.
- Robertson B, Auclair F, Menard A, Grillner S, Dubuc R (2007) GABA distribution in lamprey is phylogenetically conserved. *J Comp Neurol* 503:47-63.
- Rommelfanger KS, Wichmann T (2010) Extrastriatal dopaminergic circuits of the Basal Ganglia. *Front Neuroanat* 4:139.
- Rovainen CM (1979) Neurobiology of lampreys. *Physiological reviews* 59:1007-1077.
- Rymar VV, Sasseville R, Luk KC, Sadikot AF (2004) Neurogenesis and stereological morphometry of calretinin-immunoreactive GABAergic interneurons of the neostriatum. *J Comp Neurol* 469:325-339.
- Saitoh K, Menard A, Grillner S (2007) Tectal control of locomotion, steering, and eye movements in lamprey. *J Neurophysiol* 97:3093-3108.
- Schiffmann SN, Jacobs O, Vanderhaeghen JJ (1991) Striatal restricted adenosine A2 receptor (RDC8) is expressed by enkephalin but not by substance P neurons: an in situ hybridization histochemistry study. *Journal of neurochemistry* 57:1062-1067.
- Shik ML, Orlovsky GN (1976) Neurophysiology of locomotor automatism. *Physiological reviews* 56:465-501.
- Sidibe M, Smith Y (1999) Thalamic inputs to striatal interneurons in monkeys: synaptic organization and co-localization of calcium binding proteins. *Neuroscience* 89:1189-1208.
- Sirota MG, Di Prisco GV, Dubuc R (2000) Stimulation of the mesencephalic locomotor region elicits controlled swimming in semi-intact lampreys. *Eur J Neurosci* 12:4081-4092.
- Skinner RD, Garcia-Rill E (1984) The mesencephalic locomotor region (MLR) in the rat. *Brain Res* 323:385-389.
- Smith AD, Bolam JP (1990) The neural network of the basal ganglia as revealed by the study of synaptic connections of identified neurones. *Trends Neurosci* 13:259-265.
- Smith Y, Villalba R (2008) Striatal and extrastriatal dopamine in the basal ganglia: an overview of its anatomical organization in normal and Parkinsonian brains. *Movement disorders : official journal of the Movement Disorder Society* 23 Suppl 3:S534-547.
- Smith Y, Raju DV, Pare JF, Sidibe M (2004) The thalamostriatal system: a highly specific network of the basal ganglia circuitry. *Trends Neurosci* 27:520-527.
- Stephenson-Jones M, Floros O, Robertson B, Grillner S (2012) Evolutionary conservation of the habenular nuclei and their circuitry controlling the dopamine and 5-hydroxytryptophan (5-HT) systems. *Proc Natl Acad Sci U S A* 109:E164-173.
- Stephenson-Jones M, Samuelsson E, Ericsson J, Robertson B, Grillner S (2011) Evolutionary conservation of the basal ganglia as a common vertebrate mechanism for action selection. *Current biology : CB* 21:1081-1091.

- Surmeier DJ, Kitai ST (1994) Dopaminergic regulation of striatal efferent pathways. *Curr Opin Neurobiol* 4:915-919.
- Surmeier DJ, Carrillo-Reid L, Vargas J (2011) Dopaminergic modulation of striatal neurons, circuits, and assemblies. *Neuroscience* 198:3-18.
- Surmeier DJ, Ding J, Day M, Wang Z, Shen W (2007) D1 and D2 dopamine-receptor modulation of striatal glutamatergic signaling in striatal medium spiny neurons. *Trends Neurosci* 30:228-235.
- Svenningsson P, Nishi A, Fisone G, Girault JA, Nairn AC, Greengard P (2004) DARPP-32: an integrator of neurotransmission. *Annual review of pharmacology and toxicology* 44:269-296.
- Tepper J, Abercrombie E, Bolam J (2007) Basal ganglia macrocircuits. *Prog Brain Res* 160:3-7.
- Tepper JM, Bolam JP (2004) Functional diversity and specificity of neostriatal interneurons. *Curr Opin Neurobiol* 14:685-692.
- Tepper JM, Koos T, Wilson CJ (2004) GABAergic microcircuits in the neostriatum. *Trends Neurosci* 27:662-669.
- Tepper JM, Wilson CJ, Koos T (2008) Feedforward and feedback inhibition in neostriatal GABAergic spiny neurons. *Brain Res Rev* 58:272-281.
- Tepper JM, Tecuapetla F, Koos T, Ibanez-Sandoval O (2010) Heterogeneity and diversity of striatal GABAergic interneurons. *Front Neuroanat* 4:150.
- Thompson RH, Menard A, Pombal M, Grillner S (2008) Forebrain dopamine depletion impairs motor behavior in lamprey. *Eur J Neurosci* 27:1452-1460.
- Uchimura N, Cherubini E, North RA (1989) Inward rectification in rat nucleus accumbens neurons. *J Neurophysiol* 62:1280-1286.
- Ullen F, Orlovsky GN, Deliagina TG, Grillner S (1993) Role of dermal photoreceptors and lateral eyes in initiation and orientation of locomotion in lamprey. *Behavioural brain research* 54:107-110.
- Utter AA, Basso MA (2008) The basal ganglia: an overview of circuits and function. *Neuroscience and biobehavioral reviews* 32:333-342.
- Valjent E, Bertran-Gonzalez J, Herve D, Fisone G, Girault JA (2009) Looking BAC at striatal signaling: cell-specific analysis in new transgenic mice. *Trends Neurosci* 32:538-547.
- Van der Werf YD, Witter MP, Groenewegen HJ (2002) The intralaminar and midline nuclei of the thalamus. Anatomical and functional evidence for participation in processes of arousal and awareness. *Brain Res Brain Res Rev* 39:107-140.
- Vernier (1997) The amphioxus D1/beta receptor and the emergence of the vertebrate adrenergic system. In: GenBank NCBI Accession number. AJ005434.1p.
- Vesselkin NP, Ermakova TV, Reperant J, Kosareva AA, Kenigfest NB (1980) The retinofugal and retinopetal systems in *Lampetra fluviatilis*. An experimental study using radioautographic and HRP methods. *Brain Res* 195:453-460.
- Wachtler K (1974) The distribution of acetylcholinesterase in the cyclostome brain. I. *Lampetra planeri* (L.). *Cell and tissue research* 152:259-270.
- Wang D, Grillner S, Wallen P (2011) 5-HT and dopamine modulates CaV1.3 calcium channels involved in postinhibitory rebound in the spinal network for locomotion in lamprey. *J Neurophysiol* 105:1212-1224.
- Wikstrom MA, Grillner S, El Manira A (1999) Inhibition of N- and L-type Ca<sup>2+</sup> currents by dopamine in lamprey spinal motoneurons. *Neuroreport* 10:3179-3183.
- Wilson C, Kawaguchi Y (1996) The origins of two-state spontaneous membrane potential fluctuations of neostriatal spiny neurons. *J Neurosci* 16:2397-2410.
- Wilson CJ (2005) The mechanism of intrinsic amplification of hyperpolarizations and spontaneous bursting in striatal cholinergic interneurons. *Neuron* 45:575-585.

- Wilson CJ, Chang HT, Kitai ST (1990) Firing patterns and synaptic potentials of identified giant aspiny interneurons in the rat neostriatum. *J Neurosci* 10:508-519.
- Yoshida M, Precht W (1971) Monosynaptic inhibition of neurons of the substantia nigra by caudato-nigral fibers. *Brain Res* 32:225-228.

I



## Short communication

## A lamprey striatal brain slice preparation for patch-clamp recordings

Jesper Ericsson, Brita Robertson, Martin A. Wikström\*

*Department of Neuroscience, Karolinska Institutet, S-17177 Stockholm, Sweden*

Received 26 December 2006; received in revised form 24 May 2007; accepted 28 May 2007

**Abstract**

Striatum, the input layer of the basal ganglia is important for functions such as the selection of motor behaviour. The lamprey, a lower vertebrate, is particularly well suited as a model system for the control of motor functions as its central nervous system is similar to that of higher vertebrates and exhibits a lower level of complexity. Therefore, studies in lamprey preparations enable cellular and synaptic mechanisms to be correlated with behaviour.

The lamprey brain slice preparation presented has been developed to study the striatal microcircuits and input/output systems with patch-clamp recordings. The method involves dissection of the central nervous system, brain slice preparation, identification of the striatum, visual identification of striatal neurons and patch-clamp recordings. By combining studies in the slice preparation presented here and other lamprey preparations such as the semi-intact lamprey, we will be able to correlate striatal mechanisms on the cellular, synaptic and network levels with striatal output and motor behaviour. The method can be adapted to produce similar slice preparations from other areas of the lamprey brain.

© 2007 Elsevier B.V. All rights reserved.

**Keywords:** Basal ganglia; Lamprey; Striatum; Patch-clamp; Motor functions; Slice preparation**1. Introduction**

The lamprey, a primitive vertebrate, has been used as a model system for the study of the cellular bases of motor functions at the brain, brainstem and spinal cord levels. In particular, the motor control systems for posture and locomotion have been extensively studied (Brocard and Dubuc, 2003; Deliagina and Pavlova, 2002; Deliagina et al., 2002; Grillner, 2003).

The basal ganglia including its input layer – the striatum – is important for the selection and initiation of behaviour (Grillner et al., 2005), as well as for cognitive functions (Brown et al., 1997). The mammalian striatum receives glutamatergic input from cortex and thalamus (cf. Grillner et al., 2005; Groenewegen, 2003) and, in addition, receives inputs from a number of modulatory systems including the serotonergic system originating in the raphe nuclei, the dopamine system arising from the substantia nigra pars compacta and the histamine system (from hypothal-

amus) (Dube et al., 1988; Gerfen, 1988; Huston et al., 1997; Panula et al., 2000; Wilson et al., 1983).

GABAergic medium spiny neurons (MSN) make up approximately 95% of the striatal neurons in rodents and are the sole output neurons (Grillner et al., 2005).

They exist in two major populations expressing either dopamine D<sub>1</sub> receptors and substance P or D<sub>2</sub> receptors and enkephalin (Grillner et al., 2005; Nicola et al., 2000).

Mammalian MSN exhibit a bistable membrane potential with an up-state relatively close to the action potential firing threshold while the down-state is more hyperpolarized (~−80 mV). When in the up-state, MSN are readily activated by synaptic inputs and then, in a simplified sense, inhibits tonically active GABAergic neurons in downstream nuclei of the basal ganglia. MSN also receive intrastriatal input arising from both GABAergic and cholinergic interneurons as well as from MSN.

The lamprey striatum is located lateral to the medial ventricle of the telencephalon (Pombal et al., 1997b) and is relatively small (Fig. 1A–F) compared to its equivalent in rodents. It exhibits many similarities with the striatum of amniotes and (Pombal et al., 1997a,b) appears to be well conserved phylogenetically. The lamprey striatum exhibits immunoreactivity for GABA,

\* Corresponding author. Tel.: +46 8 5248 7345; fax: +46 8 34 95 44.  
E-mail address: martin.wikstrom@ki.se (M.A. Wikström).

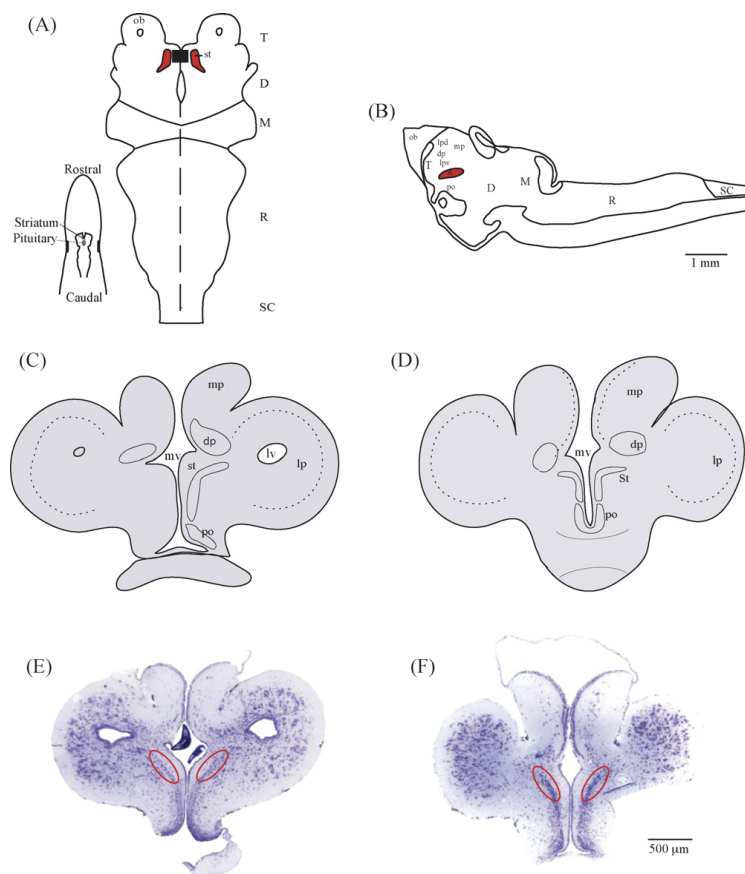


Fig. 1. Anatomical location of the lamprey striatum. (A) Dorsal view of the lamprey brain with the striatum labeled in red (st). The lamprey brain including the striatum can be observed in the intact head (smaller inset figure). (B) Sagittal view of the lamprey brain with the striatum labeled in red. (C and D) Maps of a rostral (C) and a caudal (D) coronal section of the lamprey brain showing the location of the striatum in relation to other structures. Cresyl violet-stained rostral (E) and a caudal (F) brain slice sections of the striatum (striatum labelled in red). Abbreviations are as follows: D, diencephalon; dp, dorsal pallium; lpd, dorsal part of the lateral pallium; lpv, ventral part of the lateral pallium; lp, lateral pallium; lv, lateral telencephalic ventricle; M, mesencephalon; mv, medial telencephalic ventricle; mp, medial pallium; ob, olfactory bulb; po, nucleus preopticus; R, rhombencephalon; SC, spinal cord; st, striatum; T, telencephalon; vth, nucleus ventralis thalami. (A) was adapted from El Manira et al. (1997) and (B) from Pombal et al. (1997a) (both copyright John Wiley & Sons, Inc., 1997). Reprinted with permission of Wiley-Liss, Inc., a subsidiary of John Wiley & Sons, Inc.

substance P, neurotensin and acetylcholinesterase. In addition, the striatum receives prominent serotonergic, histaminergic and dopaminergic fibers as well as inputs from thalamus and pallidum (Brodin et al., 1990a,b; Pombal et al., 1997a,b). Importantly, depletion of dopaminergic neurons with MPTP (1-methyl 4-phenyl 1,2,3,6-tetrahydropyridine) induces the same types of hypokinetic symptoms in lamprey as in mammals (Thompson et al., 2000). Efferent projections from striatum are sent to the ventral part of the lateral pallidum—the putative pallidum (Pombal et al., 1997b) which in turn, send projections to the thalamus that innervate brainstem motor centers (Ménard et al., 2007; Pombal et al., 1997b).

Little is known about the intrinsic function of the striatum in any class of vertebrates and we have therefore developed a lamprey brain slice preparation to analyze the striatal microcircuits with patch-clamp recordings from single and multiple neurons. The use of a slice preparation is necessary in order to be able to make patch-clamp recordings from visually identified neurons.

In the present paper we describe a lamprey striatal brain slice preparation for patch-clamp recordings, visualization and identification of the striatum in the preparation, and how its condition was tested. To our knowledge, the patch-clamp recordings described here are the first made in the lamprey from structures higher than the brainstem.



## 2. Methods

### 2.1. Dissection and removal of the brain

Lampreys (*Lampetra fluviatilis*,  $n=65$ ) were anaesthetized using MS-222 (100 mg/l, Sigma) and decapitated caudal to the gills. The rostral part of the lamprey (Fig. 1A) was immersed in 4–8 °C artificial cerebrospinal fluid (aCSF) containing (in mM) either NaCl, 138; KCl, 2.1; CaCl<sub>2</sub>, 1.8; MgCl<sub>2</sub>, 1.2; glucose, 4; *N*-2-hydroxyethylpiperazine-*N'*-2-ethanesulphonic acid (HEPES), 2; and l-glutamine, 0.5 (bubbled with O<sub>2</sub> for 20 min prior to use, pH adjusted to 7.4 with 1 M NaOH) or NaCl 125, KCl 2.5, MgCl<sub>2</sub> 1, NaH<sub>2</sub>PO<sub>4</sub> 1.25, CaCl<sub>2</sub> 2, NaHCO<sub>3</sub> 25 and glucose 25 (bubbled continuously with 5% CO<sub>2</sub> in O<sub>2</sub>, pH 7.4).

To have a stable preparation during the dissection it was necessary to remove as much muscle tissue as possible. Tissue ventral to the notochord was removed from the caudal end of the preparation to the level of the eyes (Fig. 1A) and included most of the gills. The preparation was then pinned down with the dorsal side up in a Sylgard (Dow Corning, Wiesbaden, Germany)-lined Petri dish filled with cold aCSF (4–8 °C), and the lateral and dorsal muscle tissue was removed along the same section as above. Next, the spinal canal was cut open and followed up to the brainstem and brain that were exposed by removing all overlying tissue. Special care was taken when cutting the pineal nerve (for review see Rovainen, 1979) as it may otherwise pull on the brain during the dissection thereby causing severe damage.

Thereafter, the spinal cord, brainstem and brain were carefully removed from the rest of the preparation. By gently lifting the caudal end of the spinal cord to cut ventral roots and remove loose tissue under it, a part of the spinal cord could be lifted, after which the process was reiterated more rostrally. Furthermore, as much as possible of meninges and fat on the dorsal side of the brain should be removed prior to lifting it as it may otherwise stick to the blade during cutting. Particular care should be taken not to damage the olfactory bulbs as they easily detach from the rest of the brain. After the brain was removed, it was immediately immersed in 4–8 °C aCSF for 2–3 min. In some trials the brain was immersed in carbonate-based aCSF with low [Ca<sup>2+</sup>] (1 mM,  $n=3$ ) or in aCSF containing tetrodotoxin (TTX (Sigma), 0.5 μM,  $n=3$ ) to reduce spontaneous neural activity before cutting and thereby hopefully increase the cell survival rate. No significant benefits from these treatments were, however, observed and they were therefore discontinued at an early stage.

### 2.2. Production of coronal brain slices

During development of the procedure different cutting techniques were tried.

We found that the best method for the production of slices was to put the brain horizontally on a piece of Agar that was placed in the specimen holder of a home-made, vertically cutting, vibratome. This method produces coronal brain slices of good quality. To avoid that the Agar piece would slide during cutting, it was cut as close to the shape of the holder as possible

and rugged up on the underside. Because of the small size of the brain (typically at most 2.5 mm thick and 3 mm wide) it was not possible to fixate the brain with glue which is normal for larger preparations. Therefore, we usually formed an elongated groove in the Agar in which the brain was placed. Care was taken to ensure that all edges in the Agar were as smooth as possible so that the small brain slices could be removed easily. The brain may also be put on a flat piece of Agar and may in such cases move some during cutting which reduces the precision although it is easier to remove the slices.

Slice thickness ranged from 200 to 600 μm. We found that a high vibration frequency combined with a slow blade advance speed produced the best slices based on cell survival and durability of the preparation. The striatum is located very close to the medial ventricle of the telecephalon (Fig. 1C–F) which sometimes resulted in tissue compression during cutting. This appeared to affect cell survival negatively, but could be counteracted by keeping the advance speed of the cutting blade as low as possible and by not cutting thinner slices than 300 μm. The thickness found to result in the best balance between cell survival rate and visibility was 400–500 μm. Due to the small size of the lamprey striatum (Fig. 1A–D, Pombal et al., 1997a,b) it is not possible to produce more than one or two striatal brain slices from one animal. The coronal slices will, however, contain the striatum from both hemispheres.

After cutting, the slices were immediately transferred to a holding chamber containing cold carbonate- or HEPES-based aCSF that was held on ice. Carbonate-based aCSF was continuously bubbled with 95% O<sub>2</sub>/5% CO<sub>2</sub>.

Other, less successful, cutting techniques were tried as well. To avoid the problem concerning movement of the preparation during cutting, embedding of the brain in Agar during horizontal and vertical slicing ( $n=10$ ) was tried. In these trials, the brain was completely “baked” into Agar with as little empty space as possible. This approach was, however, found to be suboptimal due to a number of factors. During immersion in Agar the tissue becomes heated to approximately 30 °C which affected the cell survival rate negatively. Furthermore, due to bad visibility when the brain is in Agar and as the thin and elongated brain tended to “sag” it was hard to identify exactly where the cuts were positioned. Therefore, this method was found to be unsuitable.

### 2.3. Electrophysiology and microscopy

The slice preparation was placed in a round recording chamber and held in place with a small net. Neurons were visualised using infrared (IR) illumination and differential interference contrast (IR-DIC) optics (Zeiss Axioskop 2FS+ or Olympus BX50WI), and approached under visual guidance using a remote control manipulation system (Luigs & Neumann, Ratingen, Germany). Whole-cell recordings of lamprey striatal neurons, in either voltage clamp (Fig. 2D) or current clamp configuration (Fig. 2E and F), were obtained using borosilicate patch-clamp electrodes (5–10 MΩ, 150F/10, Harvard Apparatus, Kent, UK) filled with a solution containing (in mM): MgCl<sub>2</sub>, 1.2; glucose, 10; HEPES, 10; CaCl<sub>2</sub>, 1; KCH<sub>3</sub>SO<sub>4</sub>, 102; EGTA, 10; ATP, 3.944; GTP, 0.3; phosphocreatine, 5 (265–275 mOsm, pH 7.6). In a

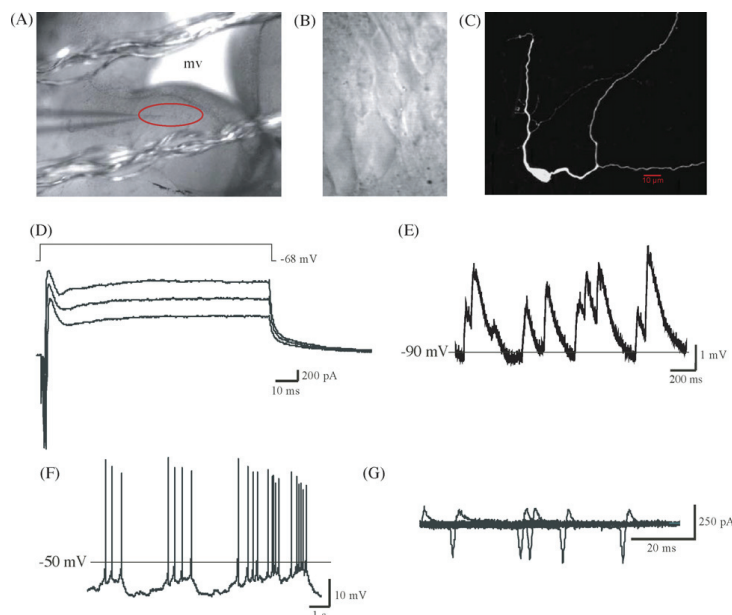


Fig. 2. The condition of the slice preparation was assessed visually and electrophysiologically. (A) Identification and recording of neurons in the slice preparation. The striatum can be seen as a band of cells lying below the medial telencephalic ventricle (mv, 10 $\times$ ). The patch-clamp electrode can be seen extending into the striatum from the left. (B) Enlarged picture of the striatum. (C) Neurobiotin-filled lamprey striatal neuron ( $n=10$ ). (D) Voltage steps ( $n=20$ ) were made in voltage-clamp to investigate if the activation and kinetics of Na<sup>+</sup> and K<sup>+</sup> currents appeared normal. (E) A current-clamp recording of a neuron receiving spontaneous synaptic input. Many neurons ( $n=10$ ) exhibited strong spontaneous depolarizing synaptic inputs, as well as plateau potentials. (F) In some cases ( $n=3$ ) action potentials could be observed superimposed on the depolarized plateaus (current-clamp recording). (G) Some lamprey striatal neurons ( $n=4$ ) fired spontaneously which could be observed with recordings in the on-cell configuration.

few cases ATP, GTP and phosphocreatine were excluded. In many cases, neurons ( $n=30$ ) were injected with 0.3% neurobiotin (Vector Laboratories Inc., CA, USA) that had been added to the intracellular solution to enable later visualization of the neurons in the confocal microscope (Zeiss LSM 510 Meta). All recordings were made using either an Axopatch 200B or a Multiclamp 700B amplifier (Molecular Devices Corp., Synnyswale, CA, USA) and digitized at 10–50 kHz by a PC computer. All membrane potential values were corrected for the liquid junction potential.

### 3. Results

Evaluation of the slice preparation was made with visual inspection and whole-cell patch-clamp recordings of identified lamprey striatal neurons. The recordings made in this study were made to investigate the condition of the slice and the neurons. A more detailed characterization of the neural properties of lamprey striatal neurons is currently being made in our lab.

#### 3.1. Identifications of the striatum in the slice

Due to its small size and the nearby location of other nuclei such as the nucleus preopticus and the dorsal and lateral pallia, it

is important to identify the striatum in the slice preparation correctly. Identification was, during the early phases of the study, made by using the brain maps from earlier studies made by Pombal et al. (1997a,b). Identification was, however, best made with a detailed map of the *L. fluviatilis* brain in coronal sections that recently has been made in our lab (Robertson et al., personal communication, Fig. 1E and F). We set up the following criteria to be able to identify the striatum in the slice: the medial telencephalic ventricle should be clearly visible and + -shaped (Fig. 1C–F). Furthermore, both the medial and lateral pallia should be present. In addition, the lateral ventricle should be clearly visible in a slice containing the rostral striatum (Fig. 1C and E). In slices meeting these criteria, the striatum could be identified in between the dorsal pallium and the nucleus preopticus (Fig. 1C–F) and could often be seen as a band of cells in the microscope even at low magnification (Fig. 2A; 10 $\times$ ).

#### 3.2. Visualization and patch-clamp recordings of striatal neurons

Visualization of the neurons was made with IR-DIC microscopy (Fig. 2B). In addition, neurobiotin-injected neurons ( $n=30$ ) were studied in the confocal microscope (Fig. 2C) to enable a detailed view. The visual impression of the neurons that

appeared neither shrunken nor swollen indicated that the neurons were healthy and that the intra- and extracellular solutions were suitable. Cell survival appeared to be best using carbonate-based aCSF.

It has been suggested that it is difficult to make patch-clamp recordings in adult lamprey neural tissue partly due to difficulty in penetrating the tissue with the patch-clamp electrode. In this study, we found that with an outward air pressure applied to the patch pipette it was possible to advance through the neural tissue. The tissue was, however, less easy to penetrate compared to rodent preparations and it was therefore necessary to apply a relatively strong outward pressure through the pipette. No apparent differences compared to rodent preparations in the ability in forming gigaseals or going into the whole-cell configuration could be found.

In order to assess how healthy the neurons in the slice were we investigated the resting membrane potential, the current responses to stepwise depolarizations in voltage-clamp (Fig. 2D,  $n=20$ ), the form and threshold of the action potential (elicited by current injection (current-clamp) or resulting from synaptic input) and any spontaneous synaptic activity. The neurons resting membrane potential (RMP) was  $-70.6 \pm 1.7$  mV ( $n=53$ ). Furthermore, the neurons received excitatory spontaneous synaptic transmission (Fig. 2E, current-clamp) that results suggest was glutamatergic as it could be blocked with CNQX ( $40 \mu\text{M}$ ,  $n=5$ ), and as it could not be reversed by depolarizations up to  $-20$  mV. Action potentials could easily be elicited by depolarizing current pulses and had a firing threshold of  $-46.7 \pm 0.7$  mV ( $n=32$ ). Some neurons ( $n=4$ ) were firing action potentials spontaneously which could be observed in on-cell configuration before breaking into the cell (Fig. 2G). In addition, many neurons ( $n=10$ ) exhibited strong membrane potential oscillations with an amplitude of 5–20 mV (Fig. 2F).

#### 4. Discussion

In the present paper we describe the development of a slice preparation for the detailed study of neuronal mechanisms in the striatum and the first patch-clamp recordings made from neurons in the lamprey telencephalon. Previously, no patch-clamp recordings have been demonstrated from higher brain areas in the lamprey. However such recordings have been made in spinal cord (Cochilla and Alford, 1997; Schwartz et al., 2005), brainstem (Alford and Dubuc, 1993) and from dissociated spinal neurons (El Manira and Bussières, 1997; Wikström et al., 1999).

The CNS of the lamprey is comparatively similar to that of higher vertebrates although with a lower level of complexity (Grillner, 2003; Grillner and Wallén, 2002). The lamprey has been shown to be an excellent model for the study of the neuronal control, on supraspinal and spinal levels, of motor functions. However, studies involving the detailed physiological characteristics of neurons have so far mostly been restricted to brainstem and spinal cord areas. To understand the control of motor actions mediated by the brain it is important to be able to study neuronal and microcircuit mechanisms in structures such as the striatum with electrophysiological means. This clearly demonstrates the

need for a brain slice preparation for the study of the detailed cellular and synaptic interactions in the lamprey striatum. Such a preparation is necessary in order to study how the striatal microcircuits operate, how striatal neurons projecting to the putative pallidum are activated and controlled, and how the basal ganglia control motor behaviour.

We have therefore developed an efficient method for the production of healthy striatal brain slices from the lamprey. The procedure presented produces a preparation of good quality that will last for 4–6 h when kept in a 4–8 °C storage solution. There are, however, a number of specific problems that have to be taken into account and actions that are crucial; (1) it is important to be very careful during the removal of the brain as it is extremely soft and the olfactory bulbs easily detach from the rest of the brain. If this happens it is necessary to discard the preparation. (2) Cell survival is best using carbonate-based aCSF. Preincubation with low  $\text{Ca}^{2+}$  concentration or TTX before cutting in order to reduce synaptic activity in the preparation affected cell survival only slightly if at all. (3) The cutting of the preparation should be done as quickly as possible ( $\leq 4$  min) as it is not possible to have it immersed in aCSF while this is being done. The reason for this is that the lamprey brain cannot be fastened with glue as is usual for rodent preparations. (4) Vertical cutting with a slow blade advance speed and a high vibration frequency during cutting worked best. (5) Care also needs to be taken to minimize movement of the preparation during cutting. This may be done by creating a groove in the Agar in which the brain is placed. After the slices have been cut they should be stored in cold (4–8 °C) normal aCSF. (6) As the slice preparation is small and the neural tissue dense, it is necessary to fixate the preparation well to avoid movement when the patch-clamp electrode is advanced through the slice. Finally, it is advantageous (7) to have a relatively strong outward air pressure on the patch-clamp electrode while advancing through the slice.

Identification of the lamprey striatum in a coronal section is best made using the maps in Fig. 1C and D. Visualization of neurons should be made with IR-DIC microscopy. In order to assess if the neurons in the slice were healthy, we measured the RMP and action potential threshold. The RMP ( $\sim -71$  mV) was on the average approximately 7 mV more depolarized than what has been reported for spinal ( $-77.4 \pm 4.5$  mV, Buchanan, 1993) neurons. This may be due to strong excitatory synaptic transmission to the striatal neurons (see Section 3) although it should be remembered that different neuronal types often exhibit differences in RMP. Furthermore, some of the neurons had a significantly more hyperpolarized RMP. The RMP for reticulospinal neurons have been reported by different authors. Rouse et al. (1998) reported it to be approximately  $-65$  mV while others have reported more hyperpolarized values ( $-74.6 \pm 0.6$  mV, Le Ray et al., 2004).

The firing threshold for the striatal neurons was  $\sim -47$  mV while it has been reported to be  $-54.4 \pm 6.5$  mV in spinal neurons (Buchanan, 1993).

A comprehensive study of the electrophysiological properties of lamprey striatal neurons was not within the scope of the present study. However, as mentioned in the results section such a characterization is currently being made in our lab.

In all, this new lamprey striatal slice preparation will enable detailed studies of the cellular and synaptic mechanisms in the lamprey striatum that can be correlated with striatal output to other structures and downstream activation of reticulospinal neurons and the spinal locomotor CPG. This should lead to important new information concerning the basal ganglia involvement in the control of motor functions. Furthermore, the technique described here can easily be adapted for the production of brain slices from other areas of the lamprey brain.

### Acknowledgements

We are grateful to Prof. Sten Grillner for advice and valuable comments on the manuscript. This work was supported by the Swedish Research Council, Magnus Bergvalls foundation and the Swedish Medical Association.

### References

- Alford S, Dubuc R. Glutamate metabotropic receptor mediated depression of synaptic inputs to lamprey reticulospinal neurones. *Brain Res* 1993;605:175–9.
- Brocard F, Dubuc R. Differential contribution of reticulospinal cells to the control of locomotion induced by the mesencephalic locomotor region. *J Neurophysiol* 2003;90:1714–27.
- Brodin L, Hökfelt T, Grillner S, Panula P. Distribution of histaminergic neurons in the brain of the lamprey *Lampetra fluviatilis* as revealed by histamine-immunohistochemistry. *J Comp Neurol* 1990a;292:435–42.
- Brodin L, Theodorsson E, Christenson J, Cullheim S, Hökfelt T, Brown JC, et al. Neotensin-like Peptides in the CNS of lampreys: chromatographic characterization and immunohistochemical localization with reference to aminergic markers. *Eur J Neurosci* 1990b;2:1095–109.
- Brown LL, Schneider JS, Lidsky TI. Sensory and cognitive functions of the basal ganglia. *Curr Opin Neurobiol* 1997;7:157–63.
- Buchanan JT. Electrophysiological properties of identified classes of lamprey spinal neurons. *J Neurophysiol* 1993;70:2313–25.
- Cochilla AJ, Alford S. Glutamate receptor-mediated synaptic excitation in axons of the lamprey. *J Physiol* 1997;499:443–57.
- Deliagina TG, Pavlova EL. Modifications of vestibular responses of individual reticulospinal neurons in lamprey caused by unilateral labyrinthectomy. *J Neurophysiol* 2002;87:1–14.
- Deliagina TG, Zelenin PV, Orlovsky GN. Encoding and decoding of reticulospinal commands. *Brain Res Brain Res Rev* 2002;40:166–77.
- Dube L, Smith AD, Bolam JP. Identification of synaptic terminals of thalamic or cortical origin in contact with distinct medium-size spiny neurons in the rat neostriatum. *J Comp Neurol* 1988;267:455–71.
- El Manira A, Bussièrès N. Calcium channel subtypes in lamprey sensory and motor neurons. *J Neurophysiol* 1997;78:1334–40.
- El Manira A, Pombal MA, Grillner S. Diencephalic projection to reticulospinal neurons involved in the initiation of locomotion in adult lampreys *Lampetra fluviatilis*. *J Comp Neurol* 1997;389:603–16.
- Gerfen CR. Synaptic organization of the striatum. *J Electron Microscop Technol* 1988;10:265–81.
- Grillner S. The motor infrastructure: from ion channels to neuronal networks. *Nat Rev Neurosci* 2003;4:573–86.
- Grillner S, Hellgren J, Ménard A, Saitoh K, Wikström MA. Mechanisms for selection of basic motor programs—roles for the striatum and pallidum. *Trends Neurosci* 2005;28:364–70.
- Grillner S, Wallén P. Cellular bases of a vertebrate locomotor system—steering, intersegmental and segmental co-ordination and sensory control. *Brain Res Brain Res Rev* 2002;40:92–106.
- Groenewegen HJ. The basal ganglia and motor control. *Neural Plast* 2003;10:107–20.
- Huston JP, Wagner U, Hasenohr RU. The tuberomammillary nucleus projections in the control of learning, memory and reinforcement processes: evidence for an inhibitory role. *Behav Brain Res* 1997;83:97–105.
- Le Ray D, Brocard F, Dubuc R. Muscarinic modulation of the trigemino-reticular pathway in lampreys. *J Neurophysiol* 2004;92:926–38.
- Ménard A, Auclair F, Bourcier-Lucas C, Grillner S, Dubuc R. Descending GABAergic projections to the mesencephalic locomotor region in the lamprey *Petromyzon marinus*. *J Comp Neurol* 2007;501:260–73.
- Nicola SM, Surmeier J, Malenka RC. Dopaminergic modulation of neuronal excitability in the striatum and nucleus accumbens. *Annu Rev Neurosci* 2000;23:185–215.
- Panula P, Karlstedt K, Sallmen T, Peitsaro N, Kaslin J, Michelsen KA, et al. The histaminergic system in the brain: structural characteristics and changes in hibernation. *J Chem Neuroanat* 2000;18:65–74.
- Pombal MA, El Manira A, Grillner S. Afferents of the lamprey striatum with special reference to the dopaminergic system: a combined tracing and immunohistochemical study. *J Comp Neurol* 1997a;386:71–91.
- Pombal MA, El Manira A, Grillner S. Organization of the lamprey striatum—transmitters and projections. *Brain Res* 1997b;766:249–54.
- Rouse DT, Quan X, McLellan AD. Biophysical properties of descending brain neurons in larval lamprey. *Brain Res* 1998;779:301–8.
- Rovainen CM. Neurobiology of lampreys. *Physiol Rev* 1979;59:1007–77.
- Schwartz EJ, Gerachshenko T, Alford S. 5-HT prolongs ventral root bursting via presynaptic inhibition of synaptic activity during fictive locomotion in lamprey. *J Neurophysiol* 2005;93:980–8.
- Thompson RH, Woolley JD, Grillner S. Forebrain dopamine depletion produces severe motor deficits in lamprey. *Soc. Neurosci. Abstr.* 2000;26:554.1.
- Wikström MA, Grillner S, El Manira A. Inhibition of N- and L-type  $Ca^{2+}$  currents by dopamine in lamprey spinal motoneurons. *Neuroreport* 1999;10:3179–83.
- Wilson CJ, Chang HT, Kitai ST. Origins of post synaptic potentials evoked in spiny neostriatal projection neurons by thalamic stimulation in the rat. *Exp Brain Res* 1983;51:217–26.

II



## Striatal cellular properties conserved from lampreys to mammals

Jesper Ericsson, Gilad Silberberg, Brita Robertson, Martin A. Wikström and Sten Grillner

*Nobel Institute for Neurophysiology, Department of Neuroscience, Stockholm Brain Institute, Karolinska Institutet, SE-171 77 Stockholm, Sweden*

**Non-technical summary** The striatum is a structure in the forebrain that plays an important role in the control of movements. Diseases that affect this region lead to severe movement disorders, such as Parkinson's disease. We show here in the lamprey, the oldest vertebrate group to emerge, that the characteristic cellular properties of neurons in striatum in many respects are similar to those of mammals. Our results show how specific ion channels, including particular potassium channels (Kir) that are open at very negative membrane potentials help shape the way these cells respond to and transmit neuronal signals. These specific features are thus conserved throughout vertebrate evolution, and contribute thereby to our understanding of the mode of operation of striatum, at a cellular level, and how movements are controlled.

**Abstract** The striatum of the lamprey, the first vertebrate group to appear in evolution, shows striking similarities to that of mammals with respect to histochemical markers, afferent and efferent projections and the effect of dopamine depletion, which leads to hypokinetic motor symptoms. The cellular properties of lamprey striatal neurons were studied here using patch-clamp recordings in acute striatal slices. Sixty-five per cent of recorded neurons were characterised by a prominent inward rectification due to a  $K^+$  conductance of the Kir type. They had a ramping response with a long delay to the first action potential due to activation of a low-voltage-activated A-type  $K^+$  current. Many such inwardly rectifying neurons (IRNs) had a hyperpolarised resting membrane potential and some had spiny dendrites. The remaining 35% of the neurons (non-IRNs) represent a heterogeneous group, including some with characteristics similar to the fast-spiking interneuron of the mammalian striatum. They showed short-lasting, large afterhyperpolarisations (AHPs) and discharged action potentials at high frequency. None of the recorded neurons were spontaneously active but they received GABAergic and glutamatergic synaptic input. The fact that most lamprey striatal neurons display inward rectification indicates that this is a conserved characteristic of striatal neurons throughout vertebrate phylogeny. This is a cellular property of critical importance for the operations of the striatum in mammals.

(Resubmitted 26 March 2011; accepted after revision 12 April 2011; first published online 18 April 2011)

**Corresponding author** S. Grillner: Nobel Institute for Neurophysiology, Department of Neuroscience, Stockholm Brain Institute, Karolinska Institutet, SE-171 77 Stockholm, Sweden. Email: sten.grillner@ki.se

**Abbreviations** AHP, afterhyperpolarisation; 4-AP, 4-aminopyridine; DAB, diaminobenzidine; IRN, inwardly rectifying neuron; Kir, inwardly rectifying potassium channels; MPTP, 1-methyl-4-phenyl-1,2,3,6-tetrahydropyridine; MSN, medium spiny neuron; PIR, post-inhibitory rebound.

## Introduction

In the mammalian striatum, 95% of all neurons are GABAergic medium spiny projection neurons (MSNs; cf. Tepper *et al.* 2007). They are characterised by a negative resting potential due to the presence of potassium channels of the inward rectifier type (Kir) that are open at negative potentials, but closed when the membrane potential is brought to more depolarised levels by synaptic excitatory drive. This property of MSNs makes them difficult to activate by the glutamatergic input from cortex and thalamus (Wilson & Kawaguchi, 1996; Tepper *et al.* 2004; Grillner *et al.* 2005). The responsiveness of MSNs is, however, regulated by the degree of dopaminergic modulatory drive (Surmeier *et al.* 2007; Redgrave *et al.* 2008). Without the presence of a dopamine input, mammals become hypokinetic and acquire Parkinsonian symptoms. Conversely, an enhanced level of dopamine leads to hyperkinesias with an unintended initiation of motor programmes.

Kir was recently shown to be a characteristic feature of MSNs in reptiles (Barral *et al.* 2010), which would suggest that Kir is an important property of striatal function in all amniotes (Kawaguchi *et al.* 1989; Farries & Perkel, 2000). Other characteristic features of MSNs are hyperpolarised resting potentials and a ramping response with a long delay to the first action potential due to low-voltage-activated A-type K<sup>+</sup> channels (Kawaguchi *et al.* 1989; Uchimura *et al.* 1989; Nisenbaum & Wilson, 1995).

Cyclostomes (jawless fish like lampreys) represent the first vertebrate group to emerge in evolution. They deviated from the evolutionary line leading up to mammals already 530–560 million years ago, around 200 million years before reptiles emerged (Olsen, 2007). Although a striatum is present in all vertebrates, no information regarding the presence of Kir is available in amphibians, fish or cyclostomes (anamniotes). Recent findings in the lamprey striatum show that it contains spiny GABAergic projection neurons that express dopamine D1 and D2 receptors, tachykinins and enkephalin (Pombal *et al.* 1997b, 2001; Auclair *et al.* 2004; Ericsson *et al.* 2010; Robertson *et al.* 2010). Striatum receives input from pallidum (cortex in mammals) and thalamus, as well as a dopaminergic, 5-HT and histaminergic input (Brodin *et al.* 1990a,b; Jimenez *et al.* 1996; Pombal *et al.* 1997a). The lamprey striatum thus receives the same type of input and expresses the same molecular markers as in mammals and other amniotes. Dopamine depletion with 1-methyl-4-phenyl-1,2,3,6-tetrahydropyridine (MPTP) renders the lamprey hypokinetic, as in Parkinson's, an effect that can be counteracted by dopamine agonists (Thompson *et al.* 2008). It thus appears that also with regard to function, the role of the basal ganglia is conserved.

In this study we wanted to characterise neurons in the lamprey striatum in terms of their electrophysiological, morphological and synaptic input, and isolate some of the key properties supporting generic striatal function in vertebrates.

## Methods

### Ethical approval

All experimental procedures conformed to the guidelines of the Stockholm municipal committee for animal experiments.

### Slice preparation

Coronal brain slices, 300–500  $\mu\text{m}$  thick, were prepared from 46 lampreys (*Lampetra fluviatilis*), as described earlier (Ericsson *et al.* 2007). Usually only one brain slice per animal containing the striatum, located lateral to the medial telencephalic ventricle (Fig. 1A and B), in both hemispheres was obtained due to the small size of the striatum. The striatum can be clearly seen as a well-defined band of cell bodies (Fig. 1A–C). These cells are GABAergic and express substance P and enkephalin, and D1 and D2 receptors (Pombal *et al.* 1997b; Robertson *et al.* 2007, 2010). Slices were kept at 4–8°C in artificial cerebrospinal fluid (aCSF) of the following composition (in mM): 125 NaCl, 2.5 KCl, 1 MgCl<sub>2</sub>, 1.25 NaH<sub>2</sub>PO<sub>4</sub>, 2 CaCl<sub>2</sub>, 25 NaHCO<sub>3</sub> and 20 glucose. The aCSF was oxygenated continuously with 95% O<sub>2</sub> and 5% CO<sub>2</sub> (pH 7.4) and was also used for perfusion during recordings at the same temperature (Badkontroller V, Luigs & Neumann, Ratingen, Germany).

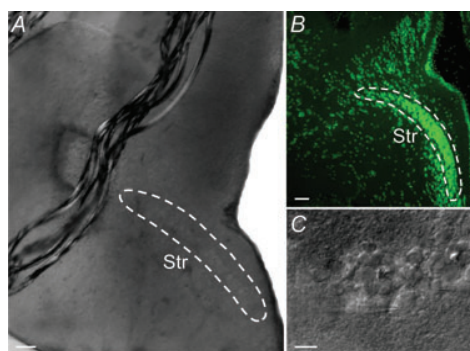


**Figure 1. Anatomical location of the striatum (Str)**

A, coronal acute brain slice in the recording chamber showing the striatal cell band inside the white lines. B, fluorescent Nissl staining of a coronal section displaying the band of striatal cell bodies. C, photograph of individual striatal neurons in the recording chamber. Scale bars = 100  $\mu\text{m}$  in A and B, 15  $\mu\text{m}$  in C.



### Electrophysiology and morphological reconstruction

Patch-clamp electrodes (7–12 M $\Omega$ ) were filled with (in mM): 102 KCH<sub>3</sub>SO<sub>4</sub>, 1.2 MgCl<sub>2</sub>, 10 Hepes, 1 CaCl<sub>2</sub>, 10 EGTA, 3.94 Mg-ATP, 0.3 Na-GTP, 5 phosphocreatine sodium salt and 10 glucose (osmolarity 265–275 mosmol l<sup>-1</sup>) or with an alternative solution with a higher chloride concentration: 105 potassium gluconate, 30 KCl, 10 Hepes, 4 Mg-ATP, 0.3 Na-GTP and 10 phosphocreatine sodium salt (osmolarity 270 mosmol l<sup>-1</sup>). Patch electrodes were prepared from borosilicate glass microcapillaries (Harvard Apparatus, Edenbridge, UK) using a two-stage puller (PP-830, Narishige, Japan). Whole-cell recordings were performed in current- or voltage-clamp mode using a Multiclamp 700B amplifier (Molecular Devices, Sunnyvale, CA, USA) and digitised at 10–50 kHz by a PC. Bridge balance and pipette capacitance compensation were automatically adjusted on the amplifier and all membrane potential values were corrected for the liquid junction potential. Neurons were visualised (see example in Fig. 1A and C) with DIC/infrared optics (Zeiss Axioskop 2FS plus, Munich, Germany) and electrodes were advanced using remote micromanipulators (Luigs & Neumann). Data was acquired with the Clampex software and analysed in Clampfit (pCLAMP, Molecular Devices).

Neurons were intracellularly stained by injection of 0.3–0.5% neurobiotin (Vector Laboratories, Burlingame, CA, USA) during recordings. Brain slices were fixed overnight in 4% formalin and 14% picric acid in 0.1 M phosphate buffer (PB) and analysed by either confocal or conventional light microscopy. For confocal imaging (Carl Zeiss LSM 510 Meta, München, Germany), slices were first incubated in streptavidin-Cy2 (1:1000, Jackson ImmunoResearch Laboratories, West Grove, PA, USA) in 0.3% Triton X-100 and 1% BSA in 0.1 M PB overnight. The slices were then washed in 0.01 M phosphate buffered saline (PBS) before being dehydrated in alcohol and transferred to methyl salicylate (Merck, NJ, USA) prior to mounting in DPX (Fluka/Sigma-Aldrich, St Louis, MO, USA). Confocal image reconstructions were made and analysed using Zeiss LSM Image Browser and ImageJ software (Rasband WS, National Institutes of Health, Bethesda, MD, USA). Some slices were instead processed with the Vectastain Elite ABC kit (Vector Laboratories). Slices were thoroughly washed in 0.01 M PBS and incubated in 0.6% hydrogen peroxidase in methanol for 20 min, rinsed in PBS and transferred to the ABC solution for 3 h. After rinsing in PBS, slices were incubated in diaminobenzidine (DAB; ImmPACT DAB, Vector Laboratories) for 5 min, then rinsed and dehydrated in alcohol prior to mounting in DPX. Subsequently, neurons were visualised in a light microscope (Olympus BX51, Melville, NY, USA) and photomicrographs were taken using Cell A (Olympus).

Formalin fixed lamprey brain sections, 20  $\mu$ m thick, were stained with a green fluorescent Nissl stain (1:1000;

Molecular Probes Europe BV, Leiden, the Netherlands) for analysis of striatal morphology.

### Electrophysiological analysis

Neurons that had stable responses with large over-shooting (reaching above 0 mV) action potentials (mean amplitude  $\sim$ 54 mV) during step depolarisations in current clamp recordings were considered healthy and were subsequently analysed (see for example Fig. 2A). Most recordings were performed in current clamp mode, with injections of hyperpolarising and depolarising current steps to investigate voltage responses. Action potentials were triggered by positive current pulses and the amplitude measured relative to the firing threshold.

The time delay to the first action potential was measured on the first current injection step that elicited an action potential, in a series of increasing steps from a baseline around  $-75$  mV. The input resistance of neurons was calculated by dividing the steady-state voltage response by the applied current injection. A rectification index was defined as the ratio between the input resistance at very hyperpolarised potentials (around  $-100$  to  $-120$  mV) and the input resistance at the resting potential, where no obvious Na<sup>+</sup> conductances had been activated. Thus, large rectification would inversely correspond to a low index since the input resistance at hyperpolarised levels is low while it is significantly higher at more depolarised levels.

To quantify the voltage 'sag' sometimes seen at hyperpolarised potentials, a sag index was calculated. The sag index was defined as the difference of the most hyperpolarised voltage and the steady-state voltage deflection of that pulse (Sag  $\Delta V$  in Fig. 4A) divided by the steady-state deflection. Thus, a large voltage sag correspond to a high sag index, so for example an index of 1 would correspond to an amplitude of the hyperpolarised voltage that was twice as large as the steady-state response.

The average action potential frequency in a spike train was measured between the first and the last action potential during a 1 s suprathreshold current injection. Spontaneous synaptic inputs were recorded using an alternative intracellular solution with 30 mM KCl in the pipette solution to ensure that GABAergic events were detected more easily as depolarising events at the resting potential. These were measured in current clamp mode and analysed by monitoring the frequency of events before and during bath application of drugs.

The following drugs were used and applied directly in the extracellular bath: the K<sup>+</sup> channel blocker 4-aminopyridine (4-AP, 100–500  $\mu$ M, Sigma-Aldrich, St Louis, MO, USA), Barium chloride (100  $\mu$ M Sigma-Aldrich), the monovalent cation current  $I_h$  antagonist ZD 7288 (50  $\mu$ M, Tocris Bioscience, Ellisville, MO, USA), the

AMPA receptor antagonist NBQX disodium salt ( $40\ \mu\text{M}$ , Tocris) and the GABA<sub>A</sub> receptor antagonist gabazine ( $40\ \mu\text{M}$ , Tocris).

### Statistics

Results are presented as means  $\pm$  standard deviation (SD) and statistical comparisons between means were made with Student's two-tailed paired *t* test with GraphPad Prism Software (GraphPad Software, San Diego, CA, USA).

### Results

Whole-cell recordings were obtained from 74 neurons that were classified into two main subgroups based on the presence or absence of inward rectification observed by injection of depolarising and hyperpolarising current steps. Pronounced inward rectification is a hallmark

of MSNs in amniotes and clearly differentiates these neurons from other striatal interneurons and is therefore of special interest (Kawaguchi *et al.* 1989; Grillner *et al.* 2005; Barral *et al.* 2010). It is identified by lower input resistance at more negative potentials due to the opening of K<sup>+</sup> (Kir) channels (Uchimura *et al.* 1989). An example of an inwardly rectifying neuron is depicted in Fig. 2A. The rectification in lamprey striatal neurons was quantified by calculating the ratio between the input resistance at  $-120\ \text{mV}$  and at resting potential (Fig. 2B and C). Two clusters of neurons with rectification ratios below or above 0.5 were apparent when plotting the rectification ratios (Fig. 2B). Forty-eight neurons (65%) had rectification values below 0.5 and displayed clear inward rectification, seen by visual inspection of the voltage responses to stepwise hyperpolarising and depolarising current injections at subthreshold values, and are referred to as inwardly rectifying neurons (IRNs). The population of neurons with rectification values above 0.5 did not show marked inward rectification (Fig. 6) and are

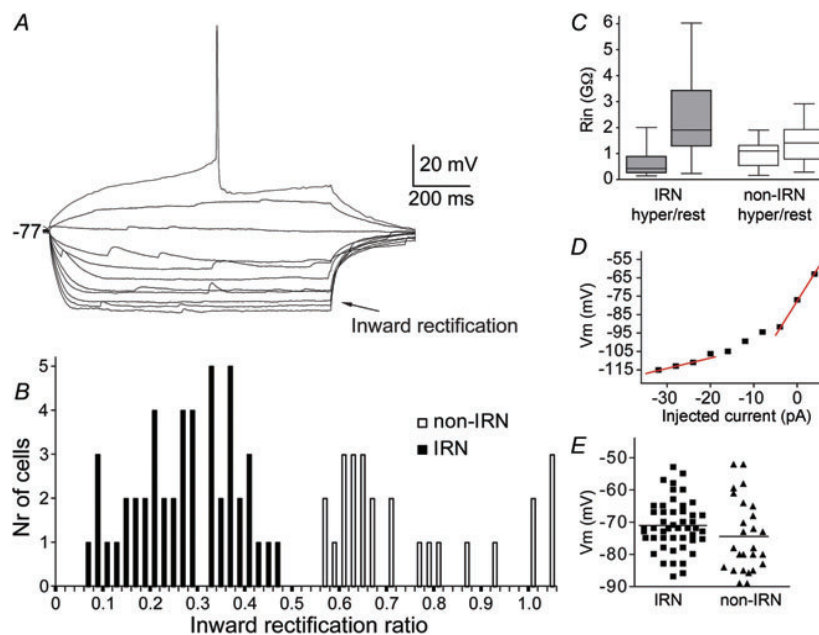


**Figure 2. Properties of IRNs and distribution of parameters of both IRNs and non-IRNs**

A, voltage responses of an IRN to hyperpolarising and depolarising 1 s current steps of 4 pA per step, elicited from rest at  $-77\ \text{mV}$ . Inward rectification is seen as relatively small voltage responses at hyperpolarised potentials (arrow) with each step and increasingly larger responses at more depolarised levels. The rectification ratio is 0.34. B, histogram of the inward rectification ratio for all neurons. Neurons with ratio below 0.5 form a population defined as IRNs and those above 0.5 as non-IRNs. C, plot of the input resistance ( $R_{in}$ ) of IRNs and non-IRNs, measured at a hyperpolarised potential ( $-120\ \text{mV}$ ) and at resting membrane potentials. D, I-V plot of the steady-state voltage deflections to current steps of the neuron displayed in A. Note the steeper slope at more depolarised potentials. E, distribution of the resting membrane potentials of recorded neurons.

Table 1. Cellular properties of lamprey striatal neurons

	IRNs	non-IRNs
Neurons (n)	48	26
Resting potential (mV)	$-71.2 \pm 7.8$	$-74.2 \pm 11.7$
Inward rectification ratio	$0.28 \pm 0.10$	$0.75 \pm 0.17$
Delay to AP (ms)	$420 \pm 135$	$345 \pm 110$
AP amplitude (thr to peak) (mV)	$54.4 \pm 10.9$	$55.4 \pm 10.2$
AP half-width (ms)	$3.3 \pm 1.6$	$3.4 \pm 1.4$
AP threshold (mV)	$-46.4 \pm 4.4$	$-46.9 \pm 4.1$
Amplitude of monophasic AHP (mV)	$-22.8 \pm 6.3$	$-18.9 \pm 6.8$
Neurons with both fAHP and sAHP (n)	6	7
Neurons with spike frequency adaptation (n)	3	7
Neurons with PIR APs (n)	18	4

All values are means  $\pm$  SD. AP, action potential; AHP, afterhyperpolarization; PIR, post-inhibitory rebound; thr, threshold.

referred to as 'non-IRNs'. We recognise that some neurons classified as non-IRNs here still exhibit a certain degree of inward rectification as indicated by the inward rectification ratio in Fig. 2B. No neurons fired action potentials at rest. The basic membrane properties of the two groups are summarised in Table 1.

### Inwardly rectifying neurons

**Basic electrophysiological properties.** IRNs displayed a characteristic voltage response due to inward rectification, hyperpolarised resting membrane potentials and a ramping response to depolarising current injections resulting in a long delay to the first action potential. Figure 2A shows the typical appearance of an IRN with an inward rectification ratio of 0.34, with an overall mean ratio for the IRN population of  $0.28 \pm 0.10$ , ranging from 0.07 to 0.45 (Fig. 2B). Many cells (25%) displayed very strong rectification (ratio  $\leq 0.20$ ). The input resistance was much lower at hyperpolarised membrane potential levels than at rest within the IRN population (Fig. 2C). The strongest rectification was normally seen below  $-90$  mV, similar to findings in rodents although not as pronounced (Kawaguchi *et al.* 1989; Jiang & North, 1991; Cepeda *et al.* 2008). The steady state  $I$ - $V$  curve in Fig. 2D shows the characteristic difference in slope between hyperpolarised and more depolarised membrane potential levels, as is evident also from the current steps in Fig. 2A. IRNs had a mean resting potential of  $-71.2 \pm 7.8$  mV, with 65% of the neurons having values between  $-70$  mV and  $-87$  mV (see Fig. 2E for distribution).

Most IRNs (87.5%) displayed a monophasic AHP (Fig. 3A). The mean size of the monophasic AHP for IRNs was  $-22.8 \pm 6.3$  mV, as measured with reference to the threshold of the action potential, rather than the resting membrane potential. The voltage dependence of the monophasic AHP is illustrated in Fig. 3A. The size of the AHP was increased upon

depolarisation and was reversed at levels around  $-75$  to  $-80$  mV, indicating that the underlying current was a  $K^+$  current. The time to peak of the AHP was variable (Fig. 3B) with a mean of  $30.5 \pm 19.9$  ms for the neurons with monophasic AHPs. Six IRNs (12.5%) displayed a biphasic AHP with the time to the second maximum ranging from 41 ms to 170 ms, and with a mean of  $89.8 \pm 45.7$  ms. The mean amplitude of the slow AHP (sAHP) was  $-15.8 \pm 5.0$  mV. The time to the peak of the fast AHP (fAHP) component was  $9.1 \pm 4.0$  ms. Half of these neurons showed a marked spike frequency adaptation with comparable properties to the neuron displayed in Fig. 6G.

Seventy per cent of IRNs showed reliable and regular spiking with a limited spike frequency adaptation during sustained current injections (Fig. 3C and D), while the other 30% of neurons had some broadening of action potentials, firing failure at depolarised levels and sometimes irregular firing patterns. Action potentials had a threshold of  $-46.4 \pm 4.4$  mV, a half-width of  $3.3 \pm 1.6$  ms and amplitude of  $54.4 \pm 10.9$  mV (see Table 1). Fifty per cent of IRNs could discharge at frequencies of 15 Hz or above for a sustained period and a few (6%) up to at least 50 Hz. Most neurons appeared to saturate at their maximum firing frequencies, while the remainder showed action potential inactivation at further depolarisation.

Some of the IRNs showed a time- and voltage-dependent sag in their response to hyperpolarising current steps (Fig. 4D), contributing with a time-dependent component of the inward rectification. The sag was estimated by a sag index (see Methods), as exemplified by the cell in Fig. 4D with a sag index of 0.31. Only a minority (33%) of the IRNs (Fig. 4F), however, had a sag index 0.2 or above, a value not reached by any of the non-IRNs. The sag was most pronounced at hyperpolarised potentials and in many of these neurons it was not visible at voltages more depolarised than

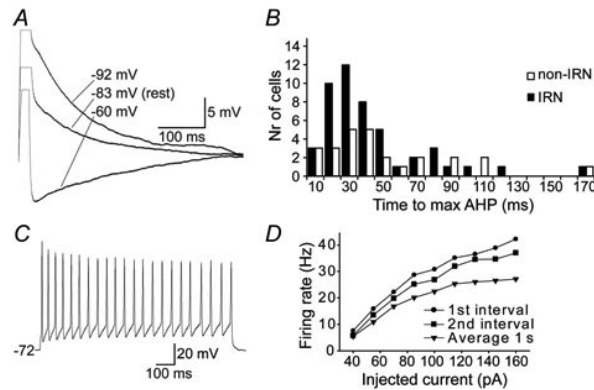


**Figure 3. Afterhyperpolarisation (AHP) and firing properties of IRNs**

A, the AHP of an IRN following the action potential elicited by a 5 ms positive current pulse. The AHP is shown at three different baseline potentials (–60, –83 and –92 mV), achieved by continuous current injections, to reveal the voltage dependence of the AHP. The AHP is reversed between –60 mV and –83 mV. B, frequency histogram of the time to maximum AHP for IRNs (black) and non-IRNs (white). C, response to suprathreshold current injections, showing the firing properties of the neuron in A. D, plot of firing rate as a function of the injected current during a 1 s current pulse in the neuron in C. The round markers indicates the instantaneous frequency of the first interval in the elicited train of action potentials and the squares the second interval. The triangles show the average firing frequency over the entire train of action potentials.

at –85 mV. At the termination of the hyperpolarising steps that were elicited from rest, a post-inhibitory rebound (PIR) depolarisation with spiking occurred (Fig. 4D) in 60% of these neurons with a sag index of 0.2 or larger. The larger the hyperpolarising steps, the greater the PIR depolarisation and the number of action potentials generated (up to 8 action potentials). PIR spikes could, however, also be elicited in a subset of IRNs without a sag when the hyperpolarising pulses were injected from

depolarised baselines around –60 mV but not at the more hyperpolarised resting state.

#### Pharmacological analysis of inward rectification in IRNs.

The Kir channels have been investigated in different species and cell types, including rat dorsal and ventral striatal cells, and they are known to be blocked by extracellular barium chloride at 100  $\mu$ M (Standen & Stanfield, 1978; Uchimura *et al.* 1989; Nisenbaum & Wilson, 1995). Through bath

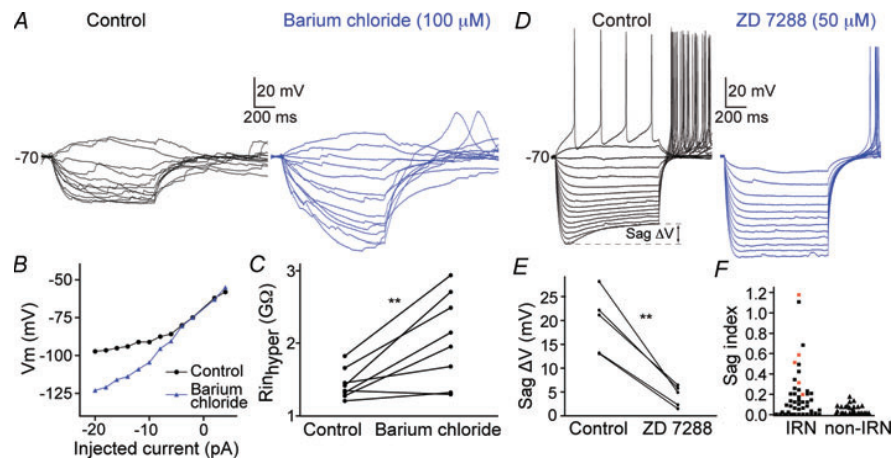


**Figure 4. Pharmacological analyses of Kir and I<sub>h</sub> in IRNs**

A, voltage responses of an IRN before (left) and during bath application of barium chloride (right) that blocks Kir-channels. B, I–V plot of the cell in A, that shifts from being upwardly concave (control) to a close to straight line (barium chloride). C, the input resistance at hyperpolarised potentials is increased during Ba<sup>2+</sup> application. D, the left voltage traces shows an IRN that also displays an I<sub>h</sub>-induced sag (see Sag  $\Delta V$ ) with a sag index of 0.31, followed by a post-inhibitory rebound with action potentials at the end of the hyperpolarising current steps. Under control conditions (left) the I<sub>h</sub> sag is seen clearly at hyperpolarised levels while bath application of the I<sub>h</sub> antagonist ZD 7288 almost completely removes the sag (right). E, the sag is reduced after application of ZD 7288 (50  $\mu$ M, n = 5). F, plot of the sag index for each IRN and non-IRN. The paler squares indicate the neurons in which ZD 7288 was applied.

application of barium chloride at this concentration, we show that the inward rectification is significantly reduced at subthreshold levels (Fig. 4A–C,  $n = 8$ ). Figure 4A shows an IRN before and during  $\text{Ba}^{2+}$  application, with increased voltage deflections between each current stimulation and prolonged time-constants. The  $I$ – $V$  relationship (Fig. 4B) changes from an upwardly concave curve to an almost straight line, reflecting a near constant input resistance below rest after the blockade with  $\text{Ba}^{2+}$ . The effect of  $\text{Ba}^{2+}$  was quantified by comparing the input resistance at hyperpolarised potentials (around  $-110$  mV) before and during barium and it increased significantly from  $1.44 \pm 0.2$  G $\Omega$  to  $2.06 \pm 0.6$  G $\Omega$  ( $P < 0.01$ ,  $n = 8$ ; Fig. 4C). The degree of rectification was associated with the change in input resistance, so that neurons with less rectification showed less change and the one neuron in Fig. 4C that did not increase its input resistance was also clearly defined as a non-IRN based on its inward rectification ratio (0.93). The application of  $\text{Ba}^{2+}$  was also accompanied by a depolarisation of neurons by 5–10 mV.

The effect of  $\text{Ba}^{2+}$  on the inward rectification in striatal neurons suggest that it is due to Kir-channels, and thus also due to a  $\text{K}^+$  conductance.

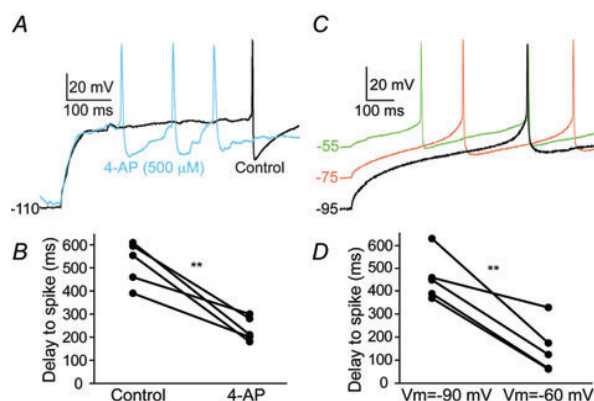
**Pharmacological analyses of  $I_h$  and A-type  $\text{K}^+$  current contribution to IRNs.** One-third of the IRNs had a voltage-dependent sag (Fig. 4D and F) that was examined by bath application of  $50 \mu\text{M}$  ZD 7288, an antagonist of the monovalent cation current  $I_h$  known to cause a voltage sag in other neurons (Harris & Constanti, 1995). Following ZD 7288 application, the sag decreased markedly from  $19.5 \pm 6.4$  mV to  $4.3 \pm 2.2$  mV ( $P < 0.01$ ,  $n = 5$ ; Fig. 4D and E). Figure 4D also shows that the inward rectification was reduced but maintained at a lower level after application of ZD 7288. In one neuron,  $\text{Ba}^{2+}$  was added 10 min following application of ZD 7288, effectively removing all inward rectification (data not

shown). ZD 7288 also affected the PIR depolarisation and the accompanying action potentials. The time to the first rebound action potential increased from  $104 \pm 24$  ms to  $235 \pm 48$  ms ( $P < 0.05$ ,  $n = 4$ ), and the number of rebound action potentials was reduced by 1–4 action potentials (Fig. 4D). These data clearly indicate that the sag is mediated by activation of an  $I_h$  current and partly also the accompanying PIR.

The characteristic ramping response and long delay to the first action potential in rat MSNs is mainly due to activation of a low-voltage-activated  $\text{K}^+$  current,  $I_A$ , activated at subthreshold membrane potentials and that inactivates after hundreds of milliseconds (Surmeier *et al.* 1991; Nisenbaum & Wilson, 1995; Shen *et al.* 2004). In lamprey, as well as mammals, this A-type  $\text{K}^+$  current is selectively depressed at low concentrations of 4-AP ( $100 \mu\text{M}$ ), while high concentrations also reduce the high-voltage-activated A-type  $\text{K}^+$  current (Rogawski *et al.* 1985; Surmeier *et al.* 1991; Nisenbaum & Wilson, 1995; Hess & El Manira, 2001). During investigation of the low-voltage-activated A-type  $\text{K}^+$  channels, neurons were held at very hyperpolarised levels to ensure that these channels were not voltage inactivated before the depolarising steps were given (Fig. 5A). 4-AP reduced the time delay to the first action potential (Fig. 5A and B) at a concentration of both  $100 \mu\text{M}$  ( $P < 0.05$ , control:  $518 \pm 93$  ms;  $100 \mu\text{M}$ :  $211 \pm 8$  ms,  $n = 3$ ) and  $500 \mu\text{M}$  ( $P < 0.01$ , control:  $522 \pm 84$  ms;  $500 \mu\text{M}$ :  $234 \pm 47$  ms,  $n = 5$ ). Similar results were obtained through voltage inactivation of the A-type  $\text{K}^+$  current by membrane depolarisation before current injections (Fig. 5C and D). The delay to the first action potential was reduced from  $460 \pm 92$  ms to  $151 \pm 99$  ms by changing the baseline membrane potential from  $-90$  mV to  $-60$  mV ( $P < 0.01$ ,  $n = 5$ ). It should be noted, however, that the long delays to first spike are present at rest in neurons (Fig. 2A and Table 1). These results suggest that an A-type  $\text{K}^+$  current

**Figure 5. Pharmacological analyses of the A-type  $\text{K}^+$  current contribution to IRNs**

A, voltage response to the first depolarising current step that elicits an action potential (black line, control) displaying the long delay to first action potential. During bath application of the  $I_A$  antagonist 4-AP at 100 and  $500 \mu\text{M}$  action potentials are evoked after a much shorter delay. Data only shown for  $500 \mu\text{M}$ . B, the time delay to the first action potential is reduced by several hundred milliseconds by 4-AP ( $500 \mu\text{M}$ ,  $n = 5$ ). C, the ramping response to first spike is also reduced by eliciting action potentials from different baseline potentials. The more depolarised baseline potential (from lower to middle to upper traces), the shorter the time-delay to first action potential. D, at  $-60$  mV, the time delay to first action potential is significantly shorter than at  $-90$  mV ( $n = 5$ ).





contributes to the ramping response with a long delay to the first spike, upon a depolarisation from a hyperpolarised level.

**Synaptic input to IRNs.** Lamprey striatal neurons receive glutamatergic spontaneous synaptic input (Ericsson *et al.* 2007). We show that striatal neurons also receive a continuous GABAergic input (Fig. 6A and B). Application of the GABA<sub>A</sub> receptor blocker gabazine (40  $\mu$ M) strongly reduced the spontaneous input ( $P < 0.01$ , control:  $5.48 \pm 1.61$  Hz; gabazine:  $2.48 \pm 1.36$  Hz,  $n = 5$ ). Further application of NBQX (40  $\mu$ M) blocked almost all of the remaining synaptic input ( $P < 0.01$ , gabazine:  $2.48 \pm 1.36$  Hz; NBQX+gabazine:  $0.10 \pm 0.17$  Hz,  $n = 5$ ). To facilitate the detection of GABAergic input at the resting membrane potential, these experiments were performed with an intracellular solution containing 30 mM chloride, thus shifting the reversal potential for GABA<sub>A</sub> responses to a predicted value around  $-35$  mV.

### Non-inwardly rectifying neurons

**Basic electrophysiological properties.** Non-IRNs represent a somewhat heterogeneous group ( $n = 26$ ) and are defined as having a rectification ratio larger than 0.5 ( $0.75 \pm 0.17$ , ranging from 0.56 to 1.05, see Fig. 2B), and  $I$ - $V$  traces with a close to linear relationship (Fig. 7A and B). The mean resting membrane potential was  $-74.2 \pm 11.7$  mV (Table 1), and 69% of the neurons had resting potentials below  $-70$  mV (Fig. 2E). Most neurons demonstrated long delays to the first action potential ( $345 \pm 110$  ms) with amplitudes of  $55.4 \pm 10.2$  mV (Table 1). The action potential threshold was

$-46.9 \pm 4.1$  mV and the half-width  $3.4 \pm 1.4$  ms. When the non-IRNs are taken as a group there are, except for the rectification ratio and the lack of  $I_h$  (Fig. 4F), no prominent differences in cellular properties compared to IRNs (see Table 1).

One subgroup of non-IRNs displayed a fast monophasic AHP following the action potential (69%; Fig. 7C), while the other exhibited a biphasic AHP (Fig. 7F). The average time to peak of the monophasic AHP (Fig. 7C) was  $29.4 \pm 16.4$  ms, and the amplitude  $-18.9 \pm 6.8$  mV, as estimated from the threshold of the action potential. The monophasic AHP reversed at the same membrane potential level as in IRNs, i.e. around  $-75$  to  $-80$  mV (Fig. 7C). Seventy-three per cent of non-IRNs with monophasic AHPs showed regular spiking with action potential frequencies ranging from 15 to 40 Hz with limited spike frequency adaptation. Three of the neurons with a monophasic AHP appeared to represent a separate subcategory of non-IRNs. They displayed significantly shorter times to peak AHP ( $8.3 \pm 3.2$  ms), narrow action potentials ( $1.75 \pm 0.06$  ms, cf. Table 1) and high frequency spiking up to 60 Hz with very modest spike frequency adaptation, as measured over 1 s, and over 80 Hz for the first interval (example in Fig. 7D and E). In addition, two of these neurons had very low input resistance, both at hyperpolarised potentials ( $340 \pm 70$  M $\Omega$ ) and at rest ( $490 \pm 7$  M $\Omega$ ).

The non-IRNs that displayed biphasic AHPs (27%, Fig. 7F) had a time to the second peak of  $90.4 \pm 42.1$  ms (Fig. 3B) with an amplitude of  $-17.4 \pm 3.6$  mV. The time to the fAHP component was  $10.3 \pm 4.3$  ms. The majority of these neurons showed a marked spike frequency adaptation (Fig. 7G and H), and a frequency range from 10–30 Hz.

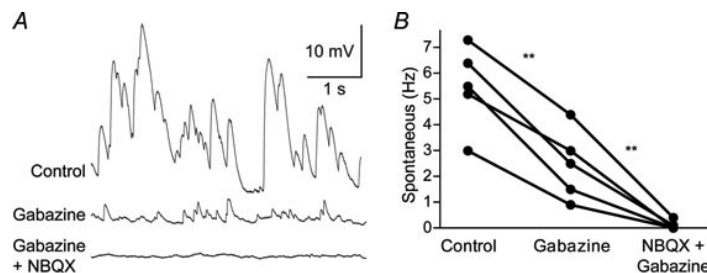


**Figure 6. Spontaneous synaptic input to IRNs**

A, current-clamp recordings of spontaneous synaptic input at  $-85$  mV. The upper trace shows synaptic input during control conditions, the second during bath application of the GABA<sub>A</sub> receptor antagonist gabazine (40  $\mu$ M) and the third during bath application of gabazine and the AMPA receptor antagonist NBQX (40  $\mu$ M) simultaneously. B, gabazine significantly reduces the spontaneous synaptic input and additional application of NBQX almost completely blocks all spontaneous synaptic input. All spontaneous synaptic input recordings were performed with intracellular solutions containing moderate concentrations of  $\text{Cl}^-$  so that GABAergic input is reversed at more depolarised potentials (theoretically around  $-35$  mV).

### Morphology and topography

**Morphological properties.** A total of 12 IRNs and 12 non-IRNs were labelled. There was no apparent difference in somatic characteristics of IRNs and non-IRNs as both had fusiform or spherical shapes. The somata diameters ranged from 8 to 15  $\mu\text{m}$  and the cell bodies were located within the striatal cell band or just lateral to the cell band where substance P expressing striatal neurons are located (Fig. 8A–E; Nozaki & Gorbman, 1986).

Most labelled neurons (8 IRNs and 8 non-IRNs) had two major processes that extended in opposite directions diagonally from the soma (see for example Fig. 8B and C), while the rest had either three to five processes or only one process. Each neuron generally had one thinner, uniform process and one thicker process with a broad base of 2–3  $\mu\text{m}$  that gradually became thinner and progressed with a thickness of 0.5–1  $\mu\text{m}$ .

The thin processes are putative axons that originated either directly from the soma or by branching off in a right angle from the base of a proximal dendrite. These processes were difficult to follow due to their thin diameters. Most of our reconstructions within the coronal plane probably represent dendrites, based on their non-uniform thickness and oblique branching. Figure 8F shows original confocal reconstructions, including the two non-IRNs in Fig. 8C, demonstrating the moderate branching exhibited by some cells. Many processes, especially those in the area between the striatum and the ventricle, had varicosities about 2  $\mu\text{m}$  apart from each other.

Neurons in the lamprey striatum have been described to have dendritic spines (Pombal *et al.* 1997b). Figure 8G shows an overview of a spiny IRN located in the caudal striatum, visualised with DAB staining. The spiny dendritic process is shown in close-up in Fig. 8H. Another

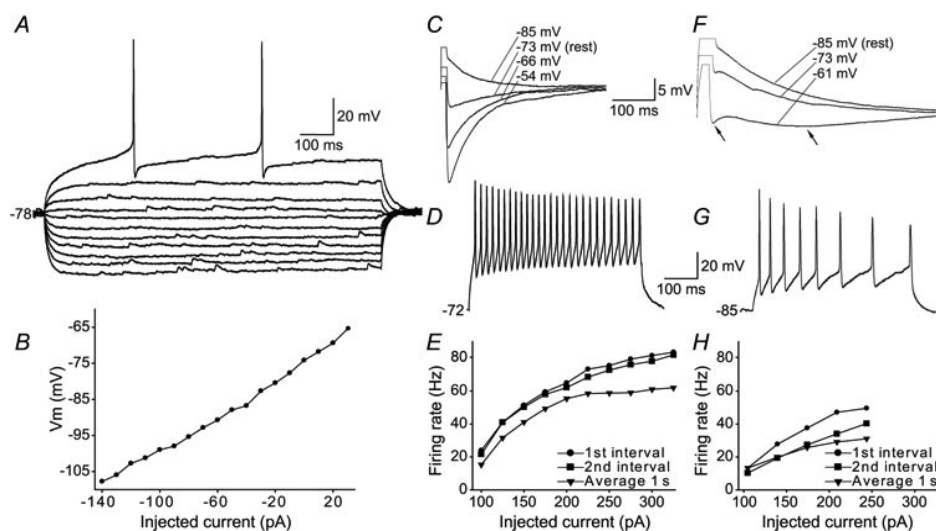


**Figure 7. Properties of non-IRNs**

A, voltage responses of a non-IRN to hyperpolarising and depolarising 1 s current steps of 10 pA per step, elicited from rest at -78 mV. The displayed neuron lacks inward rectification with a rectification ratio of 0.78 and also lacks any obvious sag. B, *I-V* plot of the steady-state voltage deflections to current steps of the neuron displayed in A showing close to a linear relationship. C, monophasic afterhyperpolarisation (AHP) response after an action potential elicited by a 5 ms positive current injection. The voltage dependence of the AHP is shown by recordings at four different baseline potentials. The reversal of the AHP takes place between -73 and -85 mV in this neuron. Scale bar for both panels C and F. D, response to suprathreshold current injections in another non-IRN with large, fast AHP showing its firing properties. Same scale bar for panels D and G. E, plot of firing rate as a function of the injected current during a 1 s current pulse of the neuron in D. The round markers show the instantaneous frequency of the first interval in the train of action potentials, the squares the second interval and the triangles the average firing frequency over the entire train of action potentials. This cell also had low input resistance ( $R_{in,hyper} = 290 \text{ M}\Omega$ ,  $R_{in,rest} = 380 \text{ M}\Omega$ ) compared to lamprey striatal neurons in general (compare to Fig. 3A). F, voltage recording of another non-IRN showing a biphasic AHP (arrows) response after the action potential, shown at three different baseline potentials. G, response to suprathreshold current injections in a neuron with biphasic AHP showing spike frequency adaptation. H, plot of firing rate as a function of the injected current of the neuron above.

spiny dendrite, visualised by confocal microscopy, is displayed in Fig. 8I. Spines appeared as thin, short stubs extending from the dendrite or as bulbs located directly on the dendritic shaft. All spiny dendrites were IRNs and they were always distal dendrites but not in perisomatic domains. We could not confirm that spines were present in all IRNs, even when well stained. This may possibly relate to the orientation of the distal dendrites in the striatal slices.

**Projections of IRNs and non-IRNs.** IRNs located in the rostral striatum had relatively short projections in the coronal plane (Fig. 8A and B). Instead, most of these processes turned in a perpendicular direction after 50–150  $\mu\text{m}$  and continued in the rostrocaudal direction ( $n = 6/7$ ) towards the pallidal regions of the lamprey (Ericsson *et al.* 2010). However, IRNs located more caudally (Fig. 8D) sent longer processes (up to 250  $\mu\text{m}$ ) within the same coronal plane and with more branching

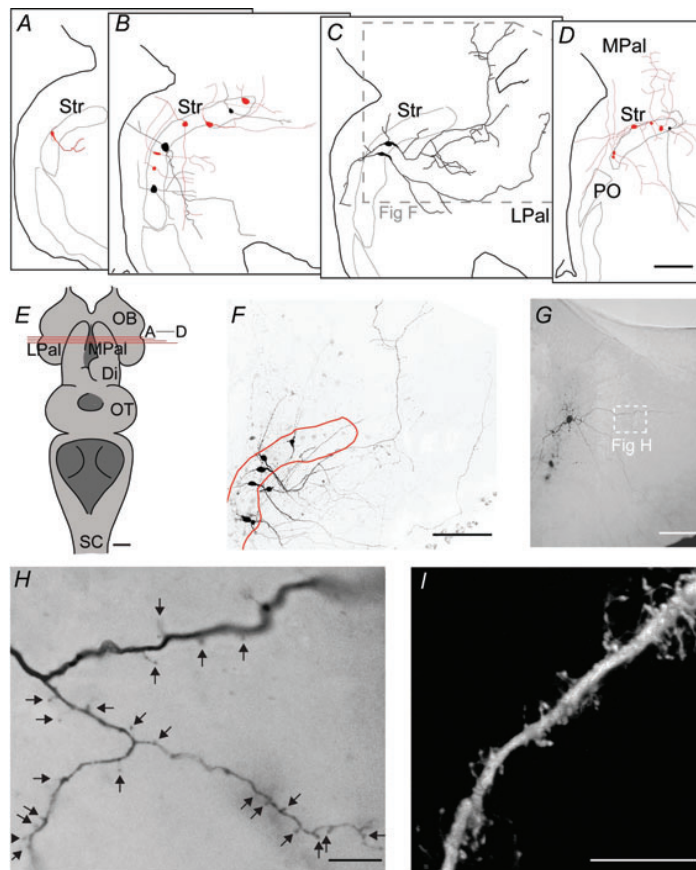


**Figure 8. Morphology and topography of striatal neurons**

A–D, schematic representations of IRNs (pale) and non-IRNs (black), in sections from rostral to caudal according to E. E, overview of the lamprey brain, including the level of coronal sectioning shown in A–D. F, confocal image showing the morphological properties of the two non-IRNs shown in C, among 4 other labelled but unrecorded neurons. See inset in C for the location in the coronal section. G, overview of a spiny IRN by light microscopy of a DAB-stained slice. H, close-up of spiny dendrites in the IRN shown in G, according to white inset. I, confocal image of another spiny dendrite labelled in the striatum. Scale bars = 100  $\mu\text{m}$  in A–D, F and G; 1 mm in E; 10  $\mu\text{m}$  in H and I. Abbreviations are as follows: Di, diencephalon; LPal, lateral pallium; MPal, medial pallium; OB, olfactory bulb; PO, nucleus preopticus; OT, optic tectum; Str, striatum.



and two of these IRNs had processes that also projected rostrocaudally. IRNs extended processes towards both the medial telencephalic ventricle and the medial and lateral pallium (Fig. 8A–D) within the coronal plane.

The processes of non-IRNs were mainly distributed within the coronal plane and only one neuron had a clear rostrocaudal projection. Many processes were long (300–700  $\mu\text{m}$ ) and in nine neurons they approached or reached into the lateral and ventrolateral pallium.

## Discussion

As summarised in the introduction, the lamprey striatum shows many similarities to that of mammals with regard to organisation of input structures and histochemical markers, and a dopamine denervation results in similar types of behavioural effects (Grillner *et al.* 2008; Ménard & Grillner, 2008; Thompson *et al.* 2008). The IRN group forms a distinct cluster with Kir channels and an inward rectification ratio ranging from 0.07 to 0.45 (see Fig. 2B). The remaining group, referred to here as non-IRNs, represents a more heterogeneous group.

### Comparison of IRNs to neurons of other vertebrates

IRNs share many of the intrinsic properties of mammalian MSNs, i.e. a fast inward rectification due to Kir-channels, hyperpolarised resting membrane potentials and a long delay to the first action potential due to activation of the low-voltage-activated A-type  $\text{K}^+$  current (Rogawski *et al.* 1985; Kawaguchi *et al.* 1989; Jiang & North, 1991; Nisenbaum & Wilson, 1995; Shen *et al.* 2007). The majority of lamprey IRNs (65%) exhibit inward rectification due only to Kir. These IRNs may serve a similar function as in mammals, where it contributes to maintain MSNs at hyperpolarised potentials until Kir-channels close upon strong excitatory input (Wilson & Kawaguchi, 1996; Stern *et al.* 1998; Grillner *et al.* 2005). Interestingly, however, around one-third of the IRNs also exhibits a large  $I_h$ -induced sag that increases the conductance at hyperpolarised potentials further and amplifies their inward rectification ratio. This subpopulation of IRNs clearly differs from rodent MSNs. Hyperpolarising current steps often triggered post-inhibitory rebound action potentials in this group of IRNs (see Fig. 4A). Potentially, a synchronised barrage of inhibitory activity limited in duration may elicit PIR spikes and thereby output from the striatum.

We show that striatal neurons receive both GABAergic and glutamatergic input, and it seems likely that the former is provided by local GABAergic microcircuits since the striatum contains almost exclusively GABAergic neurons (Robertson *et al.* 2007). The glutamatergic input presumably originates from the thalamostriatal or the lateral

and medial palliostriatal fibres (Pombal *et al.* 1997a; Northcutt & Wicht, 1997). In experiments where the synaptic input was blocked, the resting potential did not change markedly, indicating that it was not significantly influenced by the synaptic input. Once depolarised, the input resistance of IRNs was shown to increase to high values with a mean of 2400 M $\Omega$ , as compared to rodent MSNs with maximum input resistances around 600 M $\Omega$  depending on the preparation (Kawaguchi, 1993; Tepper *et al.* 2004; Cepeda *et al.* 2008). This difference may be related to the small size of lamprey neurons, but also to the distribution and density of ion channels. Inward rectification in rodents appears more pronounced than in lamprey, possibly due to a higher expression of Kir channels. In rodents, MSNs represent roughly 95% of the striatal neurons (Tepper *et al.* 2004) whereas only 65% of lamprey neurons are classified as IRNs. The population of IRNs, as defined here, may possibly be larger, as a fraction of non-IRNs have a ratio close to the dividing ratio of 0.5.

Striatal neurons are known to project to an area close to eminentia thalami, containing GABAergic projection neurons that target the mesencephalic and dienkephalic locomotor regions (MLR and DLR), as well as tectum (Ménard *et al.* 2007; Ménard & Grillner, 2008; Robertson *et al.* 2007, 2009; Stephenson-Jones *et al.* 2010). This area is suggested to be homologous to that of the mammalian globus pallidus. Recent findings also show striatal projections to an area in the caudolateral tegmentum containing GABAergic neurons projecting to tectum (Robertson *et al.* 2009). New recordings from retrogradely labelled striatal projection neurons suggest that different subsets of IRNs project to the different output regions of the basal ganglia in lamprey (Ericsson *et al.* 2010), thus corresponding to striatal projections in other vertebrates, and show that IRNs represent the striatal output neurons.

### Comparison of non-IRNs to neurons of other vertebrates

In the mammalian striatum, only interneurons lack inward rectification (Tepper & Bolam, 2004). A subgroup of non-IRNs had properties similar to the mammalian parvalbumin-expressing fast spiking interneurons, characterised by fast-spiking frequencies, very low spike frequency adaptation, low input resistance, narrow action potentials and short delays to AHPs (Kawaguchi, 1993; Tepper & Bolam, 2004).

Another subgroup was distinguished by their biphasic AHPs and marked spike frequency adaptation. The fast component of the AHP appears to be fairly similar in all lamprey striatal neurons and reversed around  $-75$  to  $-80$  mV. The main current mediating this AHP is likely to be the high-threshold transient A-type  $\text{K}^+$

current, which has been investigated in detail in the lamprey spinal cord (Hess & El Manira, 2001; Cangiano *et al.* 2002). The second, slower component seen in some neurons shows similar properties to the slow AHP in lamprey spinal neurons, due primarily to apamin-sensitive calcium-dependent  $K^+$  channels (Cangiano *et al.* 2002) with a residual 20% mediated by a Slack-like subtype of sodium-dependent  $K^+$  channel (Wallén *et al.* 2007).

The morphological data of non-IRNs showed that many of their dendritic processes are within the coronal plane where their cell bodies are located. However, we assume that non-IRNs and especially those resembling the fast-spiking type neurons represent interneurons. Few afferents to the striatum actually innervate the cell layer (Pombal *et al.* 1997*b*) and rather target the periventricular neuropil or the area between the striatal cell layer and the lateral pallium. It thus seems likely that the dendrites of putative interneurons would not respect the boundaries of the cell layer. Although the presumed axons of these cells were too thin to be traced in order to confirm that they only contact other striatal neurons, the results discussed above (e.g. Ericsson *et al.* 2010) with all output neurons identified as IRNs, further strengthen the possibility that they are interneurons.

In the lamprey striatum there is a pronounced acetylcholinesterase activity and cells have been found to express choline acetyltransferase immunoreactivity (Pombal *et al.* 1997*b*, 2001), suggesting the presence of cholinergic neurons. In rodents, large aspiny cholinergic interneurons represent around 1% of the striatal cell population (Rymar *et al.* 2004). In the present sample of cells ( $n = 74$ ), no neurons could clearly be identified as cholinergic cells.

### Concluding remarks

Our data further strengthen previous findings suggesting that the basic properties of the striatal neurons had already been developed early in vertebrate evolution, before the lamprey diverged from the main vertebrate line around 560 million years ago. Lamprey striatal neurons express some of the hallmarks of mammalian striatal neurons, including inward rectification due to Kir channels. About one-third of these neurons also display  $I_h$ -mediated voltage sags, which would ascertain that after an inhibitory hyperpolarisation there will be an  $I_h$  depolarisation that is often accompanied by PIR spikes. These characteristics may be unique to non-mammalian species. This study is the first detailed electrophysiological study of the striatal cell properties in anamniotes and indicates that the principal neuronal type and the fast-spiking interneuron were present some 250–300 million years before the anamniote–amniote transition. Thus, the basic design of the striatum and the basal ganglia circuitry implied in decision-making and action selection of motor behaviour

are present even in the less evolved lamprey, supporting a limited behavioural repertoire.

### References

- Auclair F, Lund J & Dubuc R (2004). Immunohistochemical distribution of tachykinins in the CNS of the lamprey *Petromyzon marinus*. *J Comp Neurol* **479**, 328–346.
- Barral J, Galarraga E, Tapia D, Flores-Barrera E, Reyes A & Bargas J (2010). Dopaminergic modulation of spiny neurons in the turtle striatum. *Cell Mol Neurobiol* **30**, 743–750.
- Brodin L, Hokfelt T, Grillner S & Panula P (1990*a*). Distribution of histaminergic neurons in the brain of the lamprey *Lampetra fluviatilis* as revealed by histamine-immunohistochemistry. *J Comp Neurol* **292**, 435–442.
- Brodin L, Theodorsson E, Christenson J, Cullheim S, Hökfelt T, Brown J, Buchan A, Panula P, Verhofstad A & Goldstein M (1990*b*). Neurotensin-like peptides in the CNS of lampreys: chromatographic characterization and immunohistochemical localization with reference to aminergic markers. *Eur J Neurosci* **2**, 1095–1109.
- Cangiano L, Wallén P & Grillner S (2002). Role of apamin-sensitive  $K_{Ca}$  channels for reticulospinal synaptic transmission to motoneuron and for the afterhyperpolarization. *J Neurophysiol* **88**, 289–299.
- Cepeda C, André V, Yamazaki I, Wu N, Kleiman-Weiner M & Levine M (2008). Differential electrophysiological properties of dopamine D1 and D2 receptor-containing striatal medium-sized spiny neurons. *Eur J Neurosci* **27**, 671–682.
- Ericsson J, Robertson B & Wikström MA (2007). A lamprey striatal brain slice preparation for patch-clamp recordings. *J Neurosci Methods* **165**, 251–256.
- Ericsson J, Stephenson-Jones MR, Samuelsson E, Robertson B, Hill R, Hellgren J & Grillner S (2010). The lamprey provides a vertebrate blueprint of the mammalian basal ganglia. Meeting abstract, 142.8, Federation of European Neuroscience Societies Forum.
- Farries MA & Perkel DJ (2000). Electrophysiological properties of avian basal ganglia neurons recorded in vitro. *J Neurophysiol* **84**, 2502–2513.
- Grillner S, Hellgren J, Menard A, Saitoh K & Wikström MA (2005). Mechanisms for selection of basic motor programs – roles for the striatum and pallidum. *Trends Neurosci* **28**, 364–370.
- Grillner S, Wallén P, Saitoh K, Kozlov A & Robertson B (2008). Neural bases of goal-directed locomotion in vertebrates – an overview. *Brain Res Rev* **57**, 2–12.
- Harris NC & Constanti A (1995). Mechanism of block by ZD 7288 of the hyperpolarization-activated inward rectifying current in guinea pig substantia nigra neurons in vitro. *J Neurophysiol* **74**, 2366–2378.
- Hess D & El Manira A (2001). Characterization of a high-voltage-activated IA current with a role in spike timing and locomotor pattern generation. *Proc Natl Acad Sci U S A* **98**, 5276–5281.
- Jiang ZG & North RA (1991). Membrane properties and synaptic responses of rat striatal neurones *in vitro*. *J Physiol* **443**, 533–553.

- Jimenez AJ, Mancera JM, Pombal MA, Perez-Figares JM & Fernandez-Llebrez P (1996). Distribution of galanin-like immunoreactive elements in the brain of the adult lamprey *Lampetra fluviatilis*. *J Comp Neurol* **368**, 185–197.
- Kawaguchi Y (1993). Physiological, morphological, and histochemical characterization of three classes of interneurons in rat neostriatum. *J Neurosci* **13**, 4908–4923.
- Kawaguchi Y, Wilson CJ & Emson PC (1989). Intracellular recording of identified neostriatal patch and matrix spiny cells in a slice preparation preserving cortical inputs. *J Neurophysiol* **62**, 1052–1068.
- Ménard A & Grillner S (2008). Diencephalic locomotor region in the lamprey – afferents and efferent control. *J Neurophysiol* **100**, 1343–1353.
- Ménard A, Auclair F, Bourcier-Lucas C, Grillner S & Dubuc R (2007). Descending GABAergic projections to the mesencephalic locomotor region in the lamprey *Petromyzon marinus*. *J Comp Neurol* **501**, 260–273.
- Nisenbaum ES & Wilson CJ (1995). Potassium currents responsible for inward and outward rectification in rat neostriatal spiny projection neurons. *J Neurosci* **15**, 4449–4463.
- Northcutt RG & Wicht H (1997). Afferent and efferent connections of the lateral and medial pallia of the silver lamprey. *Brain Behav Evol* **49**, 1–19.
- Nozaki M & Gorbman A (1986). Occurrence and distribution of substance P-related immunoreactivity in the brain of adult lampreys, *Petromyzon marinus* and *Entosphenus tridentatus*. *Gen Comp Endocrinol* **62**, 217–229.
- Olsen BD (2007). Understanding biology through evolution, 3rd edn, Vol. 25, p. 149.
- Pombal MA, El Manira A & Grillner S (1997a). Afferents of the lamprey striatum with special reference to the dopaminergic system: a combined tracing and immunohistochemical study. *J Comp Neurol* **386**, 71–91.
- Pombal MA, El Manira A & Grillner S (1997b). Organization of the lamprey striatum – transmitters and projections. *Brain Res* **766**, 249–254.
- Pombal MA, Marin O & Gonzalez A (2001). Distribution of choline acetyltransferase-immunoreactive structures in the lamprey brain. *J Comp Neurol* **431**, 105–126.
- Redgrave P, Gurney K, Reynolds J (2008). What is reinforced by phasic dopamine signals? *Brain Res Rev* **58**, 322–339.
- Robertson B, Auclair F, Ménard A, Grillner S & Dubuc R (2007). GABA distribution in lamprey is phylogenetically conserved. *J Comp Neurol* **503**, 47–63.
- Robertson B, Jones M, Samuelsson E, Hill R, Hellgren J & Grillner S (2009). The lamprey basal ganglia – a vertebrate blue-print. Meeting abstract, 566.10, Society for Neuroscience.
- Robertson B, Stephenson-Jones MR, Ericsson J, Diaz Heijtz R & Grillner S (2010). The direct and indirect pathways of lamprey basal ganglia. Meeting abstract, 220.2, Federation of European Neuroscience Societies Forum.
- Rogawski MA, Beinfeld MC, Hays SE, Hokfelt T & Skirboll LR (1985). Cholecystokinin and cultured spinal neurons. Immunohistochemistry, receptor binding, and neurophysiology. *Ann N Y Acad Sci* **448**, 403–412.
- Rymar VV, Sasseville R, Luk KC & Sadikot AF (2004). Neurogenesis and stereological morphometry of calretinin-immunoreactive GABAergic interneurons of the neostriatum. *J Comp Neurol* **469**, 325–339.
- Shen W, Hernandez-Lopez S, Tkatch T, Held JE & Surmeier DJ (2004). Kv1.2-containing K<sup>+</sup> channels regulate subthreshold excitability of striatal medium spiny neurons. *J Neurophysiol* **91**, 1337–1349.
- Shen W, Tian X, Day M, Ulrich S, Tkatch T, Nathanson NM & Surmeier DJ (2007). Cholinergic modulation of Kir2 channels selectively elevates dendritic excitability in striatopallidal neurons. *Nat Neurosci* **10**, 1458–1466.
- Standen NB & Stanfield PR (1978). A potential and time-dependent blockade of inward rectification in frog skeletal muscle fibres by barium and strontium ions. *J Physiol* **280**, 161–191.
- Stephenson-Jones M, Samuelsson E, Ericsson J, Robertson B & Grillner S (2010). The core architecture of the basal ganglia – insights from evolution. Meeting abstract, P-64, International Basal Ganglia Society Meeting X.
- Stern EA, Jaeger D & Wilson CJ (1998). Membrane potential synchrony of simultaneously recorded striatal spiny neurons in vivo. *Nature* **394**, 475–478.
- Surmeier D, Ding J, Day M, Wang Z & Shen W (2007). D1 and D2 dopamine-receptor modulation of striatal glutamatergic signaling in striatal medium spiny neurons. *Trends Neurosci* **30**, 228–235.
- Surmeier DJ, Stefani A, Foehring RC & Kitai ST (1991). Developmental regulation of a slowly-inactivating potassium conductance in rat neostriatal neurons. *Neurosci Lett* **122**, 41–46.
- Tepper JM & Bolam JP (2004). Functional diversity and specificity of neostriatal interneurons. *Curr Opin Neurobiol* **14**, 685–692.
- Tepper JM, Koos T & Wilson CJ (2004). GABAergic microcircuits in the neostriatum. *Trends Neurosci* **27**, 662–669.
- Tepper J, Abercrombie E & Bolam J (2007). Basal ganglia macrocircuits. *Prog Brain Res* **160**, 3–7.
- Thompson RH, Ménard A, Pombal M & Grillner S (2008). Forebrain dopamine depletion impairs motor behavior in lamprey. *Eur J Neurosci* **27**, 1452–1460.
- Uchimura N, Cherubini E & North RA (1989). Inward rectification in rat nucleus accumbens neurons. *J Neurophysiol* **62**, 1280–1286.
- Wallén P, Robertson B, Cangiano L, Low P, Bhattacharjee A, Kaczmarek LK & Grillner S (2007). Sodium-dependent potassium channels of a Slack-like subtype contribute to the slow afterhyperpolarization in lamprey spinal neurons. *J Physiol* **585**, 75–90.
- Wilson C & Kawaguchi Y (1996). The origins of two-state spontaneous membrane potential fluctuations of neostriatal spiny neurons. *J Neurosci* **16**, 2397–2410.

#### Author contributions

J.E. conducted the experiments and primary data analysis and developed the experimental design together with M.W., G.S. and S.G.; B.R. provided expertise in neuroanatomical

methods; all authors took part in the evaluation of the experimental data. J.E. wrote the manuscript in interaction with all authors, who also approved the final version of the manuscript.

#### **Acknowledgements**

This work was supported by the Swedish Research Council, HEALTH-F2-2008-201716 select-and-act, ICT-STREP 216100-LAMPETRA, and the Karolinska Institute. We are grateful to Dr Peter Wallén for valuable comments on the manuscript.

III



# Evolutionarily conserved differences in pallial and thalamic short-term synaptic plasticity in striatum

Jesper Ericsson, Marcus Stephenson-Jones, Andreas Kardamakis, Brita Robertson, Gilad Silberberg and Sten Grillner\*

Nobel Institute for Neurophysiology, Department of Neuroscience, Karolinska Institutet, SE-171 77 Stockholm, SWEDEN

\* To whom correspondence should be addressed. Nobel Institute for Neurophysiology, Department of Neuroscience, Karolinska Institutet, SE-171 77 Stockholm, SWEDEN. Tel: +46-8-52486900; Fax: +46-8-349544; E-mail: [sten.grillner@ki.se](mailto:sten.grillner@ki.se)

---

The striatum of the basal ganglia is conserved throughout the vertebrate phylum. Tracing studies in lamprey have shown that its afferent inputs are organised in a manner similar to that of mammals. The main inputs arise from the thalamus and lateral pallium (the homologue of cortex) that represents the two principal excitatory glutamatergic inputs in mammals. The aim here was to characterise the pharmacology and synaptic dynamics of afferent fibers from the lateral pallium and thalamus onto identified striatal neurons to understand the processing taking place in the lamprey striatum. We used whole-cell current clamp recordings in acute slices of striatum with preserved fibers from the thalamus and lateral pallium, as well as tract tracing and immunohistochemistry. We show that the thalamus and lateral pallium produce monosynaptic excitatory glutamatergic input through NMDA and AMPA receptors. The synaptic input from the lateral pallium displayed short-term facilitation, unlike the thalamic input that instead displayed strong short-term synaptic depression. There was also an activity-dependent recruitment of intrastriatal disynaptic inhibition from both inputs. These results indicate that the two principal inputs undergo different activity dependent short-term synaptic plasticity in the lamprey striatum. The difference observed between thalamic and pallial (cortical) input is also observed in mammals, suggesting a conserved trait throughout vertebrate evolution.

**Keywords:** Basal ganglia, synaptic dynamics, thalamostriatal, corticostriatal, lamprey

**Abbreviations:** aCSF, artificial cerebrospinal fluid; DPh, habenula projecting dorsal pallidum; EmTh, eminentia thalami; fr, fasciculus retroflexus; Hb, habenula; Hyp, hypothalamus; Kir, inwardly rectifying potassium channels; LPal, lateral pallium; MAM, mammillary area; MSNs, medium spiny neurons; NCPO, nucleus of the postoptic commissure; OB, olfactory bulbs; och, optic chiasm; ot, optic tract; OT, optic tectum; PO, preoptic nucleus; PSP, postsynaptic potential; RTR, recovery test response; SCO, subcommissural organ; Str, striatum; Th, thalamus; vLPal, ventral lateral pallium.

---

## Introduction

The input layer of the basal ganglia, the striatum, receives abundant cortical and thalamic input and serves a critical role in the integration and processing of motor-related signalling and cognitive behaviour (Graybiel, 2005; Grillner *et al.*, 2005). In the lamprey, one of the earliest vertebrates that diverged from the main vertebrate evolutionary line some 560 million years ago (Kumar and Hedges, 1998), the largest striatal input also arises from the lateral pallium (the homologue of the cortex) and the thalamus (Northcutt and Wicht, 1997; Pombal *et al.*, 1997b; Polenova *et al.*, 1993), which are in focus here. It also receives a dopaminergic, 5-HT and histaminergic input (Brodin *et al.*, 1990a; Brodin *et al.*, 1990b; Jimenez *et al.*, 1996; Pombal *et al.*, 1997b).

The organisation of the basal ganglia is to a remarkable degree conserved throughout the vertebrate phylum (Marín *et al.*, 1998; Reiner *et al.*, 1998; Smeets *et al.*, 2000; Stephenson-Jones *et al.*, 2011). Recent studies have shown that all the principal components of the basal ganglia (the striatum, globus pallidus externa and interna, subthalamic nucleus and substantia nigra pars reticulata/compacta) are present in lamprey (Pombal *et al.*, 1997a, b; Robertson *et al.*, 2006; Robertson *et al.*, 2007; Ericsson *et al.*, 2011; Stephenson-Jones *et al.*, 2011; Stephenson-Jones *et al.*, 2012). Moreover, the molecular characteristics of the striatum are similarly conserved like the expression of GABA, substance P and enkephalin and dopamine D1 and D2 receptors (Pombal *et al.*, 1997a; Robertson *et al.*, 2007; Ericsson *et al.*, 2011; Stephenson-Jones *et al.*, 2011; Robertson *et al.*, 2012). In the striatum, two main types of neurons have been described, GABAergic inwardly rectifying neurons expressing potassium channels of the Kir type and non-inwardly rectifying neurons including fast-spiking neurons (Ericsson *et al.*, 2011). The former are of two subtypes expressing substance P or enkephalin respectively. They are similar to the mammalian, avian and reptile spiny projection neurons (Kawaguchi *et al.*, 1989; Farries and Perkel, 2000; Farries *et al.*, 2005; Barral *et al.*, 2010) and project to the lamprey homologues of the globus pallidus and substantia nigra pars reticulata (Stephenson-Jones *et al.*, 2011; Stephenson-Jones *et al.*, 2012).

The afferent synaptic input to the striatum of lamprey has so far not been studied. The aim here is to characterise the synaptic effects from the lateral pallium and thalamus, representing the main afferents to the striatum. In rodents the corticostriatal and thalamostriatal synapses onto MSNs are glutamatergic, but they have distinct properties (Smith *et al.*, 2001; Smeal *et al.*, 2007; Ding *et al.*, 2008; Ding *et al.*, 2010). Activation of corticostriatal fibers leads to short-term synaptic facilitation, in contrast to thalamostriatal synapses that exhibit short-term synaptic depression. We find the same difference in synaptic properties in lamprey between the two inputs as established in mammals, suggesting the difference in activity-dependent short-term plasticity is conserved throughout vertebrate evolution.

## Methods

### Ethical Approval

All experimental procedures were approved by the local ethical committee (Stockholm's Norra Djurförsöksetiska Nämnd) and were in accordance with The Guide for the Care and Use of Laboratory Animals (National Institutes of Health, 1996 revision). During the investigation, every effort was made to minimise animal suffering and to reduce the number of animals used. Experiments were performed on a total of 79 adult river lampreys (*Lampetra fluviatilis*).

### Slice preparation

The dissection and removal of brains from deeply anaesthetised (MS-222; 100mg/L; Sigma, St. Louis, USA) animals were performed as described in detail previously (Ericsson *et al.* 2007). To facilitate the cutting of brain slices on a microtome (Microm HM 650V, Thermo Scientific, Walldorf, Germany), pre-heated liquid agar (Sigma) dissolved in water at a concentration of 4% was prepared. The agar was allowed to cool down for a few minutes before brains were embedded in the agar, on top of a metal plate placed on ice. This ensured that the agar directly solidified around the brain and that the agar was cooled down quickly to restrict it from warming the brain tissue. The agar block containing the brain was then glued to a metal plate and transferred to ice-cold artificial cerebrospinal fluid (aCSF) with the following composition (in mM): 125 NaCl, 2.5 KCl, 1 MgCl<sub>2</sub>, 1.25 NaH<sub>2</sub>PO<sub>4</sub>, 2 CaCl<sub>2</sub>, 25 NaHCO<sub>3</sub> and 8 glucose. The aCSF was oxygenated continuously with 95% O<sub>2</sub> and 5% CO<sub>2</sub> (pH 7.4). Transverse brain slices of 350-400 µm were cut at the level of the striatum (see Fig. 1) and allowed to recover at ~5°C for at least one hour before being transferred to a submerged recording chamber. Perfusion of the slices was performed with aCSF at 6-8°C (Peltier cooling system, ELFA, Solna, Sweden). In a few experiments an alternative Mg<sup>2+</sup>-free solution was used to remove the voltage-gated Mg<sup>2+</sup> block of NMDA receptors to increase the likelihood of activating these receptors. The composition of this solution was the same as the regular aCSF apart from the complete removal of MgCl<sub>2</sub>. Neurons were visualised with DIC/infrared optics (Olympus BX51WI, Tokyo, Japan).



### Electrophysiology

Whole-cell current clamp recordings were performed with patch pipettes made from borosilicate glass microcapillaries (Harvard Apparatus, Kent, UK) using a horizontal puller (Model P-97, Sutter Instruments, Novato, CA, USA). The resistance of recording pipettes were typically 7–12 M $\Omega$  when filled with intracellular solution of the following composition (in mM): 131 K-Gluconate, 4 KCL, 10 Phosphocreatine disodium salt, 10 HEPES, 4 Mg-ATP, 0.3 Na-GTP (osmolality 265–275 mOsm). To facilitate the detection of GABA currents at resting potential, an alternative intracellular solution with a higher chloride concentration was used in a few experiments in order to shift the reversal potential for GABA to more depolarised values. The composition of this solution was as follows (in mM): 105 K-Gluconate, 30 KCL, 10 Phosphocreatine disodium salt, 10 HEPES, 4 Mg-ATP, 0.3 Na-GTP. The calculated reversal potential for GABA for the two solutions was -85 mV (low intracellular Cl<sup>-</sup> concentration) and -35 mV (intermediate intracellular Cl<sup>-</sup>). Bridge balance and pipette capacitance compensation were adjusted for on the Axoclamp 2B amplifier (Molecular Devices Corp., CA, USA) and all membrane potential values were corrected for the liquid junction potential (~10 mV). Data collection and analysis was made with ITC-18 (HEKA, Lambrecht, Germany) and Igor software (version 6.03, WaveMetrics, Portland, USA). At least 20 individual responses were averaged from each stimulation locus of presynaptic fibers.

A total of 69 cells were included in the study based partly on the inclusion criteria that their resting membrane potentials were below -50 mV and had action potentials reaching above 0 mV. Extracellular stimulation (50–300  $\mu$ s) of striatal afferents were performed with a concentric bipolar metal electrode (FHC, Bowdoin, USA) connected to a constant current isolated stimulator (Digitimer, Hertfordshire, England). The stimulation intensity was set to around 1–2 times the threshold strength (typically 100–200  $\mu$ A) to evoke postsynaptic potentials. To investigate the short-term dynamics of synaptic transmission, a stimulus train of 8 pulses at 10 Hz was used together with a recovery test pulse 600 ms after the 8th pulse (see Planert et al. 2010). At a 10 Hz stimulation frequency, significant short-term synaptic plasticity has been shown in mammals (Ding et al., 2008). Postsynaptic potentials (PSPs) often started on the decay phase of previous responses, and to extract correct amplitudes the synaptic decay was either fitted by an exponential curve and subtracted or manually subtracted (see Planert et al. 2010). The paired-pulse ratio was calculated by dividing the second PSP by the first PSP in a response train, and the recovery-test response ratio by comparing the 9<sup>th</sup> PSP to the first PSP.

Before stimulation experiments were performed, the exact location of afferent fibre bundles from the lateral pallidum, thalamus and olfactory bulbs within the same transverse plane as the striatum were mapped out by neurobiotin injections to anterogradely label fibers. Pharmacological agents were bath applied through the perfusion system. Glutamate AMPA receptors were blocked by 2,3-Dioxo-6-nitro-1,2,3,4-tetrahydrobenzo[f]quinoxaline-7-sulfonamide (NBQX, 40  $\mu$ M, Tocris, Ellisville, USA) and NMDA receptors with D-(-)-2-Amino-5-phosphonopentanoic acid (AP-5, 50  $\mu$ M, Tocris). The NMDA/AMPA ratio was calculated by comparing the area under the first two responses (before GABAergic signals were recruited) where the NMDA component was calculated by subtracting the non-APV sensitive area (AMPA) from the control area. GABA<sub>A</sub> receptors were blocked by gabazine (20  $\mu$ M, Tocris). To investigate the dynamic properties of activated GABA fibers, responses were measured after application of NBQX/AP-5 and before additional application of gabazine that completely removed responses. Experiments assessing differences in short-term synaptic plasticity by altering extracellular calcium concentrations were performed in the presence of AP-5.

### Anatomy

The animals were deeply anesthetised in tricaine methane sulfonate (MS-222; 100mg/L; Sigma, St. Louis, MO, USA) diluted in fresh water. They were then transected caudally at the seventh gill, and the dorsal skin and cartilage were removed to expose the brain. During the dissection and the injections, the head was pinned down and submerged in ice cooled oxygenated HEPES buffered physiological solution (138mM NaCl, 2.1mM KCl, 1.8mM CaCl<sub>2</sub>, 1.2mM MgCl<sub>2</sub>, 4mM glucose, and 2mM HEPES), pH 7.4.

### **Retrograde tracing**

All injections were made with glass (borosilicate, OD = 1.5mm, ID = 1.17mm) micropipettes, with a tip diameter of 10 - 20µm. The micropipettes were mounted in a holder, which was attached to an air supply to enable pressure-injection of dyes and the pipette was mounted on a Narishige micromanipulator.

### **Tracing experiments**

50-200 nl of 20% Neurobiotin (Vector, Burlingame, CA; in distilled water containing fast green to aid visualisation of the spread of the injection) was pressure injected unilaterally into i) the striatum (n=9), ii) the thalamus (n=3) and iii) the lateral pallium (n=4).

### **Dissection and histology**

Following injections, the heads were kept submerged in aCSF in the dark at 4°C for 24 hours to allow retrograde transport of the tracers. The brains were then dissected out of the surrounding tissue and fixed by immersion in 4% formalin and 14% saturated picric acid in 0.1M phosphate buffer (PB) pH 7.4 for 12-24 hours, after which they were cryoprotected in 20% sucrose in PB for 3-12 hours. Transverse 20 µm-thick sections were made using a cryostat, collected on gelatin coated slides and stored at -20°C until further processing. For GABA and glutamate immunohistochemistry, tissue was fixed by immersion in 4% formalin, 1% glutaraldehyde, and 14% of a saturated solution of picric acid in 0.1M PB. The brain was postfixed for 24–48 hours and cryoprotected as described above.

### **Immunohistochemistry**

For the immunohistochemical detection of GABA and glutamate, the brains were injected, dissected and processed as described above. Sections were then incubated over night with either a mouse monoclonal anti-GABA antibody (1:1000, mAb, 3A12, kindly donated by Dr. Peter Streit, Zurich, Switzerland) (Matute and Streit, 1986; Robertson et al., 2007) or with polyclonal rabbit anti-glutamate antibody (1:500; AB133, Millipore, MA, USA). Sections were subsequently incubated with either Cy3 conjugated donkey anti-mouse IgG (GABA) or Cy3 conjugated donkey anti-rabbit IgG (glutamate), together with Cy2 conjugated streptavidin (1:1000; Jackson ImmunoResearch) for 2 hours and coverslipped.

### **Statistics**

Results are presented as mean ± standard error of mean (SEM) and statistical comparisons between means were made with two-tailed paired t-tests with GraphPad Prism Software (GraphPad Software, San Diego, USA) or Microsoft Excel (Microsoft, Seattle, USA). In figures, one star indicates  $p < 0.05$ , two stars  $p < 0.01$  and three stars  $p < 0.001$ .

## **Results**

### **Afferent input from the lateral pallium and thalamus to the striatum**

In order to identify the location of the pallial and thalamic cells projecting to the striatum, neurobiotin was injected into the striatum to retrogradely label afferent cell bodies (Fig. 1A, 1C, n=5). Retrogradely labeled cells were observed unilaterally throughout the entire rostrocaudal extent of the lateral pallium, with the highest density of cells in the dorsal two thirds of the lateral pallium and only few labeled cells in the ventral part of the lateral pallium (Fig. 1A-B). Dorsal to the striatum a few cells were also observed in the medial pallium (Fig 1A). Further caudally, retrogradely labeled cells were observed in the thalamus (Fig 1A, 1D), as previously reported (Pombal *et al.*, 1997b).

In agreement with published data a few retrogradely labeled neurons were also observed in the lateral olfactory bulbs and a cluster of neurons were retrogradely labeled in the medial olfactory bulbs (Fig. 1A). Anterograde tracing studies have confirmed that this latter population projects directly to the nucleus tuberculi posterior (Derjean *et al.*, 2010) and may not terminate in the striatum, allowing for the possibility

that this population of neurons may have been labeled through uptake from fibers of passage. In addition retrogradely labeled cells were observed in the region of the hypothalamus, in the dopaminergic nucleus tuberculi posterior, and a few cells were observed in the adjacent mammillary region (Fig 1A).

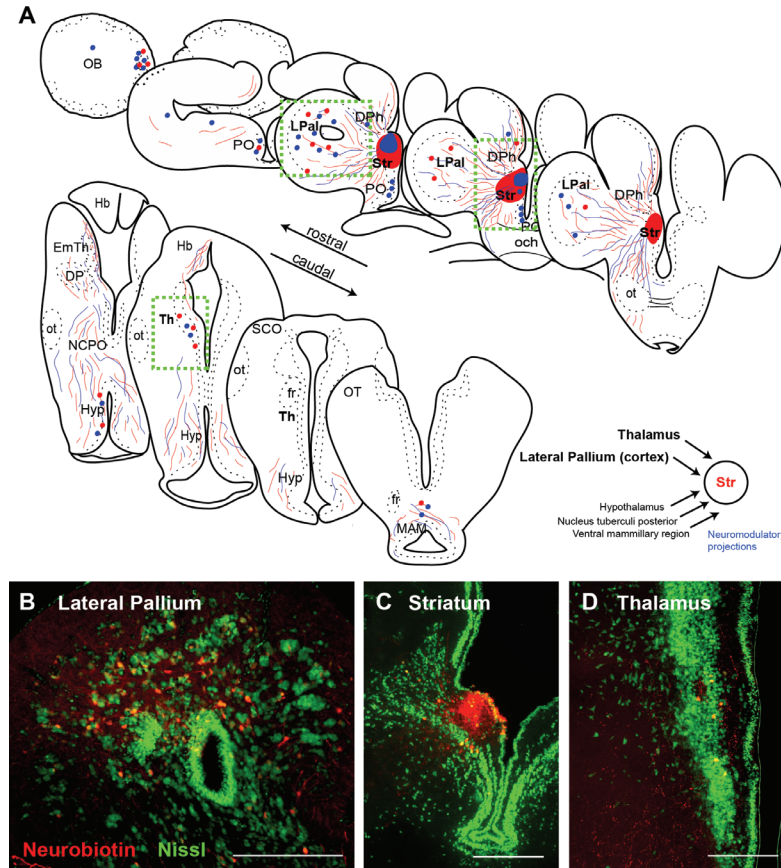


**Figure 1. Mapping of striatal afferent input**

**A**, Schematic transverse sections through the lamprey brain showing the location of retrogradely labeled cells (red and blue dots) and anterogradely labeled fibers (red and blue lines) from two injection sites (neurobiotin) into the striatum. Injection site in the striatum (**C**) resulted in retrogradely labeled neurons throughout the lateral pallium (**B**) and the thalamus (**D**). In addition, retrograde labeled neurons were observed in the olfactory bulbs, preoptic nucleus, medial pallium, hypothalamus, nucleus tuberculi posterior and mammillary area. Nissl stain in green in **B-D**. Scale bars = 200  $\mu$ m in **B**, **C** and **D**. DPh, habenula projecting dorsal pallidum; EmTh, eminentia thalami; fr, fasciculus retroflexus; Hb, habenula; Hyp, hypothalamus; LPal, lateral pallium; MAM, mammillary area; NCPO, nucleus of the postoptic commissure; OB, olfactory bulbs; och, optic chiasm; ot, optic tract; OT, optic tectum; PO, preoptic nucleus; SCO, subcommissural organ; Str, striatum; Th, thalamus.

To determine the location and projection patterns of the thalamostriatal and palliostriatal fibre tracts within the transverse brain slice used (see Methods), we injected neurobiotin into the thalamus and lateral pallium, respectively. Injections in the thalamus anterogradely labeled fibers that approached the striatum through a dense fiber tract projecting via the most lateral portion of the medial pallium (Fig. 2A), confirming the previously described thalamic projection in lamprey (Polenova and Vesselkin, 1993; Pombal *et al.*, 1997b). These thalamostriatal axons innervate the area dorsal part of striatum where many striatal dendrites are located (Ericsson *et al.*, 2011) and are also observed ventral to the striatal cell band (Fig. 2B). Fibers of a second, ventral thalamo-telencephalic projection (Northcutt and Wicht, 1997) were rarely seen.

Injections in the lateral pallium anterogradely labeled two fibre bundles, one that projected ventrally towards the striatum (Fig. 2C) where small varicose fibers terminate throughout the lateral and ventral striatal neuropil (Northcutt and Wicht, 1997). The second projected dorsally through the medial pallium and has been shown to project through the habenula commissure to the contralateral lateral pallium (Northcutt and Wicht, 1997). The anterogradely labeled fibers from the lateral pallium were observed throughout the striatum both dorsal and ventral of the striatal cell band (Fig. 2D). In contrast to the labeling from the thalamic injections, fibers were also observed through the dense striatal cell band. The results thus showed that the afferent fibers from the lateral pallium and thalamus project to the striatum through topographically separate fibre bundles, indicating that their synaptic contacts onto striatal cells may be investigated separately.

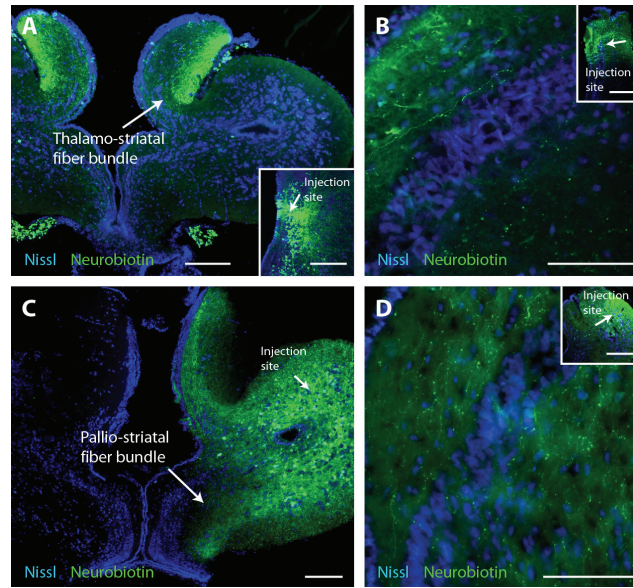


**Figure 2. Mapping of lateral palliostriatal and thalamostriatal fibers**

**A**, Anterograde labeling of thalamostriatal fibers after injection of neurobiotin in the thalamus, injection site inserted in the bottom-right part. The dense, anterogradely labeled thalamostriatal fibre tract was located in the most lateral neuropil of the medial pallium and limited to a well-defined narrow portion of the slice towards the striatum. **B**, Anterogradely labeled thalamostriatal fibers in the striatum following an injection in the thalamus (inset). **C**, Neurobiotin injections in the lateral pallium anterogradely labeled fibers throughout the lateral and ventral striatal neuropil (arrows). Injection site indicated in the lateral pallium. **D**, Anterogradely labeled palliostriatal fibers in the striatum following an injection in the lateral pallium (inset). Scale bars = 200  $\mu$ m in **A** and **C**, 100  $\mu$ m **B**, **D** and 500  $\mu$ m **B**, **D** inset.

#### **A transverse striatal slice maintains lateral palliostriatal and thalamostriatal axons**

To study the physiological responses in the striatum to stimulation of lateral pallial and thalamic afferents in an acute transverse brain slice preparation (350-400  $\mu$ m thickness, see Methods), we first investigated the responsiveness of striatal neurons to stimulations of different areas within the slice (Fig. 3A) to confirm that afferent fibers were preserved. A stimulus train readily evoked striatal postsynaptic potentials (PSPs) when applied to the thalamic fibers (Fig. 3A<sub>1</sub>, thalamic input indicated in both hemispheres by dark grey shading), to the area dorsal to the striatum (Fig. 3A<sub>2</sub>) and in the lateral pallium (LPal, Fig. 3A<sub>3-4</sub>) as well as to the most ventral part of LPal (vLPal, Fig. 3A<sub>5</sub>). The light grey shading in Figure 3A indicates areas where striatal responses were easily evoked, including the red shading indicating the stimulation area of LPal. No responses were evoked from the very lateral part of LPal (border region of the grey shading and in the unshaded area) unless significantly higher stimulation strength was used ( $> 4\times$  the threshold stimulus strength in LPal).

Activation of the thalamic fibre bundles ( $n=17$ , Fig. 3A<sub>1</sub>) elicited PSPs that reached a plateau after the second or third response, as did responses to the adjacent area located in between the thalamic fibre bundle and the striatum ( $n=8$ , Fig. 3A<sub>2</sub>). In contrast, responses from LPal ( $n=17$ , Fig. 3A<sub>3-4</sub>) in all cases summated effectively over several responses, while stimulation of the most ventral region (vLPal,  $n=10$ , Fig. 3A<sub>5</sub>) displayed a similar behaviour to that of the thalamic input. Responses were recorded from the two main cell types that have been classified in the lamprey striatum, inwardly rectifying neurons (Fig. 3B) resembling mammalian medium spiny projection neurons (MSNs) and those with little or no rectification (Fig. 3C) similar to striatal interneurons (Ericsson *et al.*, 2011). There was no difference between the postsynaptic responses of rectifying neurons ( $n=30$ ) and non-rectifying neurons ( $n=32$ , not illustrated).

The results thus show that the fibers from the lateral pallium and thalamus onto striatal neurons are preserved in the same slice and innervate both types of neurons. Below we will report on the type of synaptic transmission from the lateral pallium and thalamus and their differences in activity-dependent short-term plasticity onto striatal neurons.

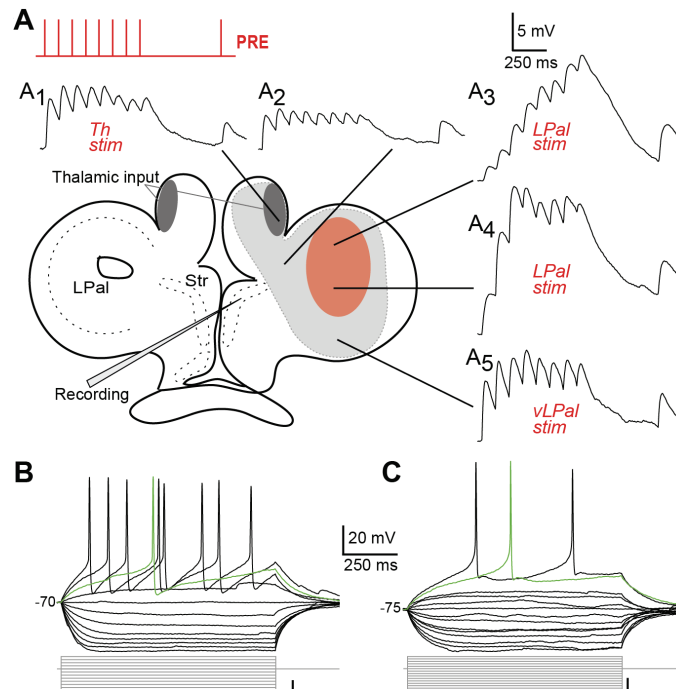


**Figure 3. Extracellular stimulation of striatal afferents**

**A**, Schematic overview of a transverse brain slice indicating the extracellular stimulation sites of striatal afferents. The light grey shading indicates areas from which striatal responses were readily evoked, including a red shading of the stimulation region in the lateral pallium. The presynaptic stimulus train of 8+1 pulses at 10 Hz is indicated in the top left corner. **A<sub>1-5</sub>**, Voltage responses to stimulation (stimulation artefacts removed) of thalamic fibers (**A<sub>1</sub>**, thalamostriatal fibers indicated by dark grey shading), the adjacent area dorsal to the striatum (**A<sub>2</sub>**), the lateral pallium (**A<sub>3-4</sub>**) and the most ventral part of the lateral pallium (**A<sub>5</sub>**). Neurons were held just below -80 mV before stimulating presynaptic fibers. **B**, Recorded neurons were a mix of inwardly rectifying neurons and non-rectifying neurons (**C**), shown by their voltage responses to hyperpolarising and depolarising current injections. The green traces represent the first, single action potentials evoked by the depolarising steps. Scale bars for the current injections indicate 10 pA.

### Input from the lateral pallium is glutamatergic and drives intrastriatal GABAergic disinaptic inhibition

In mammals the main excitatory synaptic drive to the striatum is glutamatergic, and it was important to confirm that this is the case also in lamprey. We therefore investigated the connections from the lateral



pallium in greater detail and if glutamatergic antagonists could affect the synaptic transmission. Stimulation of the lateral pallium (Fig. 4A) evoked synaptic responses (Fig. 4B, black trace) that were completely suppressed by application of AP-5 (50  $\mu$ M) and NBQX (40  $\mu$ M, Fig. 4B, blue trace). This was quantified by comparing the amplitude of the first PSP before and after drug application ( $\text{control}_{\text{PSP1}} 2.22 \pm 0.55$  mV, NBQX/AP-5 $_{\text{PSP1}} 0.027 \pm 0.03$  mV,  $p < 0.001$ ,  $n = 6$ , Fig. 4C). To investigate whether NMDA receptors contribute to the synaptic transmission, experiments were performed in  $\text{Mg}^{2+}$ -free aCSF (Fig. 4D). Application of the NMDA receptor antagonist AP-5 markedly reduced, but did not block, the synaptic transmission (Fig. 4D, grey trace). Additional application of the AMPA receptor antagonist NBQX completely removed all synaptic responses (Fig. 4D, blue trace), indicating that both receptor subtypes are activated at synapses from the lateral pallium. The NMDA to AMPA ratio was calculated to 1.84 by dividing the area under the first two pulses of the NMDA and AMPA components (see Methods).

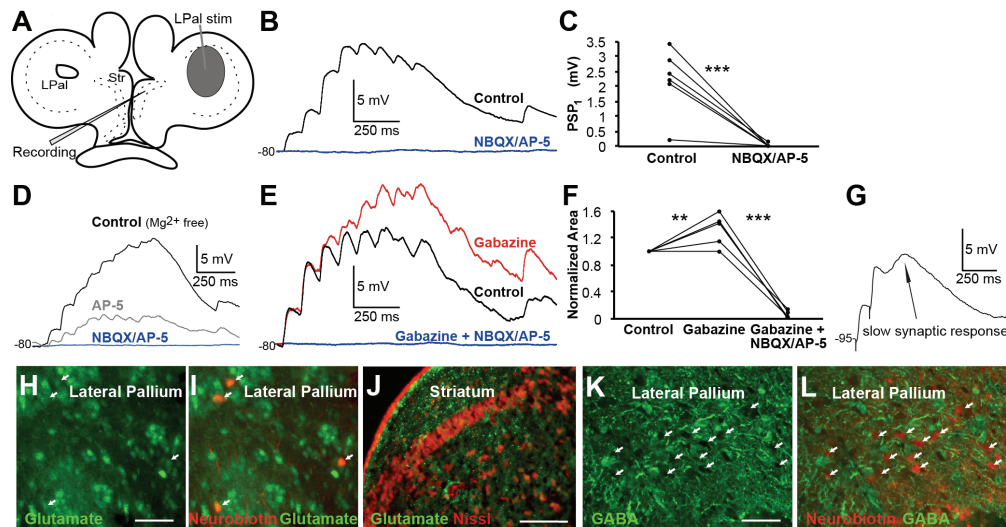


**Figure 4. Lateral palliostriatal stimulation evokes glutamatergic synaptic responses**

**A**, Schematic drawing indicating the stimulation area in LPal. **B**, Current-clamp recordings of striatal PSPs in regular aCSF evoked by LPal stimulation (artefacts removed), before (black trace) and after application of NBQX (40  $\mu$ M) and AP-5 (50  $\mu$ M, blue trace). **C**, Application of NBQX and AP-5 completely removed the postsynaptic response, quantified by comparing the first PSP response in the train before and after drug application. **D**, NMDA and AMPA receptors were investigated in  $\text{Mg}^{2+}$ -free aCSF by current-clamp recordings of striatal PSPs evoked by LPal stimulation before (black trace) and after sequential application AP-5 (grey trace) and both AP-5 and NBQX (blue trace) around -80 mV. **E**, Application of gabazine (20  $\mu$ M, red trace) increased responses in recorded neurons (rest  $V_m$  -80 mV) indicative of disinhibitory inhibition. Responses were completely removed by further application of NBQX and AP-5 (blue trace). **F**, Quantification of the effect of drugs in (**E**) was performed by comparing the normalised area under the response curve before and after application. **G**, A slow synaptic response revealed by paired-pulse stimulation (artefacts from stimulation included for clarity). The neuron was held at a hyperpolarised potential (-95 mV) where GABA is depolarising. **H**, Immunostaining for glutamate (green) in the lateral pallium. **I**, Retrogradely labeled neurons (red, indicated by arrows) in the lateral pallium were immunostained for glutamate seen by co-staining. **J**, Immunostaining showed glutamatergic fibers (green) surrounding the striatal cell band (red nissl staining). **K**, Immunostaining for GABA (green) in the lateral pallium. **L**, Retrogradely labeled neurons (red) were GABA-immunonegative as there was no co-staining with GABA. Scale bars = 50  $\mu$ m in **H** and **K**, 200  $\mu$ m in **J**. \*\* $p < 0.01$ , \*\*\* $p < 0.001$ , two-tailed paired  $t$ -tests.

To investigate if a train of depolarising synaptic potentials would also recruit a GABAergic input, we applied the GABA<sub>A</sub> receptor antagonist gabazine (20  $\mu$ M) to the slice. The red trace in Figure 4E shows that the synaptic responses were enhanced, except for the first two synaptic responses in the pulse train. In these experiments, neurons were held at -80 mV or more depolarised potentials, to ensure that GABA was hyperpolarising (calculated reversal potential at -84 mV). To quantify the effect of gabazine, we compared the normalised area under the averaged trace before and after application of the antagonist (gabazine  $133 \pm$

10% compared to control,  $p < 0.01$ ,  $n = 5$ , Fig. 4E-F). Additional application of NBQX and AP-5 completely blocked all responses (gabazine/NBQX/AP-5  $5.2 \pm 3\%$ ,  $p < 0.001$ ,  $n = 5$ , Fig. 4E-F). The GABAergic activation only occurred after the second or third excitatory postsynaptic potential (EPSP), which would suggest a disynaptic nature of these responses, moreover NBQX/AP-5 always removed the entire synaptic response indicating that no GABAergic PSPs were activated directly by the stimulation. Slower synaptic responses were also seen by paired-pulse stimulation (Fig. 4G, stimulation artefacts included for clarity) and presumably GABAergic as they diminished around its reversal potential (data not shown), here recorded at -95 mV where GABA is depolarising.

To further explore if pallial neurons projecting to the striatum indeed are glutamatergic, we combined retrograde labeling from striatum with immunohistochemistry. Retrogradely labeled cells within the lateral pallium were immunoreactive for glutamate (Fig. 4H-I) and glutamate fibers were detected throughout the striatum (Fig. 4J). In contrast, the retrogradely labeled pallial cells were GABA-immunonegative (Fig. 4K-L). These results taken together thus show that the direct lateral palliostriatal connections are glutamatergic and that this synaptic input activates both NMDA and AMPA receptors postsynaptically. Furthermore, this excitation may also recruit the intrastriatal GABAergic network as indicated by the disynaptic inhibitory responses.

#### **Input from the thalamus is glutamatergic and drives intrastriatal GABAergic disynaptic inhibition**

We next investigated whether the thalamostriatal afferent input was also glutamatergic and operated through both NMDA and AMPA receptors. Extracellular stimulations were performed strictly in the area indicated in figure 5A to selectively activate thalamic fibers, which evoked reliable responses in 17 out of 19 recorded neurons (see example in Fig. 5B, black trace). Application of NBQX and AP-5 (Fig. 5B, blue trace) completely removed all responses (control<sub>PSP1</sub>  $5.36 \pm 0.89$  mV, NBQX/AP-5<sub>PSP1</sub>  $0.080 \pm 0.033$  mV,  $p < 0.001$ ,  $n = 6$ , Fig. 5C). Experiments were also performed in  $Mg^{2+}$ -free aCSF where application of AP-5 substantially reduced the postsynaptic responses (Fig. 5D, grey trace), indicative of NMDA receptor activation. Additional application of NBQX (Fig. 5D, blue trace) completely suppressed all responses, indicative of AMPA receptor activation. The NMDA to AMPA ratio was calculated to 1.33.

As in the lateral pallium, application of gabazine increased responses at the second pulse or later (Fig. 5E, red trace), quantified by comparing the normalised area under the response (gabazine  $137 \pm 10\%$  compared to control,  $p < 0.01$ ,  $n = 5$ , Fig. 5F). Additional application of NBQX and AP-5 completely blocked all responses (gabazine/NBQX/AP-5  $2.3 \pm 1\%$ ,  $p < 0.001$ ,  $n = 5$ , Fig. 5E-F). To further corroborate that the thalamic neurons projecting to the striatum were glutamatergic, we combined retrograde labeling with immunohistochemistry. The retrogradely labeled cells within the thalamus were immunoreactive for glutamate (Fig. 5G-H), and in contrast none of the retrogradely labeled neurons were immunoreactive to GABA (Fig 5I-J).

The results thus suggest that also the thalamic input is glutamatergic and activates both NMDA and AMPA receptors, and that this excitation is able to recruit an activity-dependent disynaptic GABAergic synaptic response, as NBQX/AP-5 completely blocked all synaptic responses. In conclusion, the monosynaptic excitatory glutamatergic activation of the vertebrate striatum from the thalamus and pallium/cortex was established already in the lamprey.

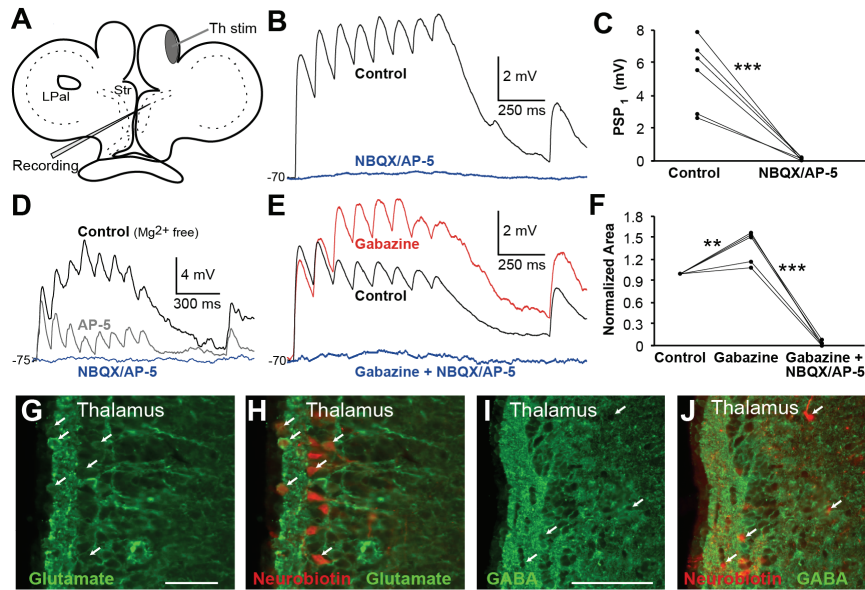


**Figure 5. Thalamostriatal synaptic responses are glutamatergic**

**A**, Schematic drawing indicating stimulation area of thalamic fibers in the most lateral region of the medial pallium. **B**, Striatal PSPs in regular aCSF in response to stimulation of thalamic fibers (black trace) and application of NBQX (40  $\mu$ M) and AP-5 (50  $\mu$ M), that completely removed all responses (blue trace), quantified by comparing the amplitude of the first PSP before and after drug application (**C**). **D**, NMDA and AMPA receptors were investigated in  $Mg^{2+}$ -free aCSF by current clamp recordings of striatal PSPs in response to stimulation of thalamic fibers (black trace) and after sequential application of AP-5 (grey trace) and both AP-5 and NBQX (blue trace) around -75 mV. **E**, Application of gabazine (20  $\mu$ M, red trace) increased responses in recorded neurons (rest Vm -70 mV), indicative of disinaptic inhibition. Responses were completely removed by further application of NBQX and AP-5 (blue trace). **F**, Quantification of the effect of drugs in (**E**). **G**, Glutamate immunostaining (green) of the thalamus showed that the cell layer is packed with glutamatergic neurons. **H**, Retrogradely labeled neurons (red) from the striatum are glutamatergic as indicated by the arrows and the co-staining. **I**, Immunostaining for GABA (green) in the thalamus. **J**, Retrogradely labeled neurons (red) were GABA-immunonegative as there was no co-staining with GABA. Scale bars = 50  $\mu$ m in **G**, 100  $\mu$ m in **I**.  $**p < 0.01$ ,  $***p < 0.001$ , two-tailed paired *t*-tests.

### Lateral palliostriatal and thalamostriatal synapses differ in their synaptic dynamics

We next investigated the short-term activity-dependent synaptic plasticity of the transmission from the lateral pallium and thalamus. Responses of the 10Hz stimulation train of 8+1 pulses were normalised to the first PSP in the pulse train (Fig 6A). The paired-pulse ratio of the second synaptic response to the first response (Fig. 6A-B, red trace/box) showed that the responses from lateral pallium displayed clear paired-pulse facilitation (PPF:  $1.38 \pm 0.10$ ). In contrast, responses from the thalamus and ventrolateral pallium showed paired-pulse depression (Th PPD  $0.56 \pm 0.07$ ; vLPal PPD  $0.61 \pm 0.12$ ;  $p < 0.001$  compared to LPal, Fig. 6A-B). Synaptic responses from the LPal were significantly facilitating for the first 300 ms after the first PSP (Fig. 6A,  $n=17$ , red trace), unlike thalamic synaptic responses that were clearly depressing throughout the 8 pulses (Fig 6A,  $n=16$ , black trace). Synaptic responses from ventrolateral pallium (Fig 6A,  $n=10$ , grey trace) were also depressing. The activity-dependent short-term synaptic facilitation of responses from LPal reached a maximum at the third pulse (ratio  $1.58 \pm 0.34$ ) but responses were still facilitatory at the fourth pulse (ratio  $1.28 \pm 0.35$ ). The synaptic dynamics of responses from the LPal were significantly different from the thalamus and vLPal for the first 300 ms after the first response; pulse 3 (Th  $0.49 \pm 0.08$ ; vLPal  $0.45 \pm 0.12$ ;  $p < 0.01$ ) and pulse 4 (Th  $0.45 \pm 0.08$ ; vLPal  $0.25 \pm 0.04$ ,  $p < 0.05$ ). In a comparison of responses of IRNs versus non-IRNs to thalamic and LPal stimulations, we did not discover any significant differences in the paired-pulse responses (Th PPRs: IRN  $0.51 \pm 0.08$ , non-IRN  $0.60 \pm 0.13$ ,  $p=0.55$ ; LPal PPRs: IRN  $1.46 \pm 0.1$ , non-IRN  $1.36 \pm 0.18$ ,  $p=0.77$ ).



To investigate if the different synapses had recovered 600 ms after the pulse train, a recovery test response (RTR, see Planert *et al.* 2010) was evoked and compared to the first PSP (last response in Fig. 6A and D). The test response recovered back to baseline during LPal stimulation (ratio  $0.99 \pm 0.16$ , Fig. 6C, n.s) whereas the thalamostriatal test response was significantly depressed compared to baseline (ratio  $0.55 \pm 0.06$ , Fig. 6C,  $p < 0.001$ ). Recovery responses from ventrolateral pallium were also depressed (ratio  $0.53 \pm 0.04$ , Fig. 6C,  $p < 0.001$ ). The differences in activity-dependent synaptic plasticity were also obtained when the same postsynaptic neuron was recorded in response to both pallial and thalamic extracellular stimulation. The paired-pulse responses were facilitatory and the test response recovered from stimulations of the LPal, while they were depressed for both thalamic and ventrolateral pallial responses (example shown in Fig. 6D). This also shows that both pallial and thalamic inputs are capable of converging upon the same striatal neuron. Synaptic responses from LPal often summated over a longer time period, effectively integrating incoming input and driving the cell towards threshold rather than reaching a plateau at subthreshold levels as did responses to thalamic input (Fig. 6C,  $n = 10/17$ ).

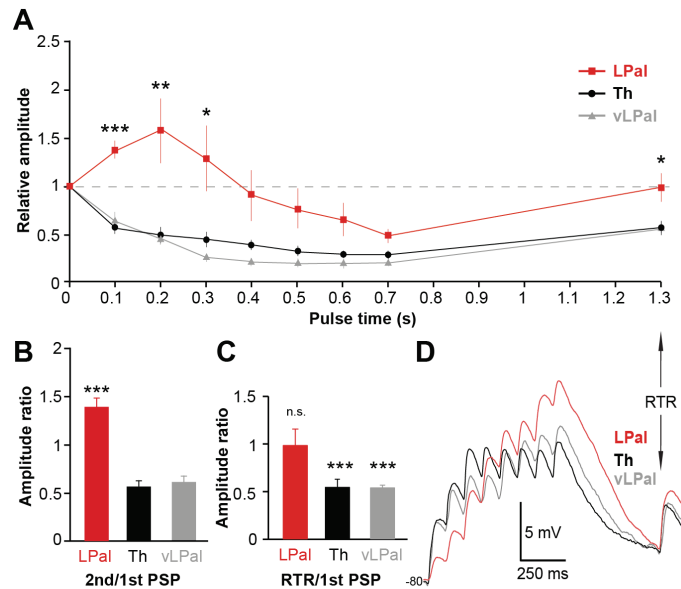


**Figure 6. Lateral palliostriatal and thalamostriatal synapses have different dynamics**  
**A**, Normalised postsynaptic responses to stimulations in LPal (red squares), vLPal (grey triangles) and thalamus (th, black circles) including the normalised recovery test response (RTR) 600 ms after the 8th pulse in the stimulus train. **B**, Comparison of the paired-pulse ratio of the second PSP to the first PSP in response to stimulations of fibers from the thalamus, LPal and vLPal (Th PPD  $0.56 \pm 0.07$ ; vLPal PPD  $0.61 \pm 0.12$ ;  $p < 0.001$  compared to LPal). **C**, Comparisons of the recovery test response of LPal, vLPal and thalamic stimulation. **D**, Postsynaptic response patterns in the same neuron to LPal (red), vLPal (grey) and thalamic (black) stimulations, baseline potential at -80 mV. \* $p < 0.05$ , \*\* $p < 0.01$ , \*\*\* $p < 0.001$ , two-tailed paired *t*-tests.

The results from the paired-pulse and recovery test responses both suggest a difference in presynaptic properties from the LPal and thalamus to striatum. The PPF and full recovery of responses from LPal are both indicative of a low presynaptic release probability, whereas the PPD and depressed recovery of thalamic and ventrolateral pallium responses suggest high presynaptic release probabilities. To investigate the release probability in further detail, we altered the external calcium concentration (Fig. 7) of the aCSF as there is a direct relationship between the probability of release and presynaptic calcium levels. By lowering the  $\text{Ca}^{2+}$  concentration from 2 mM to 0.5 mM, lateral palliostriatal paired-pulse facilitation was increased from a ratio of  $1.07 \pm 0.12$  to  $1.50 \pm 0.15$  ( $p < 0.05$ ,  $n = 5$ , Fig. 7A-B). An increase of the  $\text{Ca}^{2+}$  concentration to 4 mM did not significantly change the paired-pulse ratio but there was a trend towards synaptic depression

( $0.81 \pm 0.17$ ,  $p=0.14$ ,  $n=5$ , Fig. 7A-B). Similarly for thalamostriatal synaptic responses, lowering the  $\text{Ca}^{2+}$  concentration to 0.5 mM reduced the paired-pulse depression from  $0.59 \pm 0.095$  to  $0.87 \pm 0.10$  ( $p<0.05$ ,  $n=5$ , Fig. 7C-D). A few neurons even shifted from synaptic depression to facilitation and an increased summation of the entire response train was demonstrated (see example in Fig. 7C). Increasing the calcium concentration to 4 mM did not change the paired-pulse response ( $p=0.94$ ,  $n=5$ , Fig. 7D). Together these results indicate that lateral palliostriatal synapses have low release probabilities compared to thalamostriatal synapses with higher release probabilities that, at least partly, underlie the difference in short-term synaptic responses. Similar differences are found in cortico- and thalamostriatal short-term synaptic plasticity in rodents (Ding *et al.*, 2008; Ding *et al.*, 2010; Ellender *et al.*, 2011).

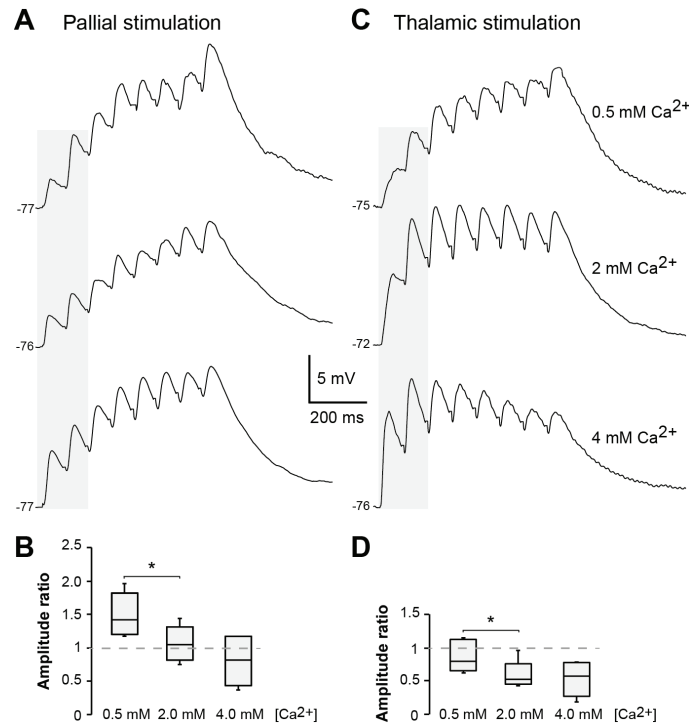


**Figure 7. Altering extracellular calcium concentration changes striatal short-term synaptic plasticity from the lateral pallium and thalamus**

**A**, Postsynaptic voltage responses to stimulation of the lateral pallium in three different extracellular  $\text{Ca}^{2+}$  concentrations: 0.5 mM (top trace), 2 mM (middle trace) and 4 mM (bottom trace). **B**, Box-plot of the paired-pulse ratio of the first two palliostriatal responses (grey shading in **A**) that was increased by lowering the  $\text{Ca}^{2+}$  concentration to 0.5 mM compared to the regular aCSF calcium concentration of 2 mM. **C**, Voltage responses to stimulation of thalamostriatal fibers in the same conditions as in **A**. **D**, Box-plot of the paired-pulse ratio of the first two thalamostriatal responses (shading in **C**) where the synaptic depression was decreased in 0.5 mM  $\text{Ca}^{2+}$  concentration.  $*p<0.05$ .

#### Intrastratial stimulation evokes a mix of GABAergic and glutamatergic responses

We also applied the same type of train stimuli within the striatum, but in this case we would anticipate coactivation of the lateral pallial, thalamic and modulatory input together with responses from the striatal microcircuit. The stimulation electrode was placed centrally or ventrally within the striatal cell band or just lateral to it (Fig. 8A). Synaptic responses were readily evoked (Fig. 8B, black trace) and application of NBQX and AP-5 significantly reduced, but did not abolish, the postsynaptic responses (control<sub>PSP1</sub>  $2.70 \pm 0.58$  mV, NBQX/AP-5<sub>PSP1</sub>  $0.69 \pm 0.15$  mV,  $p<0.05$ ,  $n=5$ , Fig. 8B-C). An additional application of gabazine (Fig. 7B, grey trace) did, however, completely remove the response (gabazine/NBQX/AP-5<sub>PSP1</sub>  $0.026 \pm 0.03$

mV,  $p < 0.01$ ,  $n = 5$ , Fig. 8B-C). Thus, in contrast to stimulation of the LPal and thalamic input, the GABAergic striatal network was directly recruited by this stimulation.

Responses to intrastratial stimulation were depressing (see Fig. 8B, black trace) and result from a mix of excitatory and inhibitory synaptic responses. Since thalamic and lateral pallial projections to the striatum are glutamatergic, the isolated GABAergic component after application of NBQX/AP-5 (Fig. 8B and D, blue traces) will most likely originate only from intrastratial synaptic interactions. The paired-pulse ratio of intrastratial GABAergic responses was  $0.74 \pm 0.07$  (Fig. 8E,  $n = 5$ ), measured from both rectifying and non-rectifying neurons. This response was significantly different from the LPal input (compare Fig. 6B and 7E,  $p < 0.01$ ) but not from that of the thalamus or the ventrolateral LPal ( $p > 0.05$ ). The recovery test response was also depressed compared to the baseline synaptic response ( $0.47 \pm 0.11$ , Fig. 8E,  $p < 0.01$ ). The results thus indicate that the intrastratial GABAergic synaptic inhibition displays short-term synaptic depression and that the recovery of synapses is longer than 600 ms.

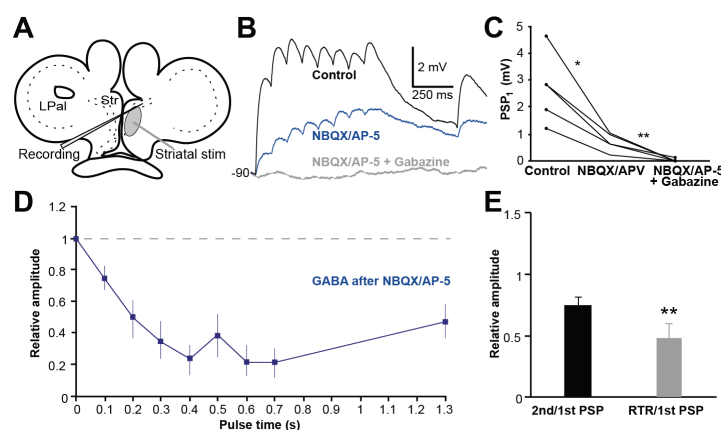


**Figure 8. Intrastratial stimulation evokes glutamatergic and GABAergic responses**

**A**, Schematic drawing indicating stimulation area in the striatum. **B**, Striatal PSPs (black trace) in response to intrastratial stimulation and application of NBQX (40  $\mu$ M) and AP-5 (50  $\mu$ M) significantly reduces postsynaptic responses (blue trace), but they were only completely removed after additional application of gabazine (20  $\mu$ M, grey trace). Neurons were held at hyperpolarised potentials where GABA is depolarising, here at -90 mV. **C**, Quantification of the synaptic effects of drugs was performed by comparing the amplitude of the first PSP in the pulse train. **D**, Normalised postsynaptic depressing intrastratial GABAergic responses, isolated after application of NBQX and AP-5. **E**, the paired-pulse ratio (black) and the recovery test ratio (grey) of GABAergic responses that are both depressed. \* $p < 0.05$ , \*\* $p < 0.01$ , two-tailed paired *t*-tests.

## Discussion

The general aim of the present study was to identify the synaptic characteristics of the input from the thalamus and lateral pallium to striatal neurons. The principal findings are that synaptic inputs to striatum from the lateral pallium and thalamus are excitatory and glutamatergic, acts via both NMDA and AMPA receptors, and that these afferents have opposite synaptic dynamics. In addition, the excitatory input recruits activity-dependent disinaptic GABAergic inhibition within the intrastratial network, which may be a result of feedforward inhibition mediated by GABAergic fast-spiking neurons or feedback inhibition by projection neurons previously described in the lamprey striatum (Ericsson *et al.*, 2011). The synaptic properties share similar characteristics to those established in mammals, indicating that the difference in short-term synaptic plasticity is conserved throughout vertebrate evolution.

### The synaptic dynamics from the thalamus is different from that of the lateral pallium

Stimulation of the thalamic fibers results in short-term synaptic depression, in contrast to the lateral pallial responses that are facilitatory. This difference in synaptic properties is similar to that of rodents, where repeated thalamic input onto MSNs evokes marked synaptic depression (Ding *et al.*, 2008; Ding *et al.*, 2010;

Ellender *et al.*, 2011), whereas the corticostriatal connection is instead facilitatory over several pulses in a stimulation train (Smith *et al.*, 2001; Ding *et al.*, 2008; Ding *et al.*, 2010; Ellender *et al.*, 2011). However, varying the interstimulus intervals of the corticostriatal activation may sometimes also lead to synaptic depression in rodents (Smeal *et al.*, 2007; Goubard *et al.*, 2011). Thus, the functional difference between the main excitatory striatal afferents in rodents appears to be present already in lamprey.

Why do we have this conserved difference in synaptic properties between cortex/pallium and thalamus from lamprey to mammals? It would seem likely that it reflects a difference in the functional role of the two inputs. Possibly the thalamic input will provide fast direct access to the striatum (e.g. from sensory input), whereas the input channeled via the cortex/pallium will require more time but be further processed and subsequently provide a more maintained signal to striatum.

The difference in short-term synaptic plasticity in rodents is due to presynaptic properties (Ding *et al.*, 2008), which appears to be the case also between lamprey thalamostriatal and lateral palliostriatal fibers onto striatal neurons. As shown in the Results section, the same neuron will receive facilitatory synapses from the lateral pallium and depressing synapses from the thalamus, supporting a presynaptic origin. The paired-pulse depression and recovery test response typical of thalamic responses are both indicative of a high presynaptic release probability and possible depletion of vesicles (Thomson, 2000), leading to progressively less release of transmitters during a prolonged stimulation. We also showed this directly by lowering the external calcium concentration that reducing synaptic depression, consistent with a high release probability at physiological calcium levels. The high release probability is also consistent with the response plateau seen during the stimulus train. Conversely, the paired-pulse facilitation and complete recovery of responses from stimulation of the lateral pallium suggest a low presynaptic release probability (Thomson, 2000). This was shown directly by the increased paired-pulse facilitation in low extracellular calcium levels. The low release probability may also explain the more efficient temporal summation, as consecutive pulses lead to an increased presynaptic calcium influx and transmitter release. However, although thalamic and lateral pallial input only produced monosynaptic glutamatergic responses, the activity-dependent recruitment of GABA at pulse three or later affects the summation or responses (Fig. 4, 5). Thus, the synaptic dynamics during prolonged activity is likely a combination of the presynaptic properties, postsynaptic depolarisation and disynaptic inhibition.

The synaptic effects of stimulation of the ventrolateral pallium are depressing. Very few cells were retrogradely labeled from the striatum in this area (Fig. 1A), which would suggest that fibers of uncertain origin were activated. A second thalamic projection has previously been described (Polenova and Vesselkin, 1993; Northcutt and Wicht, 1997) with fibers in the ventrolateral pallium. There is thus the possibility that stimulation here activates thalamic afferents onto striatal dendrites that are abundant in this area (Ericsson *et al.*, 2011). If so, these results may represent the activation of a second thalamostriatal projection that is depressing. These thalamic fibers were however few in our anatomical studies, confirming earlier results that the main thalamostriatal projection goes via the lateral region of the medial pallium (Polenova and Vesselkin, 1993).

### **The glutamatergic and disynaptic GABAergic striatal input**

Although it has been shown that striatal neurons receive spontaneous barrages of glutamatergic and GABAergic input (Ericsson *et al.*, 2007; Ericsson *et al.*, 2011), very little was known about the origin of these afferents and their synaptic characteristics. The preservation of thalamic fibers in the separate and well-defined lateral region of the medial pallium in a transverse brain slice preparation (Fig. 2A) made it possible to specifically activate this striatal input. A few neurons in the caudal medial pallium were also found to project to the striatum, but they were located on the opposite side to that of the thalamic bundle (see also Pombal *et al.*, 1997a) and are GABAergic (Robertson *et al.*, 2007). No glutamatergic cells are located in the medial pallium (Villar-Cerviño *et al.*, 2011). Taken together, these findings support our assumption that only thalamic glutamatergic fibers were activated in this region.

The fact that the thalamic and lateral pallial inputs activate both NMDA and AMPA receptors is important since NMDA receptor activation is critical for induction of different long-term changes in synaptic

transmission at many synapses, including mammalian corticostriatal synapses (Calabresi *et al.*, 1992; Partridge *et al.*, 2000).

The afferent excitation also elicited disynaptic inhibition, most likely originating in the striatum as direct striatal activation always recruits the densely packed striatal GABAergic microcircuit (Pombal *et al.*, 1997a; Menard *et al.*, 2007; Robertson *et al.*, 2007). This inhibition reduces the temporal summation of EPSPs and thereby it affects and partly controls the striatal integration of incoming excitation. In the mammalian system this is achieved via GABAergic interneurons and axon collaterals of medium spiny projection neurons (Buchwald *et al.*, 1973; Koos and Tepper, 1999; Suzuki *et al.*, 2001; Tepper *et al.*, 2004), where they provide the striatum with feedforward and feedback mechanisms (Mallet *et al.*, 2005; Gittis *et al.*, 2010; Klaus *et al.*, 2011). Striatal stimulation evoked a GABAergic depressing signal in both rectifying neurons expressing Kir-channels and non-rectifying neurons, suggesting both neuronal types are affected. It is however unknown if this occurs via fast-spiking or other GABAergic interneurons or via axon collaterals of the output neurons. As an indication however, two striatal neurons were recorded interacting via a depressing synapse activated by a stimulus train (data unpublished). It is thus possible that similar connections of inter- and/or output neurons underlie the disynaptic inhibition.

### Functional implications

The lateral pallial and thalamic signals provide different types of information to the striatum, which may be reflected in the difference in dynamic properties. The lateral pallium receives strong afferent input from the olfactory bulbs (Northcutt and Puzdrowski, 1988; Derjean *et al.*, 2010), septum, preoptic area, medial pallium and thalamus (Northcutt and Wicht, 1997). The signals to the striatum from the lateral pallium may thus be related to sensorimotor integration arising from olfactory and other sensory modalities.

Although the role of the lateral pallial area in basic motor function is not known, recent experiments show that electrical microstimulation of specific regions of the lateral pallium evokes movements of the eye, mouth and head as well as locomotion, depending on the stimulation parameters (Ocaña *et al.* 2011). These effects may be partially exerted via the lateral palliostriatal projection and movements can also be elicited by direct striatal stimulation (Menard and Grillner, 2008; Ocaña *et al.* 2011). The lateral pallium thus appears to process information closely related to motor and somatosensory signalling. The facilitatory properties of lateral palliostriatal synaptic responses may reflect an integrative function specific to this input, and the effective temporal summation may drive cells to spike during persistent activity over longer time periods. This may suggest that synchronised inputs will have a larger effect and potentially filter out small synaptic events that are uncorrelated.

The lamprey thalamus receives a different input, including direct retinal and tectal input (Vesselkin *et al.*, 1980) and input from the olfactory bulbs, the nucleus of the posterior commissure nucleus and the torus semicircularis (Polenova and Vesselkin, 1993; Northcutt and Wicht, 1997). Studies in other vertebrates have shown that the thalamus and its projection to the striatum from the intralaminar nucleus may be involved in the shift of attention and specifically signals upon salient information such as prey (Ewert *et al.*, 1999; Matsumoto *et al.*, 2001; Smith *et al.*, 2004). In mammals (Ding *et al.*, 2008; Ding *et al.*, 2010) as well as in lamprey, the thalamic input is depressing. Instead of effective temporal summation, these responses quickly reach a subthreshold plateau due to strong synaptic depression. This indicates that striatal neurons may respond most strongly to sudden, precisely timed, coincident thalamic inputs, whereas persistent activity will be depressed already at the second response.

In summary, the thalamus and lateral pallium provide the striatum with direct excitatory glutamatergic input of opposite synaptic dynamics that is conserved from lamprey to man.

## References

- Barral J, Galarraga E, Tapia D, Flores-Barrera E, Reyes A, Bargas J (2010). Dopaminergic Modulation of Spiny Neurons in the Turtle Striatum. *Cell Mol Neurobiol*.
- Brodin L, Hokfelt T, Grillner S, Panula P (1990a). Distribution of histaminergic neurons in the brain of the lamprey *Lampetra fluviatilis* as revealed by histamine-immunohistochemistry. *J Comp Neurol* **292**:435-442.
- Brodin L, Theodorsson E, Christenson J, Cullheim S, Hökfelt T, Brown J, Buchan A, Panula P, Verhofstad A, Goldstein M (1990b). Neurotensin-like Peptides in the CNS of Lampreys: Chromatographic Characterisation and Immunohistochemical Localisation with Reference to Aminergic Markers. *Eur J Neurosci* **2**:1095-1109.
- Buchwald NA, Price DD, Vernon L, Hull CD (1973). Caudate intracellular response to thalamic and cortical inputs. *Exp Neurol* **38**:311-323.
- Calabresi P, Pisani A, Mercuri NB, Bernardi G (1992). Long-term Potentiation in the Striatum is Unmasked by Removing the Voltage-dependent Magnesium Block of NMDA Receptor Channels. *Eur J Neurosci* **4**:929-935.
- Derjean D, Moussaddy A, Atallah E, St-Pierre M, Auclair F, Chang S, Ren X, Zielinski B, Dubuc R (2010). A novel neural substrate for the transformation of olfactory inputs into motor output. *PLoS biology* **8**:e1000567.
- Ding J, Peterson JD, Surmeier DJ (2008). Corticostriatal and thalamostriatal synapses have distinctive properties. *J Neurosci* **28**:6483-6492.
- Ding JB, Guzman JN, Peterson JD, Goldberg JA, Surmeier DJ (2010). Thalamic gating of corticostriatal signaling by cholinergic interneurons. *Neuron* **67**:294-307.
- Ellender TJ, Huerta-Ocampo I, Deisseroth K, Capogna M, Bolam JP (2011). Differential modulation of excitatory and inhibitory striatal synaptic transmission by histamine. *J Neurosci* **31**:15340-15351.
- Ericsson J, Robertson B, Wikstrom MA (2007). A lamprey striatal brain slice preparation for patch-clamp recordings. *J Neurosci Methods* **165**:251-256.
- Ericsson J, Silberberg G, Robertson B, Wikstrom MA, Grillner S (2011). Striatal cellular properties conserved from lampreys to mammals. *J Physiol* **589**:2979-2992.
- Ewert JP, Buxbaum-Conradi H, Glogow M, Röttgen A, Schürg-Pfeiffer E, Schwippert WW (1999). Forebrain and midbrain structures involved in prey-catching behaviour of toads: stimulus-response mediating circuits and their modulating loops. *Eur J Morphol* **37**:172-176.
- Farries MA, Perkel DJ (2000). Electrophysiological properties of avian basal ganglia neurons recorded in vitro. *J Neurophysiol* **84**:2502-2513.
- Farries MA, Meitzen J, Perkel DJ (2005). Electrophysiological properties of neurons in the basal ganglia of the domestic chick: conservation and divergence in the evolution of the avian basal ganglia. *J Neurophysiol* **94**:454-467.
- Gittis AH, Nelson AB, Thwin MT, Palop JJ, Kreitzer AC (2010). Distinct roles of GABAergic interneurons in the regulation of striatal output pathways. *J Neurosci* **30**:2223-2234.
- Goubard V, Fino E, Venance L (2011). Contribution of astrocytic glutamate and GABA uptake to corticostriatal information processing. *J Physiol* **589**:2301-2319.
- Graybiel AM (2005). The basal ganglia: learning new tricks and loving it. *Curr Opin Neurobiol* **15**:638-644.
- Grillner S, Hellgren J, Menard A, Saitoh K, Wikstrom MA (2005). Mechanisms for selection of basic motor programs--roles for the striatum and pallidum. *Trends Neurosci* **28**:364-370.
- Jimenez AJ, Mancera JM, Pombal MA, Perez-Figares JM, Fernandez-Llebrez P (1996). Distribution of galanin-like immunoreactive elements in the brain of the adult lamprey *Lampetra fluviatilis*. *J Comp Neurol* **368**:185-197.
- Kawaguchi Y, Wilson CJ, Emson PC (1989). Intracellular recording of identified neostriatal patch and matrix spiny cells in a slice preparation preserving cortical inputs. *J Neurophysiol* **62**:1052-1068.

- Klaus A, Planert H, Hjorth JJ, Berke JD, Silberberg G, Kotaleski JH (2011). Striatal fast-spiking interneurons: from firing patterns to postsynaptic impact. *Frontiers in systems neuroscience* **5**:57.
- Koos T, Tepper JM (1999). Inhibitory control of neostriatal projection neurons by GABAergic interneurons. *Nat Neurosci* **2**:467-472.
- Kumar S, Hedges S (1998). A molecular timescale for vertebrate evolution. *Nature* **392**:917-920.
- Mallet N, Le Moine C, Charpier S, Gonon F (2005). Feedforward inhibition of projection neurons by fast-spiking GABA interneurons in the rat striatum in vivo. *J Neurosci* **25**:3857-3869.
- Marín O, Smeets W, González A (1998). Evolution of the basal ganglia in tetrapods: a new perspective based on recent studies in amphibians. *Trends Neurosci* **21**:487-494.
- Matsumoto N, Minamimoto T, Graybiel AM, Kimura M (2001). Neurons in the thalamic CM-Pf complex supply striatal neurons with information about behaviorally significant sensory events. *J Neurophysiol* **85**:960-976.
- Matute C, Streit P (1986). Monoclonal antibodies demonstrating GABA-like immunoreactivity. *Histochemistry* **86**:147-157.
- Menard A, Grillner S (2008). Diencephalic locomotor region in the lamprey--afferents and efferent control. *J Neurophysiol* **100**:1343-1353.
- Menard A, Auclair F, Bourcier-Lucas C, Grillner S, Dubuc R (2007). Descending GABAergic projections to the mesencephalic locomotor region in the lamprey *Petromyzon marinus*. *J Comp Neurol* **501**:260-273.
- Northcutt RG, Puzdrowski RL (1988). Projections of the olfactory bulb and nervus terminalis in the silver lamprey. *Brain, behavior and evolution* **32**:96-107.
- Northcutt RG, Wicht H (1997). Afferent and efferent connections of the lateral and medial pallia of the silver lamprey. *Brain, behavior and evolution* **49**:1-19.
- Ocaña FM, Saitoh K, Rodriguez F, Robertson B and Grillner S (2011). Is there a motor pallium in the lamprey. *International Brain Research Organization*.
- Partridge JG, Tang KC, Lovinger DM (2000). Regional and postnatal heterogeneity of activity-dependent long-term changes in synaptic efficacy in the dorsal striatum. *J Neurophysiol* **84**:1422-1429.
- Polenova OA, Vesselkin NP (1993). Olfactory and nonolfactory projections in the river lamprey (*Lampetra fluviatilis*) telencephalon. *Journal fur Hirnforschung* **34**:261-279.
- Pombal MA, El Manira A, Grillner S (1997a). Organization of the lamprey striatum - transmitters and projections. *Brain Res* **766**:249-254.
- Pombal MA, El Manira A, Grillner S (1997b). Afferents of the lamprey striatum with special reference to the dopaminergic system: a combined tracing and immunohistochemical study. *J Comp Neurol* **386**:71-91.
- Reiner A, Medina L, Veenman C (1998). Structural and functional evolution of the basal ganglia in vertebrates. *Brain Res Brain Res Rev* **28**:235-285.
- Robertson B, Saitoh K, Menard A, Grillner S (2006). Afferents of the lamprey optic tectum with special reference to the GABA input: combined tracing and immunohistochemical study. *J Comp Neurol* **499**:106-119.
- Robertson B, Auclair F, Menard A, Grillner S, Dubuc R (2007). GABA distribution in lamprey is phylogenetically conserved. *J Comp Neurol* **503**:47-63.
- Robertson B, Huerta-Ocampo I, Ericsson J, Stephenson-Jones M, Pérez-Fernández J, Bolam P, Diaz-Heijtz R and Grillner S (2012). The Dopamine D2 Receptor Gene in Lamprey, its Expression in the Striatum and Cellular Effects of D2 Receptor Activation. *PLoS ONE* **7**:1-12; e35642
- Smeal RM, Gaspar RC, Keefe KA, Wilcox KS (2007). A rat brain slice preparation for characterizing both thalamostriatal and corticostriatal afferents. *J Neurosci Methods* **159**:224-235.
- Smeets WJ, Marín O, Gonzalez A (2000). Evolution of the basal ganglia: new perspectives through a comparative approach. *J Anat* **196 (Pt 4)**:501-517.



- Smith R, Musleh W, Akopian G, Buckwalter G, Walsh JP (2001). Regional differences in the expression of corticostriatal synaptic plasticity. *Neuroscience* **106**:95-101.
- Smith Y, Raju DV, Pare JF, Sidibe M (2004). The thalamostriatal system: a highly specific network of the basal ganglia circuitry. *Trends Neurosci* **27**:520-527.
- Stephenson-Jones M, Ericsson J, Robertson B, Grillner S (2012). Evolution of the basal ganglia; Dual output pathways conserved throughout vertebrate phylogeny. *J Comp Neurol.* **Feb 20**. doi:10.1002/cne.23087
- Stephenson-Jones M, Samuelsson E, Ericsson J, Robertson B, Grillner S (2011). Evolutionary conservation of the basal ganglia as a common vertebrate mechanism for action selection. *Current biology* : **CB 21**:1081-1091.
- Suzuki T, Miura M, Nishimura K, Aosaki T (2001). Dopamine-dependent synaptic plasticity in the striatal cholinergic interneurons. *J Neurosci* **21**:6492-6501.
- Tepper JM, Koos T, Wilson CJ (2004). GABAergic microcircuits in the neostriatum. *Trends Neurosci* **27**:662-669.
- Thomson AM (2000). Facilitation, augmentation and potentiation at central synapses. *Trends Neurosci* **23**:305-312.
- Vesselkin NP, Ermakova TV, Reperant J, Kosareva AA, Kenigfest NB (1980). The retinofugal and retinopetal systems in *Lampetra fluviatilis*. An experimental study using radioautographic and HRP methods. *Brain Res* **195**:453-460.
- Villar-Cerviño V, Barreiro-Iglesias A, Mazan S, Rodicio MC, Anadón R (2011). Glutamatergic neuronal populations in the forebrain of the sea lamprey, *Petromyzon marinus*: An in situ hybridisation and immunocytochemical study. *J Comp Neurol* **519**:1712-1735.

**Author contributions:** JE conducted the patch-clamp experiments and primary data analysis and developed the experimental design together with GS, MSJ and SG. MSJ performed the anatomical and immunohistochemical experiments and analysis. All authors took part in the evaluation of the experimental data and JE wrote the manuscript in interaction with all authors.

**Acknowledgements:** This work was supported by the Swedish Research Council, HEALTH-F2-2008-201716 Select-and-Act, ICT-STREP 216100-LAMPETRA, and the Karolinska Institute. We are grateful to Drs Peter Wallén and Abdel El Manira for valuable comments on the manuscript.



IV



# The Dopamine D2 Receptor Gene in Lamprey, Its Expression in the Striatum and Cellular Effects of D2 Receptor Activation

Brita Robertson<sup>1</sup>, Icnelia Huerta-Ocampo<sup>2</sup>, Jesper Ericsson<sup>1</sup>, Marcus Stephenson-Jones<sup>1</sup>, Juan Pérez-Fernández<sup>3</sup>, J. Paul Bolam<sup>2</sup>, Rochellys Diaz-Heijtz<sup>1</sup>, Sten Grillner<sup>1\*</sup>

<sup>1</sup> Department of Neuroscience, Karolinska Institutet, Stockholm, Sweden, <sup>2</sup> MRC Anatomical Neuropharmacology Unit, Department of Pharmacology, University of Oxford, Oxford, United Kingdom, <sup>3</sup> NeuroIam Group, Department of Functional Biology and Health Sciences, Faculty of Biology, University of Vigo, Vigo, Spain

## Abstract

All basal ganglia subnuclei have recently been identified in lampreys, the phylogenetically oldest group of vertebrates. Furthermore, the interconnectivity of these nuclei is similar to mammals and tyrosine hydroxylase-positive (dopaminergic) fibers have been detected within the input layer, the striatum. Striatal processing is critically dependent on the interplay with the dopamine system, and we explore here whether D2 receptors are expressed in the lamprey striatum and their potential role. We have identified a cDNA encoding the dopamine D2 receptor from the lamprey brain and the deduced protein sequence showed close phylogenetic relationship with other vertebrate D2 receptors, and an almost 100% identity within the transmembrane domains containing the amino acids essential for dopamine binding. There was a strong and distinct expression of D2 receptor mRNA in a subpopulation of striatal neurons, and in the same region tyrosine hydroxylase-immunoreactive synaptic terminals were identified at the ultrastructural level. The synaptic incidence of tyrosine hydroxylase-immunoreactive boutons was highest in a region ventrolateral to the compact layer of striatal neurons, a region where most striatal dendrites arborise. Application of a D2 receptor agonist modulates striatal neurons by causing a reduced spike discharge and a diminished post-inhibitory rebound. We conclude that the D2 receptor gene had already evolved in the earliest group of vertebrates, cyclostomes, when they diverged from the main vertebrate line of evolution (560 mya), and that it is expressed in striatum where it exerts similar cellular effects to that in other vertebrates. These results together with our previous published data (Stephenson-Jones *et al.* 2011, 2012) further emphasize the high degree of conservation of the basal ganglia, also with regard to the indirect loop, and its role as a basic mechanism for action selection in all vertebrates.

**Citation:** Robertson B, Huerta-Ocampo I, Ericsson J, Stephenson-Jones M, Pérez-Fernández J, et al. (2012) The Dopamine D2 Receptor Gene in Lamprey, Its Expression in the Striatum and Cellular Effects of D2 Receptor Activation. PLoS ONE 7(4): e35642. doi:10.1371/journal.pone.0035642

**Editor:** J. David Spafford, University of Waterloo, Canada

**Received:** January 26, 2012; **Accepted:** March 19, 2012; **Published:** April 26, 2012

**Copyright:** © 2012 Robertson et al. This is an open-access article distributed under the terms of the Creative Commons Attribution License, which permits unrestricted use, distribution, and reproduction in any medium, provided the original author and source are credited.

**Funding:** This work was supported by EU FP5 'Neurobotics' 001917 (to Dr. Grillner), EU FP7 'Lampetra' 21610 (to Dr. Grillner), Swedish research council, VR-M - 3026, VR-NT 621-2007-6049 (to Dr. Grillner), Karolinska Institutet's Research funds (to Dr. Robertson), FP7 Select-and-Act 201716 (to Dr. Grillner and Dr. Bolam) and Karolinska Institutet Doctoral funds (to Dr. Ericsson), Stockholm Brain Institute (to Dr. Grillner and Dr. Diaz-Heijtz), Spanish MICINN-FEDER BFU2009-13369 (to Dr. Pérez-Fernández). The funders had no role in study design, data collection and analysis, decision to publish, or preparation of the manuscript.

**Competing Interests:** The authors have declared that no competing interests exist.

\* E-mail: sten.grillner@ki.se

## Introduction

For an animal to achieve its goal it has to select between competing actions. A group of subcortical nuclei, the basal ganglia, play a key role in this process in vertebrates [1–5]. The neuronal architecture underlying selection is evolutionarily highly conserved, as all components of the basal ganglia, including the striatum and homologues of the globus pallidus, substantia nigra (*pars compacta* and *reticulata* (SNr)) and the subthalamic nucleus (STN), have been identified in the lampreys [6][7], the phylogenetically oldest vertebrates that diverged from the main vertebrate line 560 million years ago [8]. Furthermore, the lamprey striatum receives input from the cortex/pallium and thalamus [9] and GABAergic striatal neurons in both lampreys [10] and mammals [11] display inward rectification, a key feature critical in the expression of basal ganglia function.

Information in the striatum is transmitted monosynaptically by GABAergic substance P-expressing projection neurons to the

output nuclei of the basal ganglia, the globus pallidus *interna* (GPi) and the SNr (direct pathway) or polysynaptically, by enkephalin-expressing neurons projecting to the GP *externa* (GPe) and the STN and thence to the output nuclei (indirect pathway; see [7,12]). A difference between mammals on one side and lampreys and birds on the other, however, is that GPi and GPe are intermingled in the latter group but clearly distinct in mammals [7,13].

The main modulatory input to the striatum is dopaminergic in both lamprey [9] and mammals (see [14]). The functional role of dopamine in lampreys was recently studied through dopamine depletion with methyl-phenyl tetrahydropyridine (MPTP). This caused a marked hypokinesia, as in Parkinson's disease, an effect that was counteracted by treatment with dopamine agonists [15]. Dopamine receptors constitute two structurally and functionally different classes of dopamine receptors; the D1 receptor class (D1A/D1 and D1B/D5) and the D2 class (D2, D3 and D4) (see [16]). The D1 and D2 classes are thought to have different evolutionary origin and are considered to have independently and

convergently acquired the ability to bind dopamine [17]. In mammals, dopaminergic modulation of direct pathway neurons is dependent on dopamine D1 receptors, whereas modulation of indirect pathway neurons is mediated by D2 receptors. In lamprey, only a partial D1-like receptor gene has been cloned [18] and shown to be expressed in a subpopulation of striatal neurons [19]. Whether a D2 receptor is expressed in cyclostomes and if so, whether this receptor is functional is the subject of the present study. D2 receptors have previously only been identified from the level of teleosts to primates (e.g. [17,20–23]). The presence of a functional D2 receptor would provide important additional evidence of the evolutionary conservation of the receptor subtype and the operation of the basal ganglia circuitry. Here, we identify a lamprey D2 receptor gene and show its expression in a subpopulation of neurons in the striatum, where tyrosine hydroxylase-positive (TH) boutons make synaptic contact with striatal dendrites. In addition, we show that a D2 receptor agonist reduces action potential discharge of striatal neurons, in a similar manner to that observed in other vertebrates.

## Results

### Cloning and sequence analysis of lamprey dopamine D2 receptor

In order to identify a lamprey dopamine D2 receptor, the human dopamine D2 receptor long chain (accession number NM\_000795) was aligned using BLAST against the sea lamprey (*Petromyzon marinus*) genome (<http://blast.ncbi.nlm.nih.gov>). A lamprey D2 receptor-like sequence sharing an 80% identity with the human sequence was assembled and used as template. Table 1 shows the different primers used to obtain the 5' and 3' sequences. In addition, we used the 5'- and 3'-RACE PCR to amplify the respective sequences including the unconserved amino terminus and to verify the start and stop codons. At least two sets of primers were used to amplify the different regions.

The cloned D2 receptor cDNA sequence of the lamprey comprises an open reading frame of 1533 nucleotides encoding a protein of 511 amino acids. (Figure S1). The putative start codon was identified by being embedded within a strong consensus motif

for a ribosomal binding site; with a G following ATG (position +4) and a purine, G, three nucleotides upstream (position -3) (see Figure S1; [24]). In addition, the BLAST analysis showed that the length of the lamprey D2 receptor amino terminus is similar to that of other vertebrates.

The D2 receptor sequence contains two highly conserved regions. One conserved region was found in the 5' region comprising 601 nucleotides and a second at the 3' end comprising 254 nucleotides (Figure 1A). In between the two conserved regions, a sequence of 586 nucleotides, comprising the third intracellular loop, shows little identity with other vertebrate D2 receptor sequences (Figures 1A, B, see also Figure 2). An additional unconserved region was found at the 5' end comprising 95 nucleotides.

**Transmembrane domains.** The deduced amino acid sequence exhibited the typical profile of a seven transmembrane (TM) G-protein coupled receptor (GPCR). The first five TM domains were located at the conserved 5' end, and TM 6 and 7 were located at the conserved 3' end (Figures 1B and 2). As apparent in Figure 2, the lamprey dopamine D2 receptor shares a very high identity within all TM domains, with the second and third domains showing an 100% identity, when compared with the TM domains of *Homo sapiens*, *Mus musculus*, *Danio rerio* and *Anguilla anguilla*. Interestingly, when an amino acid differs in the lamprey it mostly also differs in one or several of the other species examined. The entire amino acid sequence in the lamprey shows around 60% identity with other vertebrate D2 receptor protein sequences.

The lamprey protein contains highly conserved amino acid residues that are thought to line the dopamine binding pocket within the hydrophobic TM domains, in particular valine residues in TM2, an aspartic acid residue in TM3, two serine residues in TM5, and a highly conserved WLPFF sequence and a histidine residue in TM6 [25,26]. Many characteristic features of GPCRs were identified in the protein sequence of the lamprey D2 receptor, such as a conserved DRY sequence at the end of TM3, which is mandatory for the interaction of the receptor with G proteins [27]. The lamprey protein also contains several consensus phosphorylation sites for protein kinases (PKC, PKA and CKII) and a consensus N-glycosylation site in the NH<sub>2</sub>-terminus (see

**Table 1.** Primers (5' to 3') used for the cloning of the lamprey dopamine D2 receptor gene.

	Forward primer	Reverse primer
<b>Fw-115/Re170</b>	ATGCTTGGGAGCTGCAGAGA	TGCGCGTCTCGCGTGAAAAG
<b>Fw-80/Re170</b>	GCACATTTTGGCCAAACGCGA	TGCGCGTCTCGCGTGAAAAGT
<b>Fw128/Re767</b>	TGCTCATATGCTCATCGTC	TCAAGCTTTGCACATCGTC
<b>Fw161/Re420</b>	TGCTCGATCGCCGTCT	GCTCTACAACACCCGCTACCG
<b>Fw407/Re643</b>	TGCGGATGCCCGTGCTCTACAAC	ATCTACGTGGTCCCTGCGCAAGCG
<b>Fw431/Re668</b>	CCCGCTACCGGTCTCGACGGAGAGT	GCAAAAGGGTCAACGCCAAGCGC
<b>5' RACE Re410</b>		CGATGCCCGTGCTCTACAACACC
<b>Fw469/Re957</b>	TCTGTGGTTGGGTCTGTCT	CCAACAACACTCGCTCCG
<b>Fw431/Re1497</b>	CCCGCTACCGGTCTCGACGGAGAGT	GTTCCGCAAGGCCTTCATTAAAA
<b>Fw951/Re1492</b>	GGCGAGCCAACAACACTC	ATAGAGTTCGCAAGGCCTT
<b>Fw1289/Re1497</b>	CGCAACAGAGAGAGAAGAAGCGGACTC	GTTCCGCAAGGCCTTCATTAAAA
<b>Fw1277/Re1492</b>	ATCGGAATTTTTCGCAACAG	ATAGAGTTCGCAAGGCCTT
<b>3' RACE Fw1290</b>	GCAACAGAGAGAGAAGAAGCGGACTCA	
<b>3' RACE Fw1294</b>	CAGAGAGAGAAGAAGCGGACTCAGATGC	

Fw, forward; Re, reverse.

doi:10.1371/journal.pone.0035642.t001

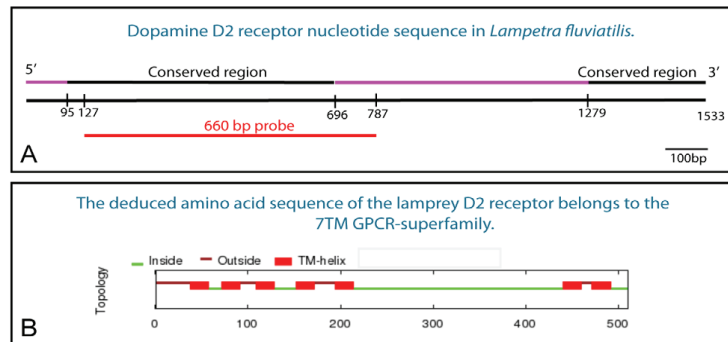


**Figure 1. The lamprey dopamine D2 receptor.** **A.** A schematic drawing of the lamprey dopamine D2 receptor nucleotide sequence showing the conserved regions (black) at the 5' and 3' ends, respectively, and the site from which the riboprobe (660 bp, red) was made. **B.** The seven transmembrane domains (TM-helix) are all located at the conserved parts of the dopamine D2 receptor. The deduced amino acid sequence of the receptor shows that it belongs to the GPCR-superfamily.  
doi:10.1371/journal.pone.0035642.g001

Figure S1; [27]. In addition, it showed the typical features of the D2 class of dopamine receptors such as a relatively long third intracellular loop and the carboxyl-terminal ending with a cysteine residue (Figure 2; [27–29]).

**Phylogenetic analysis.** We focused our phylogenetic analysis on the D2 receptor family as the BLAST analysis of the lamprey cloned sequence showed identity with the D2 receptor

family, but not with the D1 receptor family. The deduced amino acid sequence of the lamprey D2 receptor was aligned with homologous D2 receptor sequences from other known vertebrate representatives. The lamprey sequence was clustered together with other vertebrate D2 sequences, not with the D3 or D4 receptor subtypes, which shows that the lamprey sequence can be assigned to the D2 receptor subtype, based on the primary amino acid

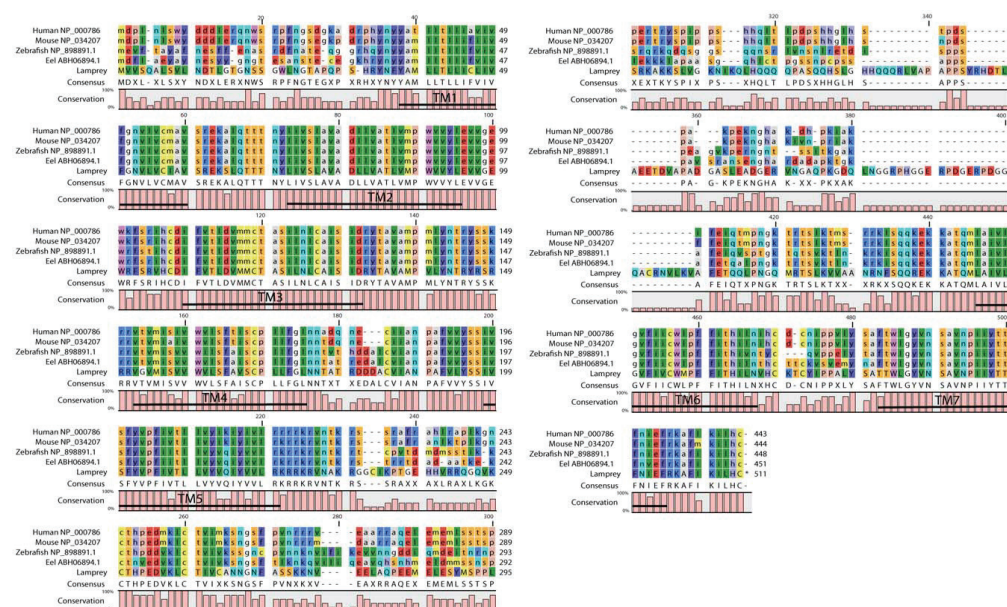


**Figure 2. Alignment of dopamine D2 receptor amino acid sequences.** Alignment of the deduced amino acid sequence from the lamprey dopamine D2 receptor with those from *Homo sapiens*, *Mus musculus*, *Danio rerio* and *Anguilla anguilla*. The seven transmembrane domains are indicated.  
doi:10.1371/journal.pone.0035642.g002

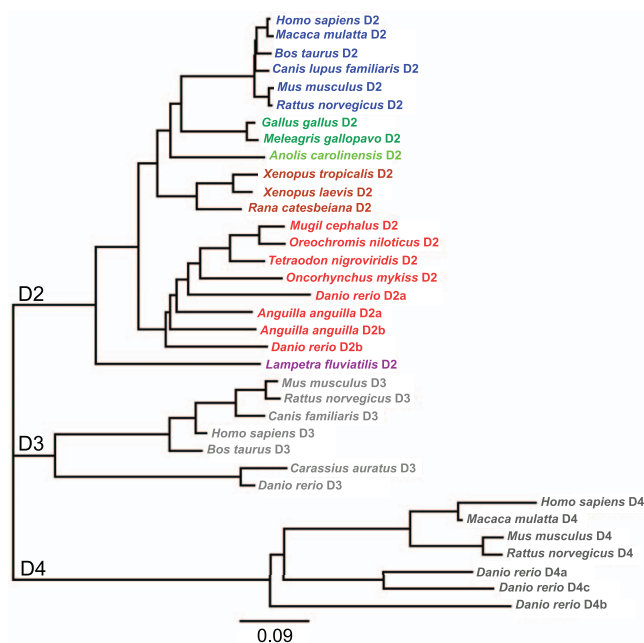


**Figure 3. Phylogenetic analysis of vertebrate dopamine receptors of the D2-family.** The distant tree was built with the neighbor-joining algorithm from alignments of the D2, D3 and D4 receptor subtypes from several vertebrate species. Data were re-sampled by 1000 bootstrap replicates to determine confidence indices within the phylogenetic tree. The scale bar refers to a phylogenetic distance of 0.09 amino acid substitution per site. The different vertebrate classes are indicated by different colors (mammals, blue; birds, dark green; reptiles, light green; amphibians, brown; fish, red; cyclostomes, mauve). GenBank accession numbers of the sequences are: *Homo sapiens* D2, AAA52761; *Macaca mulatta* D2, XP\_001085571; *Bos taurus* D2, DAA22356; *Canis lupus familiaris* D2, AAG34494; *Mus musculus* D2, NP\_034207; *Rattus norvegicus* D2, NP\_036679; *Gallus gallus* D2, NP\_001106761; *Meleagris gallopavo* D2, AAD03818; *Anolis carolinensis* D2, XP\_003217484; *Xenopus tropicalis* D2, XP\_002937871; *Xenopus laevis* D2, CAA51412; *Rana catesbeiana* D2, BAI70438; *Mugil cephalus* D2, AAU87970; *Oreochromis niloticus* D2, AAU87971; *Tetraodon nigroviridis* D2, CAF97490; *Oncorhynchus mykiss* D2, CAC87873; *Danio rerio* D2a, AAN87174; *Danio rerio* D2b, AAP94011; *Anguilla anguilla* D2a, ABH06893; *Anguilla anguilla* D2b, ABH06894; *Lampetra fluviatilis* D2, ADO23655; *Mus musculus* D3, 2105315A; *Rattus norvegicus* D3, 1614344A; *Canis lupus familiaris* D3, XP\_545106; *Homo sapiens* D3, 1705199A; *Bos taurus* D3, NP\_001179824; *Carassius auratus* D3, ABN70936; *Danio rerio* D3, AAN87173; *Homo sapiens* D4, 1709359A; *Macaca mulatta* D4, XP\_001087197; *Mus musculus* D4, 2109259A; *Rattus norvegicus* D4, AAA18588; *Danio rerio* D4a, AAW80614; *Danio rerio* D4b, AAW80615; *Danio rerio* D4c, AAW80616. doi:10.1371/journal.pone.0035642.g003

sequence (Figure 3). The tree topology further showed that the lamprey sequence is the most distant from the mammalian clade (Figure 3). The cloned lamprey D2 receptor nucleotide sequence is available in the GenBank (accession number HQ331119).

#### Dopamine D2 receptor mRNA expression

The riboprobe used contained the 5' conserved region, which includes the first five transmembrane domains (see Figure 1A and 2). When the deduced protein sequence of the riboprobe was aligned against other vertebrates using BLAST it showed a 92% identity with the *Anguilla anguilla*, 90% with *Danio rerio*, 86% with *Mus musculus*, and 86% with *Homo sapiens* D2 receptor protein sequences. The specificity of the signals obtained by *in situ* hybridization was confirmed using sense probes (see Figure 4D). Background levels from all brain regions were very low in all sections hybridized with <sup>35</sup>S-UTP-labeled riboprobes.

In the striatum (Figure 4B), a high level of D2 receptor expression was observed in the whole rostrocaudal extent visualized with either DIG- or <sup>35</sup>S-UTP-labeled riboprobes (Figure 4A and C). Only a subpopulation of neurons within the

compact striatal cell layer expressed the receptor mRNA (Figure 4C).

The preoptic area also expressed a high level of the D2 receptor (Figure 4A). A small region just ventral to striatum and dorsal to the preoptic area, the magnocellular preoptic nucleus, appears, however, devoid of D2 receptor expression (Figure 4A). Furthermore, neurons in the dorsal and lateral pallidum expressed the receptor but at a lower level (Figure 4A). More caudally, high levels of expression are observed in the habenula, thalamus and hypothalamus as well as in the mammillary region (Figure 4E–H).

Retrograde tracing from the lamprey homologue of the SNr leads to the labeling of only striatal projection neurons expressing substance P and thus belonging to the direct pathway [6]. Consistent with these previous observations we showed retrograde labeling of neurons in the striatum following the injection of neurobiotin in the SNr (Figure 5A). In sections that were double-labeled to reveal the retrogradely labeled neurons and the *in situ* hybridization signal for the D2 receptor, the labels never colocalized (Figure 5A–C; 38 retrogradely labeled neurons analyzed). This finding supports the notion that D2 receptor

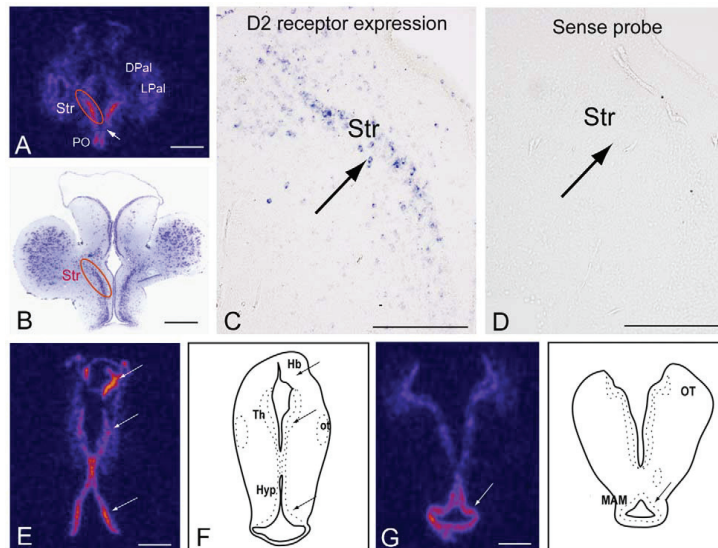


**Figure 4. Dopamine D2 receptor expression in the lamprey brain.** **A.**  $^{35}$ S-UTP-labeled D2 receptor riboprobe shows strong expression in the striatum. D2 receptor expression is also present in the dorsal and lateral pallium although less strong. Note the absence of receptor expression in the magnocellular preoptic nucleus (arrow). **B.** Nissl stained section from the striatum showing the site of receptor expression in A and C. **C.** DIG-labeled D2 receptor riboprobe expressed in a subpopulation of striatal neurons. **D.** DIG-labeled sense riboprobe showing lack of mRNA expression in the section adjacent to the one in Figure 5C. **E.**  $^{35}$ S-UTP-labeled D2 receptor riboprobe expression in the habenula, thalamus and hypothalamus. **F.** Schematic drawing of the lamprey brain indicating the habenula, thalamus and hypothalamus. **G.**  $^{35}$ S-UTP-labeled D2 receptor riboprobe shows strong expression in the mammillary area. **H.** Schematic drawing of the lamprey brain indicating the mammillary area. The pseudocoloring in **A**, **E** and **G** indicates signal intensity from low (black/blue) to high (pink/yellow). Abbreviation: *DPal*, dorsal pallium; *Hb*, habenula; *Hyp*, hypothalamus; *LPal*, lateral pallium; *MAM*, mammillary region; *ot*, optic tract; *OT*, optic tectum; *PO*, preoptic nucleus; *Str*, Striatum; *Th*, thalamus. Scale bars, A, B, E and G 500  $\mu$ m; C and D 200  $\mu$ m.  
doi:10.1371/journal.pone.0035642.g004

expressing neurons do not project directly to the output nuclei of the lamprey and are thus likely to be those striatal neurons that project to the GPe.

#### Ultrastructural localization of tyrosine hydroxylase-immunoreactive structures

Previous studies have investigated the distribution of dopamine neurons and fibers in the lamprey brain by using immunohistochemical techniques at the light microscope level [9,30]. In this study we characterized the presence of TH-immunoreactive fibers

in the striatum and performed a quantitative analysis of dopaminergic profiles at the electron microscopic level to determine synaptic incidence and the nature of the postsynaptic structures in three regions of the lamprey striatum.

The striatum is densely innervated by long, TH-positive axons, which are mainly distributed in areas III and I, with area II containing slightly fewer immunoreactive profiles (Figure 6B). In all areas, TH-positive profiles contained densely packed round vesicles (Figure 6C–E) distributed throughout the axon, and were commonly associated with two or more mitochondria. All immunolabeled structures that formed synaptic contacts, formed

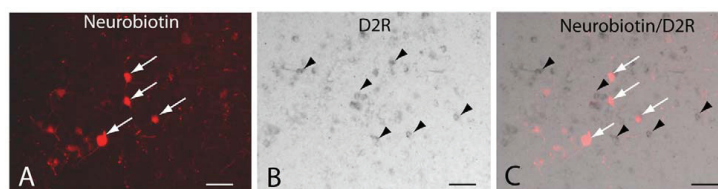


**Figure 5. Striatal projection neurons targeting substantia nigra pars reticulata (SNr) do not express the D2 receptor.** **A.** Striatal neurons retrogradely labeled after injections of neurobiotin into the SNr (white arrows). **B.** DIG-labeled D2 receptor riboprobe expressed in a subpopulation of striatal cells (black arrow heads show examples of positive cells). **C.** Merged image showing the absence of overlap between retrogradely labeled cells and D2 receptor mRNA expression. Scale bars, 100  $\mu$ m.  
doi:10.1371/journal.pone.0035642.g005



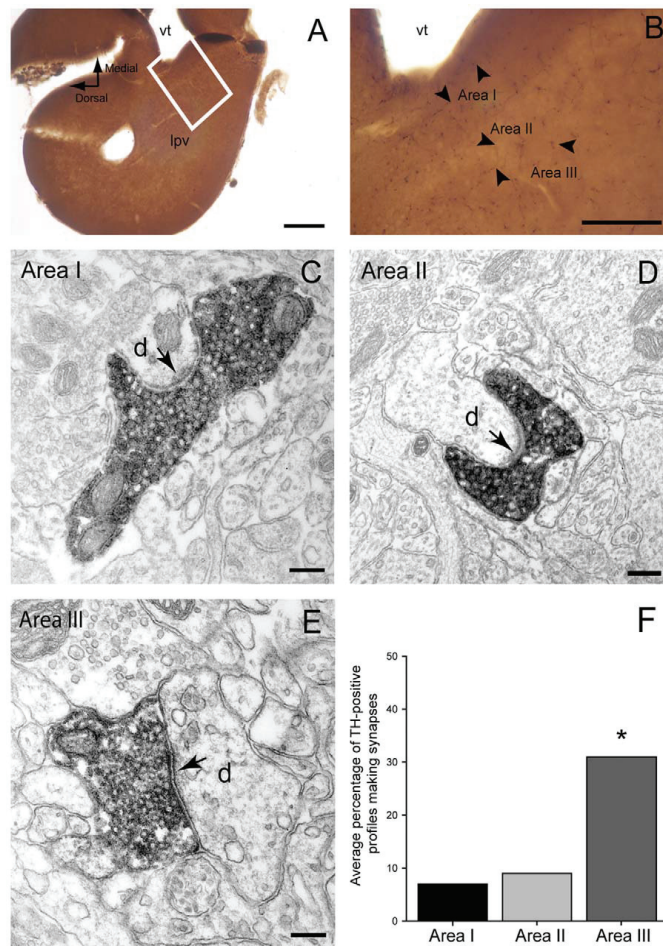


**Figure 6. Tyrosine hydroxylase (TH) immunoreactivity in the lamprey striatum.** **A and B.** Light microscope photomicrographs showing the areas (I, II and III) of the striatum that were included in the electron microscope analysis. Note the slightly higher density of TH-immunoreactive fibers (some indicated by small arrows) in Areas I and III. **C–E.** Electron micrographs of TH-immunolabeled axonal profiles forming asymmetrical synapses (arrows) with dendritic shafts (d) in Area I (C), II (D) and III (E) of the lamprey striatum. Note the densely packed vesicles and the prominent postsynaptic densities. **F.** Quantitative analysis of synaptic incidence in the three areas of striatum. The histogram shows the average percentage of TH-immunolabeled profiles which form synaptic junctions (out of a total of 75 profiles per area,  $n = 3$ ). Synaptic incidence in Area III was significantly higher when compared to Area I ( $\chi^2$  test,  $p = 0.0003$ ) and Area II ( $\chi^2$  test,  $p = 0.0022$ ). Abbreviations: vt, ventriculus medialis telencephali; lpv, ventral part of the lateral pallidum. Scale bars: A: 200  $\mu$ m, B: 100  $\mu$ m, C–E: 200 nm. doi:10.1371/journal.pone.0035642.g006

asymmetric synapses that were characterized by the presence of a long synaptic specialization, presynaptic vesicle accumulation, a thick postsynaptic density, a widened synaptic cleft and cleft material (Figure 6C–E).

In all three areas (I, II and III) the postsynaptic structures were dendrites that varied in size and shape, some of them having a stubby (Figure 6D) or spine-like appearance. We did not observe any immunopositive boutons establishing synapses of the symmetrical type (Gray's type 2) or making contact with a cell body.

The synaptic incidence analysis on the serial sections of the TH-labeled axonal profiles demonstrates that most do not form a synaptic junction within six consecutive sections. The proportion of TH-labeled axons that make synapses in area III was 31%, which was significantly higher than the synaptic incidence observed in area I ( $\chi^2$  test,  $p = 0.0003$ ) and area II ( $\chi^2$  test,  $p = 0.0022$ ), where only 7 and 9% of labeled profiles formed synapses, respectively (Figure 6F).



### The effect of D2 receptor activation on striatal neurons

In mammals and birds, selective activation of D2 receptors reduces the overall excitability of striatal projection and interneurons through modulation of intrinsic and synaptic properties [12,31,32]. To investigate the effects of D2 receptor activation on lamprey striatal neurons, we applied the selective D2 agonist, TNPA, during whole cell current-clamp recordings.

Depolarizing current steps from a slightly depolarized baseline of -65 mV applied to striatal neuron elicited a series of action potentials (Figure 7A<sub>1</sub>–A<sub>3</sub>). Application of 100  $\mu$ M TNPA markedly reduced the number of evoked spikes (Figure 7A<sub>2</sub>). Comparison of the spike frequency of evoked action potential at twice the threshold current for evoking a spike revealed a marked and significant reduction in 5 of 6 neurons in the presence of TNPA (control  $6.4 \pm 2.5$  Hz; TNPA  $3.6 \pm 3.6$ ;  $p < 0.05$ ;  $n = 6$ ; Figure 7B). The reduction was not affected by changing the baseline from which action potentials were evoked.

At the termination of hyperpolarizing current steps a post-inhibitory rebound (PIR) depolarization occurred with superimposed spikes (Figure 7A<sub>1</sub>, control). This occurs at the baseline level of -65 mV, but not at holding-potentials below -80 mV ( $n = 6$ ). During TNPA application, the number of PIR spikes (Figure 7A<sub>2</sub> and C) was markedly reduced (control  $1.9 \pm 0.9$ ; TNPA  $0.3 \pm 0.5$ ;  $p < 0.05$ ;  $n = 6$ ). Moreover, when rebound spikes were seen in the presence of TNPA, they tended to occur much later after the end of the hyperpolarizing pulse (Figure 7D). TNPA also affected the size and shape of evoked action potentials and PIR spikes (Figure 7E).

### Discussion

This study represents the first description of the lamprey dopamine D2 receptor cDNA and its expression pattern in the forebrain. We revealed a strong and distinct expression of the D2

receptor mRNA in the striatum. The same region contains TH-immunoreactive synaptic terminals. Moreover, D2 receptor agonists were found to exert similar cellular effects on striatal neurons as established in mammals [12].

### The lamprey dopamine D2 receptor gene

Our analysis of the nucleotide and deduced amino acid sequence of the lamprey D2 receptor demonstrates that it is a member of the superfamily of G-protein coupled receptors and belongs to the D2 receptor subtype. The gene has two highly conserved parts that comprise all the TM domains containing the amino acids necessary for binding of dopamine [25,26]. The unconserved intermediate part that forms the third intracellular loop differs, however, largely from other vertebrates. The longer coding sequence of the lamprey D2 receptor compared to the human long isoform, 1533 bp versus 1332 bp, is mainly due to its longer third cytoplasmic loop. A phylogenetic analysis of the cloned D2 receptor gene rooted the lamprey protein sequence at the base of the D2 receptor tree and furthest from the human D2 receptor in line with lamprey having emerged earlier than any of the other vertebrate species (approximately 560 million years ago; [8]). In mammals, birds and most teleosts, only one D2 receptor gene has been found that encodes for the two protein isoforms, the D2 long and D2 short isoforms [33,34]. Likewise, we only identified one gene encoding for a dopamine D2 receptor, as is the case for the D1-like receptor in lamprey and hagfish [16]. However, in three teleosts (zebrafish, trout and eel), multiple D2 receptors have been identified [23,35,36]. Compared to other gnathostomes, an additional duplication event (3R) is thought to have occurred in the teleost lineage [37]. It is likely that in most cases this additional duplicate has been lost, whereas a subfunctionalization of ancestral functions has been proposed to explain the conservation of both D2 receptor duplicates. In

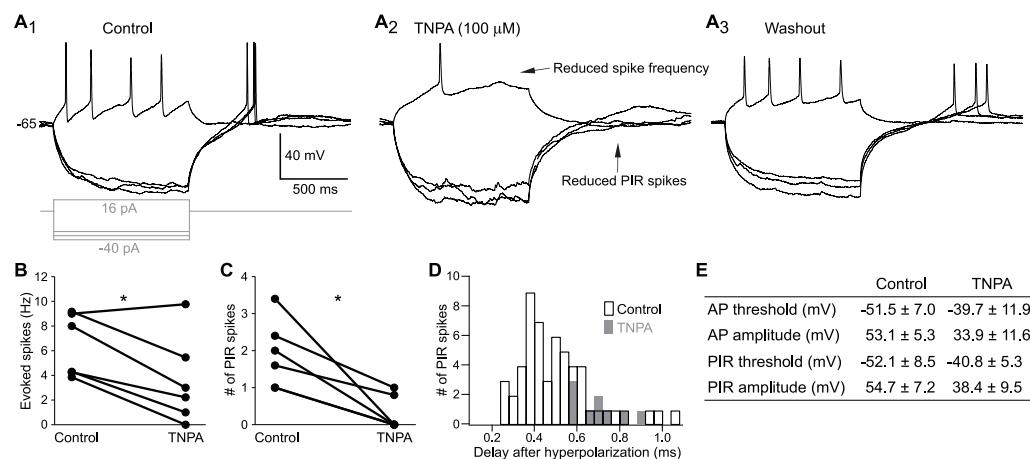


**Figure 7. Modulation of striatal neurons by a dopamine D2 agonist.** A. Voltage responses of a striatal neuron to 1 s long hyperpolarizing and depolarizing current injections during control (A<sub>1</sub>), D2 agonist application (TNPA, A<sub>2</sub>) and washout (A<sub>3</sub>). B. The number of evoked action potentials is reduced upon application of TNPA, measured here at twice the threshold stimulation. C. The average number of PIR spikes is reduced by TNPA, measured after termination of five consecutive hyperpolarizations in between -100 and -80 mV. D. The total number of PIR spikes and the time until the spike are reduced by TNPA, measured as in C. E. Table of firing properties before and during TNPA. All values presented as mean  $\pm$  SD and differences were significant for all measurements apart from the AP half-width ( $p < 0.05$ , student's t-test). Abbreviations: AP, action potential; PIR, post-inhibitory rebound; TNPA, trihydroxy-N-propyl-noraporphine 123 hydrobromide hydrate. doi:10.1371/journal.pone.0035642.g007

lampreys, at least one duplication event is thought to have occurred, but according to our results the receptor analyzed clearly corresponds to the mammalian D2 subtype. The D2 receptor is likely to be rather conserved in the vertebrate lineage even in teleosts, where the ancestral functions were maintained despite the existence of additional D2 receptors, although additional analyses are still necessary to confirm this assumption.

#### Expression of D2 receptors in the forebrain

In mammals, a clear difference between the D1 and D2 receptor expressing striatal neurons is evident at the molecular, anatomical, and physiological levels (for review see [12]). The high levels of D2 mRNA receptor expression in a subpopulation of striatal cells, as well as the absence of D2 expression in striatal cells of the direct pathway, indicate that also in lamprey, there is a segregation between these two cell-types. This is further supported by our recent studies that pallidal GPe neurons are mainly apposed by substance P-positive fibers/terminals, whereas GPe neurons are apposed by enkephalin-positive structures and that SNr projecting striatal cells are substance P-immunoreactive [6,7].

High levels of D2 receptor expression were also observed in the preoptic area, habenula, mammillary region, hypothalamus, and thalamus. In all other vertebrates investigated, these regions are rich in D2 receptor expression (e.g. [22,23,35,38,39]) which gives further evidence that our cloned D2 receptor is indeed, a member the D2 receptor subfamily. A small region of the preoptic area, the magnocellular preoptic nucleus, lacked D2 expression, as is the case in the trout [35].

Although the dopamine D2 and D3 receptors belong to the same class of dopamine receptors their expression pattern in the vertebrate brain is very different. Overall, the D2 receptor is by far the more highly expressed subtype and is found in all major brain areas receiving dopaminergic projections, particularly the dorsal striatum. The D3 receptor is not only expressed at a lower levels but it also shows a fairly restricted pattern of expression (e.g. islands of Calleja, nucleus accumbens and cerebellum) [29,40,41]. The robust general expression pattern of the D2 receptor in lamprey brain further supports our conclusion that it belongs to the D2-subfamily.

#### Dopaminergic terminals in striatum

The striatum in lampreys receives a dense dopaminergic innervation that originates in the nucleus tuberculi posterioris in the diencephalon [9]. The general distribution pattern of dopamine-immunoreactive neurons in this nucleus is similar to that obtained using antibodies against aromatic L-amino acid decarboxylase or TH [9,30,42] and furthermore this nucleus does not express the enzymes involved in the synthesis of noradrenaline or adrenaline [42] implying that the neurons are dopaminergic.

The present immunocytochemical findings confirm and extend previous findings relating to TH innervation of the lamprey striatum and demonstrate that TH-immunoreactive axonal profiles are densely packed with synaptic vesicles and form typical asymmetric synaptic specializations. Thus, similar to mammals, the lamprey striatum receives a dense innervation from TH-positive fibers. However, there are differences in the ultrastructural features in terms of their size, type of specialization and distribution of postsynaptic targets. In rodents, TH-positive boutons form symmetrical synapses (Gray's type 2) with both spines and dendritic shafts and occasionally with cell bodies [43–45]. Their synapses are very small and membrane specializations are often difficult to discern. In contrast, in the lamprey striatum dopaminergic terminals form exclusively asymmetric synapses with dendrites which, in addition, have large and prominent

synaptic specializations. Furthermore, our quantitative analysis shows that around 30% of labeled TH-positive profiles observed in Area III form synaptic contacts (when examined in 6 serial sections), whereas profiles located in Areas I and II show a significantly lower synaptic incidence (Figure 6F). Although this degree of synaptic incidence in Areas I and II is similar to that observed in mammals, the synaptic incidence in Area III is higher and may suggest that dopaminergic transmission has different characteristics in this region. It is interesting to note that a single-cell analysis of intracellularly labeled Area II striatal neurons [10] revealed that their dendrites branch more profusely in Area III, i.e. the region in which dopaminergic axons are most likely to form synapses. Overall, our study reveals new aspects of the distribution and fine structural features of the dopaminergic system of the lamprey brain. Furthermore, our data provide the structural basis to support the modulatory role of dopamine within this area and thereby its contribution to basal ganglia functions in the lamprey brain.

#### Modulation of dopamine in the striatum

D2 receptor activation modulates neuronal excitability through inhibition of voltage sensitive  $\text{Ca}^{2+}$  channels, inactivation of  $\text{Na}^{+}$  channels and activation of  $\text{K}^{+}$  channels [29,46,47]. In the present study we observed a marked reduction of discharge in lamprey striatal neurons upon D2 receptor activation, a finding that is consistent with results from reptiles, birds and mammals [31,32,48]. The D2 receptor agonist, TNPA, shifted the threshold to more depolarized levels for both action potentials and PIR spikes, as well as reducing their amplitudes. This is similar to observations in mammals where D2 activation appears to enhance slow inactivation of  $\text{Na}^{+}$  channels, an effect that also contributes to the reduction in the PIR response in cholinergic interneurons [49]. In mammalian striatal projection neurons, a reduced excitability has also been associated with a negative modulation of the L-type  $\text{Ca}_v$  1.3  $\text{Ca}^{2+}$  channel [48,50]. In the lamprey spinal cord, a depression of  $\text{Ca}_v$  1.3  $\text{Ca}^{2+}$  channels by D2 receptor activation has also been described [51]. This is consistent with our findings, where application of TNPA profoundly reduces the number of PIR spikes. The fact that PIR spikes were almost only elicited upon hyperpolarization from a depolarized baseline around  $-65$  mV or more, further suggests  $\text{Ca}_v$  1.3 channels to be involved since this is within their activation range [52].

In mammals, D2 receptors are expressed in neurons that project to the GPe, as part of the indirect pathway [53]. Selective activation of the indirect pathway medium spiny neurons leads to an inhibition of movements [54], presumably by increasing the inhibitory output of the GPe/SNr [12]. The indirect pathway has been observed in lamprey and may represent a common vertebrate mechanism for inhibiting actions [7,54]. Application of dopamine or D2 receptor antagonists cause a decrease in the excitability of mammalian indirect pathway medium spiny neurons [48,55], whereas dopamine increases the excitability of medium spiny neurons that express the D1 receptor and project directly to the GPe/SNr [56,57]. The dichotomous effects of dopamine on these pathways is therefore believed to bias the network to promote actions, by decreasing the excitability of the indirect pathway that suppresses actions and by increasing the excitability of the direct pathway that promotes actions. Our results show that lamprey striatal neurons express the D2 receptor and that D2 receptor agonists decrease the excitability of striatal neurons. This suggests that the direct and indirect pathways are not only conserved throughout vertebrate phylogeny as a common mechanism for action selection but that dopamine will play a

similar role in modulating at least D2 receptor expressing neurons to bias the network for action selection.

## Conclusion

The present identification of a functional dopamine D2 receptor and the structural basis for the modulatory role of dopamine in the lamprey striatum gives additional evidence for the presence of an indirect pathway and that the ancestral basal ganglia circuitry is evolutionary conserved. The resemblances in gene structure between different vertebrate D2 receptors furthermore show that the fundamental function of these receptors is a conserved feature.

## Material and Methods

### Ethical statement

Experiments were performed on a total of 32 adult river lampreys (*Lampetra fluviatilis*) of either sex. The experimental procedures were approved by the local ethical committee (Stockholm's Norra Djurförsöksetiska Nämnd) and were in accordance with *The Guide for the Care and Use of Laboratory Animals* (National Institutes of Health, 1996 revision). During the investigation, every effort was made to minimize animal suffering and to reduce the number of animals used.

### Molecular cloning and sequencing of the lamprey dopamine D2 receptor

**RNA isolation.** Animals (n = 9) were deeply anesthetized in tricane methane sulfonate (MS-222; 100 mg/L; Sigma-Aldrich, St. Louis, MO, USA) diluted in fresh water and the brains were quickly removed and frozen on dry ice. Total RNA was extracted using Trizol reagent (Invitrogen, La Jolla, CA, USA) or RNeasy Mini Kit (Qiagen, Valencia, CA, USA) and quantified by spectrophotometry using NanoDrop® ND-1000 spectrophotometer (NanoDrop Technologies, Wilmington, DE, USA). The integrity and purity of the RNA preparations were analysed by means of gel electrophoresis on Experion bioanalyzer (Bio-Rad Laboratories, Hercules, CA, USA). Only RNA with RQI values between 9.9 and 10 (max value 10) was used for cDNA synthesis.

**cDNA synthesis.** The first-strand cDNA synthesis from total RNA was performed with RETROscript reverse transcriptase (Ambion Inc, Huntingdon, UK) and Oligo (dT) or Random decamers. Identical results were obtained with both.

**PCR amplification.** For polymerase chain reaction (PCR) amplification, degenerate oligonucleotide primers were designed based on alignment of the human dopamine D2 receptor (GenBank accession number NM\_000795) with the lamprey (*Petromyzon marinus* WGS) genome sequences deposited in the trace archives at the NCBI (National Center for Biotechnology Information, Bethesda, MD, USA). Primers (see Table 1) were designed to amplify different parts of the predicted lamprey D2 receptor sequence using Primer3 software (Whitehead Institute/Massachusetts Institute of Technology, Boston, MA) and purchased from Invitrogen. In addition, we used the SMART RACE cDNA amplification kit (Clontech Laboratories, Palo Alto, CA; see below) to obtain the unconserved amino terminus and to verify the start and stop codons. All primers had a GC content between 50 and 61%. The amplified cDNA fragments were cleaned directly with the MinElute PCR Purification kit (Qiagen) or cloned into a pCR®II-TOPO® vector (Invitrogen, see below) and then confirmed by nucleotide sequencing (KIGene, Core Facility at Karolinska Institutet, Stockholm, Sweden).

**5'-RACE.** First strand cDNA was synthesized from total RNA using a modified lock-docking oligo (dT) primer (5'-RACE

cDNA synthesis primer) and SMARTer IIA oligo, following the manufacturer's instructions (Clontech). The first strand cDNA was used as a template for PCR amplification with a gene specific primer (Table 1) and a universal primer mix containing the complementary sequence to the SMART oligo. The 5'-RACE PCR was performed in 50 µL reactions using Clontech Advantage 2 Polymerase Mix following the manufacturer's instruction (Clontech). The amplified fragment was cloned using the TOPO TA Cloning® Kit with pCR®II-TOPO® vector and One Shot® TOP10 Chemically Competent cells following the manufacturer's instructions (Invitrogen). Transformed bacteria were grown overnight at 37°C on LB agar plates. Twelve bacteria colonies were selected and grown overnight in Terrific Broth (Sigma) at 37°C. Plasmid DNA purification was subsequently performed using the Bio-Rad Quantum Prep Plasmid Miniprep Kit (Bio-Rad Laboratories, Sundbyberg, Sweden). Purified DNA fragments were confirmed by nucleotide sequencing (KIGene).

**3'-RACE.** First strand cDNA was synthesized from total RNA using a modified lock-docking oligo (dT) primer (3'-RACE cDNA synthesis primer) according to the manufacturer's instructions (Clontech). For the gene specific primers used see Table 1.

### Sequence analysis

Sequence analysis and comparisons were made with the Basic Local Alignment Search Tool (BLAST) on NCBI and/or the CLC Sequence Viewer 6.4. The start site of translation for the putative lamprey dopamine D2 receptor was determined based upon the following: *i*) the putative start codon being embedded in a consensus motif of a ribosomal binding site (see [24], *ii*) the open reading frame using ORF finder at NCBI (<http://www.ncbi.nlm.nih.gov>) and *iii*) by BLAST analysis (comparing the putative lamprey protein sequence with D2 receptor proteins of other known vertebrate species).

Transmembrane domains predictions were made with Octopus (<http://octopus.cbr.su.se/>). Putative N-glycosylation and phosphorylation sites were analyzed using PredictProtein-Sequence Analysis, Structure and Function Prediction (<http://www.predictprotein.org>).

The amino acid sequence of the lamprey dopamine D2-like receptor was aligned with homologous D2 receptor sequences from other known vertebrate representatives using BLAST and Geneious (<http://www.geneious.com>). Dopamine D3 and D4 receptor sequences were also included in the analysis. A phylogenetic tree was constructed with the neighbor-joining method from this alignment. Detailed analysis and alignments were also made with *Homo sapiens* (NP\_000786.1), *Mus musculus* (NP\_034207.2), *Danio rerio* (NP\_898891.1) and *Anguilla anguilla* (ABH06893.1) D2 receptor proteins using CLC Sequence Viewer 6.

### Probes for *in situ* hybridization

Templates for *in vitro* transcription were prepared by PCR amplification. A 660 base pair (bp) fragment (see Figure 2A) was obtained using 5'-TGCTCATATGCCTCATCGTC-3' forward and 5'-TCAAGCTTTGCACAATCGTC-3' reverse primers. The amplified cDNA fragment was cloned into a pCR®II-TOPO® vector (Invitrogen), cleaned and confirmed by nucleotide sequencing (KIGene). Linearized plasmids (1 µg) were used to synthesize [<sup>35</sup>S] UTP- and digoxigenin (DIG)-labeled riboprobes. *In vitro* transcription was carried out using the MAXIscript™ SP6/T7 kit (Applied Biosystems, Uppsala, Sweden) and [ $\alpha$ 35-S]UTP (NEG039H; Perkin Elmer, Upplands Väsby, Sweden) or DIG RNA Labeling Mix (Roche Diagnostics, Nutley, NJ, USA) according to the manufacturer's instructions. The transcripts were

purified using NucAway™ spin columns (Applied Biosystems). Sense probes were used as negative controls.

#### *In situ* hybridization

Adult river lampreys ( $n = 12$ ) were deeply anesthetized in MS-222 (100 mg/L) diluted in fresh water. Brains were quickly removed and fixed in 4% paraformaldehyde or 4% formaldehyde in 0.01 M phosphate buffered saline (PBS) overnight at 4°C. The tissue was cryoprotected in 20% sucrose in 0.01 M PBS overnight and 20  $\mu$ m thick serial, transverse cryostat sections were cut through the brain and stored at  $-80^{\circ}\text{C}$  until further processing. In each *in situ* hybridization that we performed one series of sections was used for the anti-sense probe and the adjacent series was used for the sense probe.

***In situ* hybridization with  $^{35}\text{S}$ -UTP-labeled riboprobes.** The sections were left at room temperature for 30 min, washed in 0.01 M PBS, treated with 0.05 M HCl for 10 min, washed in DEPC-treated water and then 0.01 M PBS, acetylated in 0.25% acetic anhydride in 0.1 M triethanolamine (pH 8.0) for 15 min, washed in 0.01 M PBS and dehydrated in 70%, 80% and 100% ethanol (2 min each). Sections were air dried and prehybridized (50% deionized formamide (pH 5), 50 mM Tris-HCl (pH 7.6), 25 mM EDTA (pH 8.0), 20 mM NaCl, 0.25 mg/ml yeast tRNA, 2.5 $\times$  Denhardt's solution) for 4 h at 55°C. Sections were then hybridized overnight (14–16 h) at 55°C with labeled probes diluted to a final concentration of  $1.0 \times 10^6$  cpm/200  $\mu\text{L}$  in a solution containing 50% deionized formamide, 0.3 M NaCl, 20 mM Tris-HCl (pH 7.6), 5 mM EDTA (pH 8.0), 10 mM PBS, 0.2 mM dithiothreitol, 0.5 mg/ml yeast tRNA, 0.1 mg/ml poly-A-RNA, 10% dextran sulfate, and 1 $\times$  Denhardt's solution. After hybridization, the slides were rinsed in 1 $\times$  standard saline citrate (SSC), 0.01% sodium dodecyl sulfate (SDS; 15 min); 1 $\times$  SSC, 0.01% SDS (30 min); 50% formamide/0.5 $\times$  SSC (1 h); 1 $\times$  SSC, and 0.01% SDS (15 min) at 55°C with continuous shaking. The sections were then treated with 1  $\mu\text{g}/\text{mL}$  RNase A (Roche, Diagnostics) in RNase buffer (0.5 M NaCl, 10 mM Tris-HCl, 5 mM EDTA, pH 8.0) for 1 h at 37°C. After two additional washes in 1 $\times$  SSC, 0.01% SDS for 30 min, the sections were dehydrated in ascending alcohol series and air-dried. Sections were placed against  $\beta$ -Max film (VWR, Sweden) and stored at room temperature for 3 to 5 days. Films were developed in Kodak D19 developer for 2 min and in Kodak Unifix liquid fixative for 5 min. Films were scanned with Epson Perfection 4990 Photo scanner as gray scale film. The gray scale was converted to pseudocolors using ImageJ (NIH ImageJ version 1.45, U.S. National Institutes of Health).

***In situ* hybridization with DIG-labeled riboprobes.** Sections were handled as above excluding the HCl treatment. After prehybridization (50% formamide, 5 $\times$ SSC pH 7.0, 5 $\times$ Denhardt's, 500  $\mu\text{g}/\text{mL}$  salmon sperm DNA, 250  $\mu\text{g}/\text{mL}$  yeast RNA) for 2–4 h at 60°C, DIG-labeled sense and anti-sense riboprobes were prepared and added to the hybridization solution to a final concentration of 500 ng/mL and hybridized overnight at 60°C. An RNase treatment (20  $\mu\text{g}/\text{mL}$  in 2 $\times$ SSC) was performed for 30 min at 37°C following stringent washes in SSC (Applied Biosystems). After additional washes in maleic acid buffer (pH 7.5) the sections were incubated overnight at 4°C in alkaline phosphatase labeled sheep anti-DIG antibody (1:2000; Roche Diagnostics) in 10% heat inactivated normal goat serum (NGS; Vector Laboratories, Burlingame, CA). The alkaline phosphatase was visualized using BCIP/NBT (Roche Diagnostics) in TRIS buffer pH 9.5 without the addition of  $\text{MgCl}_2$ . The sections were dehydrated and mounted in DPX (Sigma). Photomicrographs were taken in an Olympus BX51 microscope

using the image acquisition program Cell<sup>A</sup> and adjusted for brightness and contrast with Adobe Photoshop CS4.

#### Retrograde tracing

Animals ( $n = 2$ ) were deeply anesthetized in MS-222 in ice-cooled oxygenated HEPES buffered physiological solution (in mM: 138 NaCl, 2.1 KCl, 1.8  $\text{CaCl}_2$ , 1.2  $\text{MgCl}_2$ , 4 glucose, and 2 HEPES; pH 7.4). 50–200 nL 20% neurobiotin (Vector Laboratories) was pressure injected unilaterally into the lamprey homologue of the SNr, located in the dorsolateral isthmus region. All injections were made with glass micropipettes (borosilicate, OD = 1.5 mm, ID = 1.17 mm). Following the injections, the animal were returned to their aquarium for 24 h. Following anesthesia, fixation, sectioning of the brain and *in situ* hybridization of striatal sections with DIG-labeled D2 receptor riboprobes (see above), the tissue was incubated with Cy3-streptavidin (1:1000; Jackson ImmunoResearch, West Grove, PA) to reveal the neurobiotin, rinsed in PBS and mounted in glycerol containing 2.5% DABCO (Sigma-Aldrich). The total number of retrogradely labeled cells in the striatum was counted in two animals. Photomicrographs were taken in an Olympus BX51 microscope with an Olympus XM10 CCD camera (black and white), using the image acquisition program Cell<sup>A</sup> and adjusted for brightness and contrast with Adobe Photoshop CS4.

#### Preparation and analysis of tissue for electron microscopy

**Tissue preparation.** Following anesthesia, lamprey brains ( $n = 3$ ) were immersion-fixed overnight in 4% formaldehyde, 14% saturated picric acid solution and 0.1% glutaraldehyde in 0.1 M phosphate buffer (PB; pH 7.4) at 4°C, and then transferred to 0.1 M PB until processing. The brains were embedded in 5% agar and sectioned at 50  $\mu\text{m}$  in the coronal plane using a vibrating microtome (VT1000S; Leica Microsystems, Wetzlar, Germany).

**Immunohistochemistry.** The sections were incubated in a cryoprotectant solution (0.05 M phosphate buffer, 25% sucrose, 10% glycerol) overnight, then freeze-thawed twice in liquid nitrogen in order to increase penetration of the reagents. The sections were washed thoroughly and then incubated in 10% NGS (Vector Laboratories) in PBS for 2 h at room temperature. All sections were immunolabeled to reveal TH-containing structures using a rabbit anti-TH antibody (1:500 in NGS-PBS; Millipore AB152). The sections were incubated overnight at room temperature, washed in PBS and incubated at 4°C with a biotinylated goat anti-rabbit secondary antibody (1:300 in NGS-PBS; Vector Laboratories) for about 16 h. This was followed by incubation in an avidin-biotin-peroxidase complex (ABC Elite; Vector Laboratories) for 3–4 h at room temperature. The sections were then washed in PBS followed by washes in Tris-buffer (0.5 M, pH 7.6; TB). The sections were pre-incubated in diaminobenzidine (DAB 0.025% in TB) with shaking for 15 min and the peroxidase reaction was initiated by the addition of  $\text{H}_2\text{O}_2$  to a final concentration of 0.01%. The reaction was allowed to continue for 3–5 min and stopped by several washes in TB and then PB. The sections were postfixed in 1% osmium tetroxide in PB for 15–20 min and dehydrated as described previously [45]. Following absolute ethanol, sections were washed twice in propylene oxide (Sigma) for 15 min and placed into resin overnight at room temperature (Durcupan ACM, Fluka, Gillingham, UK). They were then mounted in resin on glass slides and the resin was polymerized at 60°C for 48 h.

**Electron microscopic analysis.** It has previously been shown [9] that striatal neurons and neuropil are organized into three layers, characterized as follows: Area I is defined by the

neuropil located in the most medial part of the striatum which faces the *ventriculus medius telencephali*; Area II contains most of the striatal cell bodies arranged as a single band. These neurons possess two major processes that extend and branch in opposite directions, medially towards Area I and laterally towards Area III, which also contains scattered cell bodies. Each of these regions were investigated for the presence of TH-immunoreactive synaptic terminals and the nature of the postsynaptic targets.

Regions of the sections that contained Areas I, II and III (Figure 7 A, B) were cut out from the slide and re-embedded in Durcupan blocks. Serial sections (50–60 nm) were cut using an ultramicrotome (Leica EM UC6, Leica Microsystems) and collected on pioloform-coated, single-slot copper grids (Agar Scientific, Stansted, UK). To improve contrast, the ultrathin sections were lead-stained for 4–5 min and then examined in a Philips CM100 electron microscope.

TH-immunoreactive structures were identified by the electron dense peroxidase reaction product that adhered to the internal surface of the plasmalemma and the outer membrane of organelles and axonal profiles were identified by the presence of synaptic vesicles and often mitochondria. TH-immunolabeled profiles located in the three different areas were noted and digitally recorded at different magnifications using a Gatan CCD camera. Each profile was examined in each of the six serial sections to determine whether they form of a synaptic specialization and to characterize the nature of the postsynaptic target. Any other immunopositive axonal profile seen in a subsequent serial section was also noted and analyzed in all sections. This process was repeated on sections from different grids until 25 TH-immunopositive profiles were analyzed per area per animal. In total, 225 TH-positive profiles were included in the analysis. A total of approximately 40,000 square micrometer were examined per animal.

The digital images were analyzed using Image J, and they were adjusted for contrast and brightness using Adobe Photoshop CS3. Synapse formation throughout the serial sections was scored for each TH-positive axonal profile. For each such synapse, the postsynaptic target was characterized. All synapses observed were of the asymmetrical type (Gray's type 1) and were characterized as such by the presence of presynaptic vesicle accumulation, a thick postsynaptic density, a widened synaptic cleft and cleft material. Structures which did not fulfill these criteria were not considered as synaptic junctions.

Statistical analyses were performed using the statistical software R (version 2.13.1). Data were presented as means and standard deviations and comparisons made using chi-squared test with Yates continuity correction. Tests with  $p < 0.05$  were considered significant.

### Electrophysiology in lamprey striatal slices

Acute striatal brain slices were prepared from anesthetized (MS-222, 1 mg/100 mL) lamprey as described in Ericsson et al. [58]. Brains were quickly dissected out from decapitated lampreys in ice-cold artificial cerebrospinal fluid (aCSF) of the following composition (in mM): NaCl 125, KCl 2.5,  $\text{NaH}_2\text{PO}_4$  1.25,  $\text{MgCl}_2$  1, glucose 10,  $\text{CaCl}_2$  2 and  $\text{NaHCO}_3$  25. Sectioning of the brain

was performed with a tissue chopper (Vibratome 800 tissue Chopper, Leica Microsystems AB, Sweden) to obtain coronal slices of 350  $\mu\text{m}$  thickness. The slices were transferred to a recording chamber and continuously perfused with aCSF (pH 7.4) that was oxygenated with 95%  $\text{O}_2$  and 5%  $\text{CO}_2$ . The chamber was kept at 5–8°C with a Peltier cooling block (Elfa, Stockholm, Sweden). Slices were left to recover for at least one hour before patch clamp experiments were commenced. Recordings were performed in whole-cell current- or voltage-clamp mode with patch pipettes of 5–12 M $\Omega$  filled with (in mM): 105 K-gluconate, 30 KCl, 10 HEPES, 4 Mg-ATP, 0.3 Na-GTP and 10 phosphocreatine sodium salt (osmolarity 275 mOsm). Pipettes were prepared from borosilicate glass microcapillaries (Harvard Apparatus, Kent, UK) using a three-stage puller (Model P-97, Sutter Instruments, Novato, CA, USA). Neurons were visualized with DIC/infrared optics (Olympus BX51WI, Tokyo, Japan) and pipettes advanced with remote-controlled micromanipulators (Luigs & Neumann, Ratingen, Germany). An Axoclamp 2B amplifier (Molecular Devices Corp., CA, USA) was used together with a HS-2A headstage (Molecular Devices Corp.) for recordings and signals digitized (ITC-18, HEKA, Lambrecht, Germany) at 10–50 kHz before storage on a PC. Bridge balance and pipette capacitance compensation were adjusted on the amplifier and membrane potential values were corrected for the liquid junction potential. Data was acquired and analyzed using Igor software (version 6.03, WaveMetrics, Portland, USA).

The dopamine D2 receptor agonist TNPA (R(–)-2,10,11-Trihydroxy-N-propyl-noraporphine 123 hydrobromide hydrate; Sigma-Aldrich), was freshly prepared as 100 mM in 99.5% ethanol before dilution to 100  $\mu\text{M}$  in aCSF. TNPA was then bath-applied through the perfusion system.

Statistical analyses were performed with GraphPad Prism Software (GraphPad Software, San Diego, CA, USA) and comparisons between means were made with two-tailed paired t-tests. Results are presented as mean  $\pm$  standard deviation (SD).

### Supporting Information

**Figure S1 Nucleotide and deduced amino acid sequence of the lamprey dopamine D2 receptor.** The coding region is 1533 base pair long and its deduced amino acid sequence spans 511 amino acids. The numbering of the deduced amino acid sequence begins with the first methionine of the open reading frame, and is shown to the right of each line. The nucleotide numbers are shown to the left of each line. The untranslated regions are shown in smaller fonts. Putative N-glycosylation sites, blue squares; protein kinase C phosphorylation sites, green squares; cAMP phosphorylation site, pink square; Casein kinase II (CKII) phosphorylation site, orange squares. (TIF)

### Author Contributions

Conceived and designed the experiments: BR RDH IHO JE MSJ PB SG. Performed the experiments: BR RDH IHO JE MSJ JPF. Analyzed the data: BR RDH IHO PB JE MSJ JPF. Wrote the paper: BR RDH IHO JE PB SG.

### References

- Grillner S (1997) Ion channels and locomotion. *Science* 278: 1087–1088.
- Graybiel AM (1998) The basal ganglia and chunking of action repertoires. *Neurobiol Learn Mem* 70: 119–136.
- Redgrave P, Prescott TJ, Gurney K (1999) The basal ganglia: a vertebrate solution to the selection problem? *Neuroscience* 89: 1009–1023.
- Hikosaka O, Takikawa Y, Kawagoe R (2000) Role of the basal ganglia in the control of purposive saccadic eye movements. *Physiol Rev* 80: 953–978.
- Grillner S, Hellgren J, Menard A, Saitoh K, Wikstrom MA (2005) Mechanisms for selection of basic motor programs—roles for the striatum and pallidum. *Trends Neurosci* 28: 364–370.
- Stephenson-Jones M, Ericsson J, Robertson B, Grillner S (2012) Evolution of the basal ganglia: Dual output pathways conserved throughout vertebrate phylogeny. *J Comp Neurol*.



7. Stephenson-Jones M, Samuelsson E, Ericsson J, Robertson B, Grillner S (2011) Evolutionary conservation of the basal ganglia as a common vertebrate mechanism for action selection. *Curr Biol* 21: 1081–1091.
8. Kumar S, Hedges SB (1998) A molecular timescale for vertebrate evolution. *Nature* 392: 917–920.
9. Pombal MA, El Manira A, Grillner S (1997) Afferents of the lamprey striatum with special reference to the dopaminergic system: a combined tracing and immunohistochemical study. *J Comp Neurol* 386: 71–91.
10. Ericsson J, Silberberg G, Robertson B, Wikstrom MA, Grillner S (2011) Striatal cellular properties conserved from lampreys to mammals. *J Physiol* 589: 2979–2992.
11. Kawaguchi Y, Wilson CJ, Emson PC (1989) Intracellular recording of identified neostriatal patch and matrix spiny cells in a slice preparation preserving cortical inputs. *J Neurophysiol* 62: 1052–1068.
12. Gerfen CR, Surmeier DJ (2011) Modulation of striatal projection systems by dopamine. *Annu Rev Neurosci* 34: 441–466.
13. Reiner A, Medina L, Veenman CL (1998) Structural and functional evolution of the basal ganglia in vertebrates. *Brain Res Rev* 28: 233–285.
14. Bolam JP, Hanley JJ, Booth PA, Bevan MD (2000) Synaptic organisation of the basal ganglia. *J Anat* 196(Pt 4): 527–542.
15. Thompson RH, Menard A, Pombal M, Grillner S (2008) Forebrain dopamine depletion impairs motor behavior in lamprey. *Eur J Neurosci* 27: 1452–1460.
16. Le Crom S, Kapsimali M, Barome PO, Vernier P (2003) Dopamine receptors for every species: gene duplications and functional diversification in Craniates. *J Struct Funct Genomics* 3: 161–176.
17. Callier S, Snappyan M, Le Crom S, Prou D, Vincent JD, et al. (2003) Evolution and cell biology of dopamine receptors in vertebrates. *Biol Cell* 95: 489–502.
18. Vernier P (1997) The amphioxus D1/beta receptor and the emergence of the vertebrate adrenergic system. GenBank NCBI Accession number. AJ005434.1 p.
19. Pombal MA R-AM, Megias M, Moussa CE-H, Sidhu A, Vernier P (2007) Distribution of the dopamine D1 receptor in the lamprey brain: evolutionary implications. *Society for Neuroscience* 351.29.
20. Bunzow JR, Van Tol HH, Grandy DK, Albert P, Salon J, et al. (1988) Cloning and expression of a rat D2 dopamine receptor cDNA. *Nature* 336: 783–787.
21. Grandy DK, Marchionni MA, Makam H, Stofko RE, Alfano M, et al. (1989) Cloning of the cDNA and gene for a human D2 dopamine receptor. *Proc Natl Acad Sci U S A* 86: 9762–9766.
22. Schnell SA, You S, Foster DN, El Halawani ME (1999) Molecular cloning and tissue distribution of an avian D2 dopamine receptor mRNA from the domestic turkey (*Meleagris gallopavo*). *J Comp Neurol* 407: 543–554.
23. Pasqualini C, Weltzien FA, Vidal B, Baloch S, Rouget C, et al. (2009) Two distinct dopamine D2 receptor genes in the European eel: molecular characterization, tissue-specific transcription, and regulation by sex steroids. *Endocrinology* 150: 1377–1392.
24. Kozak M (1996) Interpreting cDNA sequences: some insights from studies on translation. *Mamm Genome* 7: 563–574.
25. Neve K, DuRand CJ, Teeter MM (2003) Structural analysis of the mammalian D2, D3 and D4 dopamine receptors. New York: Marcel Dekker.
26. Xhaard H, Rantanen VV, Nyronen T, Johnson MS (2006) Molecular evolution of adrenoceptors and dopamine receptors: implications for the binding of catecholamines. *J Med Chem* 49: 1706–1719.
27. Ferguson SS (2001) Evolving concepts in G protein-coupled receptor endocytosis: the role in receptor desensitization and signaling. *Pharmacol Rev* 53: 1–24.
28. Vallone D, Picetti R, Borrelli E (2000) Structure and function of dopamine receptors. *Neurosci Biobehav Rev* 24: 125–132.
29. Missale C, Nash SR, Robinson SW, Jaber M, Caron MG (1998) Dopamine receptors: from structure to function. *Physiol Rev* 78: 189–225.
30. Pierre-Simons J, Reperant J, Mahouche M, Ward R (2002) Development of tyrosine hydroxylase-immunoreactive systems in the brain of the larval lamprey *Lampetra fluviatilis*. *J Comp Neurol* 447: 163–176.
31. Ding L, Perkel DJ (2002) Dopamine modulates excitability of spiny neurons in the avian basal ganglia. *J Neurosci* 22: 5210–5218.
32. Barral J, Galarraga E, Tapia D, Flores-Barrera E, Reyes A, et al. (2010) Dopaminergic modulation of spiny neurons in the turtle striatum. *Cell Mol Neurobiol* 30: 743–750.
33. Monsma EJ, Jr., McVittie LD, Gerfen CR, Mahan LC, Sibley DR (1989) Multiple D2 dopamine receptors produced by alternative RNA splicing. *Nature* 342: 926–929.
34. Giros B, Sokoloff P, Martres MP, Riou JE, Emorine LJ, et al. (1989) Alternative splicing directs the expression of two D2 dopamine receptor isoforms. *Nature* 342: 923–926.
35. Vacher C, Pellegrini E, Anglade I, Ferriere F, Saligaut C, et al. (2003) Distribution of dopamine D2 receptor mRNAs in the brain and the pituitary of female rainbow trout: an in situ hybridization study. *J Comp Neurol* 458: 32–45.
36. Boehmle W, Obrecht-Pflumio S, Canfield V, Thisse C, Thisse B, et al. (2004) Evolution and expression of D2 and D3 dopamine receptor genes in zebrafish. *Dev Dyn* 230: 481–493.
37. Amores A, Force A, Yan YL, Joly L, Amemiya C, et al. (1998) Zebrafish hox clusters and vertebrate genome evolution. *Science* 282: 1711–1714.
38. Weiner DM, Levey AI, Sunahara RK, Niznik HB, O'Dowd BF, et al. (1991) D1 and D2 dopamine receptor mRNA in rat brain. *Proc Natl Acad Sci U S A* 88: 1859–1863.
39. O'Connell LA, Fontenot MR, Hofmann HA (2011) Characterization of the dopaminergic system in the brain of an African cichlid fish, *Astatotilapia burtoni*. *J Comp Neurol* 519: 75–92.
40. Bouthenet ML, Souil E, Martres MP, Sokoloff P, Giros B, et al. (1991) Localization of dopamine D3 receptor mRNA in the rat brain using in situ hybridization histochemistry: comparison with dopamine D2 receptor mRNA. *Brain Res* 564: 203–219.
41. Le Moine C, Bloch B (1996) Expression of the D3 dopamine receptor in peptidergic neurons of the nucleus accumbens: comparison with the D1 and D2 dopamine receptors. *Neuroscience* 73: 131–143.
42. Pierre J, Mahouche M, Suderevskaia EI, Reperant J, Ward R (1997) Immunocytochemical localization of dopamine and its synthetic enzymes in the central nervous system of the lamprey *Lampetra fluviatilis*. *J Comp Neurol* 380: 119–135.
43. Bouyer JJ, Joh TH, Pickel VM (1984) Ultrastructural localization of tyrosine hydroxylase in rat nucleus accumbens. *J Comp Neurol* 227: 92–103.
44. Freund TF, Powell JF, Smith AD (1984) Tyrosine hydroxylase-immunoreactive boutons in synaptic contact with identified striatonigral neurons, with particular reference to dendritic spines. *Neuroscience* 13: 1189–1215.
45. Moss J, Bolam JP (2008) A dopaminergic axon lattice in the striatum and its relationship with cortical and thalamic terminals. *J Neurosci* 28: 11221–11230.
46. Surmeier DJ, Ding J, Day M, Wang Z, Shen W (2007) D1 and D2 dopamine-receptor modulation of striatal glutamatergic signaling in striatal medium spiny neurons. *Trends Neurosci* 30: 228–235.
47. O'Keefe GC, Barker RA, Caldwell MA (2009) Dopaminergic modulation of neurogenesis in the subventricular zone of the adult brain. *Cell Cycle* 8: 2888–2894.
48. Hernandez-Lopez S, Tkatch T, Perez-Garci E, Galarraga E, Bargas J, et al. (2000) D2 dopamine receptors in striatal medium spiny neurons reduce L-type Ca<sup>2+</sup> currents and excitability via a novel PLC[ $\beta$ ]-1-IP3-calcineurin-signaling cascade. *J Neurosci* 20: 8987–8995.
49. Maurice N, Mercer J, Chan CS, Hernandez-Lopez S, Held J, et al. (2004) D2 dopamine receptor-mediated modulation of voltage-dependent Na<sup>+</sup> channels reduces autonomous activity in striatal cholinergic interneurons. *J Neurosci* 24: 10299–10301.
50. Olson PA, Tkatch T, Hernandez-Lopez S, Ulrich S, Ilijic E, et al. (2005) G-protein-coupled receptor modulation of striatal CaV1.3 L-type Ca<sup>2+</sup> channels is dependent on a Shank-binding domain. *J Neurosci* 25: 1050–1062.
51. Wang D, Grillner S, Wallen P (2011) 5-HT and dopamine modulates CaV1.3 calcium channels involved in postinhibitory rebound in the spinal network for locomotion in lamprey. *J Neurophysiol* 105: 1212–1224.
52. Lipscombe D (2002) L-type calcium channels: highs and new lows. *Circ Res* 90: 933–935.
53. Gerfen CR, Engber TM, Mahan LC, Sussel Z, Chase TN, et al. (1990) D1 and D2 dopamine receptor-regulated gene expression of striatonigral and striatopallidal neurons. *Science* 250: 1429–1432.
54. Kravitz AV, Freeze BS, Parker PR, Kay K, Thwin MT, et al. (2010) Regulation of parkinsonian motor behaviours by optogenetic control of basal ganglia circuitry. *Nature* 466: 622–626.
55. Gerfen CR (1992) The neostriatal mosaic: multiple levels of compartmental organization in the basal ganglia. *Annu Rev Neurosci* 15: 285–320.
56. Hernandez-Lopez S, Bargas J, Surmeier DJ, Reyes A, Galarraga E (1997) D1 receptor activation enhances evoked discharge in neostriatal medium spiny neurons by modulating an L-type Ca<sup>2+</sup> conductance. *J Neurosci* 17: 3334–3342.
57. West AR, Grace AA (2002) Opposite influences of endogenous dopamine D1 and D2 receptor activation on activity states and electrophysiological properties of striatal neurons: studies combining in vivo intracellular recordings and reverse microdialysis. *J Neurosci* 22: 294–304.
58. Ericsson J, Robertson B, Wikstrom MA (2007) A lamprey striatal brain slice preparation for patch-clamp recordings. *J Neurosci Methods* 165: 251–256.

V





# Dopamine differentially modulates the excitability of striatal neurons of the direct and indirect pathways in lamprey

Jesper Ericsson<sup>1\*</sup>, Marcus Stephenson-Jones<sup>1\*</sup>, Juan Pérez-Fernández<sup>2</sup>, Brita Robertson<sup>1</sup>, Gilad Silberberg<sup>1</sup> and Sten Grillner<sup>1</sup>

<sup>1</sup>Nobel Institute for Neurophysiology, Department of Neuroscience, Karolinska Institutet, SE-171 77 Stockholm, SWEDEN, <sup>2</sup>Neurolam Group, Department of Functional Biology and Health Sciences, Faculty of Biology, University of Vigo, 36310 Vigo, Spain.

\* These authors contributed equally to this work

Correspondence should be addressed to Professor Sten Grillner, Nobel Institute for Neurophysiology, Department of Neuroscience, Karolinska Institutet, SE-171 77 Stockholm, SWEDEN, [sten.grillner@ki.se](mailto:sten.grillner@ki.se)

---

Dopamine is thought to bias the mammalian and avian basal ganglia networks towards selecting actions by differentially modulating the excitability of D1 and D2 receptor expressing striatal projection neurons that project directly or indirectly to the output layer of the basal ganglia. To elucidate if this is a conserved control strategy across vertebrates, we have studied the cellular effects of dopamine on striatal projection neurons of the lamprey that represents the oldest group of extant vertebrates and hence occupies a key position in phylogeny. We performed whole-cell current clamp recordings in acute slices of retrogradely labeled direct pathway striatal neurons from the homolog of the substantia nigra pars reticulata (SNr) and neurons projecting to the mixed globus pallidus interna (GPi) and globus pallidus externa (GPe) homologs. We also used *in situ* hybridization to investigate the expression of D1- and/or D2 receptors in the different striatal projection neurons. We show that the neurons that project directly to the basal ganglia output nuclei express dopamine D1 receptors, while separate populations that project to the mixed GPi/GPe nucleus express either dopamine D1 or D2 receptors. Activation of these dopamine receptors furthermore leads to an increase in the excitability of D1 receptor expressing neurons and a decrease in the excitability of D2 receptor expressing neurons. Our results suggest that the mechanism by which dopamine modulates the activity of striatal projection neurons is conserved across the vertebrate phylum, together with the intrinsic organization of the basal ganglia.

---

## Introduction

The basal ganglia are a group of subcortical nuclei that are conserved throughout the vertebrate phylum and play a critical role in action selection and procedural learning (Redgrave et al., 1999; Stephenson-Jones et al., 2011b; Stephenson-Jones et al., 2012). The function of these nuclei is critically dependent on dopamine, released from neurons in the substantia nigra pars compacta (SNc) and ventral tegmental area. Loss of this dopaminergic innervation leads to parkinsonian symptoms, in all vertebrates studied, involving a combination of bradykinesia, rigidity and postural instability (Albin et al., 1989; Thompson et al., 2008). This suggests that as with the intrinsic basal ganglia organization, the mechanisms by which dopamine modulates these nuclei may also be conserved.

In mammals, dopamine differentially modulates the excitability of the striatal projection neurons by increasing the excitability of medium spiny neurons (MSNs) that project directly to the output layer of the basal ganglia, the globus pallidus interna (GPi)/substantia nigra pars reticulata (SNr) and decreasing the excitability of MSNs that project indirectly to these nuclei via the globus pallidus externa (GPe) (Hernandez-Lopez et al., 1997; Surmeier et al., 2007). This dichotomous effect is due to a differential expression of dopamine receptors on the two types of projection neurons, directly projecting MSNs express the dopamine D1 receptor (D1R), while indirectly projecting MSNs express the D2 receptor (D2R) (Gerfen and Surmeier, 2011). Dopamine is therefore thought to bias the basal ganglia network towards selecting actions, by increasing the excitability of the “direct” pathway, to promote actions, and decreasing the excitability of the indirect pathway, to inhibit actions (Grillner et al., 2005).

Similar to mammals, the striatum of non-mammalian vertebrates (lamprey, amphibians, reptiles and birds) receives a large dopaminergic projection from the homolog of the SNc/VTA and express D1 and D2 receptors in the striatum (Vernier, 1997; Reiner et al., 1998b; Chu et al., 2001; Pombal MA, 2007; Robertson et al., 2012). Furthermore, in turtles and birds, dopamine excites striatal neurons that express D1 receptors and inhibits neurons that express D2 receptors (Ding and Perkel, 2002; Barral et al., 2010). Despite this, in non-mammalian vertebrates it is unknown if the neurons associated with the direct and indirect pathway selectively express D1 and D2 receptors respectively, or if these neurons are differentially modulated by dopamine to bias the network towards action selection (Ding and Perkel, 2002).

As a first step in elucidating the conserved mechanisms by which dopamine facilitates movements, our aim was to use the lamprey, to determine how dopamine modulates the directly and indirectly projecting striatal neurons. This model system occupies a key position in phylogeny, with their ancestors having diverged from the main vertebrate lineage at the dawn of vertebrate evolution approximately 560 million years ago. We have studied striatal projection neurons of both the direct and indirect pathway and shown that D1R agonists preferentially modulate neurons of the direct pathway, while D2R agonists modulate neurons of the indirect pathway.

## Methods

Experiments were performed on a total of 49 adult river lampreys (*Lampetra fluviatilis*). The experimental procedures were approved by the local ethical committee (Stockholm’s Norra Djurförsöksetiska Nämnd) and were in accordance with The Guide for the Care and Use of Laboratory Animals (National Institutes of Health, 1996 revision). Every effort was made to minimize animal suffering and to reduce the number of animals used during the study.

### Slice preparation and patch-clamp experiments

Acute brain slices were prepared by dissecting out brains in ice-cold artificial cerebrospinal fluid (aCSF) with the following composition (in mM): 125 NaCl, 2.5 KCl, 1 MgCl<sub>2</sub>, 1.25, NaH<sub>2</sub>PO<sub>4</sub>, 2 CaCl<sub>2</sub>, 25 NaHCO<sub>3</sub> and 8-10 glucose. The aCSF was oxygenated continuously with 95% O<sub>2</sub> and 5% CO<sub>2</sub> and the pH (7.4) was routinely checked. To facilitate the cutting of brain slices on a microtome (Microm HM 650V, Thermo Scientific, Walldorf, Germany), pre-heated liquid agar (Sigma-Aldrich, St. Louis, MO, USA) dissolved in water at a concentration of 4% was prepared. The agar block containing the brain was then glued to a metal plate and transferred to ice-cold aCSF in the microtome chamber. Coronal brain slices of 350-400 µm were cut at the level of the striatum and allowed to recover for at least one hour in cold aCSF, before being transferred to a submerged recording chamber. Perfusion of slices was performed with aCSF at 6-8°C using a Peltier cooling system (ELFA, Solna, Sweden).

Whole-cell somatic current clamp recordings were made from labeled and unlabeled neurons with patch pipettes made from borosilicate glass microcapillaries (Harvard Apparatus, Kent, UK) using a horizontal puller (Model P-97, Sutter Instruments, Novato, CA, USA). Recording pipettes (7–12 M $\Omega$ ) were filled with intracellular solution of the following composition (in mM): 105 K-gluconate, 30 KCl, 10 HEPES, 4 Mg-ATP, 0.3 Na-GTP and 10 phosphocreatine sodium salt (osmolarity 265–275 mOsm). Bridge balance and pipette capacitance compensation were adjusted for on the Axoclamp 2B amplifier (Molecular Devices Corp., CA, USA). Neurons were visualized with DIC/infrared optics (Olympus BX51WI, Tokyo, Japan) and retrogradely labeled neurons (Rhodamine red or Alexa fluor 488-dextran) were identified by switching from infrared to epifluorescence mode. Data collection and analysis was made with ITC-18 (HEKA, Lambrecht, Germany) and Igor software (version 6.03, WaveMetrics, Portland, USA).

Passive and active electrophysiological properties were recorded in current-clamp mode by negative and positive current injections. We injected ten consecutive step currents (1 s duration) of increasing amplitudes to evoke action potentials (APs). The amplitudes of the current injections were scaled to the input resistance of individual neurons so that the second or third injection evoked one AP on average, which was used to extract single AP parameters. The current-voltage relationships were also used to analyze current-frequency relationships and the input resistance of cells. In the same experiment, step currents were kept constant after the initial scaling in order to compare the number of APs and its parameters before, during and after application of drugs. This was performed from a depolarized (-55 to -65 mV) or hyperpolarized (-80 to -90 mV) baseline and the current-clamp was monitored and adjusted for in order to compensate for any depolarization or hyperpolarization of the membrane potential initiated by drug application to keep the voltage baseline close to constant. The effects of drugs on the excitability of neurons were assessed by comparing the number of evoked action potentials evoked at near rheobase current injections. In cells that also exhibited post-inhibitory rebound (PIR) spikes, the effect of drugs was assessed by comparing the total number of PIR spikes in response to 8–10 consecutive hyperpolarizations from -100 mV to baseline.

#### Drug application and statistical analyses

Pharmacological agents were bath applied through the perfusion system. The dopamine D1 receptor agonist SKF 81297 (( $\pm$ )-6-Chloro-2,3,4,5-tetrahydro-1-phenyl-1*H*-3-benzazepine hydrobromide, Tocris) was prepared freshly and dissolved to 10  $\mu$ M (up to 20  $\mu$ M in initial experiments) in aCSF. The dopamine D2 receptor agonist TNPA (R(-)-2,10,11-Trihydroxy-N-propyl-noraporphine 123 hydrobromide hydrate; Sigma-Aldrich), was prepared freshly and first dissolved to 100 mM in 99.5 % ethanol before dilution to 100  $\mu$ M in aCSF. In sequential drug applications, the quantification of effects of the second drug was compared to the latter part of the wash period prior to application. The mixed population of striatopallidal neurons were divided into two groups (indirect/direct) by evaluating if (i) D2 activation affected excitability, (ii) D1 activation affected excitability. This grouping was based on the *in situ* hybridization results (~50% D2 or D1 receptor expressing neurons) and that D2 activation had a potent effect in responsive neurons (see also Robertson et al., 2012). In the general investigation of SKF 81297 activation (Fig. 4) and TNPA activation (Fig. 5), striatonigral, striatopallidal and unlabeled neurons that responded to either drug were included in the analysis. Statistical analyses were made with two-tailed paired t-tests. Results are presented as mean  $\pm$  standard error of mean (SEM).

#### Retrograde tracing

Lampreys were deeply anesthetized in MS-222 (100mg/L; Sigma-Aldrich) in ice-cooled oxygenated HEPES buffered physiological solution (in mM: 138 NaCl, 2.1 KCl, 1.8 CaCl<sub>2</sub>, 1.2 MgCl<sub>2</sub>, 4 glucose, and 2 HEPES; pH 7.4). All injections were made with glass (borosilicate, OD = 1.5mm, ID = 1.17mm)

micropipettes, with a tip diameter of 10 - 20µm. The micropipettes were fixed in a holder, which was attached to an air supply and a Narishige micromanipulator. 50-200 nl of 20% Neurobiotin (Vector, Burlingame, CA; in distilled water containing fast green to aid visualization of the spread of the injection) was pressure injected unilaterally into either the homolog of the SNr located in the caudal mesencephalon, or the mixed dorsal pallidum in the area ventrolateral to the eminentia thalami. Following the injections, the animals were returned to their aquarium for 16-20 h.

#### **Probes for *in situ* hybridization**

Templates for *in vitro* transcription were prepared by PCR amplification. For the D2 receptor probe, a 660 base pair (bp) fragment was obtained using 5'-TGCTCATATGCCTCATCGTC-3' forward and 5'-TCAAGCTTTGCACAATCGTC-3' reverse primers (Robertson et al., 2012) and for the D1 receptor probe, a 549 bp fragment was obtained using 5'-CTGTCCGTGCTCATCTCCTTTAT-3' forward and 5'-CCAGCCGAACCATACGAAG-3' reverse primers (Vernier, 1997). The amplified cDNA fragments were cloned into a pCR<sup>®</sup>II-TOPO<sup>®</sup> vector (Invitrogen), cleaned and confirmed by nucleotide sequencing (KIGene). Linearized plasmids (1 µg) were used to synthesize digoxigenin (DIG)-labeled riboprobes. *In vitro* transcription was carried out using the DIG RNA Labeling Mix (Roche Diagnostics, Nutley, NJ, USA) according to the manufacturer's instructions. The transcripts were purified using NucAway<sup>™</sup> spin columns (Applied Biosystems). Sense probes were used as negative controls.

#### ***In situ* hybridization**

The neurobiotin-injected animals were deeply anesthetized in MS-222 diluted in fresh water and killed by decapitation. Brains were quickly removed and fixed in 4% paraformaldehyde in 0.01M phosphate buffered saline (PBS) overnight at 4°C. They were afterwards cryoprotected in 30% sucrose in 0.01 M PBS overnight and 20 µm thick serial, transverse cryostat sections were obtained and immediately used for *in situ* hybridization. The sections were left at room temperature for 30 min, washed in 0.01 M PBS, acetylated in 0.25% acetic anhydride in 0.1 M triethanolamine (pH 8.0) for 5 min, washed in 0.01 M PBS and prehybridized (50% formamide, 5XSSC pH 7.0, 5xDenhardt's, 500 µg/mL salmon sperm DNA, 250 µg/mL yeast RNA) for 2-4 h at 60°C. DIG-labeled D1 and D2 riboprobes were prepared and added to the hybridization solution to a final concentration of 500 ng/mL, and parallel series were hybridized overnight at 60°C. An RNase treatment (20 µg/mL in 2xSSC) was performed for 30 min at 37°C following stringent washes in SSC (Applied Biosystems). After additional washes in maleic acid buffer (MABT, pH 7.5) the sections were incubated overnight at 4°C in antidigoxigenin Fab-fragments conjugated with alkaline phosphatase (1:2000; Roche Diagnostics) in 10% heat inactivated normal goat serum (Vector Laboratories, Burlingame, CA). Several washes in MABT were carried out and the alkaline phosphatase reaction was visualized using NBT/BCIP substrate (Roche Diagnostics) in staining buffer (0.1 M TRIS buffer pH 9.5 containing 100 mM NaCl and 5 mM levamisole). The staining process was stopped with washes in PBS. Those sections that had been subjected to retrograde tracing with neurobiotin were subsequently incubated with streptavidin conjugated to Cy3 (1:1000; Molecular Probes). Sections were cover slipped with glycerol containing 2.5% DABCO (Sigma-Aldrich).

## **Results**

### **Striatonigral neurons selectively express D1 receptors**

In lamprey two genes have been identified that encode for a dopamine D1 and D2 receptor respectively. D2 receptor mRNA is expressed in a subpopulation of striatal neurons (Robertson et al., 2012) and is D1R mRNA (Vernier, 1997; Pombal MA, 2007). In order to confirm that the

subpopulation of striatal neurons that project directly to the basal ganglia output nuclei, GPi/SNr, are indeed those that selectively express the D1 receptor we analyzed the striatal projection to the lamprey homolog of the SNr. As with mammals the striatal neurons projecting to the SNr exclusively express substance P and project directly to the GABAergic output neurons in the SNr (Stephenson-Jones et al., 2012). Indeed, the majority of retrogradely labeled neurons co-localize with the *in situ* hybridization signal for the D1 receptor (Fig. 1A-D;  $66.2 \pm 13.8\%$ ,  $n=5$ ). In contrast, very few of the retrogradely labeled neurons co-localize with the *in situ* hybridization signal for the D2 receptor (Fig. 1E-H;  $4.2 \pm 5.9\%$ ,  $n=4$ ).

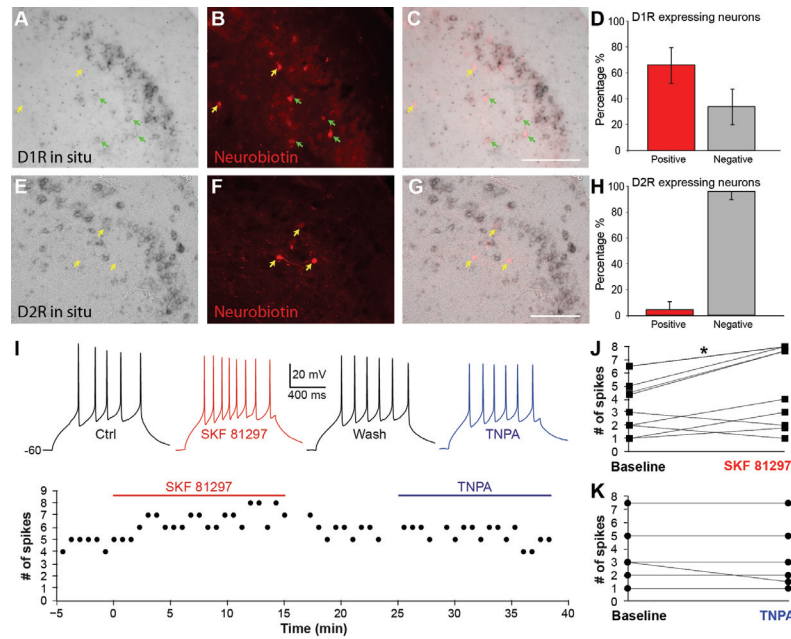


**Figure 1. Striatonigral neurons express functional D1 receptors that excite neurons**

**A**, DIG-labeled D1 receptor riboprobe expressed in a subpopulation of striatal neurons. Yellow arrows indicate neurons that are retrograde labeled but do not express D1 receptor mRNA. Green arrows indicate neurons that are retrograde labeled and express D1 receptor mRNA. **B**, Striatonigral neurons retrogradely labeled after injections of neurobiotin into the substantia nigra pars reticulata. **C**, Merged image showing the overlap between retrograde labeled cells and D1 receptor mRNA. **D**, Quantification showing the percentage of retrograde labeled neurons that express D1 receptor mRNA. **E**, DIG-labeled D2 receptor riboprobe expressed in a subpopulation of striatal neurons. Yellow arrows indicate neurons that are retrograde labeled but do not express D2 receptor mRNA. Green arrows indicate neurons that are retrograde labeled and express D2 receptor mRNA. **F**, Striatonigral neurons retrogradely labeled after injections of neurobiotin into the substantia nigra pars reticulata. **G**, Merged image showing the lack of overlap between retrogradely labeled cells and D2 receptor mRNA. **H**, Quantification showing the percentage of retrograde labeled neurons that express D2 receptor mRNA. **I**, Evoked action potentials in a retrogradely labeled striatonigral neuron during subsequent application of 10  $\mu$ M of SKF 81297 (red, second trace and bar below) and 100  $\mu$ M of TNPA (blue, last trace and bar below) shown in a corresponding plot of time and the number of spikes evoked by the same near rheobase current step. This neuron only responded to application of SKF 81297, which increased spiking seen in the plot, whereas TNPA had no effect on the number of evoked spikes. **J**, Application of SKF 81297 enhanced evoked spiking in striatonigral neurons, and all but one tested neurons were unresponsive to sequential application of TNPA (**J**). Scale bars = 200  $\mu$ M

These results thus suggest the striatal neurons that project directly to the basal ganglia output nuclei are those that express the D1 receptor. It would then be expected that D1-responsive striatonigral neurons are unresponsive to D2 receptor activation. In mammals, birds and reptiles,

dopamine D1 receptor agonists have been shown to preferentially enhance excitability while D2 receptor agonists mainly reduce excitability (Hernandez-Lopez et al., 1997; Hernandez-Lopez et al., 2000; Ding and Perkel, 2002; Barral et al., 2010). To investigate whether the retrogradely labeled neurons responded to both dopamine receptor agonists we sequentially applied D1- and D2 agonists in whole-cell patch-clamp experiments. Figure 1I shows a striatonigral neuron where application of the D1 agonist SKF 81297 (10  $\mu$ M, red trace and application time bar) excited the neuron, seen by the increased number of evoked spikes to the same positive current injection compared to the frequency prior to drug application. Wash of the D1 agonist (Fig. 1I, black trace) decreased the number of evoked spikes towards baseline although the frequency was not fully reversed. Subsequent application of the D2 agonist TNPA (100  $\mu$ M) in the same neuron did not affect the evoked spiking (Fig. 1I, blue trace and time bar). This neuron thus only responded to D1 receptor activation. Application of SKF 81297 excited 7 out of 9 neurons ( $p < 0.05$ ,  $n = 9$ , Fig. 1J) with an average increase in firing of  $47 \pm 20\%$  and one neuron did not respond at all to D1 activation (not included). Sequential application of TNPA was performed in 6 neurons out of which all but one were unresponsive (Fig. 1K,  $p = 0.36$ ) to D2 activation, but all of them were responsive to D1 activation (Fig. 1J).

These results show that striatal neurons that project directly to the output nuclei of the basal ganglia, selectively express dopamine D1 receptors, which when activated increase the excitability of these neurons.

#### **A subpopulation of striatal neurons projecting to the mixed GPi/GPe nucleus express D2 receptors that reduce excitability upon activation**

The lamprey dorsal pallidum is an intermingled GPi/GPe nucleus (Stephenson-Jones et al., 2011b) just as in birds and reptiles (Reiner et al., 1998a). Accordingly, the lamprey striatum contains two different types of neurons projecting to the dorsal pallidum, one that expresses enkephalin and that preferentially targets pallidal output neurons of the indirect pathway while the other type expresses substance P and contacts pallidal projection neurons of the direct pathway (Stephenson-Jones et al., 2011b). In mammals these separate subpopulations of direct and indirect MSNs express D1 and D2 receptors, respectively. If this organization is conserved then separate subpopulations of striatal neurons projecting to the dorsal pallidum should express either D1 or D2 receptors. In line with this just less than half of the striatal neurons, retrogradely labeled from the dorsal pallidum, co-localized with the *in situ* hybridization signal for the D2 receptor (Fig. 2A-D;  $47.1 \pm 12.8\%$ ,  $n = 6$ ).

In mammals, complete segregation or partial co-expression of D1 and D2 receptors by direct and indirect MSNs is a matter of controversy (Bertran-Gonzalez et al., 2010). To test whether either D1 or D2 agonists individually activate the mix of direct and indirect striatopallidal neurons of the lamprey, these drugs were applied sequentially during recordings. Figure 2E shows a retrogradely labeled striatopallidal neuron with evoked action potentials in response to near rheobase positive current injections from a depolarized baseline. Application of SKF 81297 (10  $\mu$ M, red trace and time bar) had no effect on the frequency of evoked spikes, while subsequent application of TNPA (100  $\mu$ M, blue trace and time bar) potently reduced the number of evoked spikes a few minutes after bath application. The dopamine D2 receptor activation by TNPA had a distinct effect on the excitability of cells by markedly reducing evoked spikes by  $45 \pm 14\%$  in 7 out of 16 cells (Fig. 2F,  $p < 0.001$ ). In these seven D2-responsive cells, application of SKF 81297 had no overall effect on excitability (Fig. 2G,  $p = 0.83$ ), although one cell was slightly excited and another inhibited by D1 activation. The data thus suggest that this subpopulation of striatopallidal neurons preferentially express D2 receptors that suppress spiking activity upon activation. These neurons are thus presumably part of the indirect pathway that preferentially targets the GPe-like neurons in the dorsal pallidum.



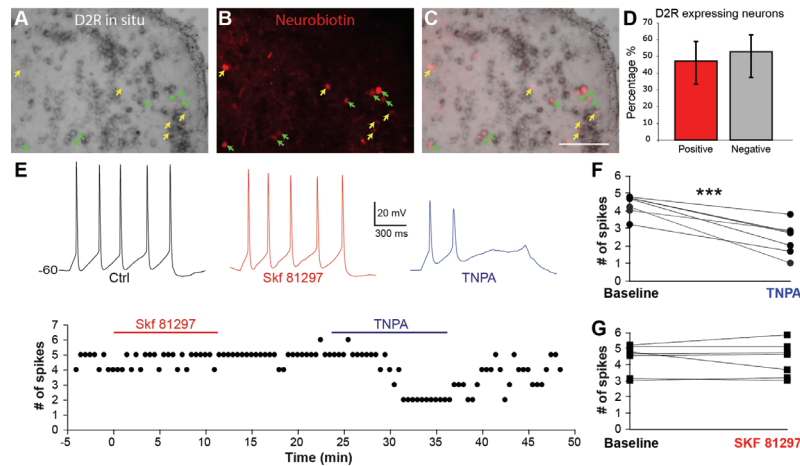


**Figure 2. One subgroup of striatopallidal neurons expresses functional D2 receptors that reduce excitability**  
**A**, DIG-labeled D2 receptor riboprobe expressed in a subpopulation of striatal neurons. Yellow arrows indicate neurons that are retrograde labeled but do not express D2 receptor mRNA. Green arrows indicate neurons that are retrograde labeled and express D2 receptor mRNA. **B**, Striatal neurons retrogradely labeled after injections of neurobiotin into the dorsal pallidum. **C**, Merged image showing the overlap between retrograde labeled cells and D2 receptor mRNA. **D**, Quantification showing the percentage of retrograde labeled neurons that express D2 receptor mRNA. **E**, Evoked action potentials in a retrogradely labeled striatopallidal neuron during sequential application of 10  $\mu$ M of SKF 81297 (red trace and bar) and 100  $\mu$ M of TNPA (blue trace and bar). This neuron does not respond to application of SKF 81297, whereas application of TNPA potently reduces the number of evoked spikes. **F**, In 7 striatopallidal cells, application of TNPA had a pronounced effect on evoked spikes that were reduced by the D2 activation. **G**, These 7 cells were not significantly affected by application of SKF 81297, although a few of the neurons slightly increased or decreased their spiking. Scale bars = 200  $\mu$ M

#### Another subpopulation of striatopallidal neurons express D1 receptors and their activation excites neurons

The results from the D2 receptor expression mapping, suggest that the other half of the striatal neurons projecting to the dorsal pallidum should represent the striatal neurons projecting to the GPi-like neurons in the dorsal pallidum and express dopamine D1 receptors (Fig. 3A-C). Again, as with the D2 receptors, just less than half of the neurons, retrogradely labeled from the dorsal pallidum, co-localized with the *in situ* hybridization signal for the D1 receptor (Fig. 3A-D;  $42.2 \pm 3.1\%$ ,  $n=2$ ).

In order to determine if these neurons selectively respond to D1 receptor agonists, both D1 and D2 receptor agonists were sequentially applied during recordings from retrogradely labeled neurons. Figure 3E shows a retrogradely labeled striatopallidal neuron that, in contrast to the previously described striatopallidal subpopulation, was excited by application of SKF 81297 (10  $\mu$ M, red trace and time bar) that increased the evoked discharge. Wash by aCSF partially reversed the effect of D1 activation. Subsequent application of TNPA (100  $\mu$ M, blue trace and time bar) had no effect on the number of evoked spikes, further indicating the existence of two segregated striatopallidal pathways. The enhanced excitability induced by D1 activation increased the number of evoked spikes by an average of  $31 \pm 7\%$  in 6 out of 16 cells (Fig. 3F,  $p<0.01$ ). In five of these six cells TNPA was subsequently applied without any effect on excitability (Fig. 3G,  $p=0.73$ ). Further, three neurons did not respond to either SKF 81297 or TNPA (not shown).

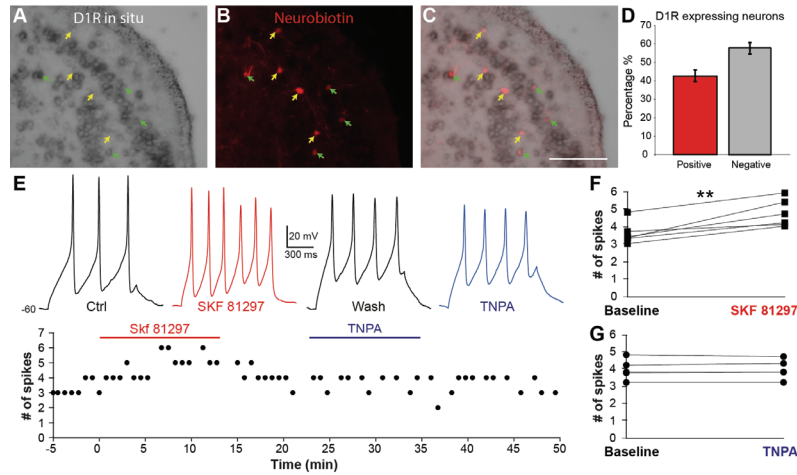


**Figure 3 One subgroup of striatopallidal neurons expresses functional D1 receptors that enhance excitability**  
**A**, DIG-labeled D1 receptor riboprobe expressed in a subpopulation of striatal neurons. Yellow arrows indicate neurons that are retrograde labeled but do not express D1 receptor mRNA. Green arrows indicate neurons that are retrograde labeled and express D1 receptor mRNA. **B**, Striatal neurons retrogradely labeled after injections of neurobiotin into the dorsal pallidum. **C**, Merged image showing the overlap between retrograde labeled cells and D1 receptor mRNA. **D**, Quantification showing the percentage of retrograde labeled neurons that express D1 receptor mRNA. **E**, Evoked action potentials in a retrogradely labeled striatopallidal neuron during sequential application of 10  $\mu$ M of SKF 81297 (red trace and bar) and 100  $\mu$ M of TNPA (blue trace and bar). This neuron responds to application of SKF 81297 by increasing spike discharge, whereas application of TNPA does not affect the number of evoked spikes. **F**, Enhanced spiking by SKF 81297 was seen in five cells that were unresponsive to TNPA (**G**). Scale bars = 200  $\mu$ m

These results suggest that the subpopulations of striatal neurons projecting to the dorsal pallidum differentially express either dopamine D1 or D2 receptors. One group of striatopallidal neurons expresses dopamine D2 receptors and their activation suppresses neuronal output while D1 activation has no effect. The other neuron type instead expresses dopamine D1 receptors that excite neurons upon activation while these neurons are unresponsive to D2 agonists. As the D1 receptors are co-localized with neurons that express substance P and project directly to the GPi in mammals, our results suggest that the D1 receptor expressing subpopulation may be the same as the “directly” projecting substance P population in lamprey. In contrast the D2 receptors may be expressed in the enkephalin population that projects to the GPe neurons in the lamprey dorsal pallidum. The mammalian organization of D1 expressing neurons projecting to the GPi, and D2 expressing neurons projecting to the GPe may thus be conserved in lamprey, even though the GPi and GPe neurons are intermingled in one nucleus, the dorsal pallidum. Taken together, these results suggest that the organization with striatal neurons of the direct and indirect pathway differentially expressing D1 and D2 receptors existed already at the origin of vertebrate evolution.

Based on these results, we pooled the data from the striatonigral neurons and the D1- but not D2-responsive striatopallidal neurons into a single group termed “direct projection neurons” (Table 1). The D2- but not D1-responsive striatopallidal neurons were pooled together with six unlabeled D2 responsive neurons into a single group termed “indirect projection neurons” (Table 1).

#### Cellular effects by D1 receptor activation

We then continued by a general analysis of the selective D1 and D2 dopamine receptor activation in striatal neurons. The dopaminergic modulation of striatal neurons is dependent on the voltage baseline in other vertebrates, where D1 receptor agonists have been shown to preferentially enhance



excitability at membrane potentials close to spike threshold and decrease it at membrane potentials close to rest (Hernandez-Lopez et al., 1997; Ding and Perkel, 2002; Barral et al., 2010). In patch-clamp recordings at a depolarized holding potential ( $\sim -55$  to  $-60$  mV, Fig 4A), a subpopulation of lamprey striatal neurons (19 out of 26 cells) were activated by the D1 agonist SKF 81297 (10  $\mu$ M) that excited neurons as seen by the increased number of evoked action potentials (Fig. 4A<sub>1</sub>). The increase in firing was evident throughout a series of current injections (Fig. 4A<sub>2</sub>) with an average increase in firing frequency of  $33 \pm 10\%$  ( $n=19$ ,  $p<0.001$ , Fig. 4A<sub>3</sub>) near rheobase current injection. In four neurons, hyperpolarizing current injections also evoked post-inhibitory rebound (PIR) action potentials after the termination of the hyperpolarization (Fig. 4A<sub>4</sub>). In these neurons, D1 receptor activation also enhanced excitability by increasing the number of PIR spikes (example in Fig. 4A<sub>1</sub>, right trace vs left trace). The spiking increased by  $84 \pm 24\%$  ( $n=4$ ,  $p<0.01$ , Fig. 4A<sub>4</sub>), quantified by the total number of PIR spikes evoked by the consecutive hyperpolarization pulses as exemplified in Figure 4A<sub>4</sub>. In addition to the increased spiking, application of SKF 81297 slightly depolarized half of the neurons ( $n=8/19$ ,  $3.3 \pm 0.3$  mV) and clearly affected the properties of action potentials (summarized in Table 1). The amplitude was reduced from  $56.8 \pm 2.5$  mV to  $47.3 \pm 3.5$  mV ( $p<0.001$ ) and the threshold shifted to a slightly more depolarized value from  $-47.4 \pm 1.7$  mV to  $-45.5 \pm 1.6$  mV ( $p<0.05$ ). The action potentials also broadened slightly from  $5.5 \pm 0.5$  ms to  $6.0 \pm 0.7$  ms ( $p<0.05$ ). In cells capable of eliciting PIR spikes, the amplitude of these spikes decreased from  $61.6 \pm 7.7$  mV to  $43.0 \pm 10.5$  mV ( $p<0.05$ ) and although 3/4 cells lowered their threshold, the overall shift was not statistically significant (baseline  $-59.3 \pm 2.1$ , SKF 81297  $-60.1 \pm 2.4$ ,  $p=0.33$ ).

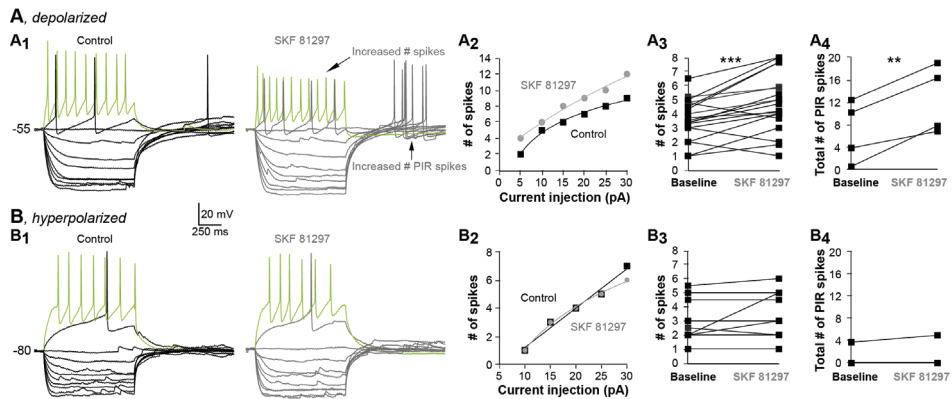


**Figure 4. D1 receptor activation by the agonist SKF 81297 excites depolarized neurons**

**A**, Evoked response patterns of striatal neurons held at depolarized membrane potentials ( $-55$  to  $-65$  mV). Application of SKF 81297 (10  $\mu$ M) enhances the firing. **A<sub>1</sub>**, Voltage responses of a neuron (striatonigral) to hyperpolarizing and depolarizing 1 s current steps of 5 pA per step, elicited from a depolarized potential at  $-55$  mV in control aCSF (left, control) or during bath application SKF 81297 (right). SKF 81297 increases the number of evoked spikes (arrow) and post-inhibitory rebound (PIR) spikes (arrow). The hyperpolarizing voltage responses are similar in control and SKF 81297, indicating that there is no change in input resistance. **A<sub>2</sub>**, Current-frequency diagram of the same neuron showing the increased number of evoked spikes during SKF 81297 (grey circles) compared to control (black squares). **A<sub>3</sub>**, Application of SKF 81297 increases the number of evoked spikes in D1R stimulated neurons, measured near rheobase. **A<sub>4</sub>**, SKF 81297 increased PIR-spikes in four neurons capable of producing such hyperpolarization-activated action potentials, quantified by the total number of PIR spikes in response to 8-10 consecutive hyperpolarizations from  $-100$  mV to baseline as in **A<sub>1</sub>**. **B**, Same protocols as in (**A**) but at hyperpolarized potentials around  $-80$  mV. **B<sub>1-2</sub>**, SKF 81297 (**B<sub>1</sub>**, right traces) has no effect on evoked potentials when they are elicited from  $-80$  mV compared to control (**B<sub>1</sub>**, left traces) and the neuron (same as in **A**) does not fire PIR spikes from this negative potential. **B<sub>3</sub>**, This was consistent for almost all cells test. **B<sub>4</sub>**, Only one of the four neurons with PIR-spikes at depolarized potentials were capable of producing such action potentials from hyperpolarized levels.

At a more negative holding potential ( $\sim -80$  mV), the enhancement in excitability disappeared (Fig. 4B). The number of evoked spikes was on average the same before and after application of SKF 81297 (Fig. 4B<sub>1-3</sub>,  $n=13$ ,  $p=0.23$ ). At this hyperpolarized baseline, three of the four neurons with PIR spikes did not fire any hyperpolarization-activated action potentials (Fig. 4B<sub>1</sub> and 4B<sub>4</sub>), indicating that the currents underlying these spikes have a more depolarized activation range. One neuron did however still produce PIR spikes, which slightly increased in number during D1 activation (Fig. 4B<sub>4</sub>). These findings show that, as in mammals (Calabresi et al., 1987; Hernandez-Lopez et al., 1997; Surmeier et al., 2007), dopamine D1 receptor activation enhances the excitability of striatal neurons only at depolarized levels. This suggests that activation of the D1 receptor modulates voltage-gated channels that are active at potentials above  $-60$  mV and that contribute to both PIRs and regular action potentials.

In addition, in experiments on the retrogradely labeled, directly projecting neurons (described in Fig. 1 and 3) where TNPA was subsequently applied after SKF 81297 this did not cause any change in action potential properties or input resistance (Table 1, Pre vs TNPA,  $p>0.05$  all values) as expected by the lack of effect on excitability.

#### Reduction of striatal excitability by D2 receptor activation

The detailed cellular responses to D2 receptor activation was also analyzed and included six unlabeled D2-responsive neurons as well as seven (7/16) striatopallidal neurons and one striatonigral (1/6) neuron that responded to TNPA (100  $\mu$ M, Fig. 1 and 2). Preliminary results in lamprey indicate that the excitability of a subpopulation of lamprey striatal neurons is reduced by a D2 receptor agonist (Robertson et al., 2012). In direct contrast to the D1 activation, application of TNPA reduced the number of both regularly evoked action potentials and PIR spikes, in a total of 14 out of 28 neurons, including non-labeled and labeled cells (Fig. 5A<sub>1</sub>). The reduction was seen throughout consecutive suprathreshold current injections (Fig. 5A<sub>2</sub>) and the average spiking frequency decreased by  $47 \pm 13\%$  ( $p<0.001$ ,  $n=14$ , Fig. 5A<sub>3</sub>). As with D1 activation, the amplitude of action potentials was markedly reduced from  $49.9 \pm 3.0$  mV to  $35 \pm 3.2$  mV ( $p<0.001$ ,  $n=14$ , Table 1) and the threshold for the action potential was shifted from  $-47.2 \pm 2.2$  mV to  $-40.5 \pm 2.8$  mV ( $p<0.01$ ,  $n=14$ , Table 1). The number of hyperpolarization-activated action potentials were significantly reduced by  $84 \pm 49\%$  ( $p<0.001$ ,  $n=8$ , Fig. 5A<sub>4</sub>) and their amplitudes were reduced from  $58.5 \pm 3.4$  mV to  $38.0 \pm 4.3$  mV ( $p<0.001$ ,  $n=6$ , Table 1). In contrast to D1 responsive neurons, the threshold for PIR-spikes was markedly depolarized from  $-52.0 \pm 3.2$  mV to  $-43.4 \pm 3.3$  mV ( $p<0.05$ ,  $n=6$ , Table 1). Another contrasting difference from D1 activated neurons was that the decreased excitability was voltage independent, and the reduced discharge persisted at hyperpolarized potentials ( $\sim -80$  mV) during TNPA application (Fig. 5B<sub>1-3</sub>,  $p<0.01$ ,  $n=7$ ). At this negative potential very few PIR spikes were evoked even during control conditions (Fig. 5B<sub>1</sub> and 5B<sub>4</sub>). The same voltage independent action with D2 receptor agonists has also been observed in birds, but not in mammals (Hernandez-Lopez et al., 2000; Ding and Perkel, 2002).

In addition, in the D2-responsive indirect projection neurons previously described (Fig. 2), subsequent application of SKF 81297 did not affect action potential properties or input resistance (Table 1, Pre vs SKF 81297,  $p>0.05$  all values) as expected by its overall lack of effect on excitability (Fig. 2).

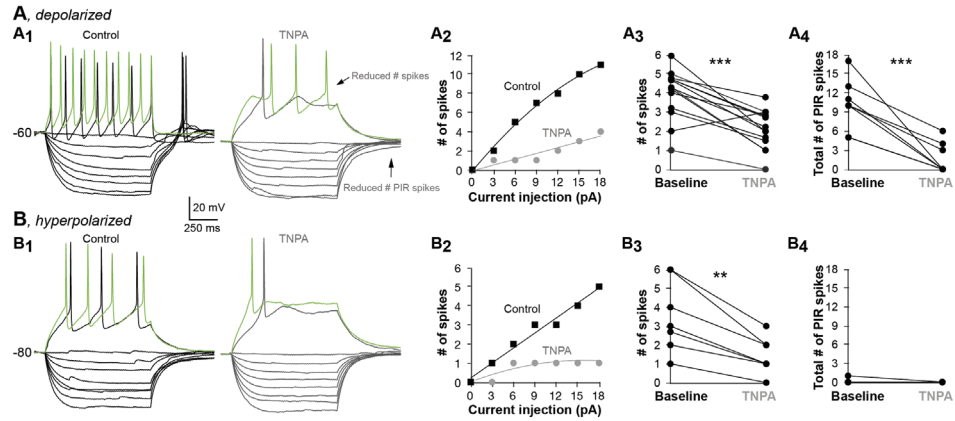


**Figure 5. D2 receptor activation by the agonist TNPA inhibits neurons**

**A**, Evoked response patterns of striatal neurons held at depolarized levels before and during application of TNPA (100  $\mu$ M) that reduce excitability. **A<sub>1</sub>**, Voltage responses of a neuron to hyperpolarizing and depolarizing 1 s current steps of 3 pA per step, elicited at membrane potentials around -55 mV in control aCSF (left, control) or during bath application TNPA (right). TNPA reduces the number of evoked spikes (arrow) and PIR-spikes (arrow). The hyperpolarizing voltage responses are similar in control and TNPA, indicating that there is no change in input resistance. **A<sub>2</sub>**, Current-frequency diagram of the same neuron showing the decreased number of evoked spikes during TNPA (grey circles) compared to control (black squares). **A<sub>3</sub>**, Application of TNPA potentially reduces the number of evoked spikes in D2 stimulated neurons, measured at near rheobase positive current injection. **A<sub>4</sub>**, TNPA strongly reduced PIR-spikes in all neurons capable of producing such hyperpolarization-activated action potentials, quantified by the total number of PIR spikes in response to 8-10 consecutive hyperpolarizations from -100 mV to baseline as in **A<sub>1</sub>**. **B**, Same protocols as in (**A**) but at hyperpolarized potentials around -80 mV. **B<sub>1,2</sub>**, TNPA (**B<sub>1</sub>**, right traces) reduces evoked potentials also when they are elicited from a hyperpolarized baseline around -80 mV compared to control (**B<sub>1</sub>**, left traces). The neuron (same as in **A**) does not fire PIR spikes from this negative potential. **B<sub>3</sub>**, The reduced spiking was consistent for all cells tested. **B<sub>4</sub>**, Only one of all neurons with PIR-spikes at depolarized potentials were capable of producing such action potentials from hyperpolarized levels.

Our results thus show that dopamine D2 receptor activation exerts opposite effects on excitability compared to D1 activation in responsive striatal projection neurons. The distinct separation of enhancing (D1-activation) or reducing (D2-activation) PIR-spiking in the subset of striatal neurons capable of producing such action potentials further emphasizes the difference in dopamine modulation of striatal projection neurons.

## Discussion

Our results suggest that the mechanism by which dopamine modulates the activity of striatal projection neurons is conserved across the vertebrate phylum, together with the intrinsic organization of the basal ganglia. As with mammalian species, the striatal neurons that project directly to the basal ganglia output nuclei express dopamine D1 receptors, while separate populations that project to the dorsal pallidum, the homolog of the GPi/GPe, express either dopamine D1 or D2 receptors. Furthermore, activation of these dopamine receptors leads to an increase in the excitability of D1 expressing neurons and a decrease in the excitability of D2 expressing neurons. Together these results suggest that the dichotomous effect of dopamine on the so called “direct” and “indirect” pathways has been conserved throughout the vertebrate phylum, likely as a mechanism to bias the network towards action selection and facilitate procedural learning.

Table 1. Effects of dopamine agonists on intrinsic properties of projection neurons

	"Direct" Projection Neurons				"Indirect" Projection Neurons			
	Baseline	SKF 81297	Pre	TNPA (no effect)	Baseline	TNPA	Pre	SKF 81297 (no effect)
Resting potential (Vm)	<b>-72.3 ± 2.2</b>	<b>-71.0 ± 2.8</b>	-	-	<b>-69.6 ± 4.1</b>	<b>-69.4 ± 4.7</b>	-	-
Amplitude of APs (mV)	<b>56.8 ± 2.5</b>	<b>47.3 ± 3.5</b>	53.8 ± 1.2	52.3 ± 4.3	<b>49.9 ± 3.0</b>	<b>35.0 ± 3.2</b>	49.4 ± 4.7	46.4 ± 5.3
Threshold for APs (mV)	<b>-47.4 ± 1.7</b>	<b>-45.5 ± 1.6</b>	-42.2 ± 2.1	-42.9 ± 2.3	<b>-47.2 ± 2.2</b>	<b>-40.5 ± 2.8</b>	-44.1 ± 3.1	-43.7 ± 2.8
Half-width of single AP (mV)	<b>5.5 ± 0.5</b>	<b>6.0 ± 0.7</b>	7.0 ± 1.2	7.0 ± 1.4	7.0 ± 1.1	7.7 ± 1.1	8.4 ± 0.7	8.1 ± 0.8
Input resistance (GΩ)	2.2 ± 0.2	2.5 ± 0.2	2.8 ± 0.3	2.7 ± 0.2	2.6 ± 0.3	2.8 ± 0.4	2.8 ± 0.5	2.7 ± 0.4
Amplitude of PIR spike (mV)	<b>61.6 ± 7.7</b>	<b>43.0 ± 10.5</b>	-	-	<b>58.5 ± 3.4</b>	<b>38.0 ± 4.3</b>	-	-
Threshold of PIR spike (mV)	<b>-59.3 ± 2.1</b>	<b>-60.1 ± 2.4</b>	-	-	<b>-52.0 ± 3.2</b>	<b>-43.4 ± 3.3</b>	-	-

Results expressed as mean ± SEM. AP, action potential; PIR, post-inhibitory rebound; "Direct Projection Neurons", pooled data from striatonigral and D1 responsive striatopallidal neurons; "Indirect", D2 responsive striatopallidal and unlabeled neurons; Pre, indicates regular aCSF prior to drug application. Bold indicate significant differences.

### Dopamine receptor expression in striatal projection neurons

Our results suggest that the majority of lamprey striatal neurons express either dopamine D1 or D2 receptors, although our electrophysiological results indicate that a small proportion of neurons may express both types of dopamine receptors. This segregation of dopamine receptor expression is also observed in mammals (Gerfen and Surmeier, 2011). Analysis of transgenic mice that express GFP under the D1 or D2 receptor promoter, have shown that these receptors are segregated, with direct and indirect projecting medium spiny neurons expressing D1 or D2 receptors, respectively (Gertler et al., 2008). Single cell RT-PCR studies have also confirmed that substance P expressing (directly projecting) striatal neurons have abundant mRNA for D1 but not D2 receptors and the majority of enkephalin expressing (indirect projecting) striatal neurons have abundant D2 but little D1 receptor mRNA, although a small percentage (approximately 10%) of enkephalin expressing neurons do contain detectable levels of D1 receptor mRNA (Surmeier et al., 1996).

Whereas most striatal projection neurons appear to express preferentially D1 or D2 receptors, RT-PCR has however indicated that there may be an overlap of receptor expression, where D1 receptors may co-localize to a various degree with the receptor subtypes of the D2 receptor family (D2-D4) (Surmeier et al., 1996; Cazorla et al., 2012), while around 25% of the D2 receptor expressing neurons also express the D5, a D1 like receptor. It should be noted that even in songbirds, where it has been suggested there is a considerable degree of D1 and D2 receptor co-expression, application of dopamine either increases or decreases the excitability of striatal neurons (Ding and Perkel, 2002).

### Ionic mechanisms

Dopamine modulates the excitability of striatal projection neurons by affecting voltage sensitive channels (Surmeier et al., 2007). The voltage dependent excitation mediated via D1 receptors in lamprey is in agreement with that previously reported in mammals (Hernandez-Lopez et al., 1997; Gerfen and Surmeier, 2011) and may be a reflection of the classical "up- and down-state" in MSNs (Wilson and Kawaguchi, 1996) where dopamine dynamically modulates neuronal activity based on the state of the animal (Mahon et al., 2003). The reduction of action potential amplitudes and the depolarizing shift of its threshold by both D1 and D2 stimulation in lamprey is likely a result of increased inactivation and decreased conductance of voltage gated Na<sup>+</sup>-channels (Cepeda et al., 1995; Carr et al., 2003; Maurice et al., 2004). There may also be modulatory effects on different potassium channels such as Kir and A-type K<sup>+</sup>-channels (Ericsson et al., 2011), which have both been implicated in dopamine modulation in other species (Hernandez-Lopez et al., 1997; Ding and Perkel, 2002). We did not, however, see any clear change in input resistance as would be expected by an effect on Kir-channels. On the other hand, the clearly contrasting effects on excitability by the two dopamine receptors may possibly be due to opposite actions on low voltage activated (LVA) L-type Ca<sub>v</sub> 1.3 Ca<sup>2+</sup> channels as has been suggested in mammals and reptiles (Hernandez-Lopez et al., 1997; Barral et al., 2010) and that activate around -60 mV (Lipscombe, 2002). This is in agreement with the capacity of lamprey striatal projection neurons to produce PIR-spikes from around -60 mV, further indicating

LVA  $\text{Ca}^{2+}$ -channels that have been shown to contribute to the PIR responses and be negatively modulated by D2 activation in lamprey spinal neurons (Wang et al., 2011). The potent increase (D1 activation) and decrease (D2 activation) of PIR-spikes and the depolarizing shift of its threshold by D2 activation only, as would be expected by an inactivation of L-type  $\text{Ca}^{2+}$ -channels, thus suggest that this may be the main target downstream of dopamine activation also in lamprey striatal neurons.

### Functional consequences

The basal ganglia circuitry underlying action selection is evolutionarily highly conserved, as homologs of the striatum, globus pallidus, substantia nigra (*pars compacta* and *reticulata*) and the subthalamic nucleus, together with the direct and indirect pathways have been identified in lamprey, one of the phylogenetically oldest vertebrates (Pombal et al., 1997a, b; Menard and Grillner, 2008; Ericsson et al., 2011; Stephenson-Jones et al., 2011a; Robertson et al., 2012; Stephenson-Jones et al., 2012). Our results now show that the differential dopaminergic modulation of the direct and indirect pathways is also highly conserved. In mammals phasic dopamine release is critical for reinforcement learning as it can influence long-term plasticity at the corticostriatal synapses (Bergman et al., 2004). Phasic release of dopamine can promote LTP at the corticostriatal synapses of the direct pathway and LTD at the corticostriatal synapses of the indirect pathway due to the differential expression of D1 and D2 receptors (Gerfen and Surmeier, 2011). Direct glutamatergic pallial (cortical)–striatal synapses are also present in lamprey with the same synaptic dynamics as those seen in mammals (Ericsson et al., 2010). Taken together these results suggest that not only is the basal ganglia circuitry for action selection conserved but also the dopaminergic modulation of this circuitry, as a common vertebrate mechanism for reinforcement learning.

### References

- Albin RL, Young AB, Penney JB (1989) The functional anatomy of basal ganglia disorders. *Trends Neurosci* 12:366-375.
- Barral J, Galarraga E, Tapia D, Flores-Barrera E, Reyes A, Bargas J (2010) Dopaminergic Modulation of Spiny Neurons in the Turtle Striatum. *Cell Mol Neurobiol*.
- Bergman H, Kimura M, Wickens J (2004) Modulation of striatal circuits by dopamine and acetylcholine. In: *Microcircuits - the interface between neurons and global brain function* (Grillner S, Graybiel A, eds), pp p. 149-162: The MIT Press.
- Bertran-Gonzalez J, Herve D, Girault JA, Valjent E (2010) What is the Degree of Segregation between Striatonigral and Striatopallidal Projections? *Front Neuroanat* 4.
- Calabresi P, Mercuri N, Stanzione P, Stefani A, Bernardi G (1987) Intracellular studies on the dopamine-induced firing inhibition of neostriatal neurons in vitro: evidence for D1 receptor involvement. *Neuroscience* 20:757-771.
- Carr DB, Day M, Cantrell AR, Held J, Scheuer T, Catterall WA, Surmeier DJ (2003) Transmitter modulation of slow, activity-dependent alterations in sodium channel availability endows neurons with a novel form of cellular plasticity. *Neuron* 39:793-806.
- Cazorla M, Shegda M, Ramesh B, Harrison NL, Kellendonk C (2012) Striatal D2 receptors regulate dendritic morphology of medium spiny neurons via Kir2 channels. *J Neurosci* 32:2398-2409.
- Cepeda C, Chandler SH, Shumate LW, Levine MS (1995) Persistent  $\text{Na}^+$  conductance in medium-sized neostriatal neurons: characterization using infrared videomicroscopy and whole cell patch-clamp recordings. *J Neurophysiol* 74:1343-1348.
- Chu J, Wilczynski W, Wilcox RE (2001) Pharmacological characterization of the D1- and D2-like dopamine receptors from the brain of the leopard frog, *Rana pipiens*. *Brain, behavior and evolution* 57:328-342.

- Ding L, Perkel DJ (2002) Dopamine modulates excitability of spiny neurons in the avian basal ganglia. *J Neurosci* 22:5210-5218.
- Ericsson J, Silberberg G, Robertson B, Wikstrom MA, Grillner S (2011) Striatal cellular properties conserved from lampreys to mammals. *J Physiol* 589:2979-2992.
- Gerfen CR, Surmeier DJ (2011) Modulation of striatal projection systems by dopamine. *Annual review of neuroscience* 34:441-466.
- Gertler TS, Chan CS, Surmeier DJ (2008) Dichotomous anatomical properties of adult striatal medium spiny neurons. *J Neurosci* 28:10814-10824.
- Grillner S, Hellgren J, Menard A, Saitoh K, Wikstrom MA (2005) Mechanisms for selection of basic motor programs--roles for the striatum and pallidum. *Trends Neurosci* 28:364-370.
- Hernandez-Lopez S, Bargas J, Surmeier DJ, Reyes A, Galarraga E (1997) D1 receptor activation enhances evoked discharge in neostriatal medium spiny neurons by modulating an L-type  $\text{Ca}^{2+}$  conductance. *J Neurosci* 17:3334-3342.
- Hernandez-Lopez S, Tkatch T, Perez-Garci E, Galarraga E, Bargas J, Hamm H, Surmeier DJ (2000) D2 dopamine receptors in striatal medium spiny neurons reduce L-type  $\text{Ca}^{2+}$  currents and excitability via a novel PLC[ $\beta$ ]-IP3-calcineurin-signaling cascade. *J Neurosci* 20:8987-8995.
- Lipscombe D (2002) L-type calcium channels: highs and new lows. *Circulation research* 90:933-935.
- Mahon S, Deniau JM, Charpier S (2003) Various synaptic activities and firing patterns in corticostriatal and striatal neurons in vivo. *Journal of physiology, Paris* 97:557-566.
- Maurice N, Mercer J, Chan CS, Hernandez-Lopez S, Held J, Tkatch T, Surmeier DJ (2004) D2 dopamine receptor-mediated modulation of voltage-dependent  $\text{Na}^{+}$  channels reduces autonomous activity in striatal cholinergic interneurons. *J Neurosci* 24:10289-10301.
- Menard A, Grillner S (2008) Diencephalic locomotor region in the lamprey--afferents and efferent control. *J Neurophysiol* 100:1343-1353.
- Pombal MA, El Manira A, Grillner S (1997a) Organization of the lamprey striatum - transmitters and projections. *Brain Res* 766:249-254.
- Pombal MA, El Manira A, Grillner S (1997b) Afferents of the lamprey striatum with special reference to the dopaminergic system: a combined tracing and immunohistochemical study. *J Comp Neurol* 386:71-91.
- Pombal MA MM, Moussa CE-H, Sidhu A, Vernier P. (2007) Distribution of the dopamine D1 receptor in the lamprey brain: evolutionary implications. *Society for Neuroscience* 35129.
- Redgrave P, Prescott TJ, Gurney K (1999) The basal ganglia: a vertebrate solution to the selection problem? *Neuroscience* 89:1009-1023.
- Reiner A, Medina L, Veenman CL (1998a) Structural and functional evolution of the basal ganglia in vertebrates. *Brain Res Brain Res Rev* 28:235-285.
- Reiner A, Medina L, Veenman C (1998b) Structural and functional evolution of the basal ganglia in vertebrates. *Brain Res Brain Res Rev* 28:235-285.
- Robertson B, Huerta-Ocampo I, Ericsson J, Stephenson-Jones M, Perez-Fernandez J, Bolam JP, Diaz-Heijtz R, Grillner S (2012) The dopamine D2 receptor gene in lamprey, its expression in the striatum and cellular effects of D2 receptor activation. *PloS one* 7:e35642.
- Stephenson-Jones M, Floros O, Robertson B, Grillner S (2011a) Evolutionary conservation of the habenular nuclei and their circuitry controlling the dopamine and 5-hydroxytryptophan (5-HT) systems. *Proc Natl Acad Sci U S A*.
- Stephenson-Jones M, Ericsson J, Robertson B, Grillner S (2012) Evolution of the basal ganglia; Dual output pathways conserved throughout vertebrate phylogeny. *J Comp Neurol*.

- Stephenson-Jones M, Samuelsson E, Ericsson J, Robertson B, Grillner S (2011b) Evolutionary conservation of the basal ganglia as a common vertebrate mechanism for action selection. *Current biology* : CB 21:1081-1091.
- Surmeier DJ, Song WJ, Yan Z (1996) Coordinated expression of dopamine receptors in neostriatal medium spiny neurons. *J Neurosci* 16:6579-6591.
- Surmeier DJ, Ding J, Day M, Wang Z, Shen W (2007) D1 and D2 dopamine-receptor modulation of striatal glutamatergic signaling in striatal medium spiny neurons. *Trends Neurosci* 30:228-235.
- Thompson RH, Menard A, Pombal M, Grillner S (2008) Forebrain dopamine depletion impairs motor behavior in lamprey. *Eur J Neurosci* 27:1452-1460.
- Vernier (1997) The amphioxus D1/beta receptor and the emergence of the vertebrate adrenergic system. In. GenBank NCBI Accession number. AJ005434.1p.
- Wang D, Grillner S, Wallen P (2011) 5-HT and dopamine modulates CaV1.3 calcium channels involved in postinhibitory rebound in the spinal network for locomotion in lamprey. *J Neurophysiol* 105:1212-1224.
- Wilson C, Kawaguchi Y (1996) The origins of two-state spontaneous membrane potential fluctuations of neostriatal spiny neurons. *J Neurosci* 16:2397-2410.





VI



# Evolution of the Basal Ganglia: Dual-Output Pathways Conserved Throughout Vertebrate Phylogeny

Marcus Stephenson-Jones, Jesper Ericsson, Brita Robertson, and Sten Grillner\*

The Nobel Institute for Neurophysiology, Department of Neuroscience, Karolinska Institutet, SE-171 77 Stockholm, Sweden

## ABSTRACT

The basal ganglia, including the striatum, globus pallidus interna and externa (GPe), subthalamic nucleus (STN), and substantia nigra pars compacta, are conserved throughout vertebrate phylogeny and have been suggested to form a common vertebrate mechanism for action selection. In mammals, this circuitry is further elaborated by the presence of a dual-output nucleus, the substantia nigra pars reticulata (SNr), and the presence of modulatory input from the cholinergic pedunculo-pontine nucleus (PPN). We sought to determine whether these additional components of the mammalian basal ganglia are also present in one of the phylogenetically oldest vertebrates, the lamprey. We show, by using immunohistochemistry, tract tracing, and whole-cell recordings, that homologs of the SNr and PPN are present in the lamprey. Thus the SNr receives direct projections from inwardly rectifying  $\gamma$ -aminobuty-

ric acid (GABA)-ergic striatal neurons expressing substance P, but it is also influenced by indirect basal ganglia projections from the STN and potentially the GPe. Moreover, GABAergic SNr projection neurons are tonically active and project to the thalamus and brainstem motor areas. The homolog of the PPN contains both cholinergic and GABAergic neurons and is connected with all the nuclei of the basal ganglia, supporting its proposed role as part of an extended basal ganglia. A separate group of cholinergic neurons dorsal to the PPN corresponds to the descending mesencephalic locomotor region. Our results suggest that dual-output nuclei are part of the ancestral basal ganglia and that the PPN appears to have coevolved as part of a mechanism for action selection common to all vertebrates. *J. Comp. Neurol.* 520:2957–2973, 2012.

© 2012 Wiley Periodicals, Inc.

**INDEXING TERMS:** substantia nigra pars reticulata; pedunculo-pontine nucleus; lamprey; globus pallidus

The basal ganglia include a group of subcortical nuclei that plays a role in a diverse range of cognitive, limbic, and motor functions (Graybiel, 1998; Grillner et al., 2005; Hikosaka et al., 2000; Redgrave et al., 1999). For mammals, detailed knowledge is available on the general structure and connectivity and modulator action of these nuclei, but the evolutionary development of this circuitry remains unclear.

Recent studies have shown that the core architecture of the basal ganglia is present in all vertebrates; homologs of the mammalian striatum, globus pallidus interna and externa (GPe), and subthalamic nucleus (STN) are present in birds and in one of the phylogenetically oldest vertebrates, the lamprey (Ericsson et al., 2007, 2011; Pombal et al., 1997b; Reiner, 2002; Stephenson-Jones et al., 2011). In addition, the “direct” and “indirect” pathways through the basal ganglia, with substance P-expressing striatal neurons projecting to the GPe and enkephalin-expressing neurons projecting indirectly to

this output nuclei via the GPe and STN, are conserved (Jiao et al., 2000; Stephenson-Jones et al., 2011). These pathways are known to play an important role in action selection (Graybiel, 1998; Grillner et al., 2005; Hikosaka et al., 2000; Redgrave et al., 1999), so it has been suggested they may form the basis of a common vertebrate selection architecture (Redgrave et al., 1999; Stephenson-Jones et al., 2011).

Grant sponsor: EU Cortex Training Program; Grant number: FP6 MEST-CT-2005-019729 (to S.G. for M.S.-J.); Grant sponsor: EU, FP5 “Neurobotics”; Grant number: 001917 (to S.G.); Grant sponsor: Swedish Research Council; Grant number: VR-M -3026; Grant number: VR-NT 621-2007-6049 (to S.G.); Grant sponsor: Karolinska Institutets Research Funds (to B.R., S.G.); Grant sponsor: FP7 Select-and-Act (to S.G.); Grant sponsor: KID (to J.E.).

\*CORRESPONDENCE TO: Prof. Sten Grillner, The Nobel Institute for Neurophysiology, Department of Neuroscience, Karolinska Institutet, SE-171 77 Stockholm, Sweden. E-mail: sten.grillner@ki.se

Received December 23, 2011; Revised January 30, 2012; Accepted February 15, 2012

DOI 10.1002/cne.23087

Published online February 20, 2012 in Wiley Online Library (wileyonlinelibrary.com)

© 2012 Wiley Periodicals, Inc.

In mammals and birds (amniotes), the output of the basal ganglia is channeled through two nuclei, the GPi and the substantia nigra pars reticulata (SNr). These two parallel-output nuclei are topographically distinct and develop from a different regions of the brain but are both influenced by “direct” and “indirect” striatal projections, and the neurons in these nuclei share molecular and physiological characteristics (Reiner et al., 1998). In addition, both of these nuclei are influenced by neuromodulatory input from the substantia nigra pars compacta (SNc) and the pedunculopontine nucleus (PPN) but differ in their projections (Karle et al., 1996; Mena-Segovia et al., 2004; Reiner et al., 1998; Smeets et al., 2000). The GPi projects via the thalamus to areas of the cortex that influence cognitive functions as well as movements and also directly to brainstem nuclei (Akkal et al., 2007; Kelly and Strick, 2004; Middleton and Strick, 2002). The SNr projects to the brainstem and areas of the thalamus that in turn influence visual processing as well as saccadic eye and head movements (Lynch et al., 1994; Sato and Hikosaka, 2002; Takakusaki et al., 2003). Although the GPi and its related circuitry, as mentioned, are conserved throughout vertebrate phylogeny, it is unclear whether a second dual-output pathway through the SNr is conserved in species such as amphibians, fish, and jawless vertebrates. Consequently, it is unknown whether the SNr represents an additional component of the common vertebrate selection architecture or whether it evolved later to accommodate the increased behavioral repertoire of advanced vertebrates.

Indirect evidence suggests that a homolog of the SNr may exist in anamniotes. In amphibians, the anterodorsal and anteroventral tegmental nuclei receive input from the striatum and project to the optic tectum, but it is unknown whether neurons in these regions are  $\gamma$ -aminobutyric acid (GABA)-ergic, as with the SNr or cholinergic as part of the PPN (Marin et al., 1997). In addition, the physiological activity of these neurons and whether they receive input from striatal neurons associated with the direct pathway are unknown. In lamprey, a jawless vertebrate, a homolog of the SNc, has been shown to be present (Pombal et al., 1997a; Thompson et al., 2008), but there is no direct evidence for a homolog of the SNr. Despite this, a group of cells in the mesencephalic tegmentum projects to the optic tectum, and cells in this region are GABAergic (Robertson et al., 2006, 2007a). This might therefore be a candidate region for a possible jawless vertebrate homolog of the SNr. Consequently, nuclei homologous to the SNr and the cholinergic PPN may be present in anamniotes, but conclusive evidence for these nuclei remains to be shown. This is important insofar as it is still not clear why there are two largely homologous parallel-output nuclei in the basal ganglia, and

an understanding of the evolutionary origin may shed light on this unresolved issue.

By using anatomical and electrophysiological techniques, we show that a dual-output nucleus homologous to the SNr is present in lamprey along with the previously characterized dorsal pallidum, the homolog of the GPi/GPe. In addition, a homolog of the PPN is present in lamprey. This nucleus is heavily interconnected with the basal ganglia and provides cholinergic input to the SNr. This suggests that the PPN is likely to have coevolved with these nuclei, lending further support to the suggestion that the PPN should be considered part of the extended basal ganglia. Together our results suggest that the complete basal ganglia organization, including dual-output nuclei, direct and indirect pathways, and the modulatory innervation from the SNc and PPN, evolved at the dawn of vertebrate evolution and has likely served as the common mechanism for action selection that vertebrates have used for the past 560 million years.

## MATERIALS AND METHODS

Experiments were performed on a total of 56 adult river lampreys (*Lampetra fluviatilis*). The experimental procedures were approved by the local ethical committee (Stockholm's Norra Djurförsöksetiska Nämnd) and were in accordance with *The guide for the care and use of laboratory animals* (National Institutes of Health, 1996 revision). During the investigation, every effort was made to minimize animal suffering and to reduce the number of animals used.

### Anatomy

The animals were deeply anesthetized in tricaine methane sulfonate (MS-222; 100 mg/liter; Sigma, St. Louis, MO) diluted in fresh water. They were then transected caudally at the seventh gill, and the dorsal skin and cartilage were removed to expose the brain. During the dissection and the injections, the head was pinned down and submerged in ice-cooled oxygenated HEPES-buffered physiological solution (138 mM NaCl, 2.1 mM KCl, 1.8 mM CaCl<sub>2</sub>, 1.2 mM MgCl<sub>2</sub>, 4 mM glucose, and 2 mM HEPES), pH 7.4.

### Retrograde tracing

All injections were made with glass (borosilicate, OD = 1.5 mm, ID = 1.17 mm) micropipettes with a tip diameter of 10–20  $\mu$ m. The micropipettes were fixed in a holder, which was attached to an air supply and a Narishige micromanipulator.

### Single-tracing experiments

Neurobiotin (50–200 nL; Vector, Burlingame, CA; 20% in distilled water containing fast green to aid visualization

of the spread of the injection) was pressure injected unilaterally into 1) different parts of the caudal mesencephalon ( $n = 9$ ), 2) the striatum ( $n = 3$ ), 3) the optic tectum ( $n = 6$ ), 4) the middle rhombencephalic reticular nucleus (MRRN;  $n = 3$ ), and 5) the PPN ( $n = 4$ ).

#### **Double-tracing experiments**

Two different combinations of injections were performed: 1) injections into the mesencephalic locomotor region (MLR) and the optic tectum ( $n = 3$ ) and 2) diencephalic locomotor region (DLR) and MLR ( $n = 3$ ). In each case, Neurobiotin (see above) was injected into one of the locations and Alexa fluor 488-dextran 10-kD (12% in distilled water; Molecular Probes Europe BV, Leiden, The Netherlands) into the other.

#### **Dissection and histology**

After injections, the heads were kept submerged in physiological solution in the dark at 4°C for 24 hours to allow retrograde transport of the tracers. The brains were then dissected out of the surrounding tissue and fixed by immersion in 4% formalin and 14% saturated picric acid in 0.1 M phosphate buffer (PB), pH 7.4, for 12–24 hours, after which they were cryoprotected in 20% sucrose in PB for 3–12 hours. Transverse 20- $\mu$ m-thick sections were made using a cryostat, collected on gelatin-coated slides, and stored at –20°C until further processing. For GABA immunohistochemistry, animals were perfused through the ascending aorta with 4% formalin, 2% glutaraldehyde, and 14% of a saturated solution of picric acid in 0.1 M PB. The brain was postfixed for 24–48 hours and cryoprotected as described above.

#### **Immunohistochemistry**

##### **Single labeling**

For immunohistochemical detection of substance P in the striatum, tyrosine hydroxylase (TH) in the nucleus tuberculi posterior, and choline acetyltransferase (ChAT) in the PPN, brains were injected and processed as described above. All primary and secondary antibodies were diluted in 1% bovine serum albumin (BSA), 0.3% Triton X-100 in 0.1 M PB. Sections were incubated overnight with rabbit polyclonal antisubstance P antisera (1:4,000; a kind gift from Prof. Lars T  renius, Stockholm, Sweden; Christensson-Nylander et al., 1986), monoclonal mouse anti-TH antibody (1:600; MAB318; Millipore, Bedford, MA) raised against TH isolated from PC12 cells, or goat polyclonal anti-ChAT (1:300; AB144P; Millipore) raised against ChAT isolated from human placenta. Sections were subsequently incubated with a mixture of Neurotrace (1:500; Molecular Probes), Cy-conjugated streptavidin (1:1,000; Jackson ImmunoResearch, West Grove, PA), and Cy-conjugated donkey anti-rabbit IgG, anti-mouse

IgG or anti-goat IgG (1:500; Jackson ImmunoResearch) for 2 hours and mounted with glycerol containing 2.5% diazabicyclanoctane (Sigma-Aldrich, St. Louis, MO).

For the immunohistochemical detection of parvalbumin and GABAergic neurons in the caudal mesencephalon, brains were dissected out and processed as described above. Sections were then incubated overnight with either a rabbit polyclonal antiparvalbumin antiserum (1:1,000; SWant, Belinzona, Switzerland; PV-28, 5.5) raised against parvalbumin isolated from rat muscle or with a mouse monoclonal anti-GABA antibody (1:1,000; mAb 3A12; kindly donated by Dr. Peter Streit, Zurich, Switzerland; Matute and Streit, 1986; Robertson et al., 2007a) raised against GABA conjugated to BSA with glutaraldehyde. Sections were subsequently incubated with Cy3-conjugated donkey anti-rabbit IgG (parvalbumin) or donkey anti-mouse IgG (GABA; 1:500; Jackson ImmunoResearch) for 2 hours and mounted.

##### **Double labeling**

For the immunohistochemical detection of substance P and enkephalin fibers in the caudal mesencephalon, injections were made into the optic tectum and processed as described above. Sections were then incubated with both a mouse monoclonal antienkephalin antibody (1:200; MAB350; Millipore) raised against Leu-enkephalin conjugated to BSA and a polyclonal guinea pig antisubstance P antiserum (1:200; T-5019, mAb 356; Peninsula Laboratories, San Carlos, CA) raised against synthetic substance-P conjugated to BSA. Sections were subsequently incubated with Cy3-conjugated donkey anti-guinea pig IgG, Cy5-conjugated donkey anti-mouse IgG (1:500; Jackson ImmunoResearch), and Cy2-conjugated streptavidin (1:1,000; Jackson ImmunoResearch) for 2 hours and coverslipped.

#### **Antibody specificity**

##### **GABA**

The antibody, mAb 3A12, was developed following immunization with GABA conjugated to BSA with glutaraldehyde (GABA-G-BSA). This clone was shown by enzyme-linked immunosorbent assay (ELISA) to bind strongly to GABA-G-BSA. Immunoreactivity of the same clone to  $\beta$ -alanine-G-BSA was 4,000 times less and even lower for glycine-, aspartate-, glutamine-, and taurine-G-BSA. Preabsorption with GABA-G-BSA completely abolished the immunohistochemical staining of rat brain sections. Double-labeling experiments with the mAb 3A12 and a commercially available rabbit anti-GABA antibody (1:100; catalog No. AB131; Chemicon, Temecula, CA) showed immunoreactivity in the same cells in the lamprey brain, and the pattern of labeling that this antibody produces in lamprey brain is similar to that previously described for

many other vertebrates (Robertson et al., 2007a). The antiserum was tested for specificity using the free-floating PAP technique on rat and human cerebellum. The immunostaining was completely abolished by preincubation of the antibody with 10–100 g of GABA-G-BSA per milliliter of diluted antibody. No immunoreactivity was detected when the primary antibody was omitted from the immunohistochemical processing.

### **Enkephalin**

This antibody has shown cross-reactivity to both Met- and Leu-enkephalin, but it does not react with similar peptides ( $\beta$ -endorphin, dynorphin) in a radioimmunoassay (Cuello et al., 1984). In addition, this antibody generates a pattern of labeling in lamprey similar to that in rats, with densely labeled fibers in areas such as the dorsal pallidum and striatum (Cuello et al., 1984; Pombal et al., 1997b; Stephenson-Jones et al., 2011).

### **Substance P**

Both antisera have been shown not to cross-react with similar peptides (somatostatin, eledoisin,  $\beta$ -endorphin, Met or Leu enkephalin) in a radioimmunoassay (Christensson-Nylander et al., 1986; Peninsula Laboratories; product information). In addition, the pattern of labeling that both antisera produce in lamprey brain is similar to that previously described for other antibodies that label substance P in lamprey and other vertebrates, such as labeled neurons in the striatum and fibers throughout the pallidum (Auclair et al., 2004; Jessell et al., 1978; Pombal et al., 1997a). Substance P-specific immunolabeling with the guinea pig antisera (Peninsula Laboratories) in rat brain was completely abolished by preabsorption with the synthetic substance P peptide (Yasuhara et al., 2008).

### **Parvalbumin**

This antiserum does not stain any structures in the brain of parvalbumin knockout mice, nor does it recognize a protein band in Western blot analysis (SWant product information; Caillard et al., 2000). In addition this antiserum produces a pattern of labeling in the lamprey striatum and pallidum similar to that in the rat brain (Canudas et al., 2005; Martin-Ibanez et al., 2010; Stephenson-Jones et al., 2011). Finally, Western blot analysis of mouse cerebellar samples revealed that this antibody recognized a single protein band of approximately 14 kDa (Caillard et al., 2000).

### **ChAT**

The specificity of the antiserum used in this study has previously been tested by Western blot analysis of brain protein extracts of rat, dogfish, sturgeon, and trout (Anadón et al., 2000) and on mouse brain lysate, in which

it recognizes a 68-kDa protein band (Millipore; supplier's information). In addition, this antibody labels cells that are known to be cholinergic, such as the motor neurons in the lamprey spinal cord (Pombal et al., 2001).

### **TH**

This antibody was shown by the supplier to recognize a protein of approximately 59–61 kDa by Western blot but does not cross-react with other similar proteins in Western blot analysis (dopamine- $\beta$ -hydroxylase, phenylalanine hydroxylase, tryptophan hydroxylase, dehydropyridine reductase). This antibody also recognized only a protein of between 59 and 61 kDa in a Western blot analysis of lamprey tissue (data not shown). In addition, this antibody recognizes cells in the nucleus tuberculi posterior, which have previously been shown to be immunoreactive for dopamine in the lamprey brain (Abalo et al., 2005). In addition, no immunoreactivity was detected when the primary antibody was omitted from the immunohistochemical processing.

### **Analysis**

Photomicrographs of key results were taken with a Zeiss Axiocam (Carl Zeiss AB, Stockholm, Sweden) or an Olympus XM10 (Olympus Sverige AB, Stockholm, Sweden) digital camera. Illustrations were prepared in Adobe Illustrator and Adobe Photoshop CS2. Images were adjusted only for brightness and contrast. Confocal z-stacks of the sections were obtained using a Zeiss laser scanning microscope 510, and the projection images were processed in the Zeiss LSM software and Adobe Photoshop CS2.

### **Electrophysiology**

#### ***Tracing prior to slice preparation for electrophysiology***

When tracer injections were combined with electrophysiological recordings, the brain was accessed by opening the skull from the level of the olfactory bulb, caudally until the obex. Throughout this procedure, the bath was perfused with HEPES solution containing MS-222 (100 mg/liter). The fluorescent tracer Alexa fluor 488 coupled to 10-kDa dextran (12% in distilled water; Molecular Probes) was injected as described above into the optic tectum or caudal mesencephalon. Animals survived and were placed back in the aquarium for 12–18 hours following injections.

#### ***In vitro slice preparation***

Animals were deeply anesthetized as described above, and the exposed brain was removed and placed in ice-cold artificial cerebrospinal fluid (aCSF; extracellular fluid) of the following composition (in mM): NaCl 125, KCl 2.5,

NaH<sub>2</sub>PO<sub>4</sub>·H<sub>2</sub>O 1.25, MgCl<sub>2</sub> 1, glucose 20, CaCl<sub>2</sub> 2, and NaHCO<sub>3</sub> 25. Coronal slices (300–400  $\mu$ m) containing the caudal mesencephalon were sectioned using a tissue chopper (Vibratome 800 tissue chopper; Leica Microsystems AB, Stockholm, Sweden). The slices were continuously perfused during the experiments and oxygenated with 95% O<sub>2</sub> and 5% CO<sub>2</sub> (pH 7.4). The method has been described in detail by Ericsson et al. (2007).

## Recordings

The slices were placed in a recording chamber and continuously perfused with aCSF and kept at 6–8°C with a Peltier cooling system. The neurons were visualized with DIC/infrared optics (Zeiss Axioskop 2FS plus [Zeiss, München, Germany] or an Olympus BX51WI [Olympus, Tokyo, Japan]). Retrogradely labeled cells were illuminated with a mercury lamp (Zeiss HBO 100 or Olympus U-RFL-T) for a brief period to avoid bleaching and visualized in the microscope by using a fluorescent filter cube. Labeled neurons were photographed before switching back to DIC/infrared for patching of identified labeled neurons.

Patch-clamp recordings were made using loose-patch, cell-attached, or whole-cell configuration with patch pipettes made from borosilicate glass microcapillaries (Harvard Apparatus, Kent, United Kingdom) with a three-stage puller (model P-97; Sutter Instruments, Novato, CA). For loose-patch and cell-attached recordings, pipettes (5–10 M $\Omega$ ) were filled with aCSF or intracellular solution of the following composition (in mM): MgCl<sub>2</sub> 1.2, glucose 10, HEPES 10, CaCl<sub>2</sub> 1, C<sub>6</sub>H<sub>11</sub>O<sub>7</sub>K 102, EGTA 10, ATP 3.944, GTP 0.3 (osmolality 265–275 mOsm). Whole-cell recordings were performed with pipettes (7–12 M $\Omega$ ) filled with intracellular solution. Bridge balance and pipette capacitance compensation were adjusted on the amplifier, and all membrane potential values were corrected for the liquid junction potential. Cells recorded in the whole-cell configuration were included if the resting membrane potential was below –50 mV, with action potentials reaching above 0 mV. Pharmacological agents were bath applied through the perfusion system. Glutamate receptors were blocked by AP-5 (50–200  $\mu$ M; Tocris, Ellisville, MO) and CNQX (40  $\mu$ M; Tocris). GABA<sub>A</sub> receptors were blocked by picrotoxin (Tocris) that was first dissolved to 50 mM in 99% ethanol and stored before being diluted 1:1,000 to a final concentration of 50  $\mu$ M in fresh aCSF during experiments. The GABA<sub>A</sub> receptor agonist muscimol (5  $\mu$ M; Tocris) was used to assess its effect on spontaneous activity.

Data were collected using either a MultiClamp 700B and Digidata 1322 (Molecular Devices, Sunnyvale, CA) or an Axoclamp 2B (Molecular Devices) and ITC-18 (HEKA, Lambrecht, Germany). Data analyses were performed

with Axograph X (version 1.3.1; Axograph, Sydney, Australia) or Igor (version 6.03; WaveMetrics, Portland, OR).

## Statistical analysis and data presentation

Statistical analysis of the data was performed in Matlab (The MathWorks) using a two-sample *t*-test; the significance threshold (*P*) was <0.05. Box plots were used for graphic presentation, with the central line representing the mean; interquartile range is marked by the box and overall distribution by the whiskers, excluding outliers. Sample statistics are expressed as mean  $\pm$  standard deviation.

## RESULTS

### Anatomical evidence for a homolog of the SNr in lamprey

As a first step in elucidating whether there are dual-output pathways in the lamprey basal ganglia, we explored whether an area in the caudal mesencephalon (Fig. 1A), which contains neurons that project to the optic tectum (Robertson et al., 2006), might represent a lamprey homolog of the mammalian SNr. In other species, the SNr neurons projecting to the optic tectum are GABAergic, express the calcium-binding protein parvalbumin, and receive input predominantly from substance P-expressing striatal medium spiny neurons (Reiner et al., 1998).

Injections of the bidirectional tracer neurobiotin into this putative SNr region (Fig. 1B; *n* = 6) resulted in retrogradely labeled neurons in the striatum. These neurons were located in the rostral striatum both within and ventral to the neuronally dense striatal band (Fig. 1C). The complementary experiment with neurobiotin injected into the striatum labeled striatal efferents in the putative SNr (pSNr; Fig. 1D; *n* = 3). These fibers were small, with varicosities, characteristic of fibers with synaptic contacts. None of these striatal fibers were observed passing dorsally into the optic tectum or caudally into the rhombencephalon, suggesting that they might terminate in this region. Cells in this area expressed GABA and the calcium-binding protein parvalbumin (Fig. 1E,H; *n* = 3). In addition, combined retrograde labeling and immunostaining revealed that projection neurons from this region, which were retrogradely labeled from the optic tectum, expressed GABA (Fig. 1E–G; *n* = 3). Processes containing substance P were also observed just ventral to the optic tectum in the putative SNr region (Fig. 1I; *n* = 3). Together these findings show that this region receives striatal input and contains GABAergic projection neurons as well as fibers and neurons immunoreactive for substance P and parvalbumin. We conclude that this area receives



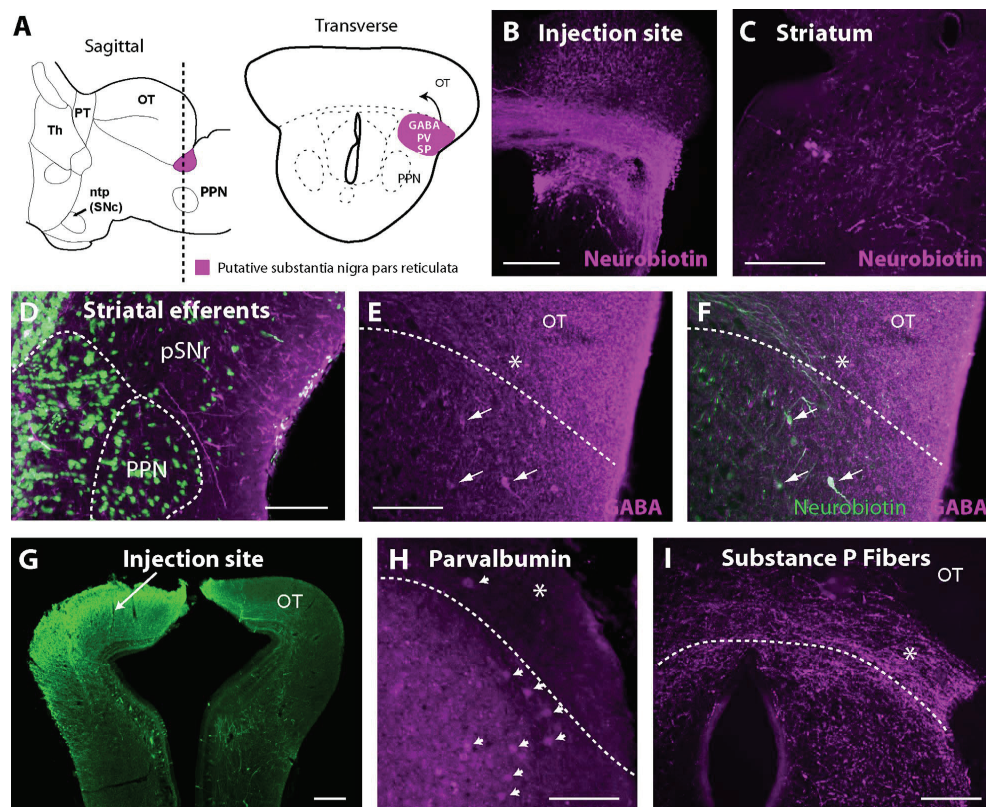


**Figure 1.** Anatomical evidence for a lamprey homolog of the substantia nigra pars reticulata. **A:** Schematic drawings of sagittal and transverse sections through the lamprey brain, indicating the location of the putative SNr. **B,C:** Neurobiotin injection (magenta) into the putative SNr region (**B**), resulting in retrogradely labeled striatal cells (**C**). **D:** Labeled efferent fibers in the putative SNr region following an injection of Neurobiotin into the striatum with a green Nissl stain. **E–G:** GABAergic retrogradely labeled cells in the putative SNr, following injections in the optic tectum (**G**). **H:** Parvalbumin-immunoreactive cells in the putative SNr region. **I:** Substance P-immunoreactive fibers in the putative SNr region. Scale bars = 200  $\mu$ m.

projections from striatum and expresses the same molecular markers as the mammalian SNr.

### Electrophysiological evidence for a homolog of the SNr in lamprey

In mammalian species, the SNr projection neurons have been shown to inhibit motor areas tonically as a result of their high level of spontaneous activity (Hikosaka et al., 2000). If these putative lamprey SNr neurons have a similar physiological role, they should also be tonically active at rest. Loose-patch recordings revealed that 53% (16/30) of the neurons within this area were spontaneously active. These neurons fired with instantaneous fir-

ing frequencies ranging between 0.6 and 3.6 Hz, with a mean frequency around 1.5 Hz (Fig. 2; bath temperature 6–8°C). To determine whether these tonically active neurons were projection neurons, we recorded from pSNr neurons that were retrogradely labeled from the optic tectum (Fig. 2A–C;  $n = 18$ ). Approximately 44% of these retrogradely labeled neurons were tonically active (eight of 18), suggesting that the SNr might tonically inhibit areas of the brain to which it projects. To determine whether this tonic activity resulted from intrinsic conductances, as it does in mammals, we investigated whether blocking glutamatergic synaptic input altered the activity. Indeed, the spontaneous activity was not significantly altered by blocking the glutamatergic synaptic input with

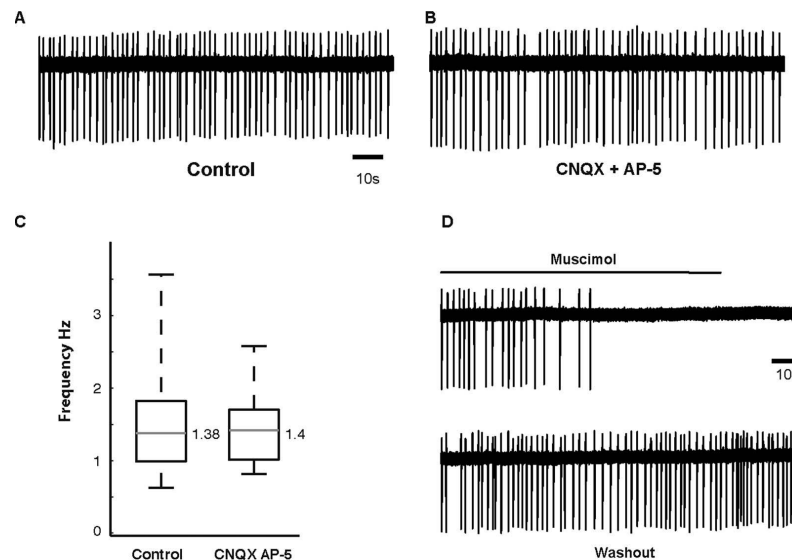


**Figure 2.** Electrophysiological evidence for a lamprey homolog of the substantia nigra pars reticulata. **A,B:** Loose-patch recording of a spontaneous repetitively firing retrogradely labeled neuron (from the tectum) before (mean frequency  $5.10 \pm 1.01$  Hz) and after (mean frequency  $4.31 \pm 1.41$  Hz) the application of the glutamatergic antagonists CNQX (40 mM) and AP-5 (40 mM). **C:** Box plots showing the normalized range and average instantaneous frequency of SNr neurons before and after application of glutamatergic receptor antagonists (control, mean =  $1.5 \pm 0.86$  Hz; CNQX and AP-5, mean =  $1.37 \pm 1.01$  Hz). **D:** Loose-patch recording of an SNr neuron before, during, and after the application of muscimol.

CNQX 40 mM and AP-5 50–200 mM (Fig. 2B,C;  $n = 6$ ). The tonic activity does not depend on glutamatergic input and thus appears to be an inherent property. This suggests that these pSNr neurons could inhibit motor regions in the absence of synaptic input. Application of muscimol 5 mM, a GABA<sub>A</sub> agonist, blocked all spontaneous activity (Fig. 1D;  $n = 6$ ). This suggests that GABAergic input from the striatum could potentially silence these neurons and thereby disinhibit the motor areas.

### Anatomical and electrophysiological characterization of the striatonigral projection

The lamprey striatum, as with all other vertebrates, contains at least two separate populations of striatal projection neurons, one expressing substance P and another expressing enkephalin (Stephenson-Jones et al., 2011). In other vertebrates, the striatal neurons projecting to the SNr express predominantly substance P and are associated with the “direct” pathway. In line with a homologous organization, immunohistochemistry revealed that the striatal neurons retrogradely labeled from the SNr in lamprey expressed substance P (Fig. 3A–D;  $n = 4$ ). These

neurons were located in the rostral striatum, in contrast to the enkephalin-expressing neurons that are located mainly in the caudal striatum (Stephenson-Jones et al., 2011). To test whether the substance P-immunoreactive fibers made putative contacts with the projection neurons, we retrogradely labeled pSNr neurons from the optic tectum ( $n = 4$ ). These projection neurons were surrounded by contacts that were immunoreactive for substance P (Fig. 3E,F;  $n = 9$ ), as with the direct (substance P–SNr–motor areas) pathway. Fibers immunoreactive for enkephalin were observed in this region, but few fibers were observed in close apposition to the retrogradely labeled projection neurons (Fig. 3E,F;  $n = 9$ ). Taken together with the retrograde labeling, this suggests that the pSNr receives input from substance P expressing striatal neurons associated with the direct pathway.

Patch-clamp recordings from striatal neurons in lamprey have shown that there are two main physiological types of neurons, inwardly rectifying neurons (IRNs) that display rectification at hyperpolarized potentials resulting from potassium channels of the Kir-type and those that do not (Ericsson et al., 2011). Inward rectification is a prominent feature of the striatal projection neurons in mammals and birds, the so-called medium spiny neurons

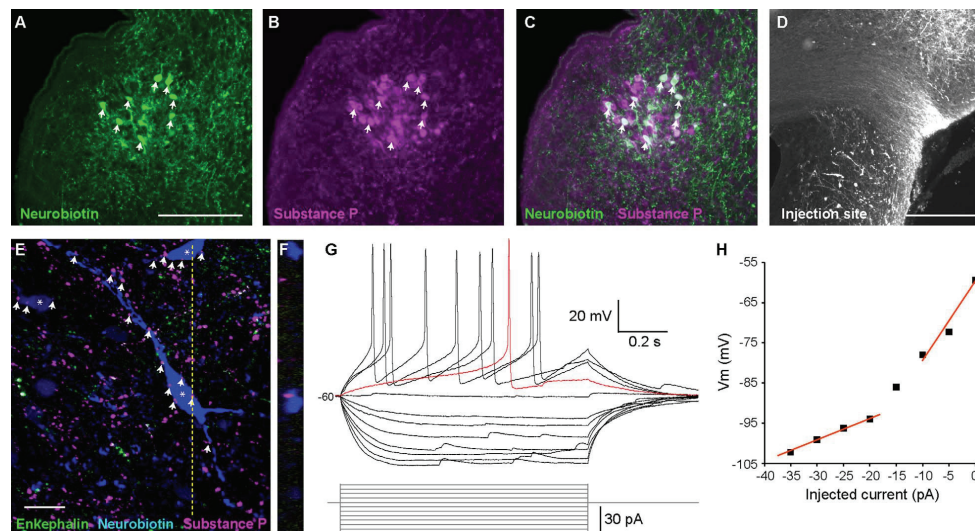


**Figure 3.** Anatomical and electrophysiological characterization of substantia nigra pars reticulata-projecting striatal neurons. **A:** Neurobiotin retrogradely labeled neurons in the striatum following an injection in the putative SNr. **B:** Substance P-immunoreactive cells in the striatum. **C:** Merged image including a blue Nissl stain. **D:** Site of Neurobiotin injection in the putative SNr. **E,F:** Confocal projection of an SNr neuron retrogradely labeled (blue) from an injection (Neurobiotin) in the optic tectum with substance P (magenta)- and enkephalin (green)-immunoreactive fibers. The yellow dotted line indicates the plane in which the z-y axis of the confocal projection is shown. **G:** Whole-cell current-clamp recording of a retrogradely labeled SNr-projecting neuron with its voltage responses to 12 consecutive current injections. Inward rectification is seen at hyperpolarized potentials as small-voltage responses for each current injection compared with larger deflections around zero and positive current injections. **H:** I-V plot of the steady-state voltage deflections to current steps of the neuron displayed in G. Note the steeper slope at more depolarized potentials. Scale bars = 200  $\mu$ m in A,D; 20  $\mu$ m in E.

(Farries et al., 2005; Planert et al., 2010). Consequently, those neurons that display this feature were suggested to represent the projection neurons in lamprey (Ericsson et al., 2011). To determine whether the SNr-projecting striatal neurons were indeed inwardly rectifying, we recorded from striatal neurons retrogradely labeled from the putative SNr. Similar to rodent MSNs and lamprey IRNs, all projection neurons had a long delay to first action potential, and eight of nine neurons displayed inward rectification (Fig. 3G). The rectification is seen clearly by visual inspection of voltage responses to current injections (Fig. 3H) and was quantified by comparing the input resistance at hyperpolarized potentials at which Kir channels are open to more depolarized values at which they are closed. The rectification ratio was  $0.42 \pm 0.08$  for these eight cells, indicating clear rectification and that their input resistance at hyperpolarized states was less than half of that at depolarized potentials. The one neuron that did not show rectification had a ratio of 0.82, similar to previously categorized non-IRNs with a ratio of  $0.75 \pm 0.17$ .

Overall, this area, ventral to the optic tectum in the caudal mesencephalon, appears to be homologous to the avian and mammalian SNr based on the input from the striatum, the presence of substance P fibers that contact the GABAergic projection neurons, the expression of parvalbumin, the electrophysiological properties of SNr projection neurons, and the electrophysiological properties of the striatal neurons that innervate the SNr (see also Discussion). We will therefore refer to this area as the *lamprey homolog of the SNr* and the neurons located within this area as *SNr neurons* for the remainder of this article.

### Connectivity of the SNr

The SNr, in other species, tonically inhibits a number of motor areas in the brainstem or cortex, via the thalamus. To investigate which regions the lamprey SNr might tonically inhibit and to determine what might influence the activity of these neurons, we investigated the connectivity of this region. Neurobiotin was injected into the caudo-ventral mesencephalon (Fig. 4A,H;  $n = 6$ ). This resulted in

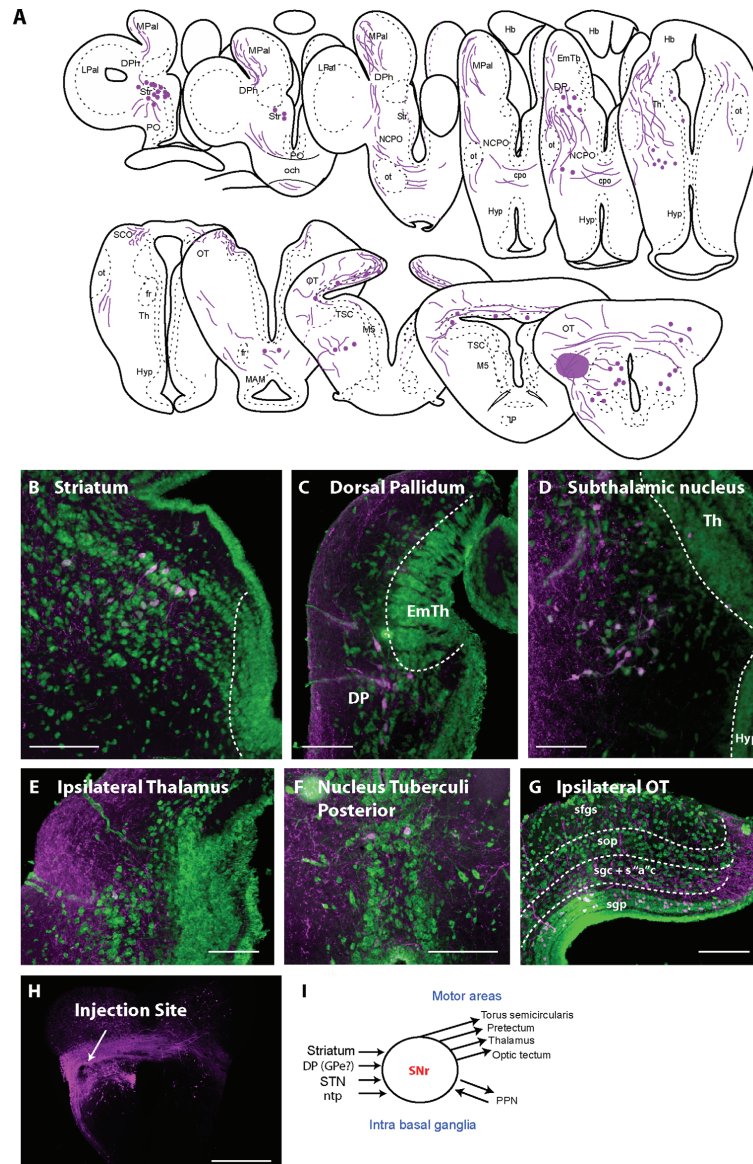


**Figure 4.** Connectivity of the substantia nigra pars reticulata. **A:** Schematic transverse sections through the lamprey brain showing the location of retrogradely labeled cells (magenta dots) and labeled fibers (magenta lines) from an injection (Neurobiotin) in the SNr region. Injections resulted in retrogradely labeled neurons in the striatum (**B**) and dorsal pallidum (**C**) and retrograde and anterograde labeling in the subthalamic region (**D**) and the thalamus (**E**). **F:** Retrogradely labeled neurons and labeled fibers in the nucleus tuberculi posterior (SNc). **G:** Retrogradely labeled neurons and fibers in the optic tectum. **H:** Site of injection in the SNr and location of retrogradely labeled cells in the lateral mesencephalon the contralateral optic tectum and the isthmus nucleus. **I:** Schematic representation of the connectivity of the SNr. All sections are counterstained with green fluorescent Nissl stain. Scale bars = 200  $\mu$ m in B–G; 100  $\mu$ m in H. The following abbreviations are used: cpo - Postoptic commissure; DP - dorsal pallidum; DPh - habenula-projecting dorsal pallidum; EmTh - eminentia thalami; fr - fasciculus retroflexus; Hb - habenula; Hyp - hypothalamus; LPal - lateral pallidum; MAM - mammillary area; MPal - medial pallidum; M5 - Mesencephalic M5 nucleus of Schober; NCPO - Nucleus of the postoptic commissure; Och - optic chiasma; ot - optic tract; OT - optic tectum; s'a'c - Stratum 'album' centrale; sfgs - Stratum fibrosum et griseum superficiale; sgc - Stratum griseum centrale; sgp - Stratum griseum periventriculare; SNr - substantia nigra pars reticulata; sop - Stratum opticum; Th - Thalamus; TSC - Torus semicircularis.



retrogradely labeled cells in the striatum, ipsilaterally on the side of the injection (Fig. 4B; depicted as red dots in Fig. 4A). In the caudal telencephalon, cells were observed ipsilaterally in a region recently identified as the dorsal pallidum (DP), the lamprey homolog of the GPi/GPe (Stephenson-Jones et al., 2011; Fig. 4C). This projection is likely to arise from GPe-like neurons, because the GPe but not GPi projects to the SNr in other vertebrates (Reiner et al., 1998). Neurons in the STN were also retrogradely labeled (Fig. 4D), suggesting that neurons in the SNr may be influenced by direct striatal projections but also by indirect striatal projections via the GPe and STN. A few retrogradely labeled cells were observed in the nucleus tuberculi posterior, the lamprey homolog of the SNc (Fig. 4F). Cells were also observed bilaterally in the deeper layers of the optic tectum, with a predominance of ipsilateral cells labeled (Fig. 4G). In the mesencephalon, cells were observed ventral to the injection site, both unilaterally on the medial border adjacent to the ventricle and bilaterally in the ventrolateral mesencephalon (Fig. 4H). It should be noted that the pattern of tectal labeling could be reproduced from injections in the reticular formation ( $n = 6$ , data not shown), which is in accordance with previously published data (Zompa and Dubuc, 1998). These injections did not label cells in any of the other areas mentioned above, suggesting that the tectal cells might have been labeled from fibers that were passing this area as part of the tectoreticular pathway and that none of the other populations continued to project to the rhombencephalon.

Labeled fibers from the injections in the SNr (Fig. 4A) were observed in a fiber tract that surrounded the optic tract; these fibers crossed the midline rostrally at the level of the optic chiasm and more caudally at the level of the postoptic commissure. Fibers passed from this tract to bilaterally innervate the thalamus (Fig. 4A,E). Fiber labeling was also observed in the nucleus tuberculi posterior (Fig. 4A,F). More caudally, fibers were present bilaterally in the pretectum and in the entire rostrocaudal extent of the deeper and intermediate layers of the optic tectum (Fig. 4G). Finally, fibers were observed bilaterally ventrolateral to the injection site; fibers reached the contralateral side by crossing in the fiber tract that passed above the SNr and below the optic tectum (Fig. 4H). The major projections of these tonically active GABAergic pallidal neurons are therefore both to brainstem motor areas and other basal ganglia nuclei that might, through reciprocal connections, influence the level of activity in the SNr (Fig. 4I).

#### Separate, intermingled populations of neurons in the SNr project to the thalamus and brainstem motor areas

To determine whether separate populations of SNr neurons could independently regulate the motor regions,

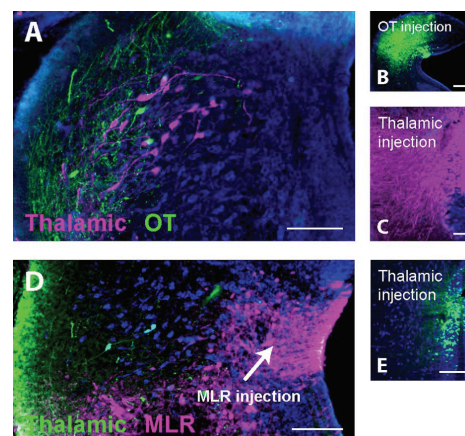


**Figure 5.** Separate pallidal subpopulations projecting to the optic tectum and thalamus are intermingled. **A:** Retrogradely (Alexa fluor 488-conjugated 10-kDa dextran) labeled neurons (green) from injections into the optic tectum (**B**) and retrogradely Neurobiotin-labeled neurons (magenta) from injections into the thalamus (**C**). **D:** Retrogradely (Alexa Fluor 488-conjugated 10 kDa dextran) labeled neurons (green) from injections into the thalamus (**E**) and retrogradely Neurobiotin-labeled neurons (magenta) from injections into the mesencephalic locomotor region (MLR; **D**). Scale bars = 200  $\mu$ m.

we explored whether the SNr populations projecting to these areas arose from distinct subpopulations. Injections in the optic tectum and thalamus but not the mesencephalic locomotor region (MLR) resulted in retrogradely labeled neurons in the SNr (Fig. 5A–E). In addition, no projections from the SNr region to the MLR were reported in a previous study on the connectivity of the MLR (Ménard et al., 2007). The retrogradely labeled neurons from the thalamus and optic tectum were all in the caudal mesencephalon just ventral to the optic tectum, the same area that receives the striatal efferents and contains the GABA- and parvalbumin-expressing neurons (see Fig. 1), supporting the evidence that the SNr projects to these motor areas. Dual injections into the thalamus and optic tectum never resulted in double-labeled SNr neurons, suggesting that the neuronal populations that project to the optic tectum were separate from those projecting to the thalamus (Fig. 5A–C;  $n = 3$  each). Although these populations are distinct, there did not appear to be a clear topographic arrangement between these separate populations; the SNr neurons in each case were intermingled. This suggests that multiple parallel pathways through the SNr could independently control each motor area.

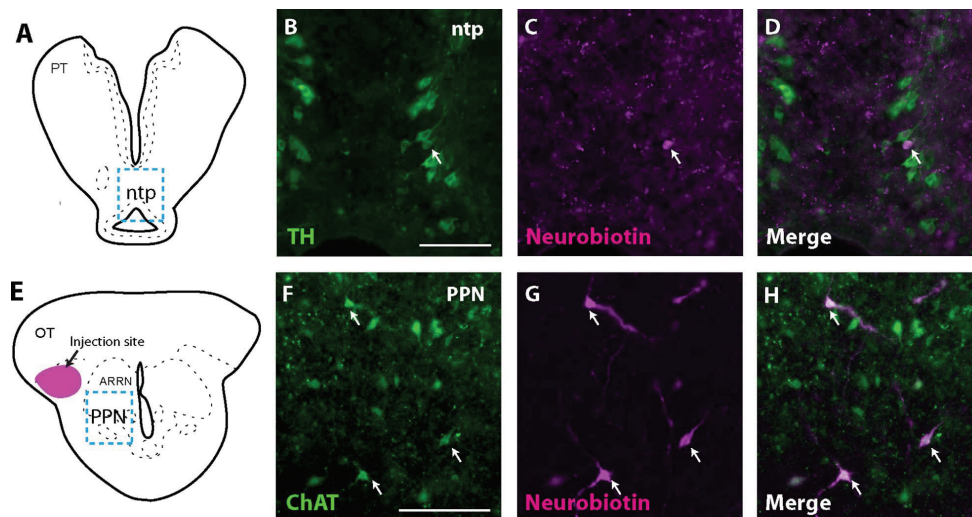


**Figure 6.** Tyrosine hydroxylase (TH)- and choline acetyltransferase (ChAT)-expressing neurons in the nucleus tuberculi posterior (ntp) and ventromedial mesencephalon project to the SNr. **A:** Schematic transverse section through the caudal diencephalon showing the location of the photomicrographs. **B:** TH immunostaining in the nucleus tuberculi posterior. **C:** Retrogradely labeled neurons from a Neurobiotin injection in the SNr. **D:** Merged image. **E:** Schematic transverse section through the mesencephalon showing the location of the injection site and the area represented in the photomicrographs. **F:** ChAT immunostaining in the putative pedunclopontine nucleus (PPN). **G:** Retrogradely labeled neurons from a Neurobiotin injection in the SNr. **H:** Merged image. Scale bars = 50  $\mu$ m in B (applies to B–D); 50  $\mu$ m in F (applies to F–H).

### Modulatory input to the SNr

To determine whether the projections from the nucleus tuberculi posterior and tegmentum might represent modulatory projections from the SNc and PPN, respectively, we combined retrograde labeling with immunohistochemistry. The retrogradely labeled neurons in the nucleus tuberculi posterior (SNc) expressed TH (Fig. 6A–D) and are therefore likely to be dopaminergic. This suggests that a connection between the SNc and the SNr is maintained despite the topographic distinction between these nuclei.

The population of neurons ventromedial to the SNr in the mesencephalon was immunoreactive for ChAT (Fig. 6E–H). In mammalian species, the SNr receives a cholinergic projection from the PPN, and, as with these cholinergic neurons in lamprey, this nucleus is located in the ventral tegmentum. The mammalian PPN also contains neurons with predominantly descending projections that have been physiologically considered to be part of the MLR (Ménard et al., 2007; Skinner and Garcia-Rill, 1984).

### Connectivity of the putative PPN

More recently, the mammalian PPN has also been suggested to form an extended part of the basal ganglia,

because it is reciprocally connected with almost all areas of the basal ganglia (Mena-Segovia et al., 2004). To examine whether the connectivity of these cholinergic neurons, in the ventral mesencephalon, is homologous to that in the PPN, we analyzed the afferent and efferent connections of this area. Injections of neurobiotin in the region of the putative PPN (Fig. 7A,I) resulted in retrogradely labeled neurons in two basal ganglia output nuclei, the habenula-projecting dorsal pallidum (DPh; Fig. 7A,B) and the DP (Fig. 7A,C), the lamprey homolog of the GPi/GPe (Stephenson-Jones et al., 2011). In the diencephalon, cells were retrogradely labeled in the STN, and a few cells were labeled in the periventricular hypothalamus (Fig. 7A,D). In the mesencephalon, cells were observed bilaterally in the deeper layers of the optic tectum, but, as with the SNr injections, these cells might have been labeled through fibers of passage as part of the tectoreticulospinal tract (Fig. 7F). More caudally, cells were observed in the contralateral SNr region (Fig. 7G) and in the contralateral PPN, and few cells were observed in the periventricular isthmus region (Fig. 7G).

Labeled fibers from the injections in the PPN (Fig. 7A) were also observed innervating a number of basal ganglia regions. As with the SNr injections, fibers from these

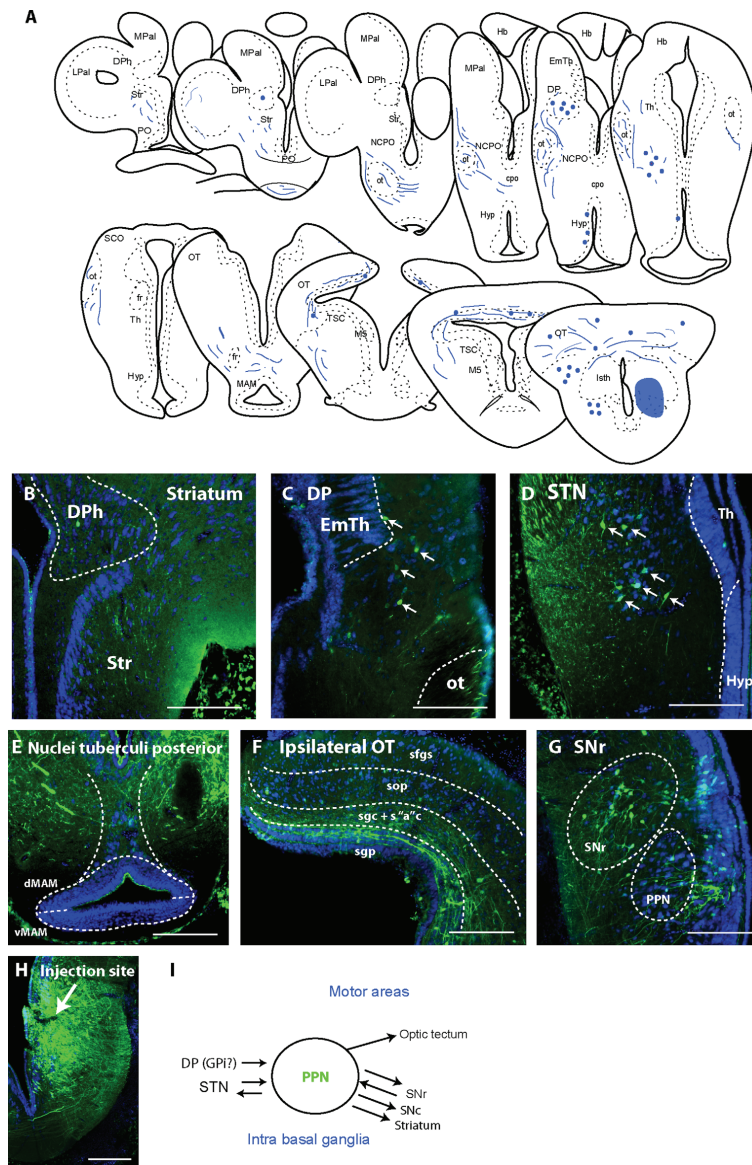


**Figure 7.** Connectivity of the pedunculopontine nucleus (PPN). **A:** Schematic transverse sections through the lamprey brain showing the location of retrogradely labeled cells (blue dots) and labeled fibers (blue lines) from an injection (Neurobiotin) in the PPN. **B:** Injections resulted in labeled fibers in the striatum and habenula-projecting pallidum (DPh) and retrogradely labeled neurons in the DPh. **C:** Retrogradely labeled cells in the dorsal pallidum (DP). **D:** Retrograde and anterograde labeling in the subthalamic region and the thalamus. **E:** Thin fibers labeled in the nucleus posterior tuberculi (SNc). **F:** Retrogradely labeled cells and fibers in the ipsilateral optic tectum. **G:** Labeled cells in the contralateral SNr and PPN region as well as in the periventricular isthmus region. **H:** Site of injection in the PPN. **I:** Schematic representation of the connectivity of the SNr. All sections are counterstained with green fluorescent Nissl stain. Scale bars = 200  $\mu$ m. The following abbreviations are used: cpo - Postoptic commissure; DP - dorsal pallidum; DPh - habenula-projecting dorsal pallidum; EmTh - eminentia thalami; fr - fasciculus retroflexus; Hb - habenula; Hyp - hypothalamus; LPal - lateral pallidum; MAM - mammillary area; MPal - medial pallidum; M5 - Mesencephalic 5 nucleus of Schober; NCPO - Nucleus of the postoptic commissure; Och - optic chiasma; ot - optic tract; OT - optic tectum; s'a'c - Stratum 'album' centrale; sfgs - Stratum fibrosum et griseum superficiale; sgc - Stratum griseum centrale; sgj - Stratum griseum periventriculare; SNr - substantia nigra pars reticulata; sop - Stratum opticum; Th - Thalamus; TSC - Torus semicircularis.



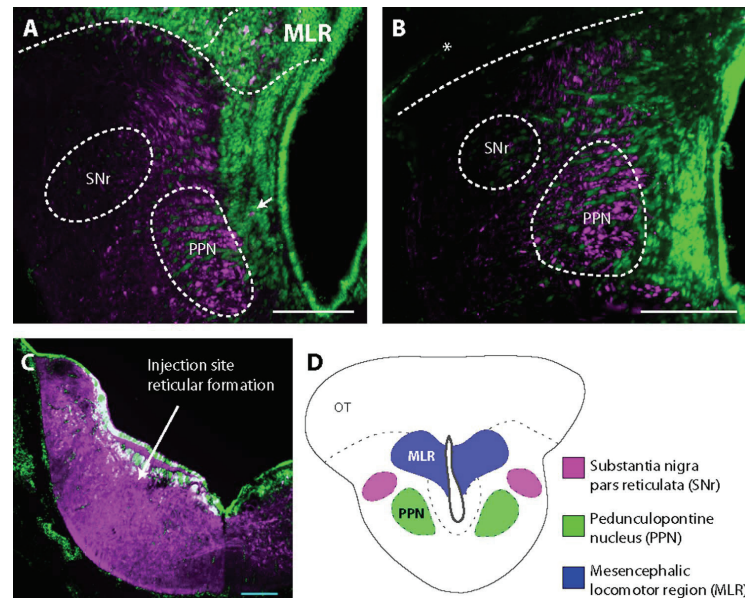


**Figure 8.** Location of the descending mesencephalic projections. **A:** Retrogradely labeled cells are observed in the isthmus nucleus, but only labeled fibers are observed passing through the PPN. **B:** Labeled fibers in the more caudal mesencephalon again showing that fibers but not cells are labeled in the region of the PPN. **C:** Location of Neurobiotin injection in the reticular formation. **D:** Schematic drawing of the caudal mesencephalon showing the location of the SNr, PPN, and cholinergic isthmus nucleus. Scale bars = 200  $\mu$ m.

injections were observed in a fiber tract that surrounded the optic tract (Fig. 7A). These fibers crossed the midline rostrally at the level of the optic chiasm and more caudally at the level of the postoptic commissure. Fibers passed from this tract and were observed in the striatum and more dorsally the DPh (Fig. 7B). A population of thin caliber fibers was observed in the STN (Fig. 7D) and the nucleus tuberculi posterior (Fig. 7E), the lamprey homolog of the SNc. More caudally, fibers were present bilaterally in the entire rostrocaudal extent of the deeper and intermediate layers of the optic tectum (Fig. 7F). The major projections of this area, as with the mammalian PPN, are therefore to basal ganglia nuclei and the optic tectum. This suggests that this nucleus may influence the activity of the basal ganglia nuclei and tectum in response to the level of basal ganglia activity as communicated through projections from the output nuclei (Fig. 7H).

As mentioned, the PPN has also been considered to be part of the MLR. To determine whether cells in this region contributed to the descending mesencephalic projections, we retrogradely labeled cells in the mesencephalon from injections in the middle rhombencephalic reticular nucleus (Fig. 8A–D). Retrogradely labeled cells were observed in the deeper layers of the optic tectum in ac-

cordance with the presence of a tectoreticulospinal projection (Zompa and Dubuc, 1998). In addition, a group of cells in the isthmus region, medial to the SNr, was also labeled (Fig. 8A); this cell group corresponds to the core of the MLR in lamprey (Ménard et al., 2007). Finally, a few retrogradely labeled neurons were located in the ventral portion of the isthmus region (Fig. 8A). In contrast, no cells were labeled within the area that we describe as the PPN (Fig. 8A,B). Despite this, large descending fibers were observed passing through the PPN (Fig. 8A,B). This suggests that the descending projections from mesencephalon arise from the MLR but not from the putative PPN.

## DISCUSSION

An understanding of whether dual-output pathways through the basal ganglia exist in all vertebrates is of fundamental importance for understanding the basic mode of operation for these nuclei (Fig. 9). Our results suggest that a nucleus homologous to the mammalian SNr, in addition to the recently described GPi homolog (Stephenson-Jones et al., 2011), exists in the lamprey, one of the phylogenetically oldest vertebrates. This suggests that the dual output pathways through the basal ganglia were

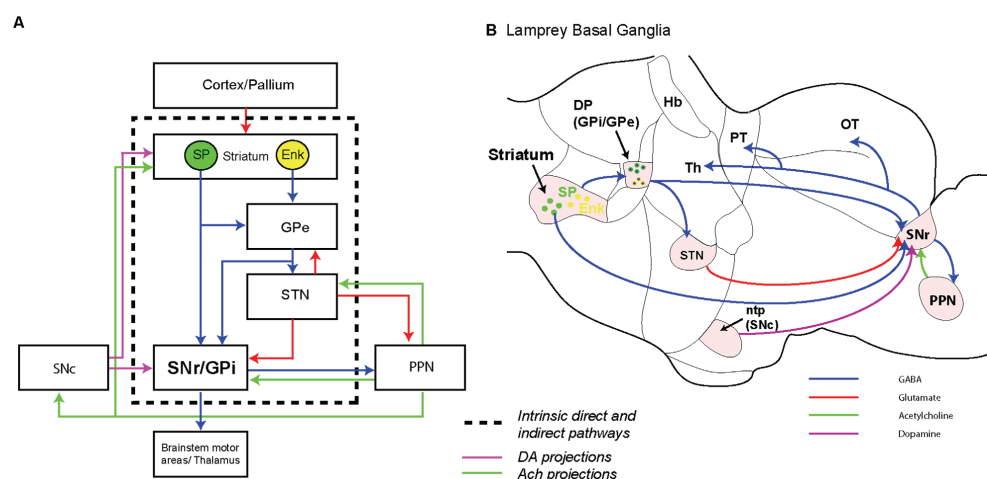


**Figure 9.** Summary of the organization of the substantia nigra pars reticulata and pedunculopontine nucleus in lamprey. **A:** Schematic showing the evolutionarily conserved architecture of the basal ganglia. Blue, red, green, and pink arrows indicate GABAergic, glutamatergic, cholinergic, and dopaminergic projections, respectively. **B:** Schematic sagittal section through the lamprey brain showing the location of the known basal ganglia nuclei and the connectivity of the SNr.

likely to have been present in the common ancestor of all vertebrates as fundamental components of evolutionary blueprint for the vertebrate basal ganglia.

### SNr evidence

The region that we describe here as a homolog of the mammalian SNr, has previously been considered to be part of the lateral isthmus nuclei. This conclusion was based on the fact that these cells projected to the optic tectum and were presumed to be cholinergic (De Arriba and Pombal, 2007; Pombal et al., 2001). We now show that these cells are GABAergic and that the cholinergic cells are located more ventromedially, as part of a potential pedunculopontine nucleus. In addition to the presence of GABAergic projection neurons, the connectivity, molecular, and physiological data that we provide here suggest that the region we describe as the SNr is an output nucleus of the basal ganglia. This conclusion is also supported by the fact that the topographic location of this nucleus is similar to that of the SNr of other vertebrates, ventrolateral to the optic tectum (Smeets et al., 2000). However, unlike the case in mammalian species (Reiner et al., 1998; Smeets, 1991), the midbrain dopaminergic neurons in lamprey are not located in apposition to the homolog of the SNr; rather, they are identified more rostrally in the nucleus tuberculi posterior (Pombal et al., 1997a). A topographic distinction between the two com-

ponents of the substantia nigra has also been observed in lizards and turtles, in which the dopaminergic neurons are located medially to the SNr (Smeets, 1991), and in birds, in which the GABAergic substantia nigra lateralis is distinct from the striatally projecting substantia nigra (Kitt and Brauth, 1986; Veenman and Reiner, 1994). For amphibians, this topographic distinction has been attributed to a lesser degree of migration of the two components of the substantia nigra, both of which develop in different regions of the brain, the SNc in the basal plate and the SNr in the alar plate (Smeets et al., 2000). The even greater topographic distinction that we observe between the lamprey dopaminergic neurons (SNc/VTA) and SNr might result from even less migration of the cell population from their developmental location. Despite this difference, our data suggest that the substantia nigra had already evolved before jawed and jawless vertebrates diverged over 560 million years ago.

Our data indicate that the lamprey SNr homolog, as with the dorsal pallidum (GPi/GPe), is influenced by both direct and indirect striatal projections. The direct projections, as with mammalian, avian, and reptilian species, arise from predominantly substance P-expressing striatal neurons, which appear to make direct contacts with the SNr projection neurons (for references see Reiner et al., 1998). In addition, striatal neurons retrogradely labeled from the SNr were immunoreactive for substance P. Taken together, these findings suggest that the direct

(striatum [substance P]–SNr–motor areas) pathway exists in the lamprey, as with all other vertebrates studied (Reiner et al., 1998). The lamprey striatonigral neurons show pronounced inward rectification and a hyperpolarized resting potential, so they may serve a function similar to that of rodent MSNs and be activated only upon strong, focused excitatory input from the pallium or thalamus. In mammalian, avian, and reptilian species, the SNr also receives enkephalin-immunoreactive projections that appear to make direct contacts with the projection neurons (Inagaki and Parent, 1984; Medina et al., 1995; Reiner and Anderson, 1990). Whether this is also the case in the lamprey is unclear, because fibers that express enkephalin were observed in the SNr, but these fibers were rarely seen in close apposition to projection neurons. Our data indicate that, in addition to the direct striatonigral pathway, the striatum might also influence the activity of the SNr indirectly via projections from the lamprey homolog of the STN and the DP (Stephenson-Jones et al., 2011). The STN receives projections from the GPe-like neurons in lamprey, suggesting that the indirect (striatum–[enkephalin]–GPe–STN–SNr) pathway may also be conserved. In mammals, neurons in the GPe also project straight to the SNr. For avian species, in which the GPe and GPI are also intermingled in the DP, experiments have demonstrated that it is the GPe-like neurons that give rise to this projection (for references see Reiner et al., 1998). The presence of dorsal pallidal projections to the SNr in lamprey therefore suggests that this second indirect pathway might also exist in an amniote species; however, further experiments are required to determine whether this projection arises from “GPe-like” neurons. This organization of dual output pathways is present in amniotes and the phylogenetically oldest vertebrates, so it is likely to be conserved throughout phylogeny as a common organization in all vertebrates including fish and amphibians and form an additional component of the blueprint for the basal ganglia.

After the identification of the GPI, this nucleus was thought to be responsible for the tonic inhibition of the motor regions that is observed in the lamprey (Ménard et al., 2007; Ménard and Grillner, 2008; Robertson et al., 2007b). The description of the additional basal ganglia output nucleus that we present here, which also has spontaneously active GABAergic projection neurons, provides an additional source for this physiological function and raises the question of the role of each of these nuclei. In lamprey, as in mammals, both the SNr and the GPI (entopeduncular nucleus) project to brainstem structures as well as to the thalamus, which in turn relays information to the cortex/pallium (Kelly and Strick, 2004). In mammals, subcompartments in SNr target different brainstem motor centers for posture, locomotion, and

eye movements, and, in the lamprey SNr, different populations target tectum and thalamus. Separate neuronal populations in the dorsal pallidum (GPI) target tectum and mesencephalic and diencephalic locomotor centers (Stephenson-Jones et al., 2011; Takakusaki et al., 2003). In primates, the relative proportion of projections to thalamus/cortex may be larger from GPI than from SNr. The two output systems therefore appear, at least partially, to act in parallel in both lamprey and mammals. It is as yet unclear why this is so. It could be that the two systems are recruited preferentially under different behavioral conditions (e.g., foraging, defense, or emotional contexts). It is important to note, however, that a large part of the standard motor repertoire of mammals and other vertebrates is mediated directly from brainstem centers. Mammals (rodents, cats, rabbits) that have had their neocortex surgically removed (see, e.g., Bjursten et al., 1976) but have the basal ganglia intact perform well-coordinated goal-directed movements that are well adapted to the environment. Clearly, these movements are controlled via the basal ganglia output nuclei SNr/GPI and the different brainstem motor centers that they regulate. This will allow the animal to explore the environment, search for food, eat, and perform other goal-directed behaviors. The control mediated via cortex/pallium may be used for more complex or demanding tasks. The relative role of SNr and GPI will have to await experiments in which the effects of the two structures can be affected selectively.

### PPN evidence

In addition to the identification of SNr, this study suggests that the PPN is present in the lamprey. In rodents, PPN appears to be subdivided into two parts that are intermingled, but the extent to which the ascending and descending components of the PPN can be separated is unclear; thus they may have arisen from separate populations. Mena-Segovia and colleagues (2004) have suggested that, in addition to its proposed role in the initiation of locomotion, the PPN should be considered as an extended part of the basal ganglia, because it is most highly interconnected with these nuclei. The PPN has been implicated in a number of functions attributed to the basal ganglia (Mena-Segovia et al., 2004). Lesions of the PPN lead to deficits in the initiation and termination of actions; rats with lesions tend to persevere with an action even after cued to stop (Florio et al., 1999). These experiments and others (for references see Winn, 2006) suggest that, as with the basal ganglia, the PPN is involved in action selection and procedural learning. In rats, cats, primates, and humans, neurons in the PPN also send descending projections to the brainstem (Mena-Segovia et al., 2008; Mitani et al., 1988; Muthusamy

et al., 2007; Ros et al., 2010). In lamprey, such descending projections were not observed from the region that we describe as the homolog of the PPN, but a projection to the reticular formation did originate from a region known as the isthmus cholinergic cell group. One explanation for the lack of descending projections from the PPN in lamprey may be that neurons in these two distinct nuclei are actually intermingled in the other species investigated. This possibility is supported by the fact that the PPN in other species is known to be a heterogeneous structure both in its function and in its anatomical composition (Mena-Segovia et al., 2004). Some neurons have exclusively descending axons (Ros et al., 2010), but other descending projections arise from collaterals of the ascending axons (Mena-Segovia et al., 2008). Connections between the PPN and the basal ganglia are prominent in the phylogenetically oldest group of vertebrates and are conserved in mammals, birds, and amphibians (Marin et al., 1999; Medina and Reiner, 1997), which supports the hypothesis that the basal ganglia and PPN are functionally and anatomically related. Insofar as the PPN and the basal ganglia nuclei both appear to be present in lamprey, our results suggest that these nuclei might have coevolved to fulfill common behavioral functions such as action selection and procedural learning.

## CONCLUSIONS

Our results demonstrate that, in addition to direct and indirect pathways through the GPI and GPe (Stephenson-Jones et al., 2011), an output nucleus homologous to the SNr is present in the phylogenetically oldest group of vertebrates, cyclostomes. This suggests that dual-output pathways were part of the blueprint for the vertebrate basal ganglia. In addition, a homolog of the PPN is present in lamprey. This nucleus is heavily interconnected with the basal ganglia and provides a cholinergic input to the SNr. This evidence lends further support to the suggestion that the PPN should be considered part of the extended basal ganglia (Mena-Segovia et al., 2004). This suggests that the PPN is likely to have coevolved with the basal ganglia as part of the common vertebrate circuitry for action selection and procedural learning.

## LITERATURE CITED

- Abalo XM, Villar-Cheda B, Anadon R, Rodicio MC. 2005. Development of the dopamine-immunoreactive system in the central nervous system of the sea lamprey. *Brain Res Bull* 66:560–564.
- Akkal D, Dum RP, Strick PL. 2007. Supplementary motor area and presupplementary motor area: targets of basal ganglia and cerebellar output. *J Neurosci* 27:10659–10673.
- Anadón R, Molist P, Rodríguez-Moldes I, López JM, Quintela I, Cerviño MC, Barja P, González A. 2000. Distribution of choline acetyltransferase immunoreactivity in the brain of an elasmobranch, the lesser spotted dogfish (*Scyliorhinus canicula*). *J Comp Neurol* 420:139–170.
- Auclair F, Lund JP, Dubuc R. 2004. Immunohistochemical distribution of tachykinins in the CNS of the lamprey *Petromyzon marinus*. *J Comp Neurol* 479:328–346.
- Björsten LM, NorrSELL K, NorrSELL U. 1976. Behavioural repertoire of cats without cerebral cortex from infancy. *Exp Brain Res* 25:115–130.
- Caillard O, Moreno H, Schwaller B, Llano I, Celio MR, Marty A. 2000. Role of the calcium-binding protein parvalbumin in short-term synaptic plasticity. *Proc Natl Acad Sci U S A* 97:13372–13377.
- Canudas AM, Pezzi S, Canals JM, Pallas M, Alberch J. 2005. Endogenous brain-derived neurotrophic factor protects dopaminergic nigral neurons against transneuronal degeneration induced by striatal excitotoxic injury. *Brain Res Mol Brain Res* 134:147–154.
- Christensson-Nylander I, Herrera-Marschitz M, Staines W, Hökfelt T, Terenius L, Ungerstedt U, Cuello C, Oertel WH, Goldstein M. 1986. Striato-nigral dynorphin and substance P pathways in the rat. I. Biochemical and immunohistochemical studies. *Exp Brain Res Exp Hirnforschung* 64:169–192.
- Cuello AC, Milstein C, Couture R, Wright B, Priestley JV, Jarvis J. 1984. Characterization and immunocytochemical application of monoclonal antibodies against enkephalins. *J Histochem Cytochem* 32:947–957.
- De Arriba MC, Pombal MA. 2007. Afferent connections of the optic tectum in lampreys: an experimental study. *Brain Behav Evol* 69:37–68.
- Ericsson J, Robertson B, Wikström MA. 2007. A lamprey striatal brain slice preparation for patch-clamp recordings. *J Neurosci Methods* 165:251–256.
- Ericsson J, Silberberg G, Robertson B, Wikström MA, Grillner S. 2011. Striatal cellular properties conserved from lampreys to mammals. *J Physiol* 589:2979–2992.
- Farries MA, Meitzen J, Perkel DJ. 2005. Electrophysiological properties of neurons in the basal ganglia of the domestic chick: conservation and divergence in the evolution of the avian basal ganglia. *J Neurophysiol* 94:454–467.
- Florio T, Capozzo A, Puglielli E, Pupillo R, Pizzuti G, Scarnati E. 1999. The function of the pedunculopontine nucleus in the preparation and execution of an externally-cued bar pressing task in the rat. *Behav Brain Res* 104:95–104.
- Graybiel AM. 1998. The basal ganglia and chunking of action repertoires. *Neurobiol Learn Mem* 70:119–136.
- Grillner S, Hellgren J, Ménard A, Saitoh K, Wikström MA. 2005. Mechanisms for selection of basic motor programs—roles for the striatum and pallidum. *Trends Neurosci* 28:364–370.
- Hikosaka O, Takikawa Y, Kawagoe R. 2000. Role of the basal ganglia in the control of purposive saccadic eye movements. *Physiol Rev* 80:953–978.
- Inagaki S, Parent A. 1984. Distribution of substance P and enkephalin like immunoreactivity in the substantia nigra of rat, cat and monkey. *Brain Res Bull* 13:319–329.
- Jessell TM, Emson PC, Paxinos G, Cuello AC. 1978. Topographic projections of substance P and GABA pathways in the striato- and pallido-nigral system: a biochemical and immunohistochemical study. *Brain Res* 152:487–498.
- Jiao Y, Medina L, Veenman CL, Toledo C, Puelles L, Reiner A. 2000. Identification of the anterior nucleus of the ansa lenticularis in birds as the homolog of the mammalian subthalamic nucleus. *J Neurosci* 20:6998–7010.
- Karle EJ, Anderson KD, Medina L, Reiner A. 1996. Light and electron microscopic immunohistochemical study of dopaminergic terminals in the striatal portion of the pigeon basal ganglia using antisera against tyrosine hydroxylase and dopamine. *J Comp Neurol* 369:109–124.

- Kelly RM, Strick PL. 2004. Macro-architecture of basal ganglia loops with the cerebral cortex: use of rabies virus to reveal multisynaptic circuits. *Prog Brain Res* 143:449–459.
- Kitt CA, Brauth SE. 1986. Telencephalic projections from mid-brain and isthmal cell groups in the pigeon. II. The nigral complex. *J Comp Neurol* 247:92–110.
- Lynch JC, Hoover JE, Strick PL. 1994. Input to the primate frontal eye field from the substantia nigra, superior colliculus, and dentate nucleus demonstrated by transneuronal transport. *Exp Brain Res Exp Hirnforschung* 100:181–186.
- Marin O, Gonzalez A, Smeets WJ. 1997. Anatomical substrate of amphibian basal ganglia involvement in visuomotor behaviour. *Eur J Neurosci* 9:2100–2109.
- Marin O, Smeets WJ, Munoz M, Sanchez-Camacho C, Pena JJ, Lopez JM, Gonzalez A. 1999. Cholinergic and catecholaminergic neurons relay striatal information to the optic tectum in amphibians. *Eur J Morphol* 37:155–159.
- Martin-Ibanez R, Crespo E, Urban N, Sergent-Tanguy S, Herranz C, Jaumot M, Valiente M, Long JE, Pineda JR, Andreu C, Rubenstein JL, Marin O, Georgopoulos K, Mengod G, Farinas I, Bachs O, Alberch J, Canals JM. 2010. Ikaros-1 couples cell cycle arrest of late striatal precursors with neurogenesis of enkephalinergic neurons. *J Comp Neurol* 518:329–351.
- Matute C, Streit P. 1986. Monoclonal antibodies demonstrating GABA-like immunoreactivity. *Histochemistry* 86:147–157.
- Medina L, Reiner A. 1997. The efferent projections of the dorsal and ventral pallidal parts of the pigeon basal ganglia, studied with biotinylated dextran amine. *Neuroscience* 81:773–802.
- Medina L, Anderson KD, Karle EJ, Reiner A. 1995. An ultrastructural double-label immunohistochemical study of the enkephalinergic input to dopaminergic neurons of the substantia nigra in pigeons. *J Comp Neurol* 357:408–432.
- Mena-Segovia J, Bolam JP, Magill PJ. 2004. Pedunculopontine nucleus and basal ganglia: distant relatives or part of the same family? *Trends Neurosci* 27:585–588.
- Mena-Segovia J, Sims HM, Magill PJ, Bolam JP. 2008. Cholinergic brainstem neurons modulate cortical gamma activity during slow oscillations. *J Physiol* 586:2947–2960.
- Ménard A, Grillner S. 2008. Diencephalic locomotor region in the lamprey—afferents and efferent control. *J Neurophysiol* 100:1343–1353.
- Ménard A, Auclair F, Bourcier-Lucas C, Grillner S, Dubuc R. 2007. Descending GABAergic projections to the mesencephalic locomotor region in the lamprey *Petromyzon marinus*. *J Comp Neurol* 501:260–273.
- Middleton FA, Strick PL. 2002. Basal-ganglia “projections” to the prefrontal cortex of the primate. *Cereb Cortex* 12:926–935.
- Mitani A, Ito K, Hallanger AE, Wainer BH, Kataoka K, McCarley RW. 1988. Cholinergic projections from the laterodorsal and pedunculopontine tegmental nuclei to the pontine gigantocellular tegmental field in the cat. *Brain Res* 451:397–402.
- Muthusamy KA, Aravamuthan BR, Kringelbach ML, Jenkinson N, Voets NL, Johansen-Berg H, Stein JF, Aziz TZ. 2007. Connectivity of the human pedunculopontine nucleus region and diffusion tensor imaging in surgical targeting. *J Neurosurg* 107:814–820.
- Planert H, Szydlowski SN, Hjorth JJ, Grillner S, Silberberg G. 2010. Dynamics of synaptic transmission between fast-spiking interneurons and striatal projection neurons of the direct and indirect pathways. *J Neurosci* 30:3499–3507.
- Pombal MA, El Manira A, Grillner S. 1997a. Afferents of the lamprey striatum with special reference to the dopaminergic system: a combined tracing and immunohistochemical study. *J Comp Neurol* 386:71–91.
- Pombal MA, El Manira A, Grillner S. 1997b. Organization of the lamprey striatum—transmitters and projections. *Brain Res* 766:249–254.
- Pombal MA, Marin O, Gonzalez A. 2001. Distribution of choline acetyltransferase-immunoreactive structures in the lamprey brain. *J Comp Neurol* 431:105–126.
- Redgrave P, Prescott TJ, Gurney K. 1999. The basal ganglia: a vertebrate solution to the selection problem? *Neuroscience* 89:1009–1023.
- Reiner A. 2002. Functional circuitry of the avian basal ganglia: implications for basal ganglia organization in stem amniotes. *Brain Res Bull* 57:513–528.
- Reiner A, Anderson KD. 1990. The patterns of neurotransmitter and neuropeptide co-occurrence among striatal projection neurons: conclusions based on recent findings. *Brain Res Rev* 15:251–265.
- Reiner A, Medina L, Veenman CL. 1998. Structural and functional evolution of the basal ganglia in vertebrates. *Brain Res Brain Res Rev* 28:235–285.
- Robertson B, Saitoh K, Ménard A, Grillner S. 2006. Afferents of the lamprey optic tectum with special reference to the GABA input: combined tracing and immunohistochemical study. *J Comp Neurol* 499:106–119.
- Robertson B, Auclair F, Ménard A, Grillner S, Dubuc R. 2007a. GABA distribution in lamprey is phylogenetically conserved. *J Comp Neurol* 503:47–63.
- Robertson B, Saitoh K, Grillner S. 2007b. GABAergic control of tectal orienting behavior in the lamprey. *Soc Neurosci Abstr* 924.5.
- Ros H, Magill PJ, Moss J, Bolam JP, Mena-Segovia J. 2010. Distinct types of non-cholinergic pedunculopontine neurons are differentially modulated during global brain states. *Neuroscience* 170:78–91.
- Sato M, Hikosaka O. 2002. Role of primate substantia nigra pars reticulata in reward-oriented saccadic eye movement. *J Neurosci* 22:2363–2373.
- Skinner RD, Garcia-Rill E. 1984. The mesencephalic locomotor region (MLR) in the rat. *Brain Res* 323:385–389.
- Smeets WJ. 1991. Comparative aspects of the distribution of substance P and dopamine immunoreactivity in the substantia nigra of amniotes. *Brain Behav Evol* 37:179–188.
- Smeets WJ, Marin O, Gonzalez A. 2000. Evolution of the basal ganglia: new perspectives through a comparative approach. *J Anat* 196:501–517.
- Stephenson-Jones M, Samuelsson E, Ericsson J, Robertson B, Grillner S. 2011. Evolutionary conservation of the basal ganglia as a common vertebrate mechanism for action selection. *Curr Biol* 21:1081–1091.
- Takakusaki K, Habaguchi T, Ohtinata-Sugimoto J, Saitoh K, Sakamoto T. 2003. Basal ganglia efferents to the brainstem centers controlling postural muscle tone and locomotion: a new concept for understanding motor disorders in basal ganglia dysfunction. *Neuroscience* 119:293–308.
- Thompson RH, Menard A, Pombal M, Grillner S. 2008. Forebrain dopamine depletion impairs motor behavior in lamprey. *Eur J Neurosci* 27:1452–1460.
- Veenman CL, Reiner A. 1994. The distribution of GABA-containing perikarya, fibers, and terminals in the forebrain and midbrain of pigeons, with particular reference to the basal ganglia and its projection targets. *J Comp Neurol* 339:209–250.
- Winn P. 2006. How best to consider the structure and function of the pedunculopontine tegmental nucleus: evidence from animal studies. *J Neurol Sci* 25:234–250.
- Yasuhara O, Aimi Y, Matsuo A, Kimura H. 2008. Distribution of a splice variant of choline acetyltransferase in the trigeminal ganglion and brainstem of the rat: comparison with calcitonin gene-related peptide and substance P. *J Comp Neurol* 509:436–448.
- Zompa IC, Dubuc R. 1998. Diencephalic and mesencephalic projections to rhombencephalic reticular nuclei in lampreys. *Brain Res* 802:27–54.





**Karolinska  
Institutet**

**Institutionen för Neurovetenskap**

## **Cellular and Synaptic Properties in the Lamprey Striatum**

**AKADEMISK AVHANDLING**

som för avläggande av medicine doktorsexamen vid Karolinska  
Institutet offentlig försvaras i Föreläsningssalen Hillarp

**Fredagen den 28 september, 2012, kl 10.00**

av

**Jesper Ericsson**

Civilingenjör

*Huvudhandledare:*

Docent Gilad Silberberg  
Karolinska Institutet  
Institutionen för Neurovetenskap

*Bihandledare:*

Professor Sten Grillner  
Karolinska Institutet  
Institutionen för Neurovetenskap  
Nobelinstitutet för Neurofysiologi

Doktor Martin Wikström  
Karolinska Institutet  
Institutionen för Neurovetenskap

Professor Jeanette Hellgren Kotaleski  
Kungliga Tekniska Högskolan  
Institutionen för Beräkningsbiologi

*Fakultetsopponent:*

Professor Rejean Dubuc  
Université de Montreal  
Department of Physiology  
Central Nervous System Group

*Betygsnämnd:*

Docent Per Svenningsson  
Karolinska Institutet  
Institutionen för Klinisk Neurovetenskap

Professor Gilberto Fisone  
Karolinska Institutet  
Institutionen för Neurovetenskap

Professor Martin Garwicz  
Lunds Universitet  
Medicinska Fakulteten  
Neuronano Research Center

**Stockholm 2012**



## ABSTRACT

The striatum is the main input structure of the basal ganglia, a group of subcortical nuclei that are central to the control of different patterns of motor behaviours and for the selection of actions, a fundamental problem facing all animals. The main focus of this thesis has been to characterize the cellular and synaptic mechanisms of the striatum and its relation to other basal ganglia nuclei in the lamprey.

To understand how the basal ganglia input structure, the striatum, processes motor related information we first needed to understand the basic architecture of the striatal microcircuitry. Individual neurons were characterized based on their electrophysiological properties and we showed that there are two main types of striatal neurons: inwardly rectifying neurons (IRNs) that are distinguished by a prominent rectification due to a  $K_{ir}$  type  $K^+$  conductance, and non-IRNs. IRNs are in this and other respects very similar to the mammalian medium spiny projection neurons (MSNs). IRNs are projection neurons of two types, those that express substance P, dopamine receptors of D1 type and GABA, or enkephaline and D2 receptors and GABA. Non-IRNs are a mixed group of neurons and contain neurons similar to the fast-spiking type found in mammals.

We then investigated how the striatum is activated by the main excitatory inputs from the lateral pallium (the homolog of the cortex) and from thalamus. As recently demonstrated in mammals, the pallium and thalamus in lamprey provide synaptic inputs with very different dynamic properties to the striatum, as evoked by extracellular stimulation of the respective pathway. Repetitive activation of the synapses from the lateral pallium result in a progressive facilitation over several hundred milliseconds due to a low presynaptic release probability. In contrast, activation of thalamic afferents instead evokes strongly depressing synapses throughout a stimulus train due to a high presynaptic release probability. The conserved difference between the thalamic and pallial inputs most likely has functional implications for processing within striatum.

The lamprey striatum receives prominent dopaminergic innervation that, when depleted, leads to hypokinetic symptoms. As dopamine is thought to bias the striatal networks towards selecting actions by differentially modulating the excitability of D1 and D2 receptor expressing striatal projection neurons, we investigated this in lamprey. We cloned the lamprey D2 receptor and demonstrated that it was expressed in striatum. We showed that the neurons that project directly to the basal ganglia output nuclei (SNr and the globus pallidus interna (GPi)) express dopamine D1 receptors, while separate populations that project to the mixed GPi/GPe nucleus express either dopamine D1 or D2 receptors. As in mammals, activation of D1 receptors furthermore leads to an increase in the excitability, whereas D2 activation decreases the excitability of IRNs.

Lastly, we identified the SNr and pedunculopontine nucleus (PPN) in lamprey and showed that the SNr provides tonic inhibition to downstream motor centers while the cholinergic neurons of the PPN modulates basal ganglia nuclei.

In summary, the organization of striatum and the properties of the synaptic input, cellular properties and molecular markers are conserved throughout vertebrate evolution.